

©[2010]

Ying Li

ALL RIGHTS RESERVED

REGULATION OF TGF β SIGNALING BY MICRORNAS

By

YING LI

A Dissertation submitted to the

Graduate School-New Brunswick

Rutgers, The State University of New Jersey

and

The Graduate School of Biomedical Sciences

University of Medicine and Dentistry of New Jersey

in partial fulfillment of the requirements for the degree of

Doctor of Philosophy

Graduate Program in Cellular and Developmental Biology

written under the direction of

Richard W. Padgett, Ph.D.

And approved by

New Brunswick, New Jersey

October 2010

ABSTRACT OF THE DISSERTATION:
REGULATION OF TGF β SIGNALING BY MICRORNAS

By

YING LI

Dissertation Director:

Richard W. Padgett

The TGF β superfamily plays important roles in various processes. With the genetic tools available, *Drosophila* has been a useful model organism to study the regulators of the TGF β pathways, which can shed light on potential treatments for many developmental disorders and diseases caused by aberrant TGF β signaling. microRNAs (miRNAs) are small non-coding RNAs, acting posttranscriptionally to regulate gene expression, that are involved in various aspects of cellular and developmental processes.

My thesis work examines the regulation of TGF β -like pathways by miRNAs. Specifically, with the combination of computational algorithms and tissue culture methods, my early work successfully identified and validated the targets of *Drosophila* miRNAs. From that, I found that *bantam*, a miRNA, can down regulate *Mad* (*Mothers against dpp*), a signaling component of TGF β . Furthermore, I used *Drosophila* as a model and demonstrated that *bantam* is a negative regulator of the Dpp (*decapentaplegic*) pathway. My results showed *bantam* down regulates *Mad* (*Mothers against dpp*) expression *in vivo* by targeting the *Mad* 3'UTR, resulting in changes in Dpp signaling. The removal of

bantam binding sites in the 3'UTR of a *Mad* transgene results in a significant increase in the viability of haploinsufficient *dpp* animals compared to a *Mad* transgene carrying intact *bantam* binding sites in the 3'UTR. Interestingly, *bantam* is up-regulated by Dpp in the wing imaginal disc, and thereby functions in a Dpp feedback loop. Furthermore, this feedback loop is important for maintaining anterior-posterior (A/P) compartment boundary stability in the wing disc through regulation of *omb* (*optomotor-blind*). Comparative genomics reveal that *bantam* is evolutionarily conserved, and miRNA target predictions suggest that human *bantam* homologs selectively target Smad5, one of two homologs of *Mad* in BMP signaling, but does not target Smad2 which functions in the activin/TGF β pathway. These data suggest that *bantam* is a conserved negative regulator of BMP/Dpp signaling.

In addition to the work in the wing disc, I extended my studies and examined the role of *bantam* in *Drosophila* brain development. My work shows that *bantam* is critical for maintaining the stem cell pools of the optic lobe, and that *bantam* has a cell-autonomously effect on glial cell proliferation and distribution, largely through targeting *omb*.

ACKNOWLEDGEMENTS

I would like to take this opportunity to express my gratitude to all those people who helped me through my Ph.D. study.

First and foremost, I would like to show my deepest gratitude to my dissertation advisor, Dr. Richard W. Padgett, for his support and guidance. Rick is a very respectable, responsible and resourceful scientist. He guided me through every stage of my Ph.D study, from the first experimental design to the final writing of this dissertation. Without his illuminating instruction, impressive kindness and patience, I could not have completed my thesis. His keen and vigorous academic observation enlightens me not only in this thesis but also in my future career.

Second, I would like to express my heartfelt gratitude to my committee members, Dr. Ken Irvine, Dr. Kim McKim, Dr. Monica Driscoll and Dr. Sunita Kramer, for their helpful scientific suggestions and comments on my dissertation and their constant encouragement and advice.

Third, I would also like to thanks to all the past and current members in Padgett lab during my time here. In particular, I want to thank Nanci Kane and Ryan Gleason for useful scientific discussions. A lot of thanks go for Nanci Kane and Harlan Robins for collaborations on several experiments.

Last but not the least my thanks go to my beloved family for their constant love and support, being confident in me all through these years. I would like to mention my special deepest thanks for my mom, a great woman, who sacrificed a lot of her personal social life by helping me taking care of my kids. Without her incredible support and help, I would never come so far to pursue my Ph.D. study, and my kids would never be so happy and healthy.

TABLE OF CONTENTS

Abstract of the Dissertation.....	ii
Acknowledgements.....	iv
Table of Contents.....	vi
List of Tables.....	ix
List of Figures.....	x

Chapter I

General Instroduction.....	1
Figures.....	37

Chapter II

Incorporation Structure to Predict microRNA targets.....	41
Abstract.....	42
Introduction.....	43
Materials and Methods.....	45
Results and Discussion.....	47
Acknowledgments.....	55
Figures.....	56
Tables.....	60

Chapter III

bantam* microRNA is a Negative Regulator of the *decapentaplegic

Pathway.....	76
Abstract.....	77
Author Summary.....	78
Introduction.....	79
Results.....	84
Discussion.....	94
Materials and Methods.....	100
Acknowledgments.....	104
Figures.....	105
Tables.....	129

Chapter IV

***bantam* microRNA Functions in the Optic Lobe.....**

Summary.....	132
Introduction.....	133
Materials and Methods.....	137
Results.....	140
Discussion.....	149
Acknowledgments.....	153
Figures.....	154

Appendix

Conservation microRNAs in Brains.....	173
Introduction.....	174
Materials and Methods.....	176
Results and Discussion.....	179
Summary.....	183
Figures.....	185
Tables.....	187
 Summary of thesis work.....	 191
References.....	196
Curriculum Vitae.....	220

LIST of TABLES

Chapter II

Table 1. Tested miRNA targets.....	60
Table 2. Top 10 targets for each miRNA.....	61

Chapter III

Table 1. Survival rates of haploinsufficient <i>dpp</i> alleles by two <i>ubi-Mad</i> transgenes.....	129
Table 2. Predicted target sites of miRNAs from <i>hsa-miR-450/542</i> cluster on Smad5 3'UTR.....	130

Appendix

Table 1. miRNAs in Drosophila larval brains and adult heads.....	187
Table 2. Conserved expression of miRNAs in brain tissues across species.....	189

LIST of FIGURES

Chapter I

Figure 1. The mammalian TGF β signaling pathways.....	37
Figure 2. The TGF β signaling pathways in <i>Drosophila</i>	39

Chapter II

Figure 1. A graph of <i>luciferase</i> reporter intensity from miRNA target genes	56
Figure 2. Both of the two <i>bantam</i> -binding sites on the 3' UTR of <i>Mad</i> are shown to contribute to repression	58

Chapter III

Figure 1. <i>bantam</i> regulates <i>Mad</i>	105
Figure 2. Loss of <i>bantam</i> binding sites in <i>Mad</i> increases rescue of <i>dpp</i> haploinsufficiency	107
Figure 3. <i>bantam</i> and <i>Mad</i> regulate each other	109
Figure 4. <i>omb</i> rescues a <i>bantam</i> wing disc defect.....	111
Figure 5. <i>bantam</i> and Dpp potentiate wing disc growth	113

Figure 6. <i>bantam</i> is evolutionarily conserved.....	115
Figure 7. Regulation of <i>bantam</i> and Dpp signaling in Drosophila wing imaginal disc cells.....	117
Figure 8. Sequence analysis of DNA 15kb upstream of Drosophila <i>bantam</i>	119
Figure 9. Conserved Smad binding sites in the regulatory sequences of <i>miR-450/542</i> cluster.....	124

Chapter IV

Figure 1. <i>bantam</i> is differentially expressed within the optic lobe.....	154
Figure 2. <i>bantam</i> is required for proliferation in the optic lobe.....	157
Figure 3. <i>bantam</i> affects photoreceptor-neuron axon projection in the optic lobe.....	159
Figure 4. <i>bantam</i> promotes glial cell proliferation in the optic lobe.....	161
Figure 5. <i>bantam</i> down regulates <i>omb</i> in the optic lobe.....	163
Figure 6. <i>omb</i> rescues <i>bantam</i>	165
Figure 7. <i>bantam</i> causes abnormal distribution of glia cells with increased number in the optic lobe.....	167

Figure 8. Over expression of *bantam* causes ectopic glial cells in the lamina..169

Figure 9. *bantam* causes ectopic glial cell cluster in the lamina.....171

Appendix

Figure 1. *miR-7* and *miR-125* are highly expressed in the Drosophila developing
brain.....185

CHAPTER I

GENERAL INTRODUCTION

1. The Transforming Growth Factor β Superfamily

The secreted transforming growth factor β (TGF β) superfamily controls a broad array of cellular functions in a developmental context dependent and cell type specific manner, such as cell proliferation, differentiation, migration and apoptosis, in a variety of multicellular organisms ranging from worms and flies to humans. Aberrant TGF β signaling caused by mutations in the ligands or their downstream components that transduce the signal have been implicated in various human diseases, such as fibrosis, autoimmune and cardiovascular diseases, cancers and developmental disorders (Massague et al., 2000; Padgett, 1999). In cancers, TGF β is a tumor suppressor in the early phase of tumorigenesis, but acts as a tumor promoter during cancer progression (Bierie and Moses, 2006).

Based on the amino acid homology within the ligand domain, TGF β superfamily is divided into three major subfamilies, TGF β s, activins, and bone morphogenetic proteins (BMPs). The TGF β family is evolutionarily conserved throughout metazoans. In humans, 33 structurally related members are found in TGF β family (Moustakas and Heldin, 2009). In *C. elegans*, there are five TGF β ligands, *daf-7*, *dbl-1*, *unc-129*, *tig-1*, and *tig-2* (Padgett et al., 1998). In *Drosophila*, there are seven TGF β ligands. Decapentaplegic (Dpp), Screw (Scw), and Glass-bottom boat (Gbb) are members of BMP family, whereas, Activin- β (Act β) and Dawdle (Daw) belong to the TGF β /activin branch. Maverick (Mav) and Myoglianin (Myo) are divergent and are not assigned to a particular ligand subfamily (Parker et al., 2004; Raftery and Sutherland, 1999). The essential framework in TGF- β signaling has been determined (Figure 1). At the surface of response cell, there are type I

and type II transmembrane receptors, which contain intracellular protein kinase domain with serine/threonine specificity. When the dimeric TGF- β ligands bind to a type II receptor, the type II receptor binds to a type I receptor, and phosphorylates the type I receptor within its glycine- and serine-rich sequence motif (GS domain) between the transmembrane and kinase domains. Once phosphorylated, the active type I receptor can then initiate the intracellular signaling cascade through Smad proteins. Smads can be divided into three functional classes: the receptor-regulated-Smads (R-Smads), the common Smad (co-Smad), and the inhibitory Smads (I-Smads). First, active type-I receptors phosphorylate R-Smads. Smad1, Smad5 and Smad8 are activated by BMP signaling, whereas Smad2 and Smad3 are activated by activin/TGF- β signaling (Feng and Derynck, 2005). The activated R-Smads then associate with the Co-Smad, Smad4, which is shared by all three signal pathways. Next the R-Smads/Co-Smad complex translocates into the nucleus, binds to DNA sequences, and either activates or represses target gene expression by binding to other transcriptional factors. Smads are composed of three domains: (1) an N-terminal Mad-homology 1 (MH1) domain, which is responsible for DNA-binding and also provides the interaction platform for various proteins, (2) the middle linker domain, which is enriched in prolines and phosphorylatable serine or threonines, and (3) the C-terminal MH2 domain, which mediates R-Smad specificity, receptor recognition, and Smad oligomerization. R-Smads and Co-Smads both contain highly conserved MH1 and MH2 domains. However, R-Smads contain an additional C-terminal SSXS motif, which can be phosphorylated by an active type I receptor (Wrana, 2000). I-Smads, Smad6 and Smad7, can be induced by TGF β signaling. But due to the lack of the MH1 domain, it can not bind to DNA, but rather acts as competitive

antagonist to prevent R-Smad phosphorylation by type I receptors, negatively regulating signal strength and duration in a negative-feed back loop (Hayashi et al., 1997; Nakao et al., 1997).

2. The Regulation of TGF β Signaling

Fine tuning of TGF β signaling is important for its functions. Strength and duration of TGF β signaling are regulated at various steps and by multiple mechanisms, both extracellularly and intracellularly (Moustakas and Heldin, 2009).

2.1. The Regulation of TGF β ligands

All TGF β ligands are synthesized as large proproteins with a C-terminal mature polypeptide followed by a N-terminal propeptide, which is proteolytically processed before secretion from the cell (Koli et al., 2001). This TGF β propeptide is referred to as the latency associated peptide (LAP), bound to TGF- β noncovalently after secretion, sequestering TGF- β in a latent form that cannot bind to receptors (Bottinger et al., 1996). This latent TGF β complex contains an additional one of four latent TGF- β -binding proteins (LTBPs), extracellular matrix proteins, which are disulfide-linked to LAP (Miyazono et al., 1993). LTBPs are found to have important roles in TGF β secretion, storage in the extracellular matrix (ECM), and eventual activation. Activation of latent TGF β involves proteolytic cleavage of LTBPs from ECM, and releasing LAPs or at least exposing the receptor binding sites of TGF β (Koli et al., 2001). Once secreted, the TGF β ligands also interact with various extracellular proteins which affect signaling through changing availability of ligands to their receptors (Umulis et al., 2009). Noggin and

Chordin are well known inhibitors of BMPs signaling (Gazzerro and Canalis, 2006). Noggin is a secreted glycosylated protein, which binds BMPs with high affinity and prevents their interaction with their specific receptors, thus inhibiting signaling. Chordin is a conserved glycosylated protein known to antagonize BMP action in the Spemann Organizer. Chordin binds specifically to BMPs, and does not bind other members of the TGF β superfamily. The chordin/BMP complex is further regulated by *tolloid*, the zinc metalloprotease, which cleaves chordin and releases free BMPs to the extracellular space (Piccolo et al., 1997). The *Drosophila* Chordin homolog, Short gastrulation (Sog), forms an inverse gradient in the blastoderm dorsal ectoderm that antagonizes Decapentaplegic (Dpp), and is required in axis formation and dorsal tissue specification (Francois et al., 1994). Recently, Viking (Vkg) and Dcg1, type IV collagen proteins in the extracellular matrix (ECM) in *Drosophila*, were reported to bind to Dpp and regulate its signaling in both the embryo and the ovary during development (Wang et al., 2008b). In the embryo, binding of type IV collagen to Dpp increased Dpp signaling by promoting Dpp gradient formation. While in the ovary, these type IV collagens showed an inhibitory effect on Dpp signaling through sequestration of the Dpp ligand (Wang et al., 2008b).

Follistatin is a soluble monomeric glycosylated polypeptide that binds activin with high affinity and inhibits most of its biological actions (Xia and Schneyer, 2009). A *Drosophila* Follistatin homologue (dFS) has been cloned (Haerry and O'Connor, 2002). *dFs* expression causes mutant phenotypes similar to the mutants of the activin ligands, *daw* and *Act β* , suggesting that *Drosophila* FS has similar functions with its vertebrate counterpart (Pentek et al., 2009).

Besides type I and type II receptors, TGF β ligands can also bind to co-receptors or the TGF β type III receptor on the cell surface which can either promote or inhibit signaling (Bernabeu et al., 2009). Normally these co-receptors do not have an intrinsic signaling function but regulate the access of TGF- β ligands to receptors. In mammals, betaglycan and endoglin are membrane-anchored proteoglycans. Endoglin is mainly expressed in vascular endothelial cells, while betaglycan is more generally distributed. In most cases, the extracellular domain of betaglycan binds TGF β superfamily ligands with high affinity, and facilitates ligands binding to their respective cognate type II and type I receptors to increase signaling (Kirkbride et al., 2008; Lopez-Casillas et al., 1993). But in the case of binding to inhibin, betaglycan shows an inhibitory effect on both BMPs and activin pathways (Farnworth et al., 2006; Lewis et al., 2000). Although endoglin has a high degree of similar amino acid sequences to those of betaglycan in the transmembrane and cytoplasmic domains, the two do not have same binding profile for TGF β superfamily ligands (Bernabeu et al., 2009). In many cell types, endoglin causes an opposite TGF β 1-dependent response. However, how exactly endoglin regulates TGF β signaling is not known (Bernabeu et al., 2009). Cripto is a glycosyl-phosphatidylinositol (GPI)-anchored proteoglycan, which is a co-receptor enhancing Nodal signaling (Constam, 2009). Two important domains characterize Cripto: a conserved CFC domain, which binds to type I receptor ALK4, and an EGF-like motif, which binds to Nodal. Cripto also recruits other proprotein convertases to the Cripto-Nodal-receptor complex, and facilitates the processing the Nodal precursor into maturity. Cripto is also found to help enrich Nodal in the early endosome (Constam, 2009). In *Drosophila*, *Dally* (*division abnormally delayed*),

a *Drosophila* member of the glypican family of integral membrane proteoglycans positively regulates Dpp signaling and plays a role in the cell cycle (Jackson et al., 1997).

2.2. The Regulation of TGF β Receptors

All TGF β ligands transmit signaling through binding to type I and type II receptors on the cell membrane. There are five type II (ActR-IIA, ActR-IIB, BMPR-II, AMHR-II and T β R-II) and seven type I receptors (ALKs 1–7) in the human genome (Massague and Gomis, 2006; Schmierer and Hill, 2007). Ligand binding brings a constitutive active type II receptor adjacent to a type I receptor, allowing the type II receptor to phosphorylate the juxtamembrane GS domain of the intracellular part of the type I receptor, turning on its kinase activity. Some proteins can bind to the GS domain of the type I receptor, inhibiting phosphorylation of type I receptory by a type II receptor, such as the immunophilin FKBP12, which is thought to provide a safeguard against leaky signaling when ligand is absent (Chen et al., 1997). Furthermore, a more recent report showed that FKBP12 also functions as an adaptor for Smad7-Smurfl complex and activin type I receptor, facilitating the degradation of the receptor (Yamaguchi et al., 2006). Various proteins are found to associate with TGF β receptor and act as negative regulators of TGF β signaling pathway. The WD-repeat protein, the B α subunit of protein phosphatase 2A (PP2A) interacts with type I TGF- β receptors and is phosphorylated by the receptor. Evidence showed that B α can enhance the growth inhibition activity of TGF- β (Griswold-Prenner et al., 1998). Another WD-repeat protein, STRAP, binds both type I and type II receptors, and recruits and stabilizes Smad7 to an activated type I receptor,

therefore preventing Smad2 and Smad3 from accessing a type I receptor (Datta and Moses, 2000).

Some intracellular proteins can function as positive regulators of TGF β signaling by facilitating Smad binding to type I receptors. In response to TGF β signaling, Axin interacts with an active type I receptor and Smad3, and facilitates Smad3 phosphorylation by the type I receptor, increasing TGF β signaling (Furuhashi et al., 2001). Disabled-2 (Dab2) associates with both type I and type II TGF β receptors as well as Smad2 and Smad3, helping to propagate signaling from the receptor to Smad (Hocevar et al., 2001).

Evidence showed that the degradation and stability of TGF β receptors play critical roles in the regulation of TGF β signaling pathway. Post-transcriptional modifications of receptors, such as ubiquitination and sumoylation, have been shown to be important in regulating the strength and duration of TGF β signaling (Lonn et al., 2009). Ubiquitination involves covalently attaching one or more ubiquitin monomers via a three-step enzymatic reaction with E1, E2, and E3 enzymes. I-Smads seem to play central roles in orchestrating ubiquitination of a type I receptor (discussed below). Sumoylation is the modification of the conjugation of SUMO (small-ubiquitin-like modifiers) to protein through SUMO ligases. TGF β type I receptor was reported to be sumoylated upon TGF β signaling. Sumoylation of the receptor facilitates recruitment and phosphorylation of Smad3, consequently increasing TGF β signaling (Kang et al., 2008).

2.3. The Roles of I-Smads

TGF β induced I-Smads, Smad6 and Smad7, were long known to compete with R-Smads to the receptor, regulating TGF β in a negative-feed back loop (Hayashi et al., 1997; Nakao et al., 1997). While Smad7 inhibits both TGF β and BMP pathways, Smad6 inhibits BMP pathways more selectively (Goto et al., 2007). In addition, I-Smads function as scaffolds for proteins that negatively regulate receptor function. Interaction of GADD34 with Smad7 subsequently recruits a catalytic subunit of protein phosphatase 1 (PP1) holoenzyme to dephosphorylate and inactivate T β RI, providing an effective mechanism for negatively mediating TGF β -induced cell cycle arrest (Shi et al., 2004). Furthermore, I-Smads recruit the HECT (homologous to the E6-associated protein C-terminus) type E3 ubiquitin ligases to receptors and cause receptor degradation. Examples include Smurfs (Smad ubiquitylation regulatory factors), WWP1 (WW domain-containing protein 1) and NEDD4-2 (neural precursor cell expressed, developmentally down-regulated 4-2) (Izzi and Attisano, 2006; Lonn et al., 2009). Recently, a chaperone protein, heat shock protein (HSP90) was reported to bind to receptors and protect those receptors from ubiquitylation by Smurf2, thus positively regulating TGF β signaling (Wrighton et al., 2008). Smad7 can also bind to the deubiquitinating enzyme, UCH37 (ubiquitin C-terminal hydrolase) via a different region from the Smurf PY interacting motif. UCH37 can reverse the ubiquitination of the type I TGF- β receptor, leading to stabilization of the receptor and also increasing the TGF β signaling (Wicks et al., 2005). More recently, the AMP-regulated kinase member SIK (salt-inducible kinase) induced by TGF β signaling was found to interact with Smad7, leading the degradation of type I receptor ALK5. Kinase activity of SIK was shown to be

required for proper T β RI degradation; however, the direct substrate of this kinase remains mysterious (Kowanetz et al., 2008).

2.4. The Regulation of Smad trafficking

Once phosphorylated by a type I receptor, R-Smad forms a complex with Co-Smad, and translocates into the nucleus. In the nucleus, phosphorylated Smad can be dephosphorylated by nuclear phosphatases, and then exported out. Nuclear shuttling of Smads is highly regulated. Transportation of the Smads complex into the nucleus is mediated by nucleoporins and importins. In their MH1 domain, all Smads contain conserved nuclear localization signals (NLSs), which play a pivotal role in the nuclear shuttling of Smads by binding to specific importins (Reguly and Wrana, 2003). In *Drosophila*, Moeskin (Msk) is important for the nuclear import of phosphorylated Mad. Mammalian orthologues of Msk, importin7 and importin8, also mediate the nuclear import of Smad1, Smad3, and Smad4 (Xu et al., 2007; Yao et al., 2008). Besides the NLS, Smads proteins also contain nuclear export signals (NESs) in their MH2 domain or linker region, which bind to specific exportins to mediate Smad exported out of nucleus (Reguly and Wrana, 2003). The significance of the linker region of Smad in relation to TGF β signaling strength and duration has been recognized as well. There are phosphorylation sites in the linker region of Smad1/Mad by MAPK (mitogen-activated protein kinase) and GSK3 (glycogen synthase kinase 3). Also, MAPK and GSK3 phosphorylations cause an inhibitory effect for BMPs/Dpp signaling by promoting cytoplasmic retention of Smad1/Mad (Eivers et al., 2009a). MAPK is activated by the receptor tyrosine kinase, which receives signaling from growth factors. GSK3 is inhibited

by Wnt signaling. Hence, MAPK and GSK3 sites in the linker region of Smad1/Mad provide a regulatory cross talk between BMP/Dpp and other signaling pathways (Eivers et al., 2009a).

Ubiquitin and SUMO modifications of Smad proteins also aid in mediating nuclear trafficking. Mono-ubiquitination of Smad4 in the nucleus promotes turnover of Smad complexes and facilitates nuclear export of Smad4 (Wang et al., 2008a). PIASy (the protein inhibitor of activated Stat y) sumo-ligase promotes Smad3 nuclear export, causing the suppression of TGF β signaling (Imoto et al., 2008). *Drosophila* utilizes similar SUMO modification to regulate Smad trafficking as well. Evidence showed that sumoylation of Medea in the nucleus promotes its nuclear export. Failure of sumoylation of Medea led to an increase of Dpp signaling in the developing embryo, suggesting that SUMO modification is an important negative method that animals employ to tune up the Dpp gradient (Miles et al., 2008).

Interaction with other proteins affects Smad trafficking as well. Shuttling protein TAZ, which is also a transcriptional regulator, was found to promote nuclear accumulation of Smad2/Smad3-Smad4 complex upon TGF β stimulation. This regulation is also important for the self-renewal of the human embryonic stem cell (Varelas et al., 2008). In *Drosophila*, Otefin (Ote), a nuclear lamin-binding protein is essential for germline stem cell (GSC) maintenance by interacting with Medea and retaining Smad complex into nucleus (Jiang et al., 2008).

2.5. Transcription regulation of Smads

Once the activated Smad complex is translocated into the nucleus, it can regulate the transcription of TGF β target genes. The conserved MH1 domain of Smads can bind specific DNA sequences to the promoters or enhancers of TGF β target genes, thus initiating transcription of these genes. A single SMAD binding site (SBE) is composed of the sequence 5'-GTCT-3' or its reverse complement 5'-AGAC-3', which can bind to MH1 domains of activated Smad3-Smad4 complexes (Shi et al., 1998; Zawel et al., 1998). In contrast, the phosphorylated Smad1 preferentially binds to a GC-rich motif (Schmierer and Hill, 2007). However, this short Smad binding element (SBE, 5'-GTCT- 3') only allows low affinity binding. In most cases, strong DNA binding by Smads is dependent on its interaction with other transcription factors, which bind to DNA with higher affinity. Currently, there have been numerous transcription factors associated with Smad complexes, modulating the specificity of their transcription activity (Feng and Derynck, 2005).

In *Drosophila*, phosphorylated Mad, the homologue of Smad1, can recognize the consensus sequence 5'-GRCGNC-3' (which is normally adjacent to the canonical SBE 5'-GTCT-3' sequence), allowing additional DNA to bind to Medea (Gao et al., 2005). The 5 base pair spacing between these sites is conferred by the binding of the transcriptional regulator Schnurri (Shn) to the Mad-Medea complex (Gao et al., 2005). Shn is a large zinc finger DNA binding protein, which acts as a repressor and is essential for Dpp mediated repression of *brinker* (*brk*) transcription (Marty et al., 2000). Transcription of *brk* is negatively regulated by Dpp signaling throughout development. Brk can bind to

many Dpp target genes in a sequence-specific (5' -GGCCYY- 3') manner to repress them in the absence of Dpp signaling (Sivasankaran et al., 2000; Zhang et al., 2001).

3. TGF β Signaling Pathways in *Drosophila*

3.1. Overview of TGF β pathways in *Drosophila*

Drosophila has both BMP-like and Activin-like signals (Figure 2). There are a total of seven TGF- β -related ligands. Three BMP-type ligands are present in *Drosophila*: Dpp (an ortholog of vertebrate BMP2 and BMP4), Gbb (a member of the BMP5, BMP6, BMP7 subgroup), and Scw (a distantly related BMP family member) (Newfeld et al., 1999; Parker et al., 2004; Raftery and Sutherland, 1999). Dpp is considered a functional ortholog of BMP2 and BMP4, showing > 75% amino acid similarity with human BMP4 (Padgett et al., 1993). The embryonic dorsal-ventral patterning defect of null *dpp* mutant can be rescued by expressing human BMP4 in *Drosophila* (Padgett et al., 1993). In mammals, BMPs are well known for their functions in skeletal development and adult bone homeostasis (Tsumaki and Yoshikawa, 2005; Winnier et al., 1995). The highly purified recombinant *dpp* protein can induce bone formation in mammalian cell culture as well (Sampath et al., 1993). Act β and Daw are *Drosophila* orthologs of vertebrate activin (Brummel et al., 1999; Kutty et al., 1998). The other ligands are more divergent. In *Drosophila*, only two type II receptors are found, Punt (Put) and Wishful thinking (Wit), which are employed by both BMP and activin pathways. Thus, signaling specificity is most dependent on recruitment of an appropriate type I receptor. There are three type I receptors in *Drosophila*: Thickveins (Tkv), Saxophone (Sax) and Atr-1/Baboon (Babo). There are also two R-Smads: Mothers against dpp (Mad) and dSmad2, but only one

single Co-Smad, Medea (Med). For BMP-like signaling in *Drosophila*, the ligands, Dpp, Gbb, and Scw, act through the type I receptor Tkv or Sax. Upon ligand binding, Sax and Tkv phosphorylate Mad. Phosphorylated Mad (P-MAD) forms a complex with the co-Smad, Medea, which then translocates into the nucleus, forming a complex with other co-factors, regulating target gene expression either by transcriptional activation or repression (Parker et al., 2004; Raftery and Sutherland, 1999). For the activin-like pathway in *Drosophila*, Daw and Act β signal through Babo and dSmad2 (Das et al., 1999; Parker et al., 2006; Serpe and O'Connor, 2006). So far, Daughters against dpp (Dad) is the only I-Smad that has been identified in *Drosophila* with a known function of exclusively inhibiting BMP/Dpp signaling in a negative feedback loop method (Tsuneizumi et al., 1997), but having no effect on the activin-like pathways (Kamiya et al., 2008).

3.2. Developmental Roles of BMP/Dpp signaling in *Drosophila*

Since the discovery of *dpp* that showed defects in imaginal disc development (Spencer et al., 1982), studies have unveiled its important functions in many developmental processes (Parker et al., 2004; Raftery and Sutherland, 1999), such as the dorsal–ventral (D-V) patterning in the blastoderm embryo, the dorsal closure of the embryo, development of the heart, salivary glands and trachea, the growth and patterning of the imaginal discs, the maintenance of germline stem cells and maturation of the glial cells in the optic lobe.

3.2.1. Roles of BMP/Dpp signaling in early embryonic patterning

During development, zygotic expression of *dpp* provides the D-V axis positional information to the embryonic ectoderm. Loss of Dpp in *dpp* mutant embryo renders a striking ventralized phenotype, in which the dorsal-lateral epidermis and dorsal-most amnioserosa are missing (Irish and Gelbart, 1987). The *dpp* gene is expressed in the dorsal 40% of the embryonic circumference (St Johnston and Gelbart, 1987), specifying distinct cell fates in the dorsal region in a dosage-dependent manner (Ferguson and Anderson, 1992). Peak level of Dpp activity specifies the dorsal extraembryonic amnioserosa tissue, while a low level of Dpp activity signifies the dorsal epidermis. The ventral ectodermal cells without Dpp activity becomes neurogenic ectoderm (Ferguson and Anderson, 1992; Wharton et al., 1993). *dpp* mRNA is expressed uniformly in the dorsal region (St Johnston and Gelbart, 1987), and Tkv, Sax, Put and Mad are all provided to the embryo from the maternal genome during oogenesis (Podos and Ferguson, 1999). Thus, a gradient of Dpp signaling in the dorsal embryo is generated by post-transcriptional modulation of ligand distribution or signaling capability. Evidence showed that a gradient of Dpp activity is generated by the combined action of three extracellular proteins: Short gastrulation (Sog), Twisted gastrulation (Tsg) and Tolloid (Tld) (Arora and Nusslein-Volhard, 1992; Decotto and Ferguson, 2001; Francois et al., 1994; Mason et al., 1994; Shimell et al., 1991). Both Sog and Tsg can form ternary complexes with Dpp and sequester Dpp ligand to its receptor, therefore acting as local antagonists of BMP signaling (Decotto and Ferguson, 2001; Ross et al., 2001). Sog, the *Drosophila* homolog of the vertebrate chordin, is expressed in the ventral-lateral region of the embryo that abut the Dpp expression domain, forming a ventral to dorsal diffusion gradient of Sog that results in an inverse gradient of Dpp (Marques et al., 1997). Tsg can facilitate strong

binding of Sog to Dpp (Ross et al., 2001). Tld is a metalloprotease, which is expressed only in dorsal cells and can cleave ligand-associated Sog and release Dpp to its receptor (Marques et al., 1997; Shimmi and O'Connor, 2003). However, the Dpp activity gradient in the dorsal region is not smooth; instead, there is a very sharp transition between cells receiving high (dorsal midline) and very low (dorsal lateral) signals. Sog and Tsg are found to be required in the formation of this sharp transition of Dpp activity (Ross et al., 2001). In *sog* or *tsg* mutant embryos, P-MAD fails to refine and intensify at the dorsal midline, and amnioserosa is missing (Ross et al., 2001). Binding of Sog to Dpp were reported to play essential roles in the long range diffusion of Dpp ligands to the dorsal midline of the embryo (Eldar et al., 2002; Shimmi et al., 2005). At the dorsolateral region where Sog protein level is high, the binding of Dpp to Sog renders it sequestered from its receptor binding. However, some Dpp ligands are freed from Dpp-Sog complex, processed by Tld, and recaptured by Sog at the dorsolateral region, further promoting its diffusion. On the other hand, at the dorsal midline region where Sog is least prevalent, Dpp is free with the help of Tld, and activates signaling (Eldar et al., 2002).

Besides Dpp, the second BMP ligand Scw also plays an important part in early embryonic patterning. The null mutant of *scw* embryo showed a partial ventralization phenotype, but less severe than null *dpp* mutant (Arora et al., 1994). However, the patterning function of Scw is entirely dependent on Dpp signaling, since activation of the Scw type I receptor Sax has no phenotype in the embryo that lacks Dpp signaling (Neul and Ferguson, 1998). Injection of *dpp* mRNA can actually rescue *scw* mutants (Nguyen et al., 1998). Much evidence also showed that the synergy between Dpp and Scw is

important, as it ensures the peak level of BMP signaling at the dorsal midline of the embryo (Arora et al., 1994; Shimmi et al., 2005; Wang and Ferguson, 2005). The transportation of the heterodimers of Dpp and Scw is favored over the homodimers of Dpp or Scw, through significantly higher affinity for Sog and Tsg compared with Dpp or Scw homodimer. Tld also processes heterodimers Dpp/Scw more efficiently than it does homodimers Dpp or Scw (Shimmi et al., 2005). Furthermore, the signaling activity of the Dpp/Scw heterodimer is much higher than either Dpp or Scw homodimers alone (Shimmi et al., 2005). Genetic and molecular analysis of receptor function revealed that Dpp functions through Tkv, while Scw functions through Sax. And the Dpp/Scw heterodimer requires the activity from both Tkv and Sax (Brummel et al., 1994; Nellen et al., 1994; Neul and Ferguson, 1998; Shimmi et al., 2005). However, the mechanisms by which the Sax signal synergizes with the Tkv pathway are not well known.

3.2.2. Roles of BMPs-like signaling in Drosophila Wing Imaginal Disc

During Drosophila development, Dpp acts as a key morphogen in many developmental stages and organs (Podos and Ferguson, 1999). Patterning and growth are tightly linked during development. However, the underlying mechanisms are not well known. The developing Drosophila wing has been a great model system for the study of Dpp cooperated functions of patterning and growth.

Drosophila imaginal discs are two-sided sacs that include the juxtaposed epithelial cells that give rise to the adult appendages. The wing imaginal discs originate as approximately 30-50 cells at the beginning of the first larval instar and go through rapid

and steady cell divisions with an average cell cycle about 8.5 hours through whole larval stages, finally totaling approximately 50,000 cells at the end of the third instar larval stage when cell proliferation stops. Adult wings are produced by eversion of wing imaginal discs. Since wing cells don't grow or divide, the size of wing is most dependent on the size of the wing imaginal disc (Day and Lawrence, 2000; Gonzalez-Gaitan et al., 1994). During development, the wing disc is patterned into four major compartments: the anterior (A) and posterior (P) compartments are separated by A/P boundary, while the dorsal (D) and ventral (V) compartments are separated by D/V boundary. Wing disc patterns are determined by morphogen gradients, with a Dpp determining pattern along the A/P boundary and Wingless (Wg) specifying pattern along the D/V boundary. At the early formation of the wing disc, the selector gene *engrailed* is already expressed in the posterior compartment, inducing secretion of *hedgehog* signaling protein. Hedgehog diffuses a short distance to the cells of the A compartment, and induces the expression of Dpp in a narrow stripe of cells along the A/P boundary, which then diffuses bidirectionally to direct the cell fates in both A and P compartments (Day and Lawrence, 2000).

The requirement of Dpp signaling for both wing disc cell growth and patterning is indisputable, because a lack of Dpp in the wing primordium reduces the wing to a stump, and ectopic expression of dpp causes additional growth that substantially redesigned the wing (Spencer et al., 1982; Zecca et al., 1995). Studies of the expression of Dpp target genes, *optomotor-blind (omb)* and *spalt (sal)*, have also demonstrated that Dpp acts directly at a distance as a gradient morphogen to exert its long-range influence on wing

patterning in a concentration-dependent manner. *omb* and *sal* are activated at different signaling thresholds and show a nested border expression region centered upon the *dpp* expression domain in the wing pouch (Nellen et al., 1996). Ectopic expression of secreted *dpp* in the clone induced the expression of *omb* and *sal* not only inside the clone, but also in the surrounding cells. On the other hand, ectopic expression of the constitutively active Dpp receptor Tkv only induces *omb* and *sal* expression inside the clone, but not in neighboring cells (Nellen et al., 1996). This indicates that Dpp is acting as a morphogen. By using the GFP-tagged Dpp, the Dpp gradient has been visualized to diffuse bidirectionally at a significant distance directly from its source (Entchev et al., 2000; Teleman and Cohen, 2000).

How does Dpp form a morphogen gradient in the wing disc? There are two major methods of gradient formation: extracellular diffusion and planar transcytosis between cells. The view of planar transcytosis in Dpp gradient formation is controversial. Observation of the GFP-tagged Dpp diffusion suggests that Dynamin-dependent endocytosis is required for spreading of Dpp. Dpp diffusion was impaired in the cells lacking Dynamin, a protein essential for endocytosis (Entchev et al., 2000; Kicheva et al., 2007). However, an experiment done by another group showed that the *dynammin* mutant did not block Dpp movement but rather inhibited Dpp signaling, suggesting that Dpp spreading is not dependent on endocytosis (Belenkaya et al., 2004).

Several studies have shown that the integral membrane proteoglycans, Dally and dally-like protein (DLP), play a role in Dpp morphogen distribution (Belenkaya et al., 2004;

Fujise et al., 2003; Jackson et al., 1997). Dpp fails to move across cells double mutant for *dally* and *dlp* in the wing disc (Belenkaya et al., 2004). The truncated form of Dpp, which lacks the domain responsible for interaction with Dally, shows the same signaling activity and protein stability as wild-type Dpp *in vitro*. However, this truncated form of Dpp has a shorter half-life *in vivo*, which indicates that the binding of Dally to Dpp stabilizes Dpp in the extracellular matrix (Akiyama et al., 2008). Dally also regulates cell response to Dpp in a cell-autonomous manner. Cells with increased levels of Dally showed increased sensitivity to Dpp (Fujise et al., 2003). However, the molecular basis by which Dally and DLP regulate Dpp signaling and distribution is not yet completely understood.

Another determinant of Dpp morphogen gradient is the Dpp receptor Tkv. In wild-type wing discs, Tkv is relatively low within the central domain of the wing disc, but high in cells at the lateral margins of the wing disc. The pattern of *tkv* expression is significant in shaping the Dpp gradient in the wing disc, since high levels of *tkv* makes the cell sensitive to Dpp signaling but also limits Dpp ligand diffusion (Lecuit and Cohen, 1998). Since Dpp signaling can negatively regulate *tkv* expression (Lecuit and Cohen, 1998), proper Dpp gradient formation can be shaped by Dpp dependent down regulation of *tkv*. *tkv* is also regulated by Hedgehog signaling, which shows strong suppression on *tkv* expression in A/P boundary cells (Tanimoto et al., 2000).

Target genes and the mechanisms underlying Dpp signaling in wing pattern are reasonably well understood, whereas the growth promoting effectors downstream of signaling are still largely mysterious. The longitudinal veins (LVs) of *Drosophila* wing

are positioned along the anteroposterior axis in response to specific levels of Dpp signaling. The fifth longitudinal (L5) wing vein in the posterior compartment depends on the border between *omb* and *brk* expression domains, while the position of the L2 wing vein in the anterior compartment is defined by the combination action of *brk* and *sal* (Cook et al., 2004; de Celis and Barrio, 2000).

Loss and gain of function studies have shown that Dpp acts as a growth promoting factor in the wing imaginal disc. Loss of *dpp* expression in the wing imaginal discs resulted in smaller wings (Spencer et al., 1982; Zecca et al., 1995), while ectopic dpp expression caused abnormally large discs (Martin-Castellanos and Edgar, 2002). In addition, cell clones mutant for *dpp*, *tkv*, or *Mad* failed to survive, whereas clones that displayed over expressed components of Dpp pathway overgrew (Adachi-Yamada et al., 1999; Burke and Basler, 1996; Martin-Castellanos and Edgar, 2002; Rogulja and Irvine, 2005). However, the mechanism of growth control by Dpp is still mostly unknown.

In the wild-type, cell divisions occur all over the wing imaginal disc in a pattern and rate that is uniform in the entire disc (Gonzalez-Gaitan et al., 1994; Milan et al., 1996; Rogulja and Irvine, 2005). Exactly how graded distribution and activity of Dpp leads to uniform growth has been a challenging question for researchers. Several models have tried to explore this conundrum (Schwank and Basler, 2010). In the threshold model, morphogen-driving cell proliferation appears to be constant in cells where Dpp signaling activity level is above a certain minimum. However, the overgrowth of cell in clones with elevated Dpp signaling does not support this model. The second model is the gradient

model in which cell proliferation in the wing discs is dependent on the slope of Dpp signaling activity (Day and Lawrence, 2000). However, this model is not supported by the evidence that overgrowth is caused by elevated homogeneous Dpp signaling (Martin-Castellanos and Edgar, 2002). Later, experimental results have led to a refined gradient model that incorporates the difference of cellular fate in the wing discs (Rogulja and Irvine, 2005). In that study, they showed evidence that cell proliferation can be transiently triggered by the Dpp signaling gradient. However, the uniform expression of Tkv^{QD} (a constitutively active Dpp receptor) inhibited the proliferation in the centre of the disc, while resulting in over proliferation in the lateral region of the disc. Hence, it was proposed that during early wing imaginal disc development, cells are programmed differently so that medial cells proliferate only in response to differences in Dpp signaling. Lateral cells proliferate not only in response to the Dpp gradient, but also to the absolute local Dpp level. However, this model cannot explain the growth at the source of Dpp production where cells are exposed to the saturating Dpp signaling. More recently, new experimental results done by Schwank et al. (2008) challenged this gradient model. It was found that wing discs overgrew when both Dpp and Brk were removed, indicating that neither Dpp nor Brk is a prerequisite for cell proliferation in the wing disc (Schwank et al., 2008). The third model is the inhibitor model, in which a growth inhibitor forms a gradient parallel to Dpp, and this inhibitor expression can be dependent or independent on Dpp signaling. Currently though, no such growth inhibitor has been experimentally validated to explain the growth by Dpp, which makes this model more speculative. The forth model is the mechanical feedback model, in which gradient of the growth factor creates certain mechanical forces in the disc, that then feedback on growth and leads to

uniform growth there (Aegerter-Wilmsen et al., 2007; Hufnagel et al., 2007; Shraiman, 2005).

3.2.3. Roles of Dpp in fly visual system

The *Drosophila* visual system is composed of a pair of compound eyes and optic ganglia, the visual processing centers of the brain. The compound eyes are composed of around 800 repeated units, called ommatidia. Each ommatidium contains eight photoreceptor neurons (R neurons) and a complement of non-neural support cells arranged in an invariant pattern. Photoreceptor cells are unipolar neurons that project directly into the different target regions in the optic lobes beginning in the third larval instar, and proceeding through about 12 hours of pupal development. Axons from photoreceptor R1-R6 neurons terminate in the lamina between two layers of lamina glial cells, the epithelial and marginal layers, and then form the lamina plexus. In contrast, R7 and R8 connect to a deeper target site known as the medulla (Cutforth and Gaul, 1997; Ting and Lee, 2007). The *Drosophila* optic lobe is derived from an embryonic optic placode that is located at the posterior head region of ectoderm. The precursor cells in the optic lobe placode start to proliferate soon after larval hatching and form two proliferation centers: the outer proliferation center (OPC) and the inner proliferation center (IOC). From these centers, cells are differentiated and four ganglia are formed (lamina, medulla, lobula and lobula plate). The OPC generates the lamina and outer medulla neurons. The IOC creates the neurons in the inner medulla, lobula, and lobula plate (Egger et al., 2007; Green et al., 1993; Hofbauer and Campos-Ortega, 1990; Nassif et al., 2003).

In the optic lobe, *dpp* is expressed in four regions in each brain hemisphere. Two lie in the glia precursor cell (GPC) region at the dorsal and ventral margin of the posterior neuroepithelium in the outer proliferation center. The other two smaller expression zones are more interior at the base of the inner proliferation center (Kaphingst and Kunes, 1994; Yoshida et al., 2005). Dpp is known to regulate neuroblast proliferation and differentiation in the optic lobe. A lack of Dpp reduced proliferation in the OPC as well as structural defects in the lamina and medulla (Kaphingst and Kunes, 1994). Later, Yoshida et al. (2005) found that Dpp signaling mediates the differentiation and migration of the lamina glia through regulating expression of *gcm* in the optic lobe (Yoshida et al., 2005). In mutant clones for *Medea*, a Dpp signal transducer, there were defects in R neuron projection patterns. Furthermore, *glial cells missing/glial cells deficient* (*gcm*), an early marker of differentiated glial cells, was found to be greatly reduced or even absent in *dpp* mutants or *Medea* clones. Whereas Dpp signaling can induce ectopic expression of *gcm* and production of mature glial cells, indicating that *gcm* expression depends on Dpp signaling in the optic lobe. The expression of a dominant-negative form of *gcm* resulted in similar abnormal R axon projections and lamina glia organization to those caused by Dpp defect (Yoshida et al., 2005).

3.3. Roles of activin-like pathway in *Drosophila*

The activin-like pathway in *Drosophila* has been studied less in comparison with the BMP/Dpp pathway. Mutants of the components of the activin pathway mainly displayed defects in neuronal modeling in mushroom bodies, morphogenesis of DC neurons (Zheng et al., 2003; Zheng et al., 2006), and motoneuron axon guidance in embryos (Parker et al.,

2006; Serpe and O'Connor, 2006). Activin pathway also shows some functions regarding proliferation, like the *babo* mutant with a small brain but also with properly patterned wings (Brummel et al., 1999; Zhu et al., 2008).

3.3.1. Roles of activin-like pathways in the mushroom bodies

In *Drosophila*, mushroom bodies (MB) are lobed neuropils that are involved in olfactory learning and memory (Pascual and Preat, 2001; Zars, 2000). MB neuron cell bodies are clustered postero-dorsally in the protocerebrum, and their dendrites form the calyx structure right below the cell body region. The axons form a forward projection, which extends ventrally toward the anterior surface of the brain, where it segregates into five terminal lobes. The α and α' lobes project toward the dorsal surface, while the β , β' and γ lobes project toward the midline of the brain. These five lobes can be grouped into three sets based on the expression levels of various MB-enriched antigens. One type of MB neuron projects its axons only into the γ lobe, referred to as γ neurons while another type projects its axon branches into both α' and β' lobes, referred as α'/β' neurons. The last type projects its axon branches into both α and β lobes, referred as α/β neurons (Crittenden et al., 1998). These MB neurons are generated sequentially so that γ neurons are born first, prior to the mid-3rd instar larval stage. α'/β' neurons are born between the mid-3rd instar larval stage and puparium formation while α/β neurons are born after puparium formation (Lee et al., 1999). During the larval stage, axons of all MB neurons bifurcate into both the dorsal and medial lobes. Shortly after puparium formation, larval MB neurons are selectively pruned according to birthdate. Degeneration of axon branches makes early-born (γ) neurons retain only their main processes in the peduncle, which then project into

the adult γ lobe without bifurcation. In contrast, the basic axon projections of the later-born (α'/β') larval neurons are preserved during metamorphosis (Lee et al., 1999).

The dActivin pathway regulates mushroom body remodeling during metamorphosis (Zheng et al., 2003). Zheng et al (2003) found a loss of function of either *babo* or dSmad2 mutants blocked the γ neuron remodeling in MBs. Loss of activin signaling in γ neuron keeps its larval axon projection pattern intact. It was also found that the ecdysone receptor B1 was reduced in those activin pathway mutants, and by restoring EcR-B1 expression, remodeling defects were significantly rescued. This indicates that *Drosophila* activin signaling modulates neuronal remodeling in part by regulating EcR-B1 expression (Zheng et al., 2003).

3.3.2. Roles of activin-like pathway in dorsal cluster (DC) neurons

Dorsal cluster (DC) neurons have their cell bodies located at the protocerebrum–optic lobe junctions and extensively innervate the optic lobes. DC neurons do not undergo extensive morphogenesis until pupal formation (Hassan et al., 2000). DC neuron dendrites densely elaborate within the lobular complex, and the axon projections traverse the entire central brain to innervate the contralateral lobular complex and further extend through the chiasm into the medulla (Zheng et al., 2006). However, the function of DC neurons is not clear.

The dActivin pathway is essential for proper morphogenesis of DC neurons (Zheng et al., 2006). Through generating DC Nb clones mutant in the activin pathway, Zheng et al.

(2006) found that mutant neurons are poorly innervated the contralateral optic lobe, and the axons often stall at the contralateral protocerebrum–optic lobe junction. Occasionally, they were repelled back to the central brain, and sometimes neurites wandered away and/or ectopically branched in the process of traversing the central brain. It was also found that the development of the mutant DC neurons was retarded (Zheng et al., 2006).

4. microRNAs

4.1. Overview of microRNAs

microRNAs (miRNAs) are a newly identified and abundant class of small non-coding RNAs. miRNAs are single stranded RNA (ssRNA) of about 22nt in length that are generated from endogenous hair-pin transcripts encoded from the miRNAs genes (Kim, 2005). miRNA genes can be located either in the intron of the protein coding genes or individually outside of the genes. There are increasing numbers of miRNA genes reported, at present, 940 in human, 171 in *Drosophila melanogaster*, and 175 in *Caenorhabditis elegans* (www.mirbase.org).

For miRNAs residing in the intron of a host gene, they are usually processed from introns and probably share the same promoter and other regulatory elements of the host gene. In some cases, miRNA genes are clustered in polycistronic transcripts and are likely to be coordinately regulated. Many, if not all, miRNAs are transcribed from flanking promoters and contain caps, a primary transcript (pri-miRNA). pri-miRNA is processed in the nucleus by a multiprotein complex called the Microprocessor, of which the core components are the RNase III enzyme Drosha and the double-stranded RNA-binding

domain (dsRBD) protein DGCR8/Pasha. Drosha cleaves pri-miRNA into about 60–80 nt long hairpin precursor miRNA (pre-miRNA), which is exported to the cytoplasm by Exportin-5 in a Ran-GTP-dependent manner. In the cytoplasm, another RNase III enzyme, Dicer, cleaves the hairpin, releasing a about 22 nt long miRNA:miRNA* duplex. The strands of this duplex separate and release a 21–25 nt mature miRNA. Plant miRNAs are further modified by methylation at the 3' end by HEN1, but no modification has been observed in *Drosophila* or *C. elegans*. Only one strand of the duplex, which is with relatively lower stability of base-pairing at its 5' end becomes a mature miRNA incorporated into RISC, whereas the miRNA* strand is typically degraded (Siomi and Siomi, 2010; Yang et al., 2005)

miRNAs function through base-pairing with the target mRNAs, usually in the 3' untranslated region (UTR). Based on the degree of complementary between miRNA-mRNA, there are two mainly kinds of mechanisms for miRNA action, translational repression or mRNA cleavage (Bagga et al., 2005; Yang et al., 2005). In plants, most mRNAs are perfectly complementary to mRNAs, which results in mRNA degradation. Whereas in animals, most miRNAs repress translation by imprecise complementary to the 3' UTR of their target mRNAs and also reduce mRNA levels (Bagga et al., 2005). Numerous studies have demonstrated that many miRNAs play important roles in various cellular processes, such as cell proliferation, apoptosis, differentiation, metabolism, development, diseases and tumors (Bushati and Cohen, 2007; Schmittgen, 2008; Yang et al., 2005). For example, *lin-4* and *let-7*, the first identified miRNAs, play important roles in controlling developmental timing in *C. elegans* (Ambros, 2003; Feinbaum and Ambros,

1999; Lee et al., 1993; Reinhart et al., 2000). *bantam* and *mir-14* were found involved in regulation of apoptosis, cell proliferation and fat metabolism in *Drosophila* (Brennecke et al., 2003; Xu et al., 2003). Some miRNAs are also found related to signaling pathways, like *mir-375*, which is a new regulator of insulin signaling through its inhibitory effect on Myotrophin (Mtpn) (Poy et al., 2004). *Bantam* was recently found to be one of the downstream targets of the Hippo pathway (Nolo et al., 2006; Thompson and Cohen, 2006). In humans, over one-third of genes are predicted to be directly targeted by miRNAs (Lewis et al., 2005).

4.2. Identification of miRNA Target genes

Importance of miRNA functions has long been recognized. However, only few miRNA targets are experimentally confirmed. With the knowledge of the binding rules derived from known miRNA-mRNA binding features, several computational algorithms have been developed for miRNA target prediction (Enright et al., 2003; Kiriakidou et al., 2004; Krek et al., 2005; Lewis et al., 2003; Mendes et al., 2009; Rehmsmeier et al., 2004; Rhoades et al., 2002; Robins et al., 2005; Yang et al., 2005; Zhang, 2005). Plant miRNA target prediction methods are relatively easy and showing great accuracy because plant miRNAs normally bind to their target mRNAs with near perfect complementarity (Rhoades et al., 2002; Zhang, 2005). On the other hand, animal miRNA targets are difficult to predict since low complementarity between animal miRNAs to their target mRNAs limits the maximum length of contiguous sequences of matching nucleotides. Various reported computational algorithms for animal miRNA target prediction includes miRanda (Enright et al., 2003), TargetScan (Lewis et al., 2003), RNAhybrid

(Rehmsmeier et al., 2004), DIANA-microT (Kiriakidou et al., 2004), and PicTar (Krek et al., 2005). Among those, miRanda, TargetScan and PicTar are three most widely used prediction algorithms. But with the limit of known miRNA-mRNA input examples, these algorithms are difficult to achieve both high specificity and high sensitivity. Moreover, the lack of high throughput and efficient experimental assays makes it hard for optimization of algorithms. There are several features of interaction between miRNAs and their target mRNAs that are commonly considered by these algorithms (Mendes et al., 2009; Yang et al., 2005), such as i) the complementarity between miRNAs and their target mRNAs, especially continuous Watson–Crick base pairing in 5' proximal half of the miRNA, ii) the conservation of miRNA target sites, iii) the thermodynamic hybridization energies of miRNA:mRNA duplexes, iv) the secondary structure of mRNA, and v) the expression profile of mRNAs. Based on these features, different algorithms choose different standards and restrictions to achieve optimization.

Compared to the high throughput bioinformatic prediction, the biological experimental methods for miRNA target identification are limited. One approach is to mis-express miRNAs and to assay mRNA down regulation by microarray (Lim et al., 2005). However, mRNAs regulated by miRNAs through translation repression would not be identified by this method. On the protein level, high throughput methods are not amendable. The most commonly used approach is the luciferase reporter gene, which contains 3'UTR of the potential miRNA target at the end of luciferase. In cases in which a miRNA acts on the 3' UTR, a decrease of the reporter is observed. But this reporter assay can only test one at a time. Furthermore, this approach does not represent the normal temporal and

physiological aspects of the interactions between miRNAs and their target mRNAs, and a rigorous analysis in animals will be required for validation (Yang et al., 2005).

4.3. Regulation of miRNA biogenesis by TGF β signaling pathway

In addition of the studies of miRNA functions, various experiments have been performed to reveal the regulation of miRNA expression. miRNA expression can be regulated both at the transcriptional level and post-transcriptional level. Many post-transcriptional regulators have been identified in regulating miRNA biogenesis, such as ADAR (adenosine deaminase acting on RNA) enzymes, the RNA helicases p68 or p72, and DGCR8 (DiGeorge syndrome critical region gene 8) (Siomi and Siomi, 2010). Recently, the study on the function of TGF β and BMP4 in differentiation of vascular smooth muscle cells (VSMCs) revealed that TGF β and BMP signaling can affect miRNA level at the post-transcriptional level by regulating miRNA processing (Davis et al., 2008). TGF β and BMP4 functions on VSMCs are due, at least in part, to their induction of *miR-21*, which targets programmed cell death protein-4 (PDCD4). The decrease in PDCD4 by *miR-21* will result in the increase of VSMC gene expression. By checking the level of pri-miR-21, pre-miR-21, and mature *miR-21* by TGF β or BMP induction in a time course, interestingly, Davis et. al. (2008) found that induction only of mature *miR-21* and pre-miR-21 after TGF β or BMP treatment, but no change in pri-miR-21. On the other hand, RNAi-mediated knockdown of R-Smad only abolished the induction of pre-miR-21 and mature *miR-21*, but did not affect pri-miR-21. These indicate that TGF β and BMP4 regulate *miR-21* processing. Further, they proved the interaction of R-Smad and RNA helicase p68, which is a critical component of Drosha microprocessor complex. By using

RNA-chromatin immunoprecipitation (ChIP), they found that Smad is present in a complex with Drosha and p68 on the pri-miR-21 after TGF β or BMP4 stimulation. They also found that recruitment of pri-miR-21 by R-Smads is induced by ligand stimulation, and recruitment of Smads to the p68–Drosha complex is pri-miRNA-specific, even though how this specificity achieved is not known. Moreover, a R-Smad mutant that is non-phosphorylatable on BMP stimulation has no change on its ability to bind pri-miR-21, indicating that TGF β or BMPs may affect the association between SMAD1 and pri-miRNAs primarily by controlling SMAD nuclear localization. Interestingly, the co-Smad, Smad4, was found not to be required for association of R-Smads with Drosha processing machinery (Davis et al., 2008). So, R-Smads associated Drosha microprocessor complex is thought different from R-Smads/Co-Smads heteromeric complex, which is preferentially associates with the cis-regulatory region of TGF β target genes. However, how cells distribute R-Smads into different functional complexes is not known.

4.4. miRNAs in Neurogenesis

In the past few year, many miRNAs have been shown to exhibit diverse roles in normal brain development and brain tumors. In zebrafish, blocking miRNA biogenesis in maternal-zygotic *dicer* (MZ*dicer*) mutant embryos caused notably morphological malformations of the nervous system, such as reduced size of the brain ventricles, missing the boundary of midbrain-hindbrain, and defects in eye and spinal cord development (Giraldez et al., 2005). These early defects in zebrafish morphogenesis can be largely rescued by *miR-430* (Giraldez et al., 2005). Gene knockout studies in mouse have also confirmed the critical roles of miRNAs in the proliferation and differentiation of

embryonic stem (ES) cells, which are the progenitor cells of neurons and glia (Kanellopoulou et al., 2005; Wang et al., 2008c). *Dicer-1* mutant mouse ES cells displayed severe defects in differentiation both *in vivo* and *in vitro* (Kanellopoulou et al., 2005). Disrupting the miRNA biogenesis in *Dgcr8* knockout ES cells caused slow proliferation and the accumulation of cells in the G1 phase of the cell cycle (Wang et al., 2008c). Studies on miRNA expression profile have revealed that some miRNAs have specific expression in undifferentiated ES cells and some undergo significant change during ES cell differentiation. For example, *miR-291a-3p*, *miR-291b-3p*, *miR-294* and *miR-295*, *miR-296* are highly expressed in undifferentiated mouse ES cells, but not detected in differentiated cells (Calabrese et al., 2007; Houbaviy et al., 2003). Expression of *miR-21*, and *miR-22* is increased dramatically upon ES cell differentiation (Houbaviy et al., 2003). Among those, *miR-291a-3p*, *miR-294* and *miR-295* are critical for maintaining ES cell proliferation by promoting G1 to S transition (Calabrese et al., 2007; Wang et al., 2008c). *miR-21* was reported to be increased in different types of tumours, such as breast carcinoma and gliomas (Davis et al., 2008; Frankel et al., 2008; Silber et al., 2009).

Many miRNAs have been identified that are specific for the brain or enriched in the brain. *miR-124* and *miR-9* are among the most studied brain-specific miRNAs. *miR-9* plays critical roles in early neural patterning, evidenced by its role in the establishment of the midbrain-hindbrain boundary in zebrafish (Leucht et al., 2008). *miR-9* also plays important roles in neural stem cell proliferation and differentiation. *miR-9* is expressed in both proliferative and differentiated cells of the brain (Kapsimali et al., 2007). Increased

expression of *miR-9* led to reduced mouse neural ES cell proliferation and promoted neural differentiation, whereas knockdown of *miR-9* increased the neural stem cell proliferation (Zhao et al., 2009). Zhao et. al. (2009) found that *miR-9* can target TLX, an essential regulator of neural stem cell self-renewal. TLX can inhibit *miR-9* expression thus forming a feedback loop to keep balance between proliferation and differentiation of neural stem cells (Zhao et al., 2009). Furthermore, over expression of *mir-124* and *mir-9* in ES-cell derived cultures can induce neuronal differentiation, and inhibit glial cell differentiation through down regulation of the signal transducer and activator of transcription 3 (STAT3) pathway (Krichevsky et al., 2006). The presence of *miR-124* seems to define the identity of neural cells, as its expression is associated with transition from proliferation to differentiation, with no expression in proliferative periventricular cells, but expression in most differentiated cells in the brain (Kapsimali et al., 2007). And in cell culture, *mir-124* is sharply increased upon the differentiation of ES cells into neurons (Conaco et al., 2006). So far, several targets of *mir-124* have been identified involved in neuronal differentiation. *miR-124* directly targets phosphatase *SCP1* (*small C-terminal domain phosphatase 1*) 3' untranslated region (UTR) to suppress SCP1 expression, which is a component of the REST transcription repressor complex with anti-neural function (Visvanathan et al., 2007). Second, *miR-124* directly targets PTBP1 (Polypyrimidine tract binding protein 1), which encodes a repressor of neuron-specific splicing. During neuronal differentiation, *miR-124* decreases PTBP1 levels, causing the accumulation of correctly spliced PTBP2 mRNA and a dramatic increase in PTBP2 protein (Makeyev et al., 2007). Moreover, *miR-124* is expressed by neuroblasts in the adult subventricular zone (SVZ) niche, regulating neuronal differentiation though

targeting Sox9, a SRY-box transcription factor (Cheng et al., 2009). SVZ is the largest germinal region in the adult mammalian brain and contains stem cells, that will give rise to neurons, astrocytes, and oligodendrocytes. Knockdown of endogenous *miR-124* during regeneration leads to delay of neuronal differentiation, while the ectopic expression of *miR-124* in SVZ cells promotes precocious neuronal differentiation (Cheng et al., 2009). Sox9 has opposite function of *miR-124*. Over expression of Sox9 in SVZ cells abolishes the production of neurons. In contrast, Sox9 knockdown caused increased neurogenesis and decreased glial formation (Cheng et al., 2009).

In addition to neuronal differentiation, there is increasing evidence for an involvement of miRNA regulatory networks in the development of certain glia cell types (e.g. oligodendrocytes). Oligodendrocytes are glial cells of the central nervous system (CNS) that synthesize multilamellar myelin membranes to ensheath axons. By studying the miRNA expression profile in two different populations of oligodendrocyte lineage cells, oligodendrocyte progenitor cells (OPCs) and premyelinating cells (OLs), Lau et al. not only identified miRNAs that are specific for oligodendrocytes but also miRNAs that were specific to differentiation (Lau et al., 2008). Abundantly expressed miRNAs in OPCs include many brain-enriched miRNAs such as *miR-9*, *miR-26a*, *miR-124a*, *miR-125b*, *miR-181b* and the *let-7* family. Over 20 miRNAs are down-regulated during differentiation including *miR-9* and *miR-124a* (Lau et al., 2008). A lot of studies have been performed to reveal the function of individual miRNA in glial cell proliferation and differentiation. *miR-219* plays important roles in promoting oligodendrocyte differentiation (Nave, 2010). *miR-125b* is strongly associated with glial

cell proliferation and also found increased in astrogliosis associated neurological disorders, such as Alzheimer's disease and in Down's syndrome (Pogue et al., 2010).

In addition, many miRNAs have changed expression levels in glial cell tumors. Gliomas are the most common malignant brain tumours (Silber et al., 2009). They are normally classified based on the morphological features into astrocytic, oligodendroglial, ependymal and choroid plexus tumours. Astrocytomas account for 80–85% of all gliomas, and among them the glioblastoma multiforme (GBM) is the most malignant one, which is virtually incurable. *miR-21*, *miR-221*, and *miR-10b* are up regulated in glioblastoma cell lines and tumor tissues. *miR-128*, *miR-181a*, *miR-181b*, *miR-181c*, *miR-124*, *miR-128a*, and *miR-137* are down regulated (Silber et al., 2009). miRNAs are also involved in the malignant progression of gliomas. Twelve miRNAs (*miR-9*, *miR-15a*, *miR-16*, *miR-17*, *miR-19a*, *miR-20a*, *miR-21*, *miR-25*, *miR-28*, *miR-130b*, *miR-140* and *miR-210*) showed increased expression, and two miRNAs (*miR-184* and *miR-328*) showed reduced expression upon progression of glioma from grade II (low-grade malignancies) to IV (the most devastating glioma) (Malzkorn et al., 2010).

Figure 1

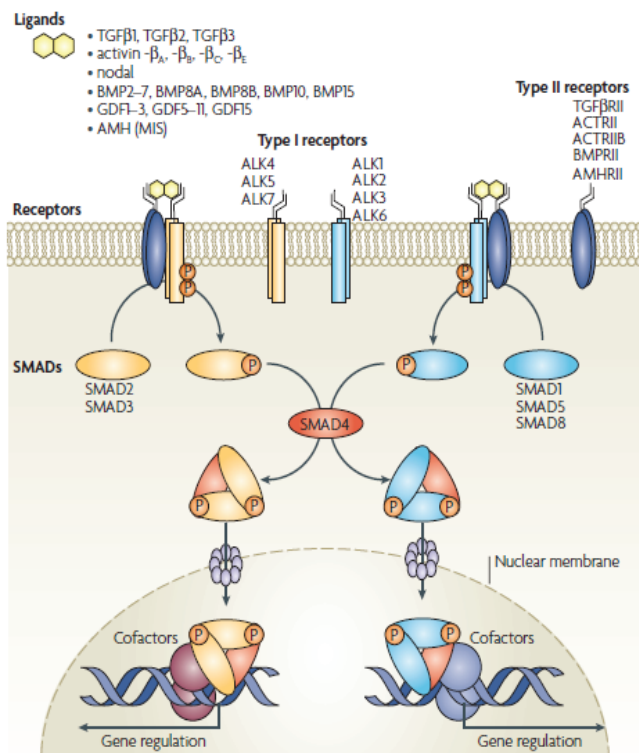


Figure 1. the mammalian TGF β signaling pathways.

At the cell surface, there are type I and type II transmembrane receptors, which contain intracellular protein kinase domain with serine/threonine specificity. When the dimeric TGF β superfamily ligands bind to a type II receptor, the type II receptor binds to a type I receptor, and phosphorylates the type I receptor. Once phosphorylated, the active type I receptor can then initiate the intracellular signaling cascade through Smads proteins. Normally, type I receptors, ALK4, ALK5 and ALK7 specifically phosphorylate Smad2 and Smad3 to propagate activin/TGF- β signaling, whereas ALK1, ALK2, ALK3 and ALK6 specifically phosphorylate Smad1, Smad5 and Smad8 to propagate BMP signaling. The activated R-Smads then associate with the Co-Smad, Smad4, which is shared by all the TGF β signal pathways. Next the R-Smads/Co-Smad complex translocates into nucleus, binds to DNA sequences, and either activates or represses target gene expression by binding to other transcriptional factors. This image was originally published in the paper (Schmierer and Hill, 2007).

Figure 2

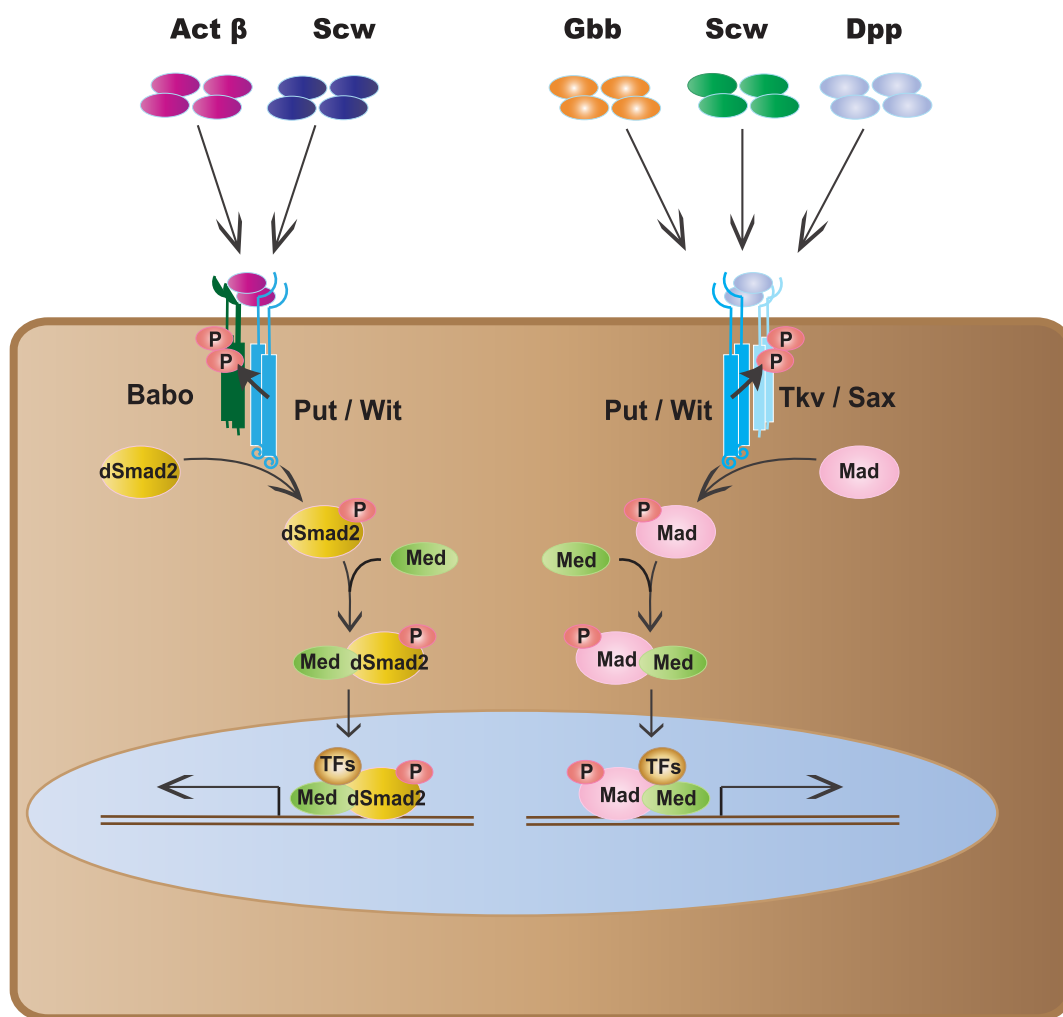


Figure 2. the TGF β signaling pathways in Drosophila.

Drosophila has both BMP-like and Activin-like signaling pathways. The cell surface type II receptors, Put and Wit, are shared by both pathways. In the BMP-like pathway, extracellular BMP-like ligands, Dpp, Gbb and Scw, act through cell surface type I receptors, Tkv or Sax, resulting the phosphorylation of Mad. Phosphorylated Mad (P-Mad) is then associated with co-Smad, Med. The P-Mad/Med complex is transported into the nucleus, and directs target gene expression. In the Activin-like pathway, extracellular ligands Act β and Daw act through a different type I receptor, Babo, resulting the phosphorylation of dSmad2, the activin-specific R-Smad. Phosphorylated dSmad2 (P-dSmad2) is then associated with co-Smad, Med. The P-Smad2/Med complex is transported into nucleus, and directs the target gene expression. TFs note transcription factors.

CHAPTER II

Incorporation Structure to Predict microRNA targets

This chapter was published in PNAS 2005 Mar 15;102(11):4006-4009.

The work in this chapter is done with the cooperation with Harlan Robins. My contribution to this chapter was in designing and performing the tissue culture experiments.

Abstract

MicroRNAs (miRNAs) are a recently discovered set of regulatory genes that constitute up to an estimated 1% of the total number of genes in animal genomes, including *Caenorhabditis elegans*, *Drosophila*, mouse, and humans [Lagos-Quintana, M., Rauhut, R., Lendeckel, W. & Tuschl, T. (2001) *Science* 294, 853–858; Lai, E. C., Tomancak, P., Williams, R. W. & Rubin, G.M. (2003) *Genome Biol.* 4, R42; Lau, N. C., Lim, L. P., Weinstein, E. G. & Bartel, D. P. (2001) *Science* 294, 858–862; Lee, R. C. & Ambros, V. (2001) *Science* 294, 862–8644; and Lee, R. C., Feinbaum, R. L. & Ambros, V. (1993) *Cell* 115, 787–798]. In animals, miRNAs regulate genes by attenuating protein translation through imperfect base pair binding to 3' UTR sequences of target genes. A major challenge in understanding the regulatory role of miRNAs is to accurately predict regulated targets. We have developed an algorithm for predicting targets that does not rely on evolutionary conservation. As one of the features of this algorithm, we incorporate the folded structure of mRNA. By using *Drosophila* miRNAs as a test case, we have validated our predictions in 10 of 15 genes tested. One of these validated genes is *Mad* as a target for *bantam*. Furthermore, our computational and experimental data suggest that miRNAs have fewer targets than previously reported.

Introduction

MicroRNAs are a class of small, ≈ 22 -nt RNAs that share properties with silencing RNAs (Doench et al., 2003). In plants, most microRNA (miRNA) genes bind sequences perfectly and lead to mRNA degradation (Bartel, 2004; Chen, 2004). However, in animals, with a notable exception (Yekta et al., 2004), they function by preventing translation without mRNA degradation (Ambros, 2001; Banerjee and Slack, 2002). The mechanism by which the bound miRNA down-regulates translation of its target mRNA remains unknown. Currently, only a handful of miRNAs have experimentally determined function *in vivo*. These miRNAs include *lin-4* and *let-7* in *Caenorhabditis elegans*, *bantam*, and *miR-14* in *Drosophila*, and *miR-23* in humans, playing vital roles in development and apoptosis (Abrahante et al., 2003; Brennecke et al., 2003; Lee and Ambros, 2001; Lin et al., 2003; Moss et al., 1997; Reinhart et al., 2000; Wightman et al., 1993; Xu et al., 2003). Even this modest set of data has some discernable common features that partially determine a set of rules governing the binding of miRNAs to their targets. It has been observed that toward the 5' end of the miRNA there is a perfect Watson–Crick base pair matching of at least seven consecutive nucleotides (Lewis et al., 2003). Recent experimental evidence has added more insights into the 3' UTR-binding rules (Doench et al., 2003; Doench and Sharp, 2004), but a complete understanding of miRNA–target interactions is not known. Because miRNA genes control many cellular processes, it is important to identify their targets with high accuracy.

Incorporating the experimentally determined features and deduced rules, we developed an algorithm for predicting miRNA targets in animals that significantly reduces

dependence on evolutionary homology without sacrificing accuracy. The algorithm consists of four parts; (i) the 5' seven nucleotides, (ii) scoring the match of the entire miRNA, (iii) incorporating 3' UTR structure of the target, and (iv) combining scores for multiple sites in the targets. Applying the algorithm to *Drosophila melanogaster*, we analyzed 73 miRNAs from the MiRNA registry (which can be accessed at www.sanger.ac.uk/Software/Rfam/mirna/index.shtml) and the 3' UTRs of 9,230 transcripts from Ensembl's Ensmart (which can be accessed at www.ensembl.org). A list of miRNAs and their predicted targets in the order ranked by our algorithm is in Table 2, which is published as supporting information on the PNAS web site.

Materials and Methods

To calculate the P value giving the probability that the correlation between free bases and real binding is random, we first folded the 3' UTR from *C. elegans lin-28*, *lin-41*, *lin-14*, *daf-12*, and *Drosophila Hid*. Then, we counted the possible binding positions in all of these genes that would give an overlap of three or more bases between the seven seed nucleotides and a region of free bases (in a loop or bubble). Dividing the total number of positions by the total number of nucleotides in the 3' UTRs gives a probability that one random seed would overlap a freebase region. This probability is 0.228. Because 12 of the 19 binding sites we are considering have seeds that overlap free bases, we compute the probability of getting 12 or more of 19, given a probability of 0.228 for each event. The result is the $P = 0.0002$.

To validate the predicted targets of *Drosophila* miRNAs, reporter assay *Drosophila* S2 cells were used to monitor changes in gene expression. First, we constructed a sensor for each target gene by replacing the 3' UTR of firefly (*Photinus pyralis*) luciferase (*Pp-luc*) with the 3' UTR of the target gene under the control of *Drosophila actin* promoter. *Pp-luc* alone in the same expression vector was used as negative control. To generate the miRNA expression constructs, miRNA genes and 100–200 bp of flanking DNA were amplified from *Drosophila* genomic DNA by PCR and cloned into vectors. Expression of the miRNA genes was induced by the *Drosophila actin* promoter. All of the miRNA gene constructs were confirmed by sequencing.

Transient transfections into S2 were used to determine the effect of the miRNA gene on the expression levels of the firefly *luciferase*. The ratio between the firefly and the *renilla reniformis luciferase (Rr-luc)* was used as an internal control for transfection efficiency. Three days after transfection, the activities of *Pp-luc* and *Rr-luc* were determined by the Dual-Glo luciferase assay (Promega). Each experiment was repeated three times, and the averages were used in comparisons.

Results and Discussion

Observing the experimentally determined miRNA target sites in *lin-14*, *daf-12*, and *lin-41* in *C. elegans* and *hid* in *Drosophila*, it was noticed that at the 5' end of the miRNA there is a perfect match of at least seven consecutive nucleotides (dubbed the seed). The necessity of this match in the functionality of a target site has been confirmed through direct experiment (Doench and Sharp, 2004). For each miRNA, we use the reverse complement of the sets of seven nucleotides in a row that end within the last three bases of the miRNA. This seed is used to establish a first cut of possible targets by searching the set of 3' UTRs from *Drosophila* for matches to these seeds.

Drawing again on both the observation of known target sites and recent direct experimental tests, we wrote a recursive program to score the entire binding site. The nonseed part of the miRNAs bind imperfectly to their targets but contribute to the overall stability. Given the small binding window of the miRNA, the known target sites form many more Watson–Crick base pairs than randomly expected. However, we cannot simply rank binding sites according to lowest binding energy for a couple reasons. First, the paper of Doench and Sharp (Doench and Sharp, 2004) provides evidence that G-U pairs do not contribute to the effectiveness of a binding site outside the seed and significantly reduce the binding if a G-U pair is found within the seed. Second, the known binding sites have not evolved to minimize binding energy. Therefore, we set up a scoring algorithm that weights A-U and G-C pairs positively, treats G-U pairs as neutral, and penalizes mismatches and gaps. Applying this scoring algorithm to the known target sites, we then choose a cutoff such that all these sites score robustly above the cutoff. We

define robust to mean that a single change in the binding site, outside of the seed, would not be able to move any of the known sites below the cutoff.

The above two criteria reduce the list of targets to a few hundred. Additional reductions in the target list can be made by examining the structure of the target 3' UTR. Folded mRNA consists of nucleotides that are base-paired and those that are free. We hypothesize that single-stranded miRNAs can only search stretches of free mRNA for potential target sites. According to Boltzmann's rules, the binding probability is proportional to the exponential of the difference in binding energies of the two states. If a stretch of RNA is unbound in one state and bound in the other, the probability of binding is relatively high. On the other hand, if the mRNA is folded so that the site of interest is base-paired with another part of the mRNA, then the energy difference between the two states is smaller, and the binding probability is smaller. Of course, there are proteins wrapping the miRNA that could potentially play a role in recognition. However, there is no evidence that the relevant proteins recognize either sequence or structure of the mRNA targets.

To test this hypothesis, we folded the 3' UTRs of the known targets in *C. elegans* and *Drosophila* and calculated the probability that the known target sites were correlated with the free nucleotides from the folded target. For the known targets of *C. elegans*, we used those listed in Banerjee and Slack (Banerjee and Slack, 2002) that meet the above two criteria, and, for *Drosophila*, we used the five *bantam* targets in *hid* listed in Brennecke *et al.* (Brennecke *et al.*, 2003). Specifically, we required that of the seven seed nucleotides

in the miRNA, at least three consecutive bases paired with free bases from the 3' UTR. We chose three bases for the following two reasons. First, the minimal length of an RNA hairpin loop is three nucleotides, which is a physical constraint from the limited flexibility of RNA. Second, recognition for base pairing of free strands require three consecutive complementary bases, and a string of two matches, then a mismatch, will not form a double strand. Because the folding algorithm is prone to error on a global scale for long sequences, we focus on the local stems produced from the folding. We restricted our set of free bases to those found in the loop at the end of a stem or the bubble located at the base of the stem. Given this restriction, we calculate the P value of 0.0002 as the probability that the correlation between known seeds and free bases is random (see *Materials and Methods*). This structural requirement for our target sites removes 80% of the false sites, whereas we lose only one-third of our real binding sites. These statistics are determined from the experimentally verified targets mentioned above. This is a substantial gain in accuracy because most real target mRNAs have multiple sites and we improve by a factor of three for each site; so, our algorithm folds the 3' UTRs of all of the *Drosophila* genes by using the vienna folding package and then throws out all potential targets that do not have an overlap with free bases as described above (Hofacker et al., 1994). We need only fold the 3' UTR because we are looking at local structure (not global), and the performance of the folding algorithm decreases dramatically as the sequence length increases. There are many other ways in which we can take structure into account such as considering alternative foldings. However, we would require more known targets to get solid statistics. We hope to improve the use of structure as more targets are discovered.

The final part of the algorithm ranks the remaining targets by computing a combined score for multiple sites within one 3' UTR. The known targets have multiple binding sites in their 3' UTR, and experimental evidence supports cooperative effects with multiple sites in each 3' UTR (Doench et al., 2003). Fitting to the experimentally generated curves from Doench *et al.* (Doench et al., 2003), we sum the scores and then take the result to the power of 1.2.

Having partially based our algorithm on observations of known targets, it is required that these targets score highly when our algorithm is applied. We met this consistency check successfully. In *C. elegans*, *lin-14* and *daf-12* were two of the top three ranking targets of miRNA *let-7*, whereas *lin-14* was also the top ranking target of miRNA *lin-4*. In *Drosophila*, *hid* ranked first as a target for the miRNA *bantam*.

We tested 19 potential targets predicted by our algorithm by use of a reporter gene in *Drosophila* S2 cells. The 3' UTR of the firefly *luciferase* gene was replaced with the 3' UTRs of the *Drosophila* targets and transfected into *Drosophila* cells (see *Materials and Methods*). Each experiment was repeated three times. Table 1 contains our algorithm's predictions regarding these 19 targets. Fifteen of the 19 targets were high-scoring targets that were chosen to represent the group of targets that scored in the top four for some miRNA. These 15 targets tested the validity of the algorithm. Ten of the 15 targets showed significant repression when the corresponding miRNA was expressed (Figure 1). For the five targets that failed, we tested the miRNA constructs to confirm that they were

functioning. We used the *bantam/hid* pair as a control because this result has been verified *in vivo*. Our result is that the algorithm predicts the top four targets for each miRNA with $\approx 67\%$ accuracy. Because the validation is in cell lines, the positive results provide evidence that the regulation has a functional role in live animals.

Three of the remaining four tested targets were chosen randomly from the group that ranked between 5 and 10 for their respective miRNAs and the final target ranked 30th for its miRNA. Experiments in cell culture showed no effect of the miRNA on the presumed targets. By using Fisher's exact test, we can say with 93% certainty that the median number of targets for each miRNA is 10 or fewer. Additionally, we can say with 97% confidence that the median number is <30 . These experiments address the question of how many targets a given miRNA is likely to have. Our results suggest that the number is smaller than previously thought.

Because our accuracy is sufficiently high, we were able to avoid requiring a cut on homology. Although homology can help improve accuracy, it comes at the expense of losing real targets. Because the *pseudoobscura* genome has not been completely annotated, we run into two major problems when trying to apply homology. The first problem is that the length of the 3' UTRs are not known, so we can only approximate the length. This problem is difficult because *Drosophila* 3' UTRs vary widely. Second, approximately one-fifth of the time the ESTs cut in the middle of a 3' UTR, prohibiting us from checking homology. Given these two limitations, we lose a substantial percentage of real targets.

As a representative example, one of the targets we validated is *Mad* regulated by *bantam*, which we would not have found had we required a homology cut. The miRNA *bantam* has been shown function in two processes (Brennecke et al., 2003). It prevents apoptosis by down-regulating the apoptotic gene *hid*. Also, mutants in *bantam* increase cell proliferation, but the target gene that interfaces with cell-cycle control is unknown. In our studies, we found that *Mad* is a target of *bantam*. Although *bantam* represses the *Mad* reporter to the same extent that it represses *hid* in our control, we wanted to confirm that the cause of repression was because of the *bantam*-binding sites in the *Mad* 3' UTR. We made point mutations in the fourth and fifth positions (as read from 3' to 5') of the two *bantam*-binding sites in the 3' UTR of *Mad*. Doench *et al.* (Doench et al., 2003) showed that mutating the fourth and fifth positions in a target site was sufficient to eliminate binding. Transfecting the points mutants into *Drosophila* S2 cells as described above, we find that mutating one site partially restores the level of luciferase in the presence of *bantam*, whereas mutating both binding sites completely restores the level (Figure 2). Because *Mad* is involved in propagating *decapentaplegic* signals, which promote proliferation in the fly, it is unlikely that the *bantam/Mad* interactions are involved in the cell-cycle regulation observed for *bantam*. Possibly more than one of the seven TGF β -like ligands signal through *Mad*, raising the possibility that the *bantam/Mad* interaction affects a different TGF β -like pathway. Alternatively, the *bantam/Mad* interaction may function through *decapentaplegic*, but in a different developmental process. Further *in vivo* experiments are warranted to examine this interaction.

To date, three algorithms are published for finding miRNA targets from a whole genome: two in *Drosophila* and one in vertebrates (Enright et al., 2003; Lewis et al., 2003; Stark et al., 2003). Two other algorithms have been applied to specific genes or miRNAs (Kiriakidou et al., 2004; Rajewsky and Socci, 2004). Only Lewis *et al.* (Lewis et al., 2003) estimated and tested a false-positive rate for targets. Lewis *et al.* (Lewis et al., 2003) tested their algorithm in humans and established a success rate of approximately two-thirds, aiming for an accurate, as opposed to comprehensive, list of targets. Their success hinged strongly on homology, limiting their targets to those where homologous genes in both mouse and rat were also predicted as strong targets of homologous miRNAs. Using either mouse or rat, but not both, dramatically drops the success rate of their algorithm. For the two *Drosophila* algorithms, we are able to directly compare results. To do the comparison, we focused on the experimentally validated genes and their corresponding miRNAs. The Enright *et al.* (Enright et al., 2003) algorithm has almost no overlapping results with our predictions. In particular, their algorithm scored only one of the 10 targets we validated experimentally in their list of the top 10 for their partner miRNAs. Because they did not experimentally validate any of their results, we are unable to run the comparison in the other direction.

The Stark *et al.* (Stark et al., 2003) algorithm provides a large list of targets of for each miRNA without determining accuracy. They chose six targets to validate partially based on their algorithm and partially based on biological intuition. Of their six validated targets, our algorithm ranks three of them in the top 10 for their partner miRNAs and two others in the top 20. One of their targets allows us to demonstrate the gain that we

achieve from our structure cut. Stark *et al.* (Stark et al., 2003) validated *reaper* as a target for *miR-2a*. Our algorithm ranks *reaper* as the number one target for *miR-2a*. If we run our algorithm without including the structure cut, *reaper* drops to 25th. Next, we compared their predictions with our validated results. From their list of the top 100 targets for each miRNA, 2 of our 10 targets scored well (in the top three), 2 scored in the 20s, and the 5 others did not make their top 60 (the final target was *Mad*, and they did not publish their *bantam* targets).

We have presented an algorithm that provides a substantial increase in accuracy for predicting miRNA targets. As more experimental data becomes available to elucidate the binding rules of miRNAs to their targets, we expect to improve our algorithm.

ACKNOWLEDGMENTS

H.R. thanks Hagar Barak and Arnold Levine for many useful discussions and helpful comments regarding the project. R.W.P. thanks Jizong Gao and Huang Wang for excellent technical assistance. We also thank Andrei Ruckenstein for useful discussions in the initial phases of this project. This work was supported by a grant from the National Institutes of Health and an Academic Excellence Grant from Rutgers University (to R.W.P.), a Busch Predoctoral Fellowship (to Y.L.), and in part by the Shelby White and Leon Levy Initiatives Fund and the David and Lucile Packard Foundation (to H.R).

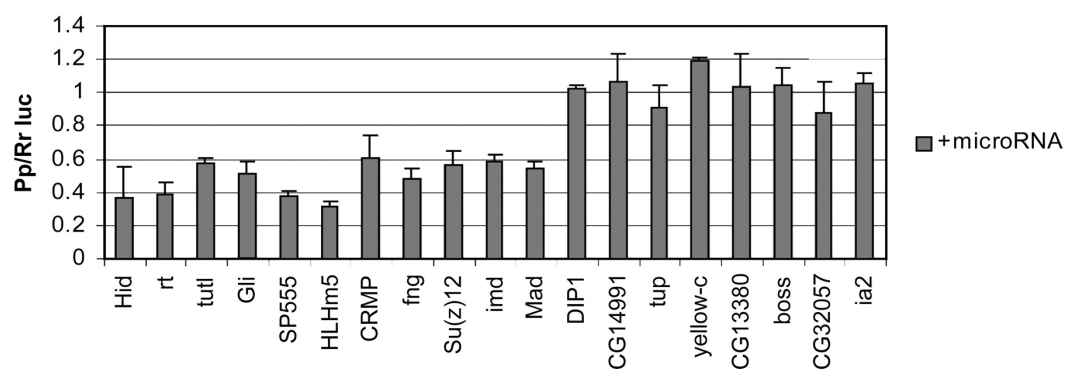
Figure 1

Figure 1. A graph of *luciferase* reporter intensity from miRNA target genes.

The 3' UTR targets are from the genes listed on the *x* axis. The particular miRNA that pairs with each gene is found in Table 1. As a control, we use *hid* as the target of *bantam*. The luciferase activity before expressing the miRNAs were normalized to 1 for all cells, so the values in the bar graph are the fraction of luciferase intensity with the miRNA expressed. Each experiment was repeated three times, given the error bars. The 11 targets on the left are regulated by a miRNA, and the 10 on the right are not.

Figure 2

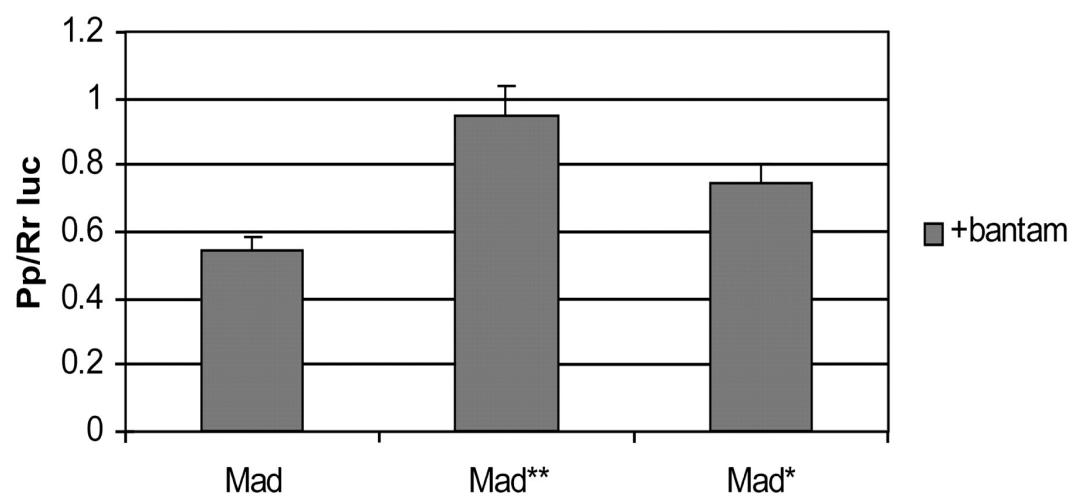


Fig. 2.

Both of the two *bantam*-binding sites on the 3' UTR of *Mad* are shown to contribute to repression. Positions 4 and 5 counting from the 5' end of the binding site are mutated in one (*) and two (**) *bantam*-binding sites, knocking out the sites. Knocking out one binding site partially restores the activity of *Mad* (*), whereas knocking out two binding sites completely restores activity (**).

Tables

Table 1. Tested miRNA targets

Target gene	miRNA	Rank	Repressed
<i>Mad</i>	<i>bantam</i>	4	Yes
<i>Hid</i>	<i>bantam</i>	1	Yes
<i>CRMP</i>	<i>miR-287</i>	2	Yes
<i>HLHm5</i>	<i>miR-7</i>	1	Yes
<i>SP555</i>	<i>miR-279</i>	1	Yes
<i>Imd</i>	<i>miR-310</i>	3	Yes
<i>Tutl</i>	<i>miR-1</i>	1	Yes
<i>Su(z) 12</i>	<i>miR-34</i>	3	Yes
<i>Rt</i>	<i>miR-12</i>	1	Yes
<i>Gli</i>	<i>miR-124</i>	1	Yes
<i>Fng</i>	<i>miR-7</i>	3	Yes
<i>DIP1</i>	<i>miR-287</i>	1	No
<i>CG14991</i>	<i>miR-303</i>	1	No
<i>tup</i>	<i>miR-278</i>	2	No
<i>Yellow-c</i>	<i>miR-317</i>	3	No
<i>CG13380</i>	<i>miR-318</i>	2	No
<i>Boss</i>	<i>miR-286</i>	5	No
<i>CG32057</i>	<i>miR-288</i>	8	No
<i>Kel</i>	<i>miR-276b</i>	6	No
<i>la2</i>	<i>miR-316</i>	30	No

Table 2. Top 10 targets for each miRNA.

The top 10 scoring targets for each miRNA are listed in order of score. The normalized score is provided for each target.

Rank	miRNA	Score	SHORT NAME	FULL TARGET NAME
1	<i>bantam</i>	0.79	<i>W</i>	<i>Wrinkled</i>
2	<i>bantam</i>	0.66	<i>CG33067</i>	
3	<i>bantam</i>	0.51	<i>CG13333</i>	
4	<i>bantam</i>	0.45	<i>Mad</i>	<i>Mothers against dpp</i>
5	<i>bantam</i>	0.37	<i>kel</i>	<i>kelch</i>
6	<i>bantam</i>	0.35	<i>CG8964</i>	
7	<i>bantam</i>	0.35	<i>HDAC6</i>	
8	<i>bantam</i>	0.33	<i>CG30097</i>	
9	<i>bantam</i>	0.33	<i>Gad1</i>	<i>Glutamic acid decarboxylase 1</i>
10	<i>bantam</i>	0.32	<i>TpnC73F</i>	<i>Troponin C at 73F</i>
1	<i>let-7</i>	0.43	<i>CG6070</i>	
2	<i>let-7</i>	0.4	<i>CG10625</i>	
3	<i>let-7</i>	0.39	<i>CG18135</i>	
4	<i>let-7</i>	0.37	<i>Eip63F-2</i>	<i>Ecdysone-induced protein 63F 2</i>
5	<i>let-7</i>	0.35	<i>RpS26</i>	<i>Ribosomal protein S26</i>
6	<i>let-7</i>	0.34	<i>CG10186</i>	
7	<i>let-7</i>	0.34	<i>twis</i>	<i>twins</i>
8	<i>let-7</i>	0.33	<i>Rh50</i>	
9	<i>let-7</i>	0.33	<i>CG11120</i>	
10	<i>let-7</i>	0.31	<i>CG12163</i>	
1	<i>miR-1</i>	0.59	<i>tutl</i>	<i>turtle</i>
2	<i>miR-1</i>	0.46	<i>crb</i>	<i>crumbs</i>
3	<i>miR-1</i>	0.45	<i>spas</i>	<i>spastin</i>
4	<i>miR-1</i>	0.44	<i>CG8500</i>	
5	<i>miR-1</i>	0.43	<i>CG2127</i>	
6	<i>miR-1</i>	0.39	<i>CG31182</i>	
7	<i>miR-1</i>	0.37	<i>CG12789</i>	
8	<i>miR-1</i>	0.37	<i>CG6417</i>	
9	<i>miR-1</i>	0.36	<i>CG31176</i>	
10	<i>miR-1</i>	0.3	<i>CG17224</i>	
1	<i>miR-10</i>	0.35	<i>Bem46</i>	
2	<i>miR-10</i>	0.31		
3	<i>miR-10</i>	0.3	<i>Dro</i>	<i>Drosocin</i>
4	<i>miR-10</i>	0.3	<i>CG7125</i>	
5	<i>miR-10</i>	0.28	<i>CG32514</i>	
6	<i>miR-10</i>	0.26	<i>GRHR11</i>	
7	<i>miR-10</i>	0.25	<i>CG10132</i>	
8	<i>miR-10</i>	0.25	<i>botv</i>	<i>brother of tout-velu</i>
9	<i>miR-10</i>	0.23	<i>Trl</i>	<i>Trithorax-like</i>
10	<i>miR-10</i>	0.22	<i>CG8360</i>	
1	<i>miR-100</i>	0.32	<i>CG32921</i>	
2	<i>miR-100</i>	0.26	<i>tacc</i>	<i>transforming acidic coiled-coil protein</i>

3	<i>miR-100</i>	0.23	<i>CG10830</i>	
4	<i>miR-100</i>	0.2	<i>DopR2</i>	<i>Dopamine receptor 2</i>
5	<i>miR-100</i>	0.18	<i>sra</i>	<i>sarah</i>
6	<i>miR-100</i>	0.17	<i>SoxN</i>	<i>SoxNeuro</i>
7	<i>miR-100</i>	0.16	<i>CG11638</i>	
8	<i>miR-100</i>	0.15	<i>CG17985</i>	
9	<i>miR-100</i>	0.15	<i>CdsA</i>	<i>CDP diglyceride synthetase</i>
10	<i>miR-100</i>	0.15	<i>CG17786</i>	
1	<i>miR-11</i>	0.33	<i>CG8249</i>	
2	<i>miR-11</i>	0.33	<i>spas</i>	<i>spastin</i>
3	<i>miR-11</i>	0.32	<i>CG13594</i>	
4	<i>miR-11</i>	0.32	<i>CG7081</i>	
5	<i>miR-11</i>	0.32	<i>Rh7</i>	<i>Rhodopsin 7</i>
6	<i>miR-11</i>	0.31	<i>CG12163</i>	
7	<i>miR-11</i>	0.29	<i>CG15316</i>	
8	<i>miR-11</i>	0.28	<i>Cyp6a2</i>	<i>Cytochrome P450-6a2</i>
9	<i>miR-11</i>	0.28	<i>MtnD</i>	<i>Metallothionein D</i>
10	<i>miR-11</i>	0.28	<i>CG32791</i>	
1	<i>miR-12</i>	0.57	<i>rt</i>	<i>rotated abdomen</i>
2	<i>miR-12</i>	0.43	<i>Rep2</i>	
3	<i>miR-12</i>	0.41	<i>CG15592</i>	
4	<i>miR-12</i>	0.4	<i>CG15422</i>	
5	<i>miR-12</i>	0.39	<i>Unc-76</i>	
6	<i>miR-12</i>	0.39	<i>CG8944</i>	
7	<i>miR-12</i>	0.38	<i>Prm</i>	<i>Paramyosin</i>
8	<i>miR-12</i>	0.36	<i>CG33205</i>	
9	<i>miR-12</i>	0.34	<i>CG9919</i>	
10	<i>miR-12</i>	0.33	<i>PpN58A</i>	<i>Protein phosphatase N at 58A</i>
1	<i>miR-124</i>	0.57	<i>Gli</i>	<i>Glialactin</i>
2	<i>miR-124</i>	0.56	<i>CG14617</i>	
3	<i>miR-124</i>	0.42	<i>sl</i>	<i>small wing</i>
4	<i>miR-124</i>	0.42	<i>sktl</i>	<i>skittles</i>
5	<i>miR-124</i>	0.34	<i>CG32853</i>	
6	<i>miR-124</i>	0.32	<i>CG32920</i>	
7	<i>miR-124</i>	0.3	<i>CG12789</i>	
8	<i>miR-124</i>	0.3	<i>PR2</i>	<i>Fak-like tyrosine kinase</i>
9	<i>miR-124</i>	0.3	<i>Ama</i>	<i>Amalgam</i>
10	<i>miR-124</i>	0.29	<i>ap</i>	<i>apterous</i>
1	<i>miR-125</i>	0.29	<i>CG32030</i>	
2	<i>miR-125</i>	0.26	<i>CG15884</i>	
3	<i>miR-125</i>	0.23	<i>CG4615</i>	
4	<i>miR-125</i>	0.22	<i>CG14781</i>	
5	<i>miR-125</i>	0.19	<i>CG11779</i>	
6	<i>miR-125</i>	0.19	<i>CG3719</i>	
7	<i>miR-125</i>	0.18	<i>CG33111</i>	
8	<i>miR-125</i>	0.18	<i>CG2222</i>	
9	<i>miR-125</i>	0.16	<i>msh-2</i>	<i>male-specific lethal 2</i>
10	<i>miR-125</i>	0.15	<i>Nplp1</i>	<i>Neuropeptide-like precursor 1</i>
1	<i>miR-133</i>	0.37	<i>CG11655</i>	
2	<i>miR-133</i>	0.26	<i>slo</i>	<i>slowpoke</i>

3	<i>miR-133</i>	0.26	<i>CG15743</i>	
4	<i>miR-133</i>	0.25	<i>fas</i>	<i>faint sausage</i>
5	<i>miR-133</i>	0.24	<i>CG12565</i>	
6	<i>miR-133</i>	0.23	<i>Ada2S</i>	<i>Transcriptional adapter 2S</i>
7	<i>miR-133</i>	0.23	<i>CG31006</i>	
8	<i>miR-133</i>	0.22	<i>Rep2</i>	
9	<i>miR-133</i>	0.2	<i>Kaz1</i>	
10	<i>miR-133</i>	0.2	<i>CG9576</i>	
1	<i>miR-13a</i>	0.37	<i>spas</i>	<i>spastin</i>
2	<i>miR-13a</i>	0.36	<i>CG8451</i>	
3	<i>miR-13a</i>	0.36	<i>CG11533</i>	
4	<i>miR-13a</i>	0.35	<i>CG7995</i>	
5	<i>miR-13a</i>	0.35	<i>CG10300</i>	
6	<i>miR-13a</i>	0.34	<i>DnaJ-H</i>	<i>DnaJ homolog</i>
7	<i>miR-13a</i>	0.32	<i>CG4851</i>	
8	<i>miR-13a</i>	0.31	<i>rpr</i>	<i>reaper</i>
9	<i>miR-13a</i>	0.3	<i>CG7955</i>	
10	<i>miR-13a</i>	0.3	<i>CG6752</i>	
1	<i>miR-13b</i>	0.37	<i>CG4851</i>	
2	<i>miR-13b</i>	0.36	<i>CG8451</i>	
3	<i>miR-13b</i>	0.34	<i>CG11533</i>	
4	<i>miR-13b</i>	0.32	<i>CG7955</i>	
5	<i>miR-13b</i>	0.32	<i>HLHm&dgr;</i>	<i>E(spl) region transcript m&dgr;</i>
6	<i>miR-13b</i>	0.31	<i>CG8249</i>	
7	<i>miR-13b</i>	0.31	<i>CG3893</i>	
8	<i>miR-13b</i>	0.3	<i>Hey</i>	<i>Hairy/E(spl)-related with YRPW motif</i>
9	<i>miR-13b</i>	0.3	<i>robo</i>	<i>roundabout</i>
10	<i>miR-13b</i>	0.29	<i>msl-2</i>	<i>male-specific lethal 2</i>
1	<i>miR-14</i>	0.4	<i>CG12942</i>	
2	<i>miR-14</i>	0.35	<i>CG14017</i>	
3	<i>miR-14</i>	0.3	<i>CG6805</i>	
4	<i>miR-14</i>	0.29	<i>CG9570</i>	
5	<i>miR-14</i>	0.28	<i>CG17141</i>	
6	<i>miR-14</i>	0.27	<i>Hr78</i>	<i>Hormone-receptor-like in 78</i>
7	<i>miR-14</i>	0.26	<i>CG32955</i>	
8	<i>miR-14</i>	0.26	<i>CG33161</i>	
9	<i>miR-14</i>	0.25	<i>Gp93</i>	<i>Glycoprotein 93</i>
10	<i>miR-14</i>	0.24	<i>CG13363</i>	
1	<i>miR-184</i>	0.34	<i>CG11050</i>	
2	<i>miR-184</i>	0.31	<i>CG32119</i>	
3	<i>miR-184</i>	0.3	<i>kek2</i>	<i>kekkon-2</i>
4	<i>miR-184</i>	0.3	<i>Nrx</i>	<i>Neurexin</i>
5	<i>miR-184</i>	0.29	<i>CG14505</i>	
6	<i>miR-184</i>	0.29	<i>CG8121</i>	
7	<i>miR-184</i>	0.28	<i>CG31170</i>	
8	<i>miR-184</i>	0.27	<i>CG7663</i>	
9	<i>miR-184</i>	0.27	<i>CG5623</i>	
10	<i>miR-184</i>	0.25	<i>CG8191</i>	
1	<i>miR-210</i>	0.51	<i>LIMK1</i>	<i>LIM-kinase1</i>
2	<i>miR-210</i>	0.39	<i>AcCoAS</i>	<i>Acetyl Coenzyme A synthase</i>

3	miR-210	0.38	CG5554	
4	miR-210	0.37	CG1902	
5	miR-210	0.36	CG8596	
6	miR-210	0.33	ppa	partner of paired
7	miR-210	0.31	CG17667	
8	miR-210	0.31	l(3)10615	
9	miR-210	0.3	CG8179	
10	miR-210	0.3	CG30101	
1	miR-219	0.6	CG32111	
2	miR-219	0.45	Trl	Trithorax-like
3	miR-219	0.38	CG10987	
4	miR-219	0.37	PpD5	Protein phosphatase D5
5	miR-219	0.37	CG11596	
6	miR-219	0.36	CG10809	
7	miR-219	0.35	CG32683	
8	miR-219	0.34		
9	miR-219	0.33	CG31660	
10	miR-219	0.27	CG32922	
1	miR-263a	0.42	CG3638	
2	miR-263a	0.37	CG3975	
3	miR-263a	0.34	PGRP-LF	Peptidoglycan recognition protein LF
4	miR-263a	0.31	CG17802	
5	miR-263a	0.31	tok	tolkin
6	miR-263a	0.3	CG18131	
7	miR-263a	0.29	Cks	Cyclin-dependent kinase subunit
8	miR-263a	0.29	Sin3A	
9	miR-263a	0.29	CG5494	
10	miR-263a	0.28	Pk17E	Protein kinase-like 17E
1	miR-263b	0.35	W	Wrinkled
2	miR-263b	0.35	crm	cramped
3	miR-263b	0.33	BicC	Bicaudal C
4	miR-263b	0.33	CG33156	
5	miR-263b	0.31	GluCl&agr;	
6	miR-263b	0.3	PpD3	Protein phosphatase D3
7	miR-263b	0.3	CG11334	
8	miR-263b	0.29	fz2	frizzled 2
9	miR-263b	0.29	CG7609	
10	miR-263b	0.27	CG3638	
1	miR-274	0.56	CG12581	
2	miR-274	0.43	milt	milt
3	miR-274	0.41	RhoGAP19D	
4	miR-274	0.39	CG32177	
5	miR-274	0.37	E2f	E2F transcription factor
6	miR-274	0.36	HDAC4	
7	miR-274	0.29	CG11486	
8	miR-274	0.29	unc-13-4A	
9	miR-274	0.28	ple	pale
10	miR-274	0.26	RhoGEF2	
1	miR-275	0.45	CG30080	
2	miR-275	0.37	CG13216	

3	miR-275	0.37	<i>hkb</i>	<i>huckebein</i>
4	miR-275	0.3	<i>hig</i>	<i>hikaru genki</i>
5	miR-275	0.3	<i>CG7816</i>	
6	miR-275	0.28	<i>CG7370</i>	
7	miR-275	0.28	<i>CG14883</i>	
8	miR-275	0.28	<i>PyK</i>	<i>Pyruvate kinase</i>
9	miR-275	0.26	<i>CG9517</i>	
10	miR-275	0.25	<i>CG15739</i>	
1	miR-276a	0.48	<i>CG8475</i>	
2	miR-276a	0.38	<i>CG13645</i>	
3	miR-276a	0.37	<i>CG16833</i>	
4	miR-276a	0.35	<i>CG9216</i>	
5	miR-276a	0.34	<i>kel</i>	<i>kelch</i>
6	miR-276a	0.31	<i>bs</i>	<i>blistered</i>
7	miR-276a	0.31	<i>Efl&ggr;</i>	
8	miR-276a	0.3	<i>Iris</i>	<i>Iris</i>
9	miR-276a	0.28	<i>CG4839</i>	
10	miR-276a	0.28	<i>CG14490</i>	
1	miR-276b	0.57	<i>CG8475</i>	
2	miR-276b	0.48	<i>CG9216</i>	
3	miR-276b	0.37	<i>CG13645</i>	
4	miR-276b	0.33	<i>CG16833</i>	
5	miR-276b	0.33	<i>Efl&ggr;</i>	
6	miR-276b	0.33	<i>kel</i>	<i>kelch</i>
7	miR-276b	0.33	<i>Mipp2</i>	<i>Multiple inositol polyphosphate phosphatase 2</i>
8	miR-276b	0.31	<i>CG14490</i>	
9	miR-276b	0.3	<i>tam</i>	<i>tamas</i>
10	miR-276b	0.26	<i>CG31211</i>	
1	miR-277	0.61	<i>CG6070</i>	
2	miR-277	0.53	<i>jumu</i>	<i>jumeau</i>
3	miR-277	0.51	<i>Fatp</i>	<i>Fatty acid (long chain) transport protein</i>
4	miR-277	0.51	<i>Bmcp</i>	
5	miR-277	0.46	<i>ebi</i>	<i>ebi</i>
6	miR-277	0.46	<i>toc</i>	<i>toucan</i>
7	miR-277	0.42	<i>CG6406</i>	
8	miR-277	0.42	<i>Sk2</i>	<i>Sphingosine kinase 2</i>
9	miR-277	0.42	<i>CG3618</i>	
10	miR-277	0.41	<i>CG32343</i>	
1	miR-278	0.38	<i>CG3638</i>	
2	miR-278	0.39	<i>tup</i>	<i>tailup</i>
3	miR-278	0.34	<i>CG15678</i>	
4	miR-278	0.33	<i>CG3308</i>	
5	miR-278	0.31	<i>CG3036</i>	
6	miR-278	0.31	<i>CG31722</i>	
7	miR-278	0.31	<i>CG33154</i>	
8	miR-278	0.31	<i>CG31358</i>	
9	miR-278	0.3	<i>CG32912</i>	
10	miR-278	0.28	<i>Gas8</i>	<i>Growth arrest specific protein 8</i>
1	miR-279	0.39	<i>SP555</i>	
2	miR-279	0.33	<i>CG7655</i>	

3	miR-279	0.3	CG2947	
4	miR-279	0.29	CG17732	
5	miR-279	0.28	DopR2	Dopamine receptor 2
6	miR-279	0.27	La	La autoantigen-like
7	miR-279	0.26	CG9083	
8	miR-279	0.25	CG8044	
9	miR-279	0.25	CG31211	
10	miR-279	0.24	msl-3	male-specific lethal 3
1	miR-280	0.93	ed	echinoid
2	miR-280	0.9	Ptp99A	Protein tyrosine phosphatase 99A
3	miR-280	0.9	CG12163	
4	miR-280	0.82	CG12295	
5	miR-280	0.8	cag	
6	miR-280	0.78	CG18177	
7	miR-280	0.77	CG6329	
8	miR-280	0.73	CG30437	
9	miR-280	0.65	bun	bunched
10	miR-280	0.65	CG9413	
1	miR-281	0.4	osp	outspread
2	miR-281	0.4	RhoGEF2	
3	miR-281	0.35	CG8745	
4	miR-281	0.3	Nep4	Neprilysin 4
5	miR-281	0.3	fs(1)h	female sterile (1) homoeotic
6	miR-281	0.29	CG5869	
7	miR-281	0.29	CG7990	
8	miR-281	0.28	CG7979	
9	miR-281	0.28	CG32772	
10	miR-281	0.27	CG30497	
1	miR-282	0.53	CG10823	
2	miR-282	0.45	CG8851	
3	miR-282	0.41	vav	
4	miR-282	0.41	wapl	wings apart-like
5	miR-282	0.4	CG8866	
6	miR-282	0.4	GluCl&agr;	
7	miR-282	0.39	Mob1	
8	miR-282	0.38	CG11880	
9	miR-282	0.38	Yippee	
10	miR-282	0.37	Dad	Daughters against dpp
1	miR-283	0.78	TpnC73F	Troponin C at 73F
2	miR-283	0.78	VACHT	
3	miR-283	0.56	heix	heixuedian
4	miR-283	0.58	CG7372	
5	miR-283	0.56	ase	asense
6	miR-283	0.55	Talin	
7	miR-283	0.49	Rgl	Ral guanine nucleotide exchange factor 2
8	miR-283	0.49	ss	spineless
9	miR-283	0.48	R	Roughened
10	miR-283	0.48	Ac76E	Adenylyl cyclase 76E
1	miR-284	0.52		
2	miR-284	0.5	CG12362	

3	miR-284	0.46	oho23B	overgrown hematopoietic organs at 23B
4	miR-284	0.44	CG7712	
5	miR-284	0.42	NetB	Netrin-B
6	miR-284	0.39	CG16807	
7	miR-284	0.38	cher	cheerio
8	miR-284	0.38	mod(mdg4)	modifier of mdg4
9	miR-284	0.37	Prosap	
10	miR-284	0.36	CG1338	
1	miR-285	0.36	CG32956	
2	miR-285	0.3	CG10512	
3	miR-285	0.3	CG5071	
4	miR-285	0.28	CG32954	
5	miR-285	0.28	Tim17a2	
6	miR-285	0.27	CG8046	
7	miR-285	0.26	TMS1	
8	miR-285	0.26	CG17712	
9	miR-285	0.25	CG2765	
10	miR-285	0.25	CG32530	
1	miR-286	0.36	CG4911	
2	miR-286	0.33	SP555	
3	miR-286	0.33	CG31498	
4	miR-286	0.32	CG8677	
5	miR-286	0.32	boss	bride of sevenless
6	miR-286	0.31	Dcr-2	Dicer-2
7	miR-286	0.31	CG11268	
8	miR-286	0.3	CG30015	
9	miR-286	0.29	CG14021	
10	miR-286	0.27	CG12806	
1	miR-287	0.63	DIP1	DISCO Interacting Protein 1
2	miR-287	0.6	CRMP	Collapsin Response Mediator Protein
3	miR-287	0.5	Lis-1	Lissencephaly-1
4	miR-287	0.44	CG8268	
5	miR-287	0.41	CG32245	
6	miR-287	0.37	CstF-64	Cleavage stimulation factor 64 kilodalton subunit
7	miR-287	0.36	CG6946	
8	miR-287	0.36	sd	scalloped
9	miR-287	0.34	CG11093	
10	miR-287	0.28	mbf1	multiprotein bridging factor 1
1	miR-288	0.53	CG2608	
2	miR-288	0.52	sbb	scribbler
3	miR-288	0.45	Syx7	Syntaxin 7
4	miR-288	0.45	Scamp	
5	miR-288	0.41	CG9588	
6	miR-288	0.4	CG7297	
7	miR-288	0.39	blp	black pearl
8	miR-288	0.38	CG32057	
9	miR-288	0.37	CG6639	
10	miR-288	0.37	CG18746	
1	miR-289	0.99	stich1	sticky chl
2	miR-289	0.99	CG7372	

3	miR-289	0.93	CG15594	
4	miR-289	0.88	CG32111	
5	miR-289	0.76	NetB	Netrin-B
6	miR-289	0.74	G&agr;49B	G protein &agr;49B
7	miR-289	0.73	Ser	Serrate
8	miR-289	0.68	CG7228	
9	miR-289	0.67	stau	staußen
10	miR-289	0.67	Shc	SHC-adaptor protein
1	miR-2a	0.39	rpr	reaper
2	miR-2a	0.37	CG8451	
3	miR-2a	0.35	Ih	
4	miR-2a	0.35	spas	spastin
5	miR-2a	0.34	CG7995	
6	miR-2a	0.33	CG11533	
7	miR-2a	0.32	Eip63F-2	Ecdysone-induced protein 63F 2
8	miR-2a	0.32	CG15177	
9	miR-2a	0.32	CG6752	
10	miR-2a	0.32	Pvf2	PDGF- and VEGF-related factor 2
1	miR-2b	0.38	CG8451	
2	miR-2b	0.38	CG12163	
3	miR-2b	0.38	Pvf2	PDGF- and VEGF-related factor 2
4	miR-2b	0.34	CG7429	
5	miR-2b	0.34		
6	miR-2b	0.32	rpr	reaper
7	miR-2b	0.31	CG16886	
8	miR-2b	0.31	CG3376	
9	miR-2b	0.3	Hey	Hairy/E(spl)-related with YRPW motif
10	miR-2b	0.3	CG7995	
1	miR-2c	0.37	rpr	reaper
2	miR-2c	0.35	CG8451	
3	miR-2c	0.34	CG7995	
4	miR-2c	0.34	CG12163	
5	miR-2c	0.33	Ih	
6	miR-2c	0.33	CG17145	
7	miR-2c	0.33	spas	spastin
8	miR-2c	0.31	Doc3	Dorsocross3
9	miR-2c	0.3		
10	miR-2c	0.3	Eip63F-2	Ecdysone-induced protein 63F 2
1	miR-3	0.47	esn	espinas
2	miR-3	0.45	D19A	
3	miR-3	0.36	wg	wingless
4	miR-3	0.34	BicC	Bicaudal C
5	miR-3	0.34	mab-2	
6	miR-3	0.31	DAT	Dopamine transporter
7	miR-3	0.31	Pbprp3	Pheromone-binding protein-related protein 3
8	miR-3	0.31	CG31188	
9	miR-3	0.27	CG13380	
10	miR-3	0.27	CG17462	
1	miR-30	0.34	BicC	Bicaudal C
2	miR-30	0.33	CG10353	

3	<i>miR-30</i>	0.31	<i>kek2</i>	<i>kekkon-2</i>
4	<i>miR-30</i>	0.28	<i>CG3814</i>	
5	<i>miR-30</i>	0.28	<i>CG15817</i>	
6	<i>miR-30</i>	0.27	<i>Cyp28a5</i>	
7	<i>miR-30</i>	0.27	<i>qkr54B</i>	<i>quaking related 54B</i>
8	<i>miR-30</i>	0.27	<i>CG32057</i>	
9	<i>miR-30</i>	0.26	<i>CG33005</i>	
10	<i>miR-30</i>	0.26	<i>RpI12</i>	
1	<i>miR-303</i>	0.62	<i>CG14991</i>	
2	<i>miR-303</i>	0.57	<i>CG30044</i>	
3	<i>miR-303</i>	0.5	<i>spen</i>	<i>split ends</i>
4	<i>miR-303</i>	0.35	<i>CG4005</i>	
5	<i>miR-303</i>	0.35	<i>CG1287</i>	
6	<i>miR-303</i>	0.35	<i>CG10192</i>	
7	<i>miR-303</i>	0.34	<i>CG15878</i>	
8	<i>miR-303</i>	0.34	<i>CG30497</i>	
9	<i>miR-303</i>	0.31	<i>M(2)21AB</i>	<i>Minute (2) 21AB</i>
10	<i>miR-303</i>	0.31	<i>kel</i>	<i>kelch</i>
1	<i>miR-304</i>	0.47	<i>CG13884</i>	
2	<i>miR-304</i>	0.42	<i>CG15910</i>	
3	<i>miR-304</i>	0.41	<i>CG4629</i>	
4	<i>miR-304</i>	0.41		
5	<i>miR-304</i>	0.4	<i>wt5</i>	<i>warts</i>
6	<i>miR-304</i>	0.39	<i>Drl-2</i>	<i>Derailed 2</i>
7	<i>miR-304</i>	0.39	<i>CG32809</i>	
8	<i>miR-304</i>	0.37	<i>slo</i>	<i>slowpoke</i>
9	<i>miR-304</i>	0.36	<i>Con</i>	<i>Connectin</i>
10	<i>miR-304</i>	0.35	<i>CG16974</i>	
1	<i>miR-305</i>	0.73	<i>CG30086</i>	
2	<i>miR-305</i>	0.6	<i>cic</i>	<i>capicua</i>
3	<i>miR-305</i>	0.45	<i>sif</i>	<i>still life</i>
4	<i>miR-305</i>	0.39	<i>lbm</i>	<i>late bloomer</i>
5	<i>miR-305</i>	0.37	<i>CG18506</i>	
6	<i>miR-305</i>	0.37	<i>RhoGAP19D</i>	
7	<i>miR-305</i>	0.36	<i>CG17361</i>	
8	<i>miR-305</i>	0.34	<i>Gclc</i>	<i>Glutamate-cysteine ligase catalytic subunit</i>
9	<i>miR-305</i>	0.31	<i>CG12071</i>	
10	<i>miR-305</i>	0.3	<i>CG11371</i>	
1	<i>miR-306</i>	0.41	<i>hig</i>	<i>hikaru genki</i>
2	<i>miR-306</i>	0.39	<i>CG13216</i>	
3	<i>miR-306</i>	0.35	<i>CG3493</i>	
4	<i>miR-306</i>	0.32	<i>CG8630</i>	
5	<i>miR-306</i>	0.29	<i>CG31814</i>	
6	<i>miR-306</i>	0.29	<i>CG33154</i>	
7	<i>miR-306</i>	0.27	<i>CG7609</i>	
8	<i>miR-306</i>	0.26	<i>CG6700</i>	
9	<i>miR-306</i>	0.26	<i>PyK</i>	<i>Pyruvate kinase</i>
10	<i>miR-306</i>	0.25	<i>CG30080</i>	
1	<i>miR-307</i>	0.37	<i>pxb</i>	
2	<i>miR-307</i>	0.35	<i>CG8300</i>	

3	miR-307	0.32	CG15093	
4	miR-307	0.29	CG33174	
5	miR-307	0.29	CG17271	
6	miR-307	0.27	CG2017	
7	miR-307	0.27	CG4940	
8	miR-307	0.26	CG3868	
9	miR-307	0.25	mRpl48	mitochondrial ribosomal protein L48
10	miR-307	0.25	CG9576	
1	miR-308	0.4	CG1667	
2	miR-308	0.38	CG31190	
3	miR-308	0.36	CG12950	
4	miR-308	0.35	CG8858	
5	miR-308	0.34	CG8177	
6	miR-308	0.33	CG9248	
7	miR-308	0.32	sano	serrano
8	miR-308	0.31	nompC	no mechanoreceptor potential C
9	miR-308	0.31	CG8134	
10	miR-308	0.3	CG8451	
1	miR-310	0.37	CG13338	
2	miR-310	0.37	CG6424	
3	miR-310	0.37	imd	immune deficiency
4	miR-310	0.3	FucTA	
5	miR-310	0.3	CG31191	
6	miR-310	0.3	CG17180	
7	miR-310	0.29	CG6652	
8	miR-310	0.29	elav	embryonic lethal, abnormal vision Cyclic-AMP response element binding protein A
9	miR-310	0.28	CrebA	
10	miR-310	0.27	CG14408	
1	miR-311	0.39	CG31728	
2	miR-311	0.38	Kap- α 3	karyopherin α 3
3	miR-311	0.36	CG14073	
4	miR-311	0.34	CG31191	
5	miR-311	0.34	CG3837	
6	miR-311	0.33	CG13189	
7	miR-311	0.32	CG15549	
8	miR-311	0.3	α -Man-IIb	
9	miR-311	0.3	sv	shaven
10	miR-311	0.23	CG13338	
1	miR-312	0.45	α -Man-IIb	
2	miR-312	0.36	rgr	regular
3	miR-312	0.35	Pu	Punch
4	miR-312	0.35	ST6Gal	Sialyltransferase
5	miR-312	0.35	CG31191	
6	miR-312	0.31	D19A	
7	miR-312	0.27	Hr39	Hormone receptor-like in 39
8	miR-312	0.27	CG13338	
9	miR-312	0.26	salm	spalt major
10	miR-312	0.24	CG14073	
1	miR-313	0.45	salm	spalt major
2	miR-313	0.42	CG15549	

3	miR-313	0.39	CG3837	
4	miR-313	0.36	Kap- $\&$ agr;3	karyopherin $\&$ agr;3
5	miR-313	0.34	CG5660	
6	miR-313	0.33	CG14073	
7	miR-313	0.32	CG31871	
8	miR-313	0.32	CG5830	
9	miR-313	0.32	CG7433	
10	miR-313	0.32	CG2254	
1	miR-314	0.49	CG9335	
2	miR-314	0.47	CG14869	
3	miR-314	0.33	CG6014	
				Sensitized chromosome inheritance
4	miR-314	0.31	Mcm10	modifier 19
5	miR-314	0.31	CG30116	
6	miR-314	0.31	cpo	couch potato
7	miR-314	0.3	salm	spalt major
8	miR-314	0.3	CG30032	
9	miR-314	0.29	CG5359	
10	miR-314	0.28	pim	pimples
1	miR-315	0.53	exu	exuperantia
2	miR-315	0.52	Pde6	Phosphodiesterase 6
3	miR-315	0.51	Axn	Axin
4	miR-315	0.47	Nrv2	Nervana 2
5	miR-315	0.47	unc-13-4A	
6	miR-315	0.45	CG7342	
7	miR-315	0.44	CG17816	
8	miR-315	0.44	cpo	couch potato
9	miR-315	0.42	Gyc76C	Guanyl cyclase at 76C
10	miR-315	0.41	Tim17a1	
1	miR-316	0.64	CG32204	
2	miR-316	0.62	CG10948	
3	miR-316	0.5	G $\&$ agr;49B	G protein $\&$ agr;49B
4	miR-316	0.44	Appl	$\&$ bgr; amyloid protein precursor-like
5	miR-316	0.42	CG18265	
6	miR-316	0.39	CG6180	
7	miR-316	0.39	vvl	ventral veins lacking
8	miR-316	0.38		
9	miR-316	0.33	CG32316	
10	miR-316	0.31	CG10011	
1	miR-317	0.41	CG11763	
2	miR-317	0.39	yellow-c	yellow-c
3	miR-317	0.36	CG5792	
4	miR-317	0.36	CG10512	
5	miR-317	0.35	eas	easily shocked
6	miR-317	0.34	Keap1	
7	miR-317	0.34	RhoGAP100F	
			nAcR $\&$ bgr;-	
8	miR-317	0.33	21C	nicotinic acetylcholine receptor beta 21C
9	miR-317	0.33	CG1599	
10	miR-317	0.33	Trn	Transportin
1	miR-318	0.42	Glut3	Glucose transporter type 3

2	<i>miR-318</i>	0.41	<i>esn</i>	<i>espinas</i>
3	<i>miR-318</i>	0.41	<i>CG13380</i>	
4	<i>miR-318</i>	0.39	<i>Optix</i>	<i>Optix</i>
5	<i>miR-318</i>	0.37	<i>CG4213</i>	
6	<i>miR-318</i>	0.35	<i>CG8108</i>	
7	<i>miR-318</i>	0.34	<i>Toll-6</i>	<i>Toll-6</i>
8	<i>miR-318</i>	0.34	<i>Rp112</i>	
9	<i>miR-318</i>	0.33	<i>CG2991</i>	
10	<i>miR-318</i>	0.33	<i>Fas3</i>	<i>Fasciclin 3</i>
1	<i>miR-31a</i>	0.34	<i>PpN58A</i>	<i>Protein phosphatase N at 58A</i>
2	<i>miR-31a</i>	0.34	<i>CG32594</i>	
3	<i>miR-31a</i>	0.32	<i>CG2103</i>	
4	<i>miR-31a</i>	0.3	<i>Act79B</i>	<i>Actin 79B</i>
5	<i>miR-31a</i>	0.29	<i>CG4751</i>	
6	<i>miR-31a</i>	0.28		
7	<i>miR-31a</i>	0.28	<i>Cyp6a14</i>	
8	<i>miR-31a</i>	0.28	<i>sqd</i>	<i>squid</i>
9	<i>miR-31a</i>	0.28	<i>su(Hw)</i>	<i>suppressor of Hairy wing</i>
10	<i>miR-31a</i>	0.27	<i>CG31771</i>	
1	<i>miR-31b</i>	0.33	<i>CG11247</i>	
2	<i>miR-31b</i>	0.33	<i>PpN58A</i>	<i>Protein phosphatase N at 58A</i>
3	<i>miR-31b</i>	0.32	<i>Act79B</i>	<i>Actin 79B</i>
4	<i>miR-31b</i>	0.32	<i>Ice</i>	<i>Ice</i>
5	<i>miR-31b</i>	0.29	<i>CG4751</i>	
6	<i>miR-31b</i>	0.29	<i>Best2</i>	<i>Bestrophin 2</i>
7	<i>miR-31b</i>	0.29	<i>CG15316</i>	
8	<i>miR-31b</i>	0.28	<i>CG5532</i>	
9	<i>miR-31b</i>	0.28	<i>su(Hw)</i>	<i>suppressor of Hairy wing</i>
10	<i>miR-31b</i>	0.28	<i>CG17841</i>	
1	<i>miR-33</i>	0.47	<i>CG11066</i>	
2	<i>miR-33</i>	0.44	<i>CG6114</i>	
3	<i>miR-33</i>	0.34	<i>mus81</i>	
4	<i>miR-33</i>	0.36	<i>en</i>	<i>engrailed</i>
5	<i>miR-33</i>	0.37	<i>CG32835</i>	
6	<i>miR-33</i>	0.34	<i>CG12016</i>	
7	<i>miR-33</i>	0.34	<i>Ost48</i>	<i>Oligosaccharyltransferase 48kD subunit</i>
8	<i>miR-33</i>	0.34	<i>GalNAc-T2</i>	<i>UDP-N-acetyl-&agr</i>
9	<i>miR-33</i>	0.32	<i>Dscam</i>	<i>Down syndrome cell adhesion molecule</i>
10	<i>miR-33</i>	0.32	<i>CG5854</i>	
1	<i>miR-34</i>	0.45	<i>Rbp4</i>	<i>RNA-binding protein 4</i>
2	<i>miR-34</i>	0.44	<i>Su(z)12</i>	
3	<i>miR-34</i>	0.41	<i>CG11030</i>	
4	<i>miR-34</i>	0.41		
5	<i>miR-34</i>	0.4	<i>CG8389</i>	
6	<i>miR-34</i>	0.39	<i>CG14290</i>	
7	<i>miR-34</i>	0.39	<i>CG32737</i>	
8	<i>miR-34</i>	0.37	<i>Sh</i>	<i>Shaker</i>
9	<i>miR-34</i>	0.36	<i>Hsc70-4</i>	<i>Heat shock protein cognate 4</i>
10	<i>miR-34</i>	0.32	<i>Eip74EF</i>	<i>Ecdysone-induced protein 74EF</i>
1	<i>miR-4</i>	0.42	<i>RhoGAP100F</i>	

2	miR-4	0.41	<i>Rim</i>	
3	miR-4	0.38	<i>CG2254</i>	
4	miR-4	0.37	<i>Thiolase</i>	<i>Thiolase</i>
5	miR-4	0.36	<i>oaf</i>	<i>out at first</i>
6	miR-4	0.34	<i>CG6634</i>	
7	miR-4	0.34	<i>msl-1</i>	<i>male-specific lethal 1</i>
8	miR-4	0.34	<i>CG8426</i>	
9	miR-4	0.34	<i>Pde8</i>	<i>Phosphodiesterase 8</i>
10	miR-4	0.34	<i>CG3308</i>	
1	miR-5	0.54	<i>CG9384</i>	
2	miR-5	0.42	<i>nerfin-1</i>	<i>nervous fingers 1</i>
3	miR-5	0.39	<i>CG8789</i>	
4	miR-5	0.35	<i>CG2217</i>	
5	miR-5	0.34	<i>CG8008</i>	
6	miR-5	0.33	<i>CG10192</i>	
7	miR-5	0.32	<i>CG6707</i>	
8	miR-5	0.31	<i>CG13213</i>	
9	miR-5	0.31	<i>Sap47</i>	<i>Synapse-associated protein 47kD</i>
10	miR-5	0.3	<i>CG14985</i>	
1	miR-7	0.63	<i>HLHm5</i>	<i>E(spl) region transcript m5</i>
2	miR-7	0.51	<i>CG6700</i>	
3	miR-7	0.5	<i>fng</i>	<i>fringe</i>
4	miR-7	0.39	<i>CG2247</i>	
5	miR-7	0.38	<i>CG7737</i>	
6	miR-7	0.37	<i>CG31660</i>	
7	miR-7	0.37	<i>Faa</i>	<i>Fumarylacetoacetase</i>
8	miR-7	0.36	<i>CG2316</i>	
9	miR-7	0.35	<i>CG10344</i>	
10	miR-7	0.35	<i>CG4413</i>	
			<i>nAcR&bgr;-</i>	
1	miR-79	0.4	<i>96A</i>	<i>nicotinic Acetylcholine Receptor beta 96A</i>
2	miR-79	0.4	<i>msl-1</i>	<i>male-specific lethal 1</i>
3	miR-79	0.39	<i>CG12207</i>	
4	miR-79	0.38	<i>CdGAPr</i>	
5	miR-79	0.38	<i>CG2702</i>	
6	miR-79	0.36	<i>CG11228</i>	
7	miR-79	0.34	<i>HLHm5</i>	<i>E(spl) region transcript m5</i>
8	miR-79	0.34	<i>wb</i>	<i>wing blister</i>
9	miR-79	0.34	<i>CG3308</i>	
10	miR-79	0.33	<i>CG33157</i>	
1	miR-8	0.43	<i>CG6522</i>	
2	miR-8	0.41	<i>CG12772</i>	
3	miR-8	0.4	<i>CG12734</i>	
4	miR-8	0.39	<i>smi35A</i>	<i>smell impaired 35A</i>
5	miR-8	0.38	<i>Fsh</i>	<i>Fsh-Tsh-like receptor</i>
6	miR-8	0.37	<i>CG15745</i>	
7	miR-8	0.34	<i>CG32365</i>	
8	miR-8	0.33	<i>CG3860</i>	
9	miR-8	0.33	<i>CG5735</i>	
10	miR-8	0.32	<i>LvpH</i>	<i>Larval visceral protein H</i>
1	miR-87	0.52	<i>trio</i>	

2	<i>miR-87</i>	0.44	<i>Cad87A</i>	
3	<i>miR-87</i>	0.42	<i>CG32062</i>	
4	<i>miR-87</i>	0.4	<i>Hnf4</i>	<i>Hepatocyte nuclear factor 4</i>
5	<i>miR-87</i>	0.38	<i>CG8108</i>	
6	<i>miR-87</i>	0.38	<i>CG14224</i>	
7	<i>miR-87</i>	0.37	<i>CG3975</i>	
8	<i>miR-87</i>	0.37	<i>CG6282</i>	
9	<i>miR-87</i>	0.36	<i>CG5208</i>	
10	<i>miR-87</i>	0.34	<i>CG31607</i>	
1	<i>miR-9</i>	0.56	<i>CG32062</i>	
2	<i>miR-9</i>	0.49	<i>CG10508</i>	
3	<i>miR-9</i>	0.46	<i>CG1815</i>	
4	<i>miR-9</i>	0.45	<i>botv</i>	<i>brother of tout-velu</i>
5	<i>miR-9</i>	0.44	<i>CG9849</i>	
6	<i>miR-9</i>	0.43	<i>CG11533</i>	
7	<i>miR-9</i>	0.41	<i>CG11533</i>	
8	<i>miR-9</i>	0.39	<i>CG10041</i>	
9	<i>miR-9</i>	0.38	<i>CG15220</i>	
10	<i>miR-9</i>	0.36	<i>Ank2</i>	
1	<i>miR-92a</i>	0.42	<i>CG13338</i>	
2	<i>miR-92a</i>	0.36	<i>Mob1</i>	
3	<i>miR-92a</i>	0.35	<i>FucTA</i>	
4	<i>miR-92a</i>	0.33	<i>imd</i>	<i>immune deficiency</i>
5	<i>miR-92a</i>	0.3	<i>hig</i>	<i>hikaru genki</i>
6	<i>miR-92a</i>	0.3	<i>&agr;-Man-II</i>	<i>&agr; Mannosidase II</i>
7	<i>miR-92a</i>	0.3	<i>CG12071</i>	
8	<i>miR-92a</i>	0.29	<i>CG15203</i>	
9	<i>miR-92a</i>	0.28	<i>CG7609</i>	
10	<i>miR-92a</i>	0.24	<i>RhoGEF2</i>	
1	<i>miR-9a</i>	0.73	<i>Syn</i>	<i>Synapsin</i>
2	<i>miR-9a</i>	0.6	<i>CG10041</i>	
3	<i>miR-9a</i>	0.52	<i>CG9849</i>	
4	<i>miR-9a</i>	0.51	<i>sif</i>	<i>still life</i>
5	<i>miR-9a</i>	0.5	<i>CG14821</i>	
6	<i>miR-9a</i>	0.49	<i>Ank2</i>	
7	<i>miR-9a</i>	0.48	<i>CG7378</i>	
8	<i>miR-9a</i>	0.46	<i>lox2</i>	<i>lysyl oxidase-like 2</i>
9	<i>miR-9a</i>	0.46	<i>CG32850</i>	
10	<i>miR-9a</i>	0.45	<i>pfk</i>	<i>piefke</i>
1	<i>mir-iab-4-5</i>	0.44	<i>CG32919</i>	
2	<i>mir-iab-4-5</i>	0.43	<i>jeb</i>	<i>jelly belly</i>
3	<i>mir-iab-4-5</i>	0.35	<i>pros</i>	<i>prospero</i>
4	<i>mir-iab-4-5</i>	0.35	<i>dally</i>	<i>division abnormally delayed</i>
5	<i>mir-iab-4-5</i>	0.33	<i>Taf5</i>	<i>TBP-associated factor 5</i>
6	<i>mir-iab-4-5</i>	0.32		
7	<i>mir-iab-4-5</i>	0.32	<i>hep</i>	<i>hemipterous</i>
8	<i>mir-iab-4-5</i>	0.32	<i>Or33a</i>	<i>Odorant receptor 33a</i>
9	<i>mir-iab-4-5</i>	0.3	<i>Hsf</i>	<i>Heat shock factor</i>
10	<i>mir-iab-4-5</i>	0.3	<i>enok</i>	<i>enoki mushroom</i>
1	<i>miR-iab-4-3</i>	0.47	<i>tim</i>	<i>timeless</i>

2	<i>miR-iab-4-3</i>	0.36	<i>Dak1</i>	
3	<i>miR-iab-4-3</i>	0.35		
4	<i>miR-iab-4-3</i>	0.35	<i>CG8443</i>	
5	<i>miR-iab-4-3</i>	0.34	<i>unc-13</i>	
6	<i>miR-iab-4-3</i>	0.33	<i>Cha</i>	<i>Choline acetyltransferase</i>
7	<i>miR-iab-4-3</i>	0.32	<i>CG7371</i>	
8	<i>miR-iab-4-3</i>	0.32	<i>CG31522</i>	
9	<i>miR-iab-4-3</i>	0.31	<i>CG12424</i>	
10	<i>miR-iab-4-3</i>	0.31	<i>CG12360</i>	

CHAPTER III

***bantam* microRNA is a Negative Regulator of the *decapentaplegic* Pathway**

Ying Li,¹ Harlan Robins,² Nanci S. Kane¹ and Richard W. Padgett^{1*}

This chapter was submitted to (Journal Plos Genetics)

My contribution to this chapter is involved in designing and performing all the experiments except the viability crosses, and the analysis of the data and writing the manuscript.

Abstract

decapentaplegic (dpp), the *Drosophila* homolog of the vertebrate bone morphogenetic protein, BMP, is crucial for patterning and growth in many developmental contexts. The Dpp pathway is regulated at many different levels to exquisitely control its activity. We show that *bantam*, a microRNA (miRNA), down regulates *Mad* (*Mothers against dpp*) expression *in vivo* by targeting the *Mad* 3'UTR, resulting in changes in Dpp signaling. Over expression of *bantam* decreases P-MAD levels and negatively affects Dpp pathway transcriptional target genes. The removal of *bantam* binding sites in the 3'UTR of a *Mad* transgene results in a significant increase in the viability of haploinsufficient *dpp* animals compared to a *Mad* transgene carrying intact *bantam* binding sites in the 3'UTR. We provide evidence that *bantam* is up-regulated by Dpp in the wing imaginal disc, and thereby functions in a Dpp feedback loop. Furthermore, we show that this feedback loop between *bantam* and Dpp signaling is important for maintaining anterior-posterior (A/P) compartment boundary stability in the wing disc through regulation of *optomotor-blind (omb)*. *bantam* must affect other growth pathways, as it only partially regulates *omb* through Dpp, and only partially works in parallel to promote cell proliferation with Dpp signaling. Interestingly, comparative genomics reveal that *bantam* is evolutionarily conserved, and miRNA target predictions suggest that human *bantam* homologs selectively target Smad5, the homolog of *Mad* in BMP signaling, but do not target Smad2 in the activin/TGF β pathway. In summary, our results support the hypothesis that *bantam* miRNA is a conserved negative regulator of BMP/Dpp signaling.

Author Summary

The transforming growth factor β (TGF β) signaling pathway is conserved in all animal species and is involved in many cellular processes in development and diseases, including cancer. Our studies, performed in *Drosophila melanogaster*, focused on the interactions between the main components of TGF β signaling, the receptor-regulated-Smad (R-Smad), *Mothers against dpp* (*Mad*), and the microRNA (miRNA) *bantam*. miRNAs are an abundant class of small, non-coding RNAs that negatively regulate gene expression by interfering with messenger RNAs (mRNA) translation or by mRNA degradation. In this study, we provide evidence that the miRNA *bantam* down regulates *Mad* in a negative feedback loop and that the Dpp pathway up-regulates *bantam*. Data are provided that shows modulation of downstream Dpp markers by *bantam*. To show that these transcriptional changes lead to phenotypic changes in the animals, we reported that the presence or absence of *bantam* binding sites on *Mad* affects viability of animals. Furthermore, through sequence analyses, we reveal that *Drosophila bantam* and its human homologs are evolutionarily conserved, as are their putative targets. This sequence similarity supports the hypothesis that regulation of BMP/ Dpp signaling by *bantam* is functionally conserved.

INTRODUCTION

A fundamental question in development is how growth, cell fate specification, and pattern formation are spatially and temporally regulated to control the final shape and size of an organ. *Decapentaplegic* (*dpp*), an ortholog of vertebrate BMP2 and BMP4 (Padgett et al., 1993), regulates both patterning and growth in *Drosophila* development (Spencer et al., 1982). Dpp acts through a well-characterized transduction pathway (Parker et al., 2004; Raftery and Sutherland, 1999). First, *dpp* ligand binds the type I receptor Thickveins (Tkv). Upon ligand binding, Tkv phosphorylates a receptor-regulated-Smad (R-Smad), Mothers against dpp (Mad). Next, phosphorylated Mad (P-MAD) forms a complex with the common Smad (co-Smad), Medea, which then translocates into the nucleus, forming a complex with other complementary co-factors, regulating target gene expression either by transcription activation or depression.

In larval wing imaginal discs, *dpp* expression in a narrow stripe of cells along the anterior-posterior compartment boundary is essential for proper growth and patterning. Dpp functions as gradient morphogen to divide the wing disc into different regions by directing the expression of different combinations of target genes. The graded distribution of *dpp* ligands leads to nested expression domains of target genes, such as *spalt* and *optomotor-blind* (*omb*), and to the reciprocal gradient expression of *brinker* (*brk*). The characteristic expression patterns of these target genes play important roles in the positioning of wing veins along the anteroposterior axis (Affolter and Basler, 2007).

Besides patterning, Dpp also functions as a growth-promoting factor. Ectopic expression of either *dpp* or an activated Dpp receptor, Tk^{Q253D} , causes overgrowth (Martin-Castellanos and Edgar, 2002). Loss or severe reduction of *dpp* expression in the wing primordium reduces the wing to a small stump (Spencer et al., 1982). Cell clones lacking Dpp signaling fail to survive, suggesting that Dpp also functions as a survival factor for wing cells (Burke and Basler, 1996; Martin-Castellanos and Edgar, 2002). However, the underlying mechanism of growth control by Dpp is not completely understood.

miRNAs are an evolutionarily conserved, abundant class of small, non-coding RNAs, which are about 22 nucleotides in length. To date, 940 miRNAs have been identified in the human genome, and 171 miRNAs in the *Drosophila* genome (www.mirbase.org) (Ambros, 2003). Each miRNA is thought to target multiple genes in their respective genomes. In metazoans, miRNAs typically down regulate gene expression by binding to complementary sequences in the 3' untranslated region (3' UTR) of their target mRNAs, resulting in inhibition of protein translation and mRNA degradation. Although the overall complementation of miRNAs to their target mRNAs is imprecise, the region between nucleotides 2 through 8 at the 5' end of the miRNA (so-called "seed" region) and target mRNA maintains high complementation (Brennecke et al., 2005; Didiano and Hobert, 2006; Jackson et al., 2006; Krek et al., 2005; Lewis et al., 2005; Robins et al., 2005). Recently, studies have shown that the 3 - 9 nucleotide region of miRNAs can function as a seed region as well (Nahvi et al., 2009). miRNAs play widespread and critical roles in a variety of cellular processes including proliferation, differentiation, apoptosis,

development, and tumor growth (Ambros, 2003; Bushati and Cohen, 2007). However, few miRNAs have been reported with confirmed targets in signaling pathways.

bantam was one of the first miRNAs studied in *Drosophila* and has many important functions (Brennecke et al., 2003; Hipfner et al., 2002). Originally thought to be unique to *Drosophila* and related species, it is now known that *bantam* has conserved orthologs not only in related arthropods, but also in vertebrates (Ibáñez-Ventoso et al., 2008). First identified in a gain-of-function screen for genes that affect tissue growth (Hipfner et al., 2002), the *bantam* gene encodes a 23 nucleotide miRNA that is expressed in a spatio-temporally restricted manner throughout development. *bantam* miRNA stimulates cell proliferation through unknown downstream targets and inhibits apoptosis through its regulation of the pro-apoptotic gene *head involution defective (hid)* (Brennecke et al., 2003). Studies of elevated *bantam* expression in *hippo* mutant cells provided evidence that *bantam* is a downstream target of the Hippo tumor-suppressor pathway (Nolo et al., 2006; Thompson and Cohen, 2006). Furthermore, Yorkie (Yki), a transcriptional effector of the Hippo pathway, induces *bantam*, and *bantam* over expression is sufficient to rescue the growth defects of *yki* mutant cells (Nolo et al., 2006; Thompson and Cohen, 2006). In eye imaginal discs, Yki acts together with Homothorax (Hth) and Teashirt (Tsh), up-regulating *bantam* to promote cell proliferation and survival in the progenitor domain (Peng et al., 2009). Hth and Yki are bound to a DNA sequence ~14 kb upstream of the *bantam* hairpin in eye imaginal disc cells by chromatin immunoprecipitation, suggesting that this regulation might be direct.

Other roles for *bantam* in cellular regulation have been uncovered. *bantam* expression in interommatidial cells in the larval eye imaginal discs modulates the survival of cells mutant for Retinoblastoma-family proteins (Tanaka-Matakatsu et al., 2009). In addition, germline stem cell (GSC) maintenance in adult *Drosophila* testes and ovaries requires *bantam* (Shcherbata et al., 2007; Yang et al., 2009). In the *Drosophila* nervous system, *bantam* inhibits polyQ- and tau-induced neurodegeneration (Bilen et al., 2006). Furthermore, a core circadian clock gene, *clock*, is regulated by *bantam* in circadian cells (Kadener et al., 2009). Finally, scaling growth of dendrite arbors in the *Drosophila* peripheral nervous system is also regulated by *bantam*. *bantam* functions in epithelial cells to non-autonomously regulate growth of class IV dendrites of sensory neurons (Parrish et al., 2009).

Our previous study showed that *Mad* is the target of *bantam in vitro* in *Drosophila* S2 cells (Robins et al., 2005), which raises the question of whether *bantam* regulates *Mad* in animals. Here, we provide evidence that *Mad* is down regulated by *bantam in vivo* and that this regulation affects the viability of animals. We present a model that *bantam* regulates Dpp signaling in a feedback loop, which is important for maintaining anterior-posterior (A/P) compartment boundary stability in the wing disc through regulation of *omb*. In addition, *bantam* and Dpp function at least partially in parallel to promote cell proliferation. Finally, we show that the vertebrate *bantam* family consists of an expanded group with conserved “seed” sequences that likely target the 3’ UTRs of Smad5, the vertebrate homolog of *Mad*. Complementary sequences to *bantam* are not found in

Smad2, indicating that only the BMP Smads are targeted. In summary, our results support that *bantam* miRNA is a conserved negative regulator of BMP/Dpp signaling.

Results

***bantam* represses *Mad* through its 3' UTR**

Based on a computational algorithm to predict target genes for miRNAs, and validated by luciferase reporter assays in *Drosophila* S2 cells, data were presented that *Mad* is a target of *bantam* (Robins et al., 2005). By analyzing the *Mad* 3'UTR sequence, we found three putative *bantam* binding sites in the *Mad* 3'UTR, two of which are physically close to each other and are evolutionarily conserved, while the third is more questionable given its borderline score in our algorithm. Point mutations introduced in these two conserved *bantam* binding sites demonstrated that they were responsible for most of *bantam*'s regulatory effect on *Mad*. Mutations in one site partially inhibited the effects of *bantam*, whereas mutations in both binding sites removed almost all of *bantam*'s inhibitory effects (Robins et al., 2005),

To ask whether *bantam* regulates *Mad* in *Drosophila*, we made transgenes expressing the *green fluorescent protein* (GFP) under the transcriptional control of a *tubulin* promoter. We placed either a wild-type *Mad* 3'UTR or mutated *Mad* 3'UTR at the 3' end of the GFP coding sequence to create wild-type *Mad* sensor or mutated *Mad* sensor, respectively. The *bantam* sensor, which contained two copies of perfect *bantam* target sequence in the 3'UTR of GFP, was used as a negative indicator of *bantam* expression level to view patterns of *bantam* expression in the animal (Brennecke et al., 2003). *bantam* reduced the levels of the sensor through an RNAi effect and thus indicated high levels of the miRNA by lowering levels of the sensor. The comparable transgene construct, *tubulin*-GFP, which had no *bantam* binding sites at the 3'UTR, was used as a

control sensor. Under the same exposure, the wild-type *Mad* sensor showed similar patterns to the *bantam* sensor in the wing pouch, indicating that in regions of high *bantam* expression, the wild-type *Mad* sensor had been down regulated. The mutated *Mad* sensor lacked this pattern, showing high expression levels in the whole disc similar to the control (Figure 1). Since the mutated *Mad* sensor differed from the wild-type *Mad* sensor by only two mutations in each of the two putative *bantam* binding regions, the expression pattern difference between them suggests that *bantam* has an inhibitory effect on *Mad* through *bantam* binding sites on the *Mad* 3'UTR in wing imaginal discs.

Mutation of *bantam* binding sites increased *Mad* rescue of the *dpp* haploinsufficiency

Based on the cell culture results, we hypothesized that during development *bantam* modifies the cellular response to Dpp signaling by acting as a negative modulator, down regulating translation of *Mad* mRNA. Even if *bantam* alters *Mad* levels, compensatory changes in the pathway may overcome *Mad* changes, resulting in wild-type animals.

Compensatory rescue, which can lead to viable animals when genes are over expressed, has been seen in other systems. Notably, four copies of *bicoid* expand its gradient in early embryos, but animals emerge wild type (Driever and Nusslein-Volhard, 1988). To test if the changes on *Mad* expression by *bantam* have effects on viability, we used a sensitized genetic background with *dpp* haploinsufficient mutant alleles. *Drosophila* haploinsufficient for *dpp* die as embryos with few escapers but can be partially rescued with ubiquitous expression of *Mad* (*ubi-Mad*) (Das et al., 1998; Sekelsky et al., 1995). If *bantam* affects *Mad* in developing animals, then mutations in the *Mad* 3' UTR *bantam* binding sites should result in an increase in the levels of *Mad*, increasing viability.

We generated a wild-type and mutated *ubi-Mad* transgene to test this hypothesis. The first transgene carried wild-type *Mad* 3'UTR (*ubi-Mad-w3'UTR*), and the second carried a mutated *Mad* 3'UTR (*ubi-Mad-m3'UTR*) with the two *bantam* binding sites mutated in the sequences complementary to the *bantam* seed sequences. We tested two different *dpp* haploinsufficient alleles, *dpp*^{H61} and *dpp*^{H46} (Spencer et al., 1982; St Johnston et al., 1990). For both *dpp* haploinsufficient alleles, *dpp*^{H61} and *dpp*^{H46}, we had similar results: mutant *ubi-Mad-m3'UTR* had a better survival rate with the *dpp* haploinsufficiency strains than wild-type *ubi-Mad-w3'UTR*. *ubi-Mad-m3'UTR* produced average survival rates of 39.5% and 33.57% for *dpp*^{H61} and *dpp*^{H46} respectively, while *ubi-Mad-w3'UTR* produced average survival rates of 25.16% (p<0.0005) and 19.55% (p<0.016) for *dpp*^{H61} and *dpp*^{H46} respectively (Figure 2 and Table 1).

***bantam* negatively affects Dpp target genes**

Since changes in the binding of *bantam* to *Mad* sequences affects the viability of animals, we examined known downstream targets of Dpp for changes in their expression. Over expression of *bantam* along the A/P boundary in the wing imaginal disc by *patched-Gal4* displayed a large decrease in the *bantam* sensor in the middle of the disc (Figure 3D), indicating that *bantam* was highly expressed in this location. In addition, P-MAD antibody staining illustrated that P-MAD was greatly decreased by *bantam* (Figure 3E, Figure 3B). The level of Dpp signaling can be monitored by changes in the level of the phosphorylated form of Mad with P-MAD antibody staining (Yakoby et al., 2008). We also examined two Dpp transcriptional target gene levels, *optomotor-blind* (*omb*, a

synonym for *bifid* in FlyBase) and *brinker* (*brk*), by using enhancer trap lines for these two genes. *omb* is a *Drosophila* T-box gene positively regulated by Dpp (Nellen et al., 1996) and is expressed in a broad region in the middle of the wing disc (Figure 3G). *omb* is required for mediating several Dpp functions, including activation of the Dpp target genes *vestigial* and *spalt*, and for repression of *tkv* and *master of thick veins* (del Alamo Rodriguez et al., 2004). *brk* encodes a transcriptional repressor and is a key target of the Dpp pathway that is negatively regulated by Dpp signaling throughout embryonic and larval development (Campbell and Tomlinson, 1999; Jazwinska et al., 1999). *brk* was highly expressed in the lateral regions of the wing disc, forming a gradient reciprocal to the Dpp gradient (Figure 3I). *bantam* expression by *patched*-Gal4 decreased *omb-lacZ* along the A/P boundary in the wing imaginal disc (Figure 3H). *bantam* expression by *engrailed*-Gal4 expanded *brk-lacZ* expression toward the A/P border (Figure 3J). All of these results demonstrated that *bantam* can down regulate Dpp signaling.

Over expression of *bantam* caused an apical fold defect along the wing disc A/P boundary similar to defects in *omb* hypomorphs

omb expression is required in posterior cells to stabilize the A/P boundary in the wing discs and *omb* hypomorphic alleles have an apical fold morphogenetic defect in the middle of the wing disc (Shen et al., 2008; Umemori et al., 2007). When *bantam* was over expressed by Mz1369-Gal4, we found that there was ectopic folding in the middle of the wing disc (Figure 4B and Figure 4E), similar to the folding caused by hypomorphic *omb*. Mz1369-Gal4 was expressed throughout the entire wing imaginal disc (Figure 4C) (Hiesinger et al., 1999) and was used to drive expression of *bantam*. We tested whether

bantam was acting through *omb* by modulating *omb* expression levels. If *bantam* was acting on a gene other than *omb*, increasing *omb* expression would not rescue animals. In wild type animals, *omb* is expressed broadly in the wing pouch (Shen et al., 2008) (Figure 4A). In Mz1369-Gal4 > *UAS-bantam* animals, *omb* expression was decreased in the wing disc and, to a greater extent, in the posterior compartment (Figure 4B). When *omb* was over expressed with the Mz1369-Gal4 driver, most animals died as embryos (del Alamo Rodriguez et al., 2004). However, when *omb* was over expressed with *bantam* using the Mz1369-Gal4 driver, approximately 40% of the discs (n=35) appeared wild type (Figure 4F), and the remaining discs had a less severe phenotype (Figure 4G) than when *bantam* was over expressed alone (Figure 4E). These results implied that the ectopic folding caused by *bantam* was at least in part due to the decrease in *omb* by *bantam*'s inhibitory effect on Dpp signaling.

***bantam* functions through Dpp to alter proliferation of discs**

Both *bantam* and Dpp signaling are known to be important for wing disc growth (Brennecke et al., 2003; Martin-Castellanos and Edgar, 2002; Spencer et al., 1982). To determine if the growth properties of *bantam* function through Dpp, we expressed *bantam* or an activated Dpp receptor (CA-Tkv) in the whole wing imaginal disc and then examined the size of the disc. When *bantam* or CA-Tkv was over expressed with Mz1369-Gal4, the wing imaginal disc was slightly larger than wild type (Figure 5E and 5H) as previously noted (Brennecke et al., 2003; Martin-Castellanos and Edgar, 2002). When *Daughters against dpp* (*Dad*) was over expressed to block Dpp signaling, the wing imaginal disc was not visible (data not shown). When *bantam* and *Dad* were both over

expressed, most larvae had no wing discs, and a few had small clusters of cells, which did not have normal wing disc morphology (Figure 5J). These results indicate that Dpp signaling is necessary for *bantam* to function at least partially in cell proliferation. When both *bantam* and CA-Tkv were over expressed, wing discs grew much larger than when either one was over expressed alone (Figure 5K). We interpret this to mean that *bantam* and the Dpp pathway amplify each other in cell proliferation.

We also examined the status of cell proliferation in the wing discs. In the wild-type discs, there was even proliferation in the whole disc as determined by EdU staining (Figure 5A). When *bantam* was over expressed using Mz1369-Gal4, there was increased proliferation in the entire disc, but more dramatically in the posterior lateral region where cells showed more sensitivity to *bantam* (Figure 5D). Using Mz1369-Gal4 to over express CA-Tkv, proliferation was increased in the lateral regions but inhibited in the middle of the disc (Figure 5G). When both *bantam* and CA-Tkv were over expressed with Mz1369-Gal4, the whole disc increased proliferation (Figure 5K). Proliferation patterns provided further evidence that cells in the wing disc possess region specific properties in response to growth signaling. Cells in the lateral region of the wing disc were stimulated to enter a new cell cycle by both *bantam* and CA-Tkv, but the cells in the middle of the wing disc responded only to *bantam*, not to CA-Tkv. This region-specific proliferation suggests that the mechanisms of action for regulation of cell proliferation by Dpp and by *bantam* function at least partially in parallel.

We generated mutant clones of *bantam* in the wing disc in order to observe the consequences of removing *bantam* on *dpp* signaling. As previously noted, *bantam* clones are very small, but slightly larger clones can be generated using Minutes to give a growth advantage to mutant tissue (Brennecke et al., 2003; Thompson and Cohen, 2006). We generated small clones of *bantam* and found that the levels of P-Mad were unchanged (data not shown). This result was not unexpected as we think that *bantam* modulates Dpp signaling rather than acting as an on/off switch. Similar observations of verified targets were seen in experiments of *bantam* and Mei-P26. *bantam* was shown to interact with the 3' UTR sequences of Mei-P26, yet *bantam* clones did not possess increased levels of Mei-26 protein (Herranz et al., 2010), suggesting *bantam* fine-tunes this pathway as well.

***bantam* expression is regulated by Dpp signaling**

Reciprocal feedback loops between miRNAs and pathways they regulate can play important roles in their functions (Carthew, 2006; Chang et al., 2004; Fazi et al., 2005). To determine if Dpp signaling and *bantam* function in a feedback loop, we modulated Dpp signaling activity to examine the effect on *bantam*. An activated Mad (generated by removing putative MAP kinase sites in the linker region) (Eivers et al., 2009a; Eivers et al., 2009b; Kretzschmar et al., 1997) was over expressed by an *engrailed*-Gal4 driver in the posterior compartment of the wing imaginal disc (Eivers et al., 2009b; Kretzschmar et al., 1997). Using the *bantam* sensor to monitor *bantam* levels, we found that the *bantam* sensor was greatly decreased in the lateral region (Figure 3L). This decline in the *bantam* sensor indicated that increased Dpp signaling increased *bantam* expression in the wing disc. In separate experiments using a miRNA microarray, we also found that *bantam* was

up-regulated more than two fold by Dpp signaling in third instar larval brains (unpublished data).

A previous study revealed that *bantam* has a large cis-regulatory region (Peng et al., 2009), so we analyzed the DNA sequence 15 kb upstream of *bantam* for the following known consensus sequences for *Mad* (GRCGNC) (Kim et al., 1997), *brk* (GGCGYY) (Sivasankaran et al., 2000; Zhang et al., 2001), and the canonical Smad binding sequence (GTCT) (Shi et al., 1998; Zawel et al., 1998) (where N is any; R is A or G, Y is C or T). Although *Mad* binds to a slightly different sequence than the canonical vertebrate sequences, *Medea* is reported to bind to the canonical vertebrate sequences (Gao et al., 2005). Our analyses of the upstream region revealed a total of 36 *Mad* binding sites and 16 *brk* binding sites in the 15kb *bantam* upstream cis-regulatory region (Figure 8). Some genes contain a *dpp* responsive silencer element, which can be directly repressed by *dpp* signaling. This region does not contain a Dpp-responsive silencer element (GRCGNCNNNNNGTCT) (Gao et al., 2005; Muller et al., 2003), suggesting that Dpp signaling directly up-regulates *bantam*.

***bantam* is evolutionarily conserved**

Long thought to be novel in *Drosophila*, a human ortholog of *bantam*, *hsa-miR-450b-3p*, was identified in cancer cells (Landgraf et al., 2007). In humans, many miRNAs are clustered in the genome, are transcribed from a polycistron, and function cooperatively (Wong et al., 2010). The *hsa-miR-450b-3p* gene is located within a 1.25 kb region of the *hsa-miR-450/542* cluster (Figure 6A). It is possible that *hsa-miR-450b-3p* is transcribed

together with its neighboring miRNAs, *hsa-miR-450a-1*, *hsa-miR-450a-2*, *hsa-miR-542*, and *hsa-miR-450b*. One gene in the cluster, *hsa-miR-450b*, encodes two unrelated miRNAs, one of which is related to *bantam* (*hsa-miR-450b-3p*). Interestingly, analysis of the sequences of the miRNAs from the *hsa-miR-450/542* cluster revealed sequence similarity in the seed sequences of two pairs of miRNAs from this cluster, which suggests they may function in a similar manner (Figure 6B). *hsa-miR-450b-3p* was highly conserved to *bantam* from bases 2-14 at the 5' end seed sequence and to *hsa-miR-542-5p*, which possesses eight continuous bases conserved in the 5' seed region (Figure 6C). G:U pairing in the seed region is tolerated *in vivo* for efficient interaction between miRNA and its target mRNA (Didiano and Hobert, 2006). In addition, *hsa-miR-542-3p* is unique among these miRNAs and is not similar to the other miRNA genes in the complex (Figure 6B).

If these human miRNAs function in a manner similar to their *Drosophila* orthologs, they may be also regulated by Smad proteins in a feedback loop. We compared the flanking gene sequences of *hsa-miR-450/542* in human and mouse and found that their upstream regulatory sequences are conserved (~55%) (Figure 9). This conservation of DNA sequences suggested that the mechanism for regulating transcription of this miRNA cluster might be conserved. so we examined the flanking sequences for the presence of Smad binding sites. We found five canonical Smad binding elements (GTCT) (Shi et al., 1998; Zawel et al., 1998), which were conserved in nine mammals (Figure 6A and Figure 9), suggesting that human *bantam* homologs are likely regulated by BMP signaling. To date, no functional studies have been done on these human *bantam* homologs.

If a regulatory feedback loop exists in vertebrates as in *Drosophila*, then human *bantam* should target one or more of the BMP Smads, Smad1, Smad2, or Smad9. Many miRNAs are evolutionarily conserved, and occasionally their targets are conserved, but to a lesser degree (John et al., 2004). We employed different miRNA target prediction algorithms, miRanda (John et al., 2004) and Targetscan (Lewis et al., 2005), to examine whether human *bantam* homologs would target BMP Smads. Both algorithms predicted that Smad5 was a putative target of the human *bantam* homologs (Figure 6D and Table 2). In addition to the binding sites for *bantam* homologs, Smad5 also contained putative sites for *hsa-miRNA-450b-5p* and *hsa-miRNA-450a*, and putative sites for *hsa-miRNA-542-3p* (Figure 6D and Table 2), suggesting that Smad5 may be regulated by other unrelated miRNA genes in the *hsa-miRNA-450/542* cluster. We also analyzed Smad2, an activin/TGF β pathway specific R-Smad, for binding sites. Interestingly, we found that the Smad2 3'UTR had no binding sites for *bantam* homologs, even though it had three sites for *hsa-miRNA-450b-5p/450a* and two sites for *hsa-miRNA-542-3p*.

DISCUSSION

***bantam* is a negative regulator of Dpp**

In this report, we provided evidence that *bantam* is a negative regulator of the Dpp pathway *in vivo*. In previous cell assay studies, we showed that *Mad* is down regulated by *bantam* (Robins et al., 2005), but whether this regulation was important in animals was not substantiated. In support of these original findings, we confirmed the presence of *bantam* binding sites in the *Mad* 3'UTR through mutational analysis. By using sensors containing 3'UTR sequences expressed in the wing imaginal discs, we showed that these sequences are necessary for regulation by *bantam*. Over expression of *bantam* changes levels of P-Mad and Dpp transcriptional target genes, *omb* and *brk*. These changes in Dpp signaling are not overcome during development. Using a sensitized genetic system with haploinsufficient *dpp* alleles, we saw that the transgene, *ubi-Mad-m3'UTR*, with mutated *bantam* binding sites in its 3'UTR, gave rise to a statistically significant better survivor ratio for *dpp* mutant flies than the *Mad* transgene with wild-type 3'UTR. Taken together, these data indicate that *bantam* regulates *Mad* at the physiological level and thereby modulates Dpp signaling activity.

***bantam* regulates aspects of Dpp functions**

The mechanisms of action of miRNAs on biological events vary. Some miRNAs act as a switch, such as *C. elegans* *lsy-6* and *miR-273*, which are thought to operate in a double negative-feedback loop to specify left-right asymmetry of chemosensory neurons (Chang et al., 2004; Johnston and Hobert, 2003). Other miRNAs are thought to function more subtly to fine-tune the biological processes they are regulating by ensuring the

appropriate level of gene expression during different developmental processes. For example, *Drosophila mir-9a* regulates the level of expression of its target gene *senseless* to ensure the generation of precise numbers of sensory organs in *Drosophila* embryos and adults (Li et al., 2006). Our results demonstrated that *bantam* is a negative regulator of the Dpp pathway. However, we do not believe that *bantam* is acting as a switch; instead, we propose that *bantam* functions as a fine-tuner of Dpp signaling to regulate the signaling strength or the gradient of Dpp signaling.

omb is required in the posterior cells to prevent aberrant apical fold formation at the A/P boundary of the wing disc, and hypomorphic *omb* alleles exhibit ectopic folding (Shen et al., 2008; Umemori et al., 2007). We found that over expression of *bantam* down regulated *omb* in the imaginal discs and caused ectopic folding in the wing imaginal discs, as has been observed in hypomorphic *omb* alleles (Shen et al., 2008; Umemori et al., 2007). Furthermore, over expression of *omb* partially rescued the folding defects caused by *bantam*. These results provide evidence that *bantam* works partially through *Mad* since *dpp* regulates *omb*. The partial rescue of *omb* folding defects could be explained by regulation of *omb* by other genes, such as *Wg*, which regulates *omb* in conjunction with Dpp (Grimm and Pflugfelder, 1996).

Dpp acts as a survival factor for wing disc cells by preventing activation of the c-Jun amino-terminal kinase (JNK)-dependent apoptotic pathway (Adachi-Yamada et al., 1999; Bryant, 1988). We found a lack of wing disc development when we blocked Dpp signaling with Dad, further supporting Dpp's role as a survival factor. *bantam* inhibits

apoptosis through targeting of the pro-apoptotic gene, *head involution defective (hid)* (Brennecke et al., 2003). However, in our work, we found that *bantam* cannot bypass the inhibitory effect of *Dad* on wing disc cell growth (Figure 5J), which suggests that *bantam* cannot alleviate *Dad*-induced activation of JNK-dependent apoptosis. *reaper*, *hid*, and *grim* are all essential cell death inducing-genes in *Drosophila* (Chen et al., 1996; Grether et al., 1995; White et al., 1994). Loss of *bantam* in clones does not result in an increase in apoptosis, suggesting *bantam* is not the main determinant for cell death (Tanaka-Matakatsu et al., 2009). JNK signaling acts upstream of *reaper* by transcriptional up-regulation (McEwen and Peifer, 2005). It is possible that blocking *Dpp* activates JNK-induced apoptosis through cell death genes other than *hid*, or a combination of *hid* and other genes; therefore, inhibition of *hid* alone by *bantam* could not rescue *Dad*-induced apoptosis.

Both *bantam* and *Dpp* signaling affected growth by coordinately increasing rates of cell proliferation and cell growth (Hipfner et al., 2002; Martin-Castellanos and Edgar, 2002). How *bantam* and *Dpp* affect the molecules in the cell cycle machinery is not well understood. In mammalian cells, Cyclin D1 (CycD) and its kinase partner Cdk4 act as positive cell cycle regulators to link extracellular cues to cell cycle machinery (Sherr, 1996). The characteristic increase in the number of cells caused by *bantam* or *dpp* signaling is very similar in both *dpp* and CycD/Cdk4 pathways (Datar et al., 2000). However, genetic studies demonstrated that CycD/Cdk4 is not required for either *bantam* or *Dpp*'s effects on growth (Hipfner et al., 2002; Martin-Castellanos and Edgar, 2002) and therefore, they must be acting at a different point in the cell cycle.

Are *bantam* and Dpp signaling functioning in sequential or in parallel modes of action to promote growth? In our work, we saw that *bantam* and CA-Tkv promote growth synergistically (Figure 5K). Coexpression of both *bantam* and CA-Tkv resulted in larger wing discs than when only *bantam* or CA-Tkv were expressed alone. In addition, there is a region-specific response of cell proliferation to *bantam* and Dpp signaling in the wing disc. In the middle region of the wing disc, cells can be stimulated to enter S phase by *bantam* but not by CA-Tkv, while in the lateral regions, cells can be stimulated by both (Figure 5D and 5G). Thus, we believe that *bantam* and Dpp operate at least in part through parallel mechanisms of action to regulate cell cycle machinery. The precise mechanism of how Dpp regulates growth is poorly understood. Several models attempt to explain Dpp's roles in growth regulation (Affolter and Basler, 2007; Schwank and Basler, 2010); however, none of them fully explain all of the data. As a fine-tuner of the pathway, we believe that *bantam* would not block Dpp signaling totally by down regulation of *Mad*. When *bantam* is over expressed with CA-Tkv, its down regulation of *Mad* might not counteract all of the stimulation by CA-Tkv. Thus, both *bantam* and Dpp signaling promote proliferation, synergistically boosting the growth effect.

Feedback loop between *bantam* and Dpp

Several reports provide evidence that feedback loops between miRNAs and their targets play important roles in their functions. In *Drosophila*, reciprocal negative feedback between *mir-7* and its target *Yan* reinforces the photoreceptor differentiation induced by the EGF signal in developing eyes (Li and Carthew, 2005). The similar negative feedback

regulatory circuitry involving *miR-223* and two transcriptional factors, NFI-A and C/EBP α , is important in human granulocytic differentiation (Fazi et al., 2005). In *C. elegans*, a positive feedback loop between *lin-12*, *mir-61*, and *vav-1* was reported to maximize LIN12 activity and specify the secondary vulva cell fate (Yoo and Greenwald, 2005). In our work, we provided evidence that *bantam* can affect Dpp pathway activity by binding to its target *Mad* mRNA, and we also determined that *bantam* levels were increased when the Dpp pathway was activated. Based on these results, we proposed a model suggesting a negative feedback loop between *bantam* and Dpp signaling (Figure 7). In cells expressing *bantam*, Dpp signaling activity can be fine-tuned through *bantam*'s negative regulatory effect on *Mad*, which in turn ensures the precise transcription of Dpp target genes in specific temporal and spatial patterns during development. Upon the stimulation of the Dpp pathway, cells may increase the level of *bantam*, which can further down regulate the Dpp pathway to a level needed for development.

It is possible that this feedback loop regulation between *bantam* and Dpp could be regulated only in a specific developmental context as a way to fine-tune the regulation of the pathway. When the Dpp pathway was activated in the entire posterior compartment of the wing imaginal disc, *bantam* levels increased dramatically in the posterior lateral region, but not obviously in the middle of the wing disc close to the A/P boundary (Figure 3L). This result is consistent with the low expression pattern of *bantam* in the middle of the wing disc where Dpp exhibits high activity in wild type (Figure 3K). Likewise, *bantam* is regulated by a growing number of genes. For example, *Notch* signaling inhibits *bantam* expression in the wing disc (Herranz et al., 2008). *bantam* is

also a target of the Hippo pathway (Nolo et al., 2006; Thompson and Cohen, 2006), so it would be good candidate for mediating crosstalk between different signaling pathways. Future studies to understand how *bantam* is integrated into other signaling pathways and to clarify how components in these other pathways affect *bantam* expression will be of interest.

The regulation of *bantam* and its integration into BMP pathways is likely an ancient feature. At least two *bantam*-like genes are present in vertebrates and have putative targets in Smad5, a conserved Smad related to Mad. Neither of these *bantam* homologs appear to target Smad2/3, the TGF β and activin Smads, suggesting *bantam* functions in the BMP pathway exclusively. It is interesting to note that *bantam* does not appear to target Smad1, a close relative of Smad5. Perhaps subtle differences in levels or tissue expression occur as a result of *bantam* binding sites in Smad5 but not in Smad1 (Eivers et al., 2009a; Monteiro et al., 2004; Zwijsen et al., 2003). It will be interesting to explore the relationship between vertebrate *bantam* and Smad homologs in future experiments.

MATERIALS AND METHODS

Drosophila strains and genetics

The GAL4/ UAS system was used to over express transgenes (Elliott and Brand, 2008; Phelps and Brand, 1998). *patched*-Gal4 and *engrailed*-Gal4 drivers were obtained from the Bloomington Drosophila Stock Center (Bloomington, IN). Mz1369-Gal4 is expressed uniformly in the wing discs and in the optic lobe of the brain (Hiesinger et al., 1999). The following four strains were used: (1) *GS-bantam*, which contains an insertion of the Gene Search UAS element upstream near the *bantam* gene, allowing *bantam* to be over expressed by Gal4 (Cho et al., 2006); (2) *UAS-omb* (Hofmeyer et al., 2008); (3) UAS-CA-Tkv (S-H. Cho and R.W.P., unpublished results); and (4) *UAS-Mad4ap*, an activated *Mad*, which contains a mutation of the serines into alanines at the four possible mitogen-activated protein kinase (MAPK) sites in the *Mad* linker region (S-H. Cho and R.W.P., unpublished results). MAPK phosphorylation prevents nuclear accumulation of Smads, therefore inhibiting signaling (Eivers et al., 2009a; Eivers et al., 2009b; Kretschmar et al., 1997). Other flies strains used in this study include: a *bantam* sensor (a P element line which contains *tub-EGFP* and two copies of the *bantam* target sequence in the 3'UTR) (Brennecke et al., 2003), *omb-lacZ* (Tsuneizumi et al., 1997), and *brk-lacZ* (Minami et al., 1999). *dpp*^{H61}/CyO, *P23* and *dpp*^{H46}/CyO, *P23* are haploinsufficient for *dpp* (Spencer et al., 1982; St Johnston et al., 1990).

Generation of *Mad* transgenes

The wild type *Mad* 3'UTR was amplified from genomic DNA with the following primers, 5'AATCCTAGGGCTTAAGATGAGGCTCGAGTC and

5'CGGTCTAGAATTATCGTCTACTTATTTTTCTGCG. Then the AvrII-XbaI fragment of *Mad* 3'UTR was cloned downstream of *tub-EGFP* into the 3'UTR in CaSpeR4.

To generate constructs with a mutated *Mad* 3'UTR, the wild-type *Mad* 3'UTR was first subcloned into pBluescript II SK(+) between NotI-XbaI. The following pair of primers 5'CAATTACAAAATGGTATAACTATTTACAATGTACTACATGCTATAATATTAATGATCTATGCCC and

5'GGGCATAGATCATTAATATTATAGCATGTAGTACATTGTAAATAGTTATACCATTTTGTAATTG were used to mutate the first *bantam* binding site. The following pair of primers

5'TGTACTACATGCTATAATATTAATGTACTATGCCCATTGGCAAAACAGTTCT and

5'AGAACTGTTTTGCCAATGGGCATAGTACATTAAATATTATAGCATGTAGTAC

A were used to mutate the second *bantam* binding site (Stratagene). The mutagenesis was confirmed by sequencing. The NotI-XbaI fragment of the mutated *Mad* 3'UTR was cloned downstream of *tub-EGFP* into the 3'UTR in CaSpeR4. The *ubi-Mad-w3'UTR* and *ubi-Mad-m3'UTR* constructs were made by cloning the above *Mad* sequences downstream of the *ubiquitin* promoter in CaSpeR.

Viability of *dpp* mutant

The *dpp*^{H61} and *dpp*^{H46} alleles contain a deletion of most of the 3' coding exon of *dpp* and are haploinsufficient (Spencer et al., 1982; St Johnston et al., 1990). Heterozygous

dpp^{H61}/+ and *dpp*^{H46}/+ animals are embryonic lethal with rare escapers. These stocks are kept by balancing with *CyO*, *P23*, a standard *CyO* balancer plus a transgene containing a copy of the *dpp Hin* region that rescues the *dpp* null mutants (Padgett et al., 1993; Wharton et al., 1993). For viability experiments, we crossed *dpp*^{H61}/*CyO*, *P23* or *dpp*^{H46}/*CyO*, *P23* males with heterozygous *ubi-Mad-w*'3'UTR/+ or *ubi-Mad-m3*'UTR/+ virgin females. Flies were grown at 25°C and collected at day 17 for counting. Survival rate of the offspring was calculated as the number of flies with straight wings divided by the total number of flies (survival rate = $CyO^{+} / CyO^{+} + CyO$).

Histology and imaging

X-Gal staining

Third instar larvae were rinsed and dissected in chilled 1x Ringers solution (Van de Bor et al., 1999). Larval heads with discs attached were fixed in formalin (Sigma) for 10 minutes and then rinsed 1x 10 minutes in assay buffer (5 mM KH₂PO₄, 5 mM K₂HPO₄, 2 mM MgCl₂, 100 mM KCl, 4 mM K₃[Fe(III)(CN)₆], 4 mM K₄[Fe(II)(CN)₆]). Next, they were incubated in pre-warmed reaction buffer (1.5 mg/ml X-Gal in assay buffer) for four hours or overnight at room temperature. Finally, samples were rinsed in assay buffer to stop the reaction.

Antibody staining

Third instar larvae were dissected in chilled 1x Ringers solution. Disc tissue was fixed in formalin (Sigma) for 10 minutes at room temperature. Primary antibodies used for

staining were rabbit anti-P-MAD (diluted as 1:4000) (Yakoby et al., 2008), rat anti-DE-cadherin (diluted 1:20, Developmental Studies Hybridoma Bank, DCAD2), rabbit anti- β -GAL (diluted 1:8000, Cappel). Secondary antibodies, conjugated to Cy3, were used for detection (diluted 1:200, Jackson ImmunoResearch Lab). Wing imaginal discs were mounted in Vectashield mounting medium (Vector Laboratories) and analyzed using confocal microscopy.

EdU Staining

EdU staining (Salic and Mitchison, 2008) was performed using Click-iT EdU Alexa Fluor Imaging kits from Molecular Probes (Invitrogen, Inc). Briefly, dissected larvae were incubated with EdU (20 μ M) at room temperature for 10 minutes, washed with PBS, and fixed in formalin (Sigma) for 18 minutes. After washing, larvae were incubated with Alexa fluor azide for 30 minutes at room temperature. After washing, whole brains were dissected and mounted in Vectashield mounting medium.

ACKNOWLEDGEMENTS

We would like to thank Drs. K. Hofmeyer, S. Cohen and N. Yakoby, the Bloomington Stock Center, and the Developmental Studies Hybridoma Bank at the University of Iowa for generously supplying the fly stocks and reagents.

Figure 1

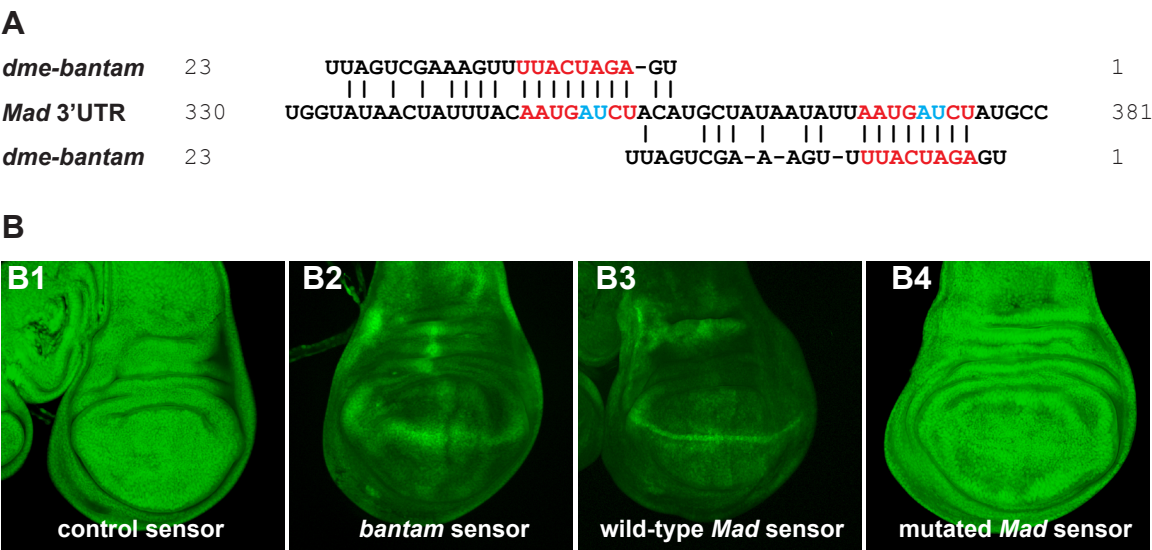
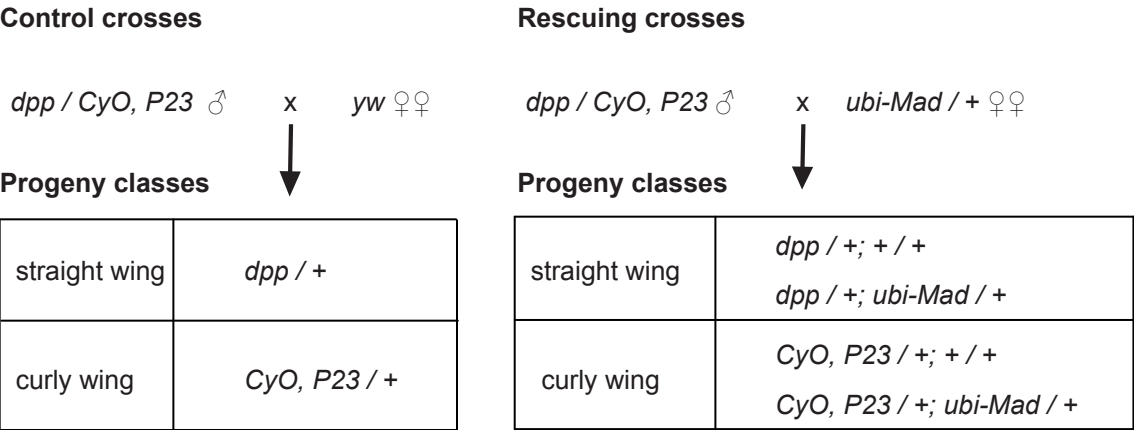


Figure 1. *bantam* regulates *Mad*.

(A) The *Mad* 3' UTR contains two *bantam* binding sites. Alignments are shown between *bantam* miRNA and the *Mad* 3' UTR. Notice perfect matches to the seed region of these two adjacent *bantam* sites. Positions 5 and 6 of the mature *bantam* binding sequence (shown in blue) are changed in the mutated *Mad* sensor, from AU to UA. (B) *In vivo* regulation of *Mad* by *bantam* in wing imaginal discs. All sensor constructs are expressed with a *tubulin* promoter driving EGFP. (B1) Control sensor without *bantam* binding sites shows expression ubiquitously, (B2) *bantam* sensor containing two perfectly complementary copies of the *bantam* binding sequence in the 3' UTR where the expression of *bantam* is low, (B3) sensor construct containing wild-type *Mad* 3' UTR, (B4) sensor construct containing two mutated *bantam* binding sites in the *Mad* 3' UTR, which shows ubiquitous expression as in (B1).

Figure 2

A



Survival rate = straight wing flies / total flies

B

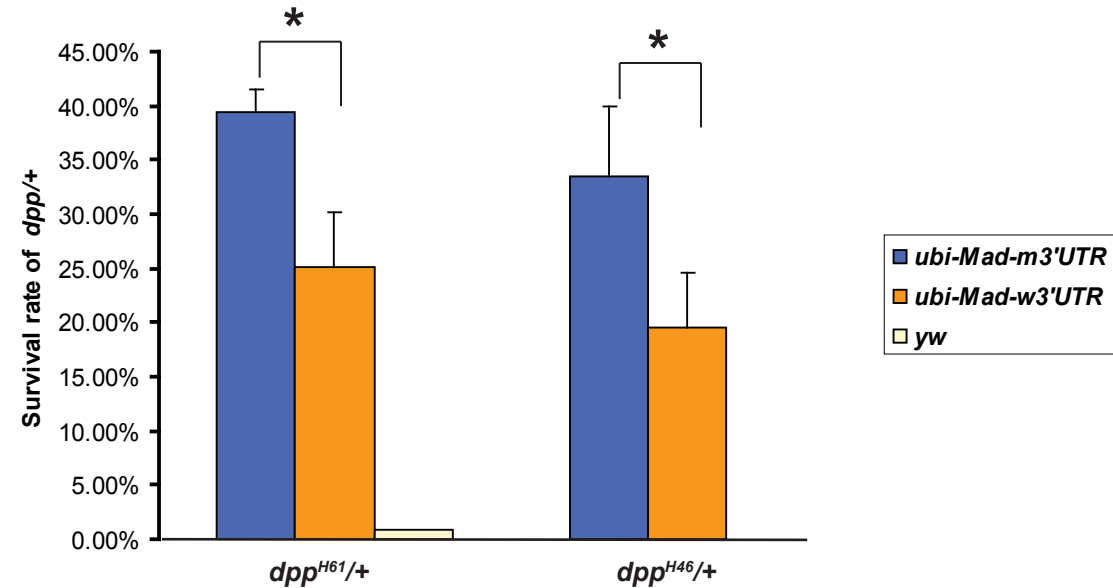


Figure 2. Loss of *bantam* binding sites in *Mad* increases rescue of *dpp* haploinsufficiency.

(A) Outline of control crosses and rescuing crosses, the progeny classes, and the formula used to calculate survival rate of *dpp*/+. (B) Histograms show that *ubi-Mad-m3'UTR* (blue) containing the mutated 3' UTR *bantam* binding site significantly improves survival rate compared to *ubi-Mad-w3'UTR* (orange), which contains the wild type 3' UTR sequences. Both haploinsufficient *dpp* alleles, *dpp*^{H61}, and *dpp*^{H46} showed significant rescue ($p < 0.0005$ and $p < 0.016$, respectively). The value of each bar represents the average survival rate from several individual transgenic lines for each construct. *ubi-Mad-m3'UTR* has two mutated *bantam* binding sites in the *Mad* 3' UTR, while *ubi-Mad-w3'UTR* contains a wild-type *Mad* 3' UTR. The *ubi-Mad-m3'UTR* and *ubi-Mad-w3'UTR* classes are statistically different from each other. The yellow bar indicates escapers of the haploinsufficiency, which is $< 1\%$ for both alleles.

Figure 3

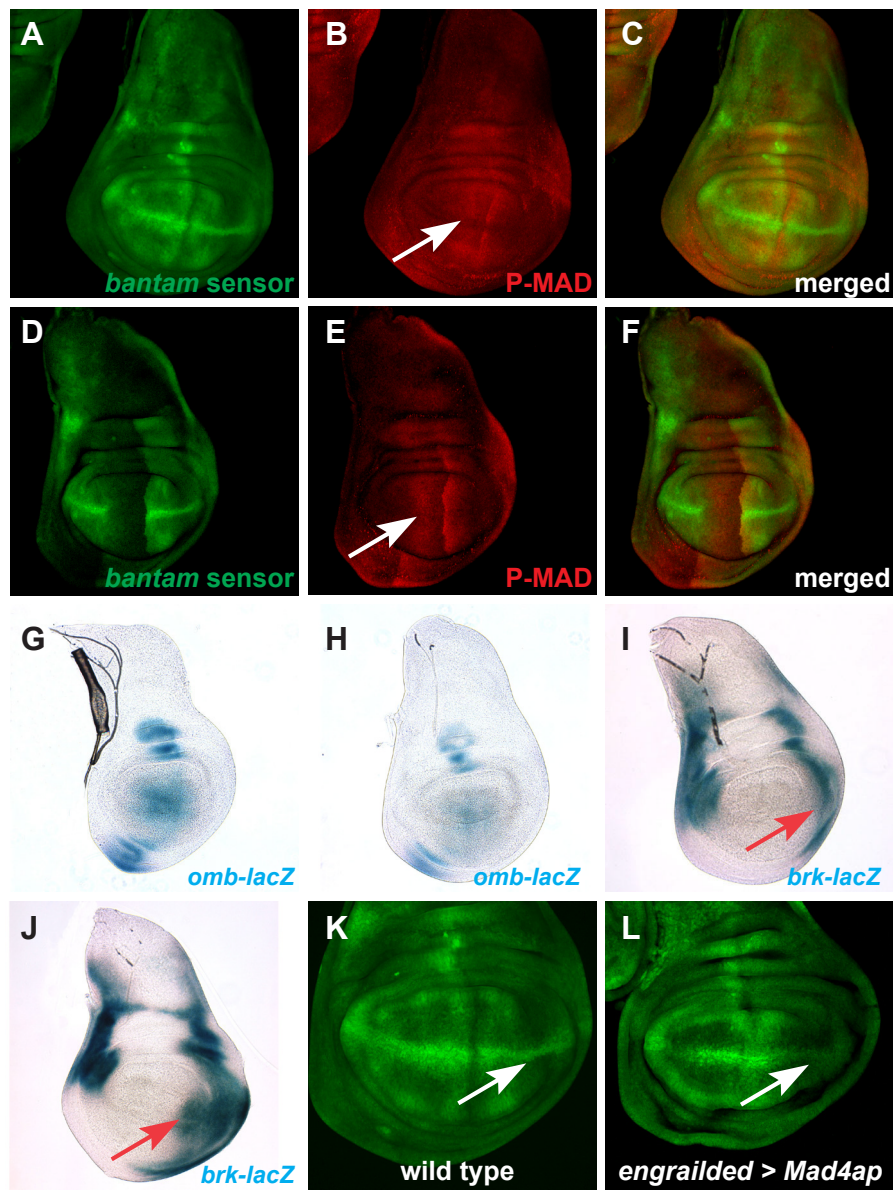


Figure 3. *bantam* and *Mad* regulate each other.

(A) Discs are oriented with anterior to the left and ventral down. Wild-type wing disc shows *bantam* expression using a *bantam* sensor (high GFP indicates low levels of *bantam*), (B) P-MAD staining displays high levels of *dpp* activity. P-MAD is highest along the A/P boundary. (C) merged views of A and B, (D-F) over expression of *bantam* by *ptc*-Gal4 along the A/P boundary of the wing disc. (D) The *bantam* sensor indicates higher expression of *bantam* along the A/P boundary. (E) P-MAD expression decreases along the A/P boundary as *bantam* increases, (F) merged panels of D and E. Arrows in B and E indicate altered expression of P-Mad at the A/P boundary. (G-J) X-Gal staining was used to monitor the expression levels in wing discs of the enhancer trap lines for *omb* and *brk*, two downstream target genes of Dpp. Wild type (G, I) and *bantam* over expression (H, J) were incubated with X-Gal for same length of time. (H) When *bantam* was over expressed along the A/P boundary by *ptc*-Gal4, *omb* expression is decreased. (J) When *bantam* was over expressed in the posterior compartment by *engrailed*-GAL4, *brk* expression is expanded toward the posterior compartment as indicated by the arrow. (K, L) *Mad* controls *bantam* levels. (K) the *bantam* sensor levels in a wild-type disc, (L) *bantam* sensor expression in wing disc in which activated *Mad* is expressed by *engrailed*-GAL4 induces expression in the posterior compartment. Note that the *bantam* sensor is decreased along the A/P boundary and more obviously in the posterior lateral region. No comparable changes were seen in the anterior compartment where *Mad* was not expressed.

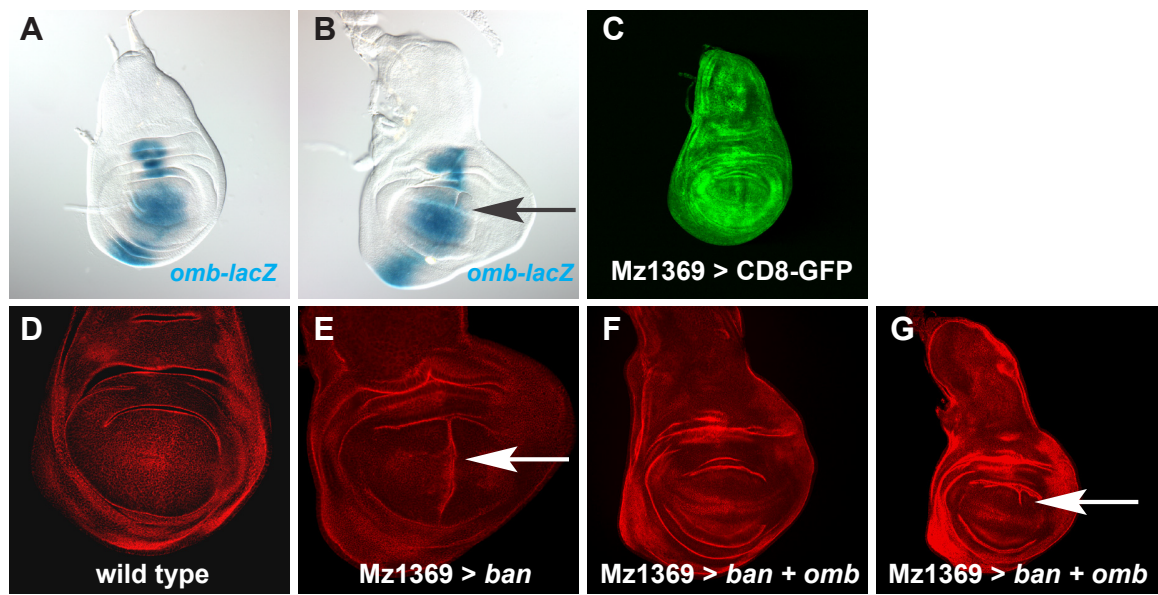
Figure 4

Figure 4. *omb* rescues a *bantam* wing disc defect.

A) X-Gal staining was used to view expression of enhancer trap line *omb-lacZ* in a wild-type wing disc. (B) *omb-lacZ* expression in Mz1369-Gal4 > *UAS-bantam* (*ban*). (C) expression pattern of Mz1369-Gal4 in the wing imaginal disc. The CD8-GFP is localized to cell membranes. The arrow indicates an apical fold defect. Notice an expansion of the posterior compartment of the wing disc. (D-G) discs stained with anti-DE-cadherin to view the morphology of wing discs, (D) wild-type wing disc, (E) over expression of *bantam* by Mz1369-Gal4. *bantam* causes an apical fold morphology defect along the A/P boundary (arrow, in E and G). Coexpression of *bantam* with *omb* can fully rescue *bantam* (F), or partially rescue *bantam* (G).

Figure 5

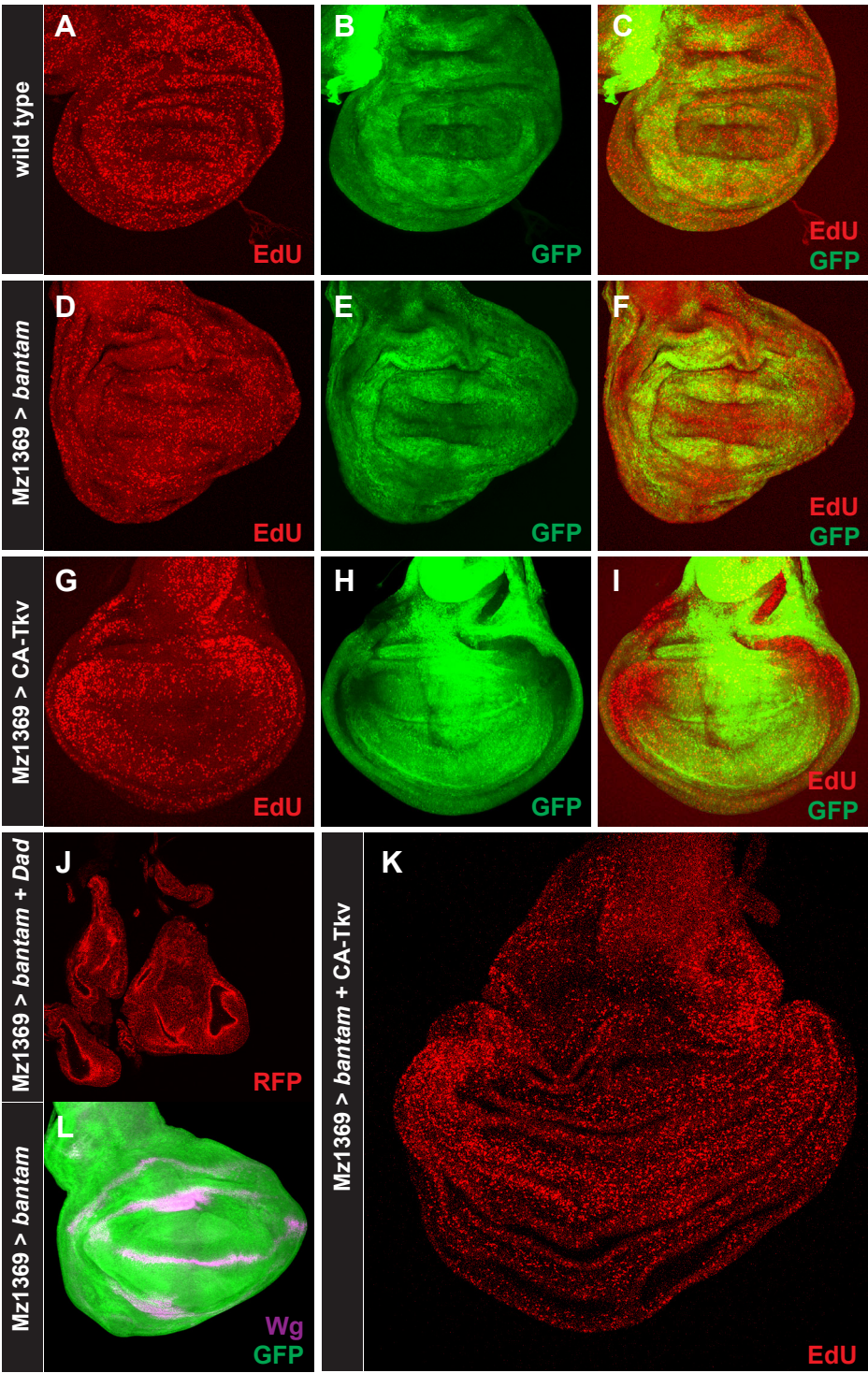


Figure 5. *bantam* and Dpp potentiate wing disc growth.

The Mz1369-Gal4 driver is used to express either *UAS-CD8-GFP*, *UAS-bantam*, *UAS-CA-Tkv*, *UAS-RFP* (red fluorescent protein), or *UAS-Dad*. All wing discs are at the same magnification. EdU staining (red) in (A, D, G, K) is used to view proliferation of cells. GFP (green) in (B, E, H) and RFP (red) in (J) are used to view wing disc expression by the Mz1369-Gal4 driver. The CD8-GFP is localized to membranes. Genotype: (A, B, C) Mz1369-Gal4 > *UAS-CD8-GFP*; (D, E, F) Mz1369-Gal4 > *UAS-CD8-GFP* + *UAS-bantam*; (G, H, I) Mz1369-Gal4 > *UAS-CD8-GFP* + *UAS-CA-Tkv*; (J) Mz1369-Gal4 > *UAS-RFP* + *UAS-bantam* + *UAS-Dad*; (K) Mz1369-Gal4 > *UAS-bantam* + *UAS-CA-Tkv*. (L) *wingless* staining in Mz1369-Gal4>*bantam* shows expression in the wing blade region.



Figure 6. *bantam* is evolutionarily conserved.

(A) Schematic view of the genome location of the *hsa-miR-450/542* gene cluster in a 1.25 kb region, which is 3.15kb from the gene AC004383. Lower bar shows the relative position of each miRNA (purple) and canonical Smad binding sites (yellow). Genes are oriented 3'-5'. (B) Three groups of mature miRNAs from *hsa-miR-450/542* cluster (five miRNAs total). (C) RNA sequence alignments of *Drosophila bantam* miRNA to its homologs in *C. elegans* and human. (D) Schematic bar showing position of human Smad5 sites for miRNAs from *hsa-miR-450/542* cluster. Sites for the human homolog *hsa-miR-450b-3p* are shown with a red arrow, sites for *hsa-miR-450-5p* are shown with a purple arrow, and sites for *hsa-miR-542-3p* are shown with a green arrow. (E) One example showing that a site in the Smad5 3'UTR can be recognized by both human *hsa-miR-450-3p* and *Drosophila bantam*.

Figure 7

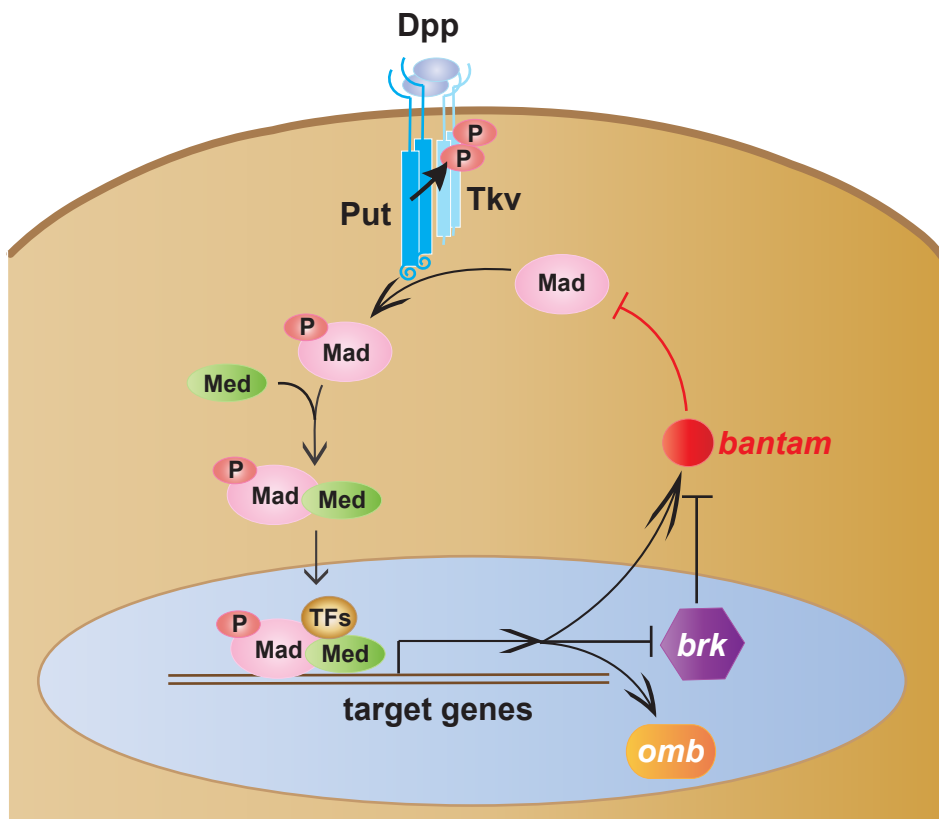


Figure 7. Regulation of *bantam* and Dpp signaling in *Drosophila* wing imaginal disc cells.

In our model, we propose feedback loop regulation between *bantam* and Dpp in the wing imaginal disc. First, extracellular *dpp* ligands bind to the cell surface type I and type II receptors, Put and Tkv, respectively. Constitutively active Put phosphorylates Tkv, which in turn phosphorylates the R-Smad, Mad. P-MAD forms a complex with the Co-Smad, Medea, and translocates into the nucleus, where tissue specific transcription is activated or repressed with the cooperation of other transcription factors (TFs). In the cells expressing *bantam*, Dpp signaling can be fine-tuned by *Mad* protein levels through the inhibitory effect of *bantam* on *Mad*. *bantam* is up-regulated by Dpp to further ensure the appropriate Dpp activity for developmental requirements.

Figure 8 *bantam* gene with upstream 15kb sequence (BDGP5.13:3L:627208:642288:1)

```

-15000 GGGACTAGCT TGGTCGTAAA ATAAAAATGTT GAGTTGTCCT AGAAAAAATC GTAATTCGGC
-14940 TTACGTAATA TCCCTCTGTG GACCTAATCT AAGCAACCAT ATTTATAAGA TATTGAATTG
-14880 CACCTTATTT ATATAATAAT AGCACGTAAT TACTCTATAC ATATTTCTAA ATATTCCTTT
-14820 CCCGCGTCGT TCCCGTACAC TACACAATCA TTAAGAAACG CCATGTATTG ATTTGACTTA
-14760 GCCTTAATCA CATGGCAGTG CAATTACAAT GCTGATATAA ATAAAAATAA ACTCGTTTTA
-14700 CGCTTATTAT TAGAACCATT TAATGCTGGT TGCTAATTGT TTTGAGTCTA AATTCTCATT
-14640 TACATGAGCA AACTGTTCTG TACTGGCTTG TTTATAGATA TTCGGGAGGA TTAAAGCGAA
-14580 ATAAATACGA ATTGATGGAC CTTAAATACA TTAGAAATGT CGACGTACAA GAAATAAACC
-14520 AAGAAAGCTA GGTTCGATT ACAATTTTTT GGATTGTTTA AAAAATTAAA ACTTTTCAAA
-14460 GGGAAATCCA AACGTGCAGA CGGCATAACA CGGATAACTT TTGTTAATCG ATTAACAAAA
-14400 CTTTCGTAAA TTATACACAA GTTATGCAAA AATTAAAAAG CCATTCGAA ATTTTGGATC
-14340 CCCAAAACCG CAAACCATGC GATAAATAGT TATGATTGCC TTTGCCAAAT CGGCCATTTT
-14280 GCTTTCGATC GTTTCGTTAA TGAAATTTTC TCGCTGTGCT TAGACACCGC TCTCGCACGC
-14220 CAATGCAATC GAGCAGCTAG GCTTTCGCTG TAGGCGAGAG AGGGACGGAG CAAGTATCTG
-14160 GGCAGTGTG CGTGTGTGTG TGTGTACGAG GTTGTGTTTC TATGTTTTTC CGAACACTGG
-14100 GGAGCAACGA CAACAAAAGC AGACAGAGCG GGCCAAAAAA TGTTAGATGC CGACCGCCCT
-14040 CCGCAGGCC CGTTTCCAAT TCCGATTCCA ATTCCGATGC CGAGTACCC GATTGTGTGG
-13980 CGTCAAACCAT TACATGCAAA CTCACACCTA CAGGCGATGC CGGCAGAGTC GTCGGCAGAG
-13920 GCCGCGGCAA GCGCGCATTC ATTCATACTT GTTGCTCTGC TCCTGTATCT GTATCAGTGT
-13860 GAACTCCCCG CTAATGTGTT GGTGTGTTGG TGTATGGGTA TGTGTTGAT TGCGCCGCAA
-13800 ACTAAAGTTT CGTGAGGCAT TTGTTTCAGT ACGTCACCGA CAGTGCCATC GAAAAGAAGG
-13740 AGGAGGCGGT GAGCCGACT CAGCACTTGG GAATTATAGT GTGTAGAGTG TTGAGTATGG
-13680 AGTAGGACTG TCGCTGGCAT CTGCTCACAC TGTTAAGGGG TTCTTTGTCA AGTAACGTGC
-13620 CGGGATTCTT TCAATTCTCG AATCTTTAAG AGTCAATAGT GTCTTCGAAC AAGTGTAGTG
-13560 TACCTAACGT TTAAATTGCC CAAAAAAATT TGCAACTTTT TTACGACGCA GTTGCAAAGA
-13500 AAACAAAGCA AGCCAGCCAA GAGCAACTTA AACGACGTAT TTAACAATAA AAAAAAACG
-13440 AAAAAACCTA AAGCGAGAGA GCGAAACTA GGGGAACACA ACAACAACA ACGCGACAAC
-13380 AACAGAATT AAAAAACAAAC TCGCTTGCGA CTTTGTAGCC TCGCAACTGA ATAATTAATA
-13320 TTAGAAGCGG AAAAGTAAAT AAAAAAATA AAAAAACAA TAAATAAATT TCAATAAAG
-13260 AACC CGAAAC GCTTATACAT ACATATGTAC GTACGTACAT ATATAAGTAT TTGGAAAGAA
-13200 CAAAAAATGG CGCACAAAGA AACTGTGAAC TTATACAATC AAAAAAATTT TATTTGATTG
-13140 CATGTCCATA TATATGTATG TGTACATGTG AACTTTGTAC CAGTGACAAAT GACGACAG
-13080 ACGCAGATGA TGATTAAGGC AGCGATGATG AATGAAACTG TGCCCTACGC TGATGTACGA
-13020 CCGATGTACT ATCAATGAAA GGGCCTACAA GATACAGAGA TATAAGATAA ATCAAAACAA
-12960 ACACACCCTA TAACAGAGTT GTGGGGTGGG AGTGGATAAG CTCTTTATAC ACACTCTTTT
-12900 GGCGGCGTGC ATTGAACATA TTTGTCTGTT TTGCTCTTGC TGTTTTTTTG TACGCGACTA
-12840 GTTTTCCTCG TTTTCGTTCT TTTGCCTTTT TATAATACCC TCTGTGTATT TATTTAAAGC
-12780 GCAATGTTT TAGATACGAC ATATAGCCAG GGGGAGGGCG GCGATGGGG CTACGAGGGG
-12720 GCGGGGACCA GACCAGAGCT AGCCAGTCAG ACCGCTGTCG ACAAATAAAA CAACAAAGTA
-12660 AACTACAGAA ACAACTAAAA GGCAAACTTG CCTATCTGCC TAGCCTTATA TTGATGTTGT
-12600 TGGTGTGTTG TTGTAGCTGC TCTGTGTTGT GCTGAATTC AGTGC GTGTG CTCAGCATTT
-12540 AACTAACTG GCACACACGC ACACCAACAC CAGCGAACGG AAAACGAAAA AAAAAATTAA
-12480 AACACACCAA CACTCAACAA CAGCCACACA AAGAGGCACA CCAACAGACA CACCAACACC
-12420 ATCACACTGA GTTGTGAGGG CTGGCAGTCT AGTGCTTATA TAATCACCGT CTAATGGGCT
-12360 TTGTTTGTA GTATTGAATG CAATTTGTTT AAAAATGTTT TATTTCAATTA TTACGTGTGT
-12300 TAAATGTGC AGCGCCCTTG TGTGCATGCA GTGCAACTCG AACAGCTGTT TGCCATAACA
-12240 CAAAACAGCT GTTCCACTGC AAGTCCTAAA AAAGAAAAAA TAAGTAAAGG AAAACAAAAA
-12180 GAGCGACTGC GACGCCGGCT GCGCAGCCAT GTGTCCTTAC AGCAGTCAAT TTGAGAGACT
-12120 TTCTTGCGCA CCAAAAAAAT ATCAAGTATA CGCAACCGAC ACCGCAATCG GGAGAGCGAG
-12060 CGAGCGACCG AGTGCTCTCT CCCCGGGCG TTGCCAGATT GTCATTTACT GTTATTTAAG
-12000 TGAATCCATA TACAGGCAAG CTTGCGAAAG GGGAAACCACA GTTGACCCGG TAAATTAATT
-11940 AAAACTATTA TAACTGAAG CTTAAAAATA ACTATTATGG GTTATACCTA AAATTAATAA
-11880 CACTAACCGT GCTAAAAATA ATATAATTCT TACAAATTGA GCTTGAGCTA ACTGATCTTG
-11820 TTAATAATAT TATAATATTG TAGTGTGAGC ATTAATAAAG TGTTGCATAC TTTTGAAAT
-11760 GTTTTATCCC GGTAAAGCCC ATATCCAGG CAATTTTCTT AAACGTATTG AGTTTAAAT
-11700 GTTTATTTTG TAACAAATTT TTGTTTCAGAA GGACAAATGG TTTTCAATTA CAGAAGTCAA
-11640 CTGCAACCCA GTTAGCGTAT TTGAATGAAA TCACTTAATT CGATAATTGA ACATTGTTAC
-11580 GAGTATTATT AATATTTTTT GTGCGCCTCT GGTAAATTGA AACCCATTAG GGTGCCCCAA
-11520 GCGCCGCGGT AATTGCGTGA GCGCAAAAC TAGTGCGCAA AATGAGTTTG CAGCCCCAAT
-11460 GCGTATTGTC CGTACTATAT AGTACGTAAT AAACAGCCAA GGCGCAATAT GCGCAGCTTC
-11400 AATACAGAGC CGACAGATAC GGATACAGAT GGGCACACAC TAAATAGTTT TTCGGAAGGG
-11340 GTTTTCGCTG TTTTCGGGCT TTCGGGCTAT CGGGCTGTCG GGGGCCGAGG CCTACCCAGT
-11280 TCTGAATGGT TGCTGTGGGC GTTATTGTTG TACTTGGAGG CGCTTATTC GAGCCTCAAG
-11220 TTCGCATCGA GGAATGAAC TGGCAACAGA GTCGCCATGT GTATCTGTGT TTATAGTTAT
-11160 TGTTGTATGG TAGTTTTTTC TGCTTTTTGT AGTAGTTTCT GTCTTTCTAT TATATTTAAA

```

```

-11100 TGCGCAATTA AGATTGGCAC TGCCCGTGGC AGCGCAACAA CAACACGAAA CACAAGAAAA
-11040 CAACAGCAAC AGAAGCGGTA ACAAGATCAA AGTATTCACA AAATGAACC AGTTTGAGTT
-10980 TTACGCATTT ATCATTCGTC GTCCGAATCT GATCAAAATC GCACAACCTA AATCCGCGAA
-10920 CAGCAGATCT TTGGCTGTAG ATAAAAACA CGAGCCAAGA ATTAAAAATA TTTCGTTTTTC
-10860 TGGGGGTAAA ATTAACCACA TGCTCCATGT TCCATATTCG TGATTGATCG ATCCGCTTTG
-10800 ACACGAATAT TTTGTTTAAT TTGTGGGAAC CAAAACATAA TGGCAAGACA TTAAGGGTTT
-10740 AACTACAAAT TGGTAAGACA GGAATGTTTG TCAAGCCTCC AATTAGCAAG TTGCTTTCTC
-10680 TTCAAATGAT AATGTCACCT AATGGGAAAT GCGTTTAGTC AGAAAACCTAC AAGTGAATAG
-10620 ATATATATAT ATTTCTGTTT CTGTCACCTT GATTCCAAC TATTTGAAGA TTTTAAAGAT
-10560 CCAATATTAT ATATTAATAA CTTTGAACCA AAATATAACG TATACGTATG GTAAAAATTA
-10500 AATTTCCTCAG CTTAAACACG CGAACATTTT AAAACTATAG AACTTCTCTC GAGCTGCAGT
-10440 GAACTTTAAT CCAAAAAATA CTTATTTTTA AGACACCTC TATCCTAGAT GCTCTATGAC
-10380 ATTTTATGGC TTTTAATTGA CCAGACGCTG TCGACATGT CCAACGATAA TGATCCGTTT
-10320 AGTTATTTTT GTATAGACAG CGATTTATTT ATAAATGCCG CGACGGATCT CTCCTTCTGC
-10260 CAGCTATATT CTGCTAGCTA TATCTGCCAC AGTGTCTGCC ATAATTAGGC GCACAGTTGG
-10200 CGCAATTAA GCGCTGGCCA AAGTCTTTTA CAAGCGAACG TCATCGAGCA GCATAAATAA
-10140 TCGCAATCCA AATACGCGCG CAACAAATA TTAACAAGAT TTGAGATCTG AGAGGAAATC
-10080 GCGGCATCGC CTGGAAATCG TTTAGCTTCT TCGTCTTTT TTGTTTGGCT CTGACGTAAA
-10020 ATGGCCCGAG TCAATTCGA TTTCAATTCAG CTCTCGATGA CGTACACATT GGCCTCTCAA
-9960 CGACCACCAC ACACCGAACA CCACCCACCG CCCACCACCC ACCGCACAC GGCACCTTAC
-9900 ATTGCCGCGC CAGACAACCT TGTAAAGTTT TTGTGCGTCA TTGCGCGCTG CTATTTTTTC
-9840 AGCCACGGCT CTTTCCCTTC TGGGCAGCCG TTGTTTTGCA ATATTATCGC CGCCGCATCT
-9780 CCAATAATAA TATCAACTCG TAAATGTCCA GGCCTGCGC AAAAATTACA CAGATATATG
-9720 TACATGTGGT ACATTCATAA GTTTCCTTGC GTGCGTCATA GTTTTCTGTA ATTCTCGATC
-9660 TCGTTACTGC CTGGCCATTT CCATATCTAC TTACAATATG TACATATATG TATGTATATA
-9600 TATTTCTAAT CTGTCGGCGG CTGTGTATCG TACTCATCGA GTTTCCTCCG AAGTGACTAA
-9540 GTGGCATGGC TACTTCTCG GCTATTCTGG GCTTATTTGT ATATGGACTT GGAGCTGGTC
-9480 ATGGATTGGT TCTGGTTCAT AGGTCGCTG TGAATCAATC TGCAAAATGT CAAATTCGAT
-9420 TTCTTATTCT GGGAACTATC AAATCGTTGC CGTTTTCTAA TCTCTATAAA TACCAAGGGT
-9360 CGTTAGAAAT TCAGAGAATT CTTAGTGAAT CAGATCGGAC TTAGTAGGTA GTTTTTTACG
-9300 AGTTGCGACG AGTTTTTAAA TACTTTTCTC TAAGCGCCAT ATGTCCTTTT TTAGCAATAA
-9240 TAAAAAATAA GCAATTAAGT GGCACCTCTA ACTAGTGCAG ACTCAGGACA ATTCAGGCAA
-9180 ATGCGAGGGG TTGAGATTCC TGAGGACTGA CTGACTGACT AGCTGAATGG GTATCAGAAC
-9120 CGACCACATC GCCTTGGGTA TTCTGATTCA GATGTACATG TGCCCCCGG ACATCGTGCC
-9060 ATATCAAAATC CTATATAATC CGAACAAGAG GCTGGGAATC AAGCGTGTAT TCAAGCGACT
-9000 TATTTAGACA CTCGCTCGCA TTTGCACTTG AATGAGTTAG TTGTGTTGTT TGTGTTGTT
-8940 CGGTTTACTT CCGTTGCTAC TATAATGGGT GTACGCGAGT GTGCACGTGT GTGGGTGTGC
-8880 TGAGCGTATA TATGCGGATC TGAGTGTGGG TGATGTGTG TATTATGTTT TTGTCGCTGC
-8820 CTGCGATTTT CATTCATTAA ATGCAAGCGC AGCACACACA CACACACATG CGCAGATTGC
-8760 GACGGCACGC ACACACGAAT ACGTATTCGA TTCATTCTA AATTCATGCA GCAGCAGCAG
-8700 CAGCAGCAAC AAACGCCGCC CCCTCCTCCC ACGCTACAC TGCGGCCTCT GCCACTGGCT
-8640 CTGCTCGCT GGGCCTCG TATCATCGT CCAACAACA CAAAAACGCG AGCACTATGG
-8580 CAGCAGCAAC CTCAAATGCG CTCTTGCTAC TGCTGCCGAT GCCTGCAAG AAATGACGCG
-8520 AAATATGAA ATATCCCAAT GCTGGAAATA ATAGTTTTTG CTGGTTAGCG TGATTTTTTG
-8460 GGCACAGAAT CTTTTCAGT TATCGTTTAA AGAAAAATGT ACCACTTGCT AGAAAAATAA
-8400 TGTAGCCTAC TTACCAGCTT TAAATGCTTT AGAGATTTAA AAAATATTTA ACTATTCAGG
-8340 CACGATTTCT TACTGTGTCC CTCTGTTTTA TCTCTGGCAA ACATCGCACC GTGGTTCGCG
-8280 TTCCAAGTCT CCATTTCCAC AATTTCCTCC TTCCAACCCC CCTCCCAATG CTTCTGTTGA
-8220 TTTTATAGAT TCGTCTCTAA TTTCAATGAA ATTCATTGTA GCACGCATAG CACGGCAGCA
-8160 ACAACACCAT CAACAATCAC TGATAAGTTC GGATCGGATC CGTATCTCTA TCGTTTGTCTG
-8100 TTGTTTGCTA TGGGGTCAGT CATTCAATGG GATCGACCCG AGCATAGCAT GCCCCATCCA
-8040 AGTTCCCTTA ATGTGCTGAT TTCGTTTCA CACAATATAC GATTGTGTTT GCAATTATGG
-7980 TAATAAAATA ATAAAAACTC TATTAAACGT ACTCCCGGTA CGCGATTATA CCAATAACCT
-7920 AAAAAAATAA ATGAGAACTA TAAATAAATG GTACATACAT ATATACGCTA CAGTATCGAT
-7860 CCAGTATCAG TCGGAGTCAA GTCTTACTTG GCCAACTCTT GGCATCTAAA ATTGAAATTA
-7800 ATACTATCCC ACTAATATCG ACCCTGTGAC TACTATTATT TTGCCACAA CTGTGATTAT
-7740 GCACTGTGTA CGGTTATGAA TGAATGAAGT TCACACACAC TCGCACACTG GCACTCACCC
-7680 ACACGTGCAG CTAGCTACCC ACACATACCC AACTCGGGT TTGCTTCGTC GGTGTGGTTT
-7620 TGGTCACTT ATTTCCGGCT GGGCGCTTTT GGCTGGGTTT ATATTTATAG CTGGGCTGTC
-7560 GGAACCTCTT CTTCAATCAG AGCGTAAGTCT TCTGCCTACT TACGGCTCTT CACCAGGTGC
-7500 TTCTTCTCTG CCTTGTGCTT CAACATGTTG CACACTTAAA AAAAAATCGG ACTTCTTCTG
-7440 AATACAAAAT TTAAGAGCGT TTTAAAGGGA GAACTATTTA ATGGAAGGAA TGTAAATTTG
-7380 TATATGTTCA TTTCAAAATC TCGAAGATGA AATTTTTTTC AAATTAATTT TCAACTCGA
-7320 TTCCAAGTG ACTTTTCTCT CTGTGTGCTG TGTGTGCCAC TCCAAAAATG CAGTTGGCAG
-7260 CACTTCCTCA TTTGGACGCA CCGGAAGTGA GCGGAAATGC TCGCACACTC GCATTAGTCA
-7200 CTTTTGTTTT CACTTCTTGA GACACCCGCC CGCACCATGT GTCCCATATA TCCCACATA
-7140 TGTATATGTA CATACATATA TCCCACCTT AGCTTCCGTT GATAAAATCC AGTCCCGCA
-7080 CCTCCCGTCC CGATCCCACT GGCTGCTATT TATGGCGAAA GTGTTTGGTG GAGTTTGTGA
-7020 TTGTTGGGCT CCCGAGTTCA ATAGTGCTTT GAACTCTAGC TGCCCTCTTT GCCGTCTCTT

```

```

-6960 TCGTTTCGTG TGTGTCTGAC TCTTTCTGGC TGGGAATGCA TCGAAAATAG AGCGGCAAAAT
-6900 TGTCTGGCTG CTTCTGCTGC TCTTGCTGCT GCTTTGGCTT TGGCTTTAGC TTTAGCTTCA
-6840 GCTATAGCCG TGGCGAAAAA GGGCGAATGA ATGGGTCTCA GATCAGGAAA GGC GGCGGCG
-6780 GTGGCGGCAG AGCGGGCGAC GACGATTGTG GGAGGGGCAC TACTTCCGCT GCGAGGCTTA
-6720 CGCAAAAAGA CGTTAAATTT ATGAATATGA ATGAGCCTCC TCCACTCGCA GCGATCGCCG
-6660 GTCGTCCGCA CGCTGCATC ACATGGCATG GAGGCAACGA AACTGGGCCA AATGTCATTA
-6600 ATACATCAGA TCCGGACATG CGAGCGGGAA GCATATAGCA AATCATGCGT TGACAGCGGG
-6540 AACCACGCAG ATAGTGACGA AGAGGGGGGG GAGGGGAGTC TCGTAGCATC TAGTAGGCCG
-6480 GGCAGCATTG GCCGGGGCGA CGCCACATT TGGAGCGGAT TCCAACTCC GACGACGACT
-6420 GCTACTCCTA CTTGGCCACA TCCACATCCG ATTGCAGCCA GCTTGTGTGT GGTTGGCCGA
-6360 GGAATGTGCT ATTATTATGC CAACCGAGCG AAGAGAGAGC GCTTGGCCAC TCCACGATTT
-6300 TCTGCATCCG CCTCGCGGGA ATGCGAATGC CATAGAACGG GGTGGGGTAT ATGCTGTTTA
-6240 GGGAGCTTAC CTAGATGTTA GTTGATCGAA ATGCTACAAC TTCCACTATA TAGTTATTTA
-6180 AAGATAAAAG ATACATATAT ATAACCCCTG GTCAGAACAA AAGTACGGCG CTTTTGCAAG
-6120 TGTCGGCATT GGGCCAGTGA CACAGACTTG TGAAGAGACA GAGATGCGGA TGCAACTATC
-6060 CAACTGGAAT ATGGCCACAA AGGCGGGCGC TGGCCAGTGC ATTCAACTGG AATTTGGGTC
-6000 GGGTGGCGTG GCAAGATGCA AGCGGCAAGA CGCTCGAATG CGCTTTCTTC CACAGCCACA
-5940 GTCACATCCA CTGCCATTTC CATATTCACT CCTGCTCCGG TTCTTGCGCC TCCCCCCAA
-5880 TTTCCCCCTT TCATTATCAG CGGGTTCATT CAGGAGGGAA ATGGGGACTG GTGGGTGGGG
-5820 CCGCGTGCGT CGGGCGGTTT GTTAGCGGGC CAATTGTGTG CACTACTGCC TCTGTTTTTC
-5760 TTTCCATTTT TTTTCTGCGC TTTCAATTGT GCGACTTTGT GCGCGTGCCC AACACTTGTA
-5700 TGCTAATGCA ACAGCCTTCG CTTTCCAGC ACAGTGGGAA CAGAAAAGCA GTTACCCGAA
-5640 CAAAGCATAT GATTTAATAT AGATGTATAG GTATATTTTT TGATATCCTT TAGGATCTGT
-5580 GTAGATGTGG TGATAGATCT CTTAGGCATT CTTACCAACC GGACATCAGC TTCAGCTTTT
-5520 ACCCGTCCGA GTACCAATCC GACCCACTGT ACCGCCCAT TGCTTCAATT GCAGTTGCAG
-5460 TTGATGGCTC TCGAGTGTGC GTGTGCCCAT TTGCAGCGG GTCAGCGTCA GCGGCTTATC
-5400 TCCTCCAACC TGGCGGCGAC TGCGGCGACTG CACCACCGTG CAAATGCAAC TGCACCTGCG
-5340 AGTGCAACTG ACGAGCCACT GTTAATTTTG CCAAGTTTTT TTTGCTGCCC AGTTTTTGCT
-5280 GCTGTGCAAG TCTCTCATGC ATAAATTTGT ACACGACATA ATTTTTTCATG AAATGGGTGG
-5220 GATCCTCCCG GTGC GGCGTC GTTGTGACG TCTTTTTCCG ACATCTAACC AAGTCGAGTG
-5160 TCGCGGTATC TACTATATAG CCACCGGCTA TATCCACATT CACATCCATC CCGTTGCGGT
-5100 TGTTTTGGGC AGGTTCCGGT CACTTTTTGC CGGCTGACCG CGCTCACTCG AGTAGAAATT
-5040 ATGTGCAATT TGTCTAGCCA GGGGTCTGCT CTCTAGTCTC TAGACTCTAG ACTCCACAAC
-4980 AGTCTGCAGT TCGATTCCGA TTTCAATAGA CTCCGCCGCG CCGTGTACGG TTGCACATAA
-4920 AGGAAGTTCG CTGGTATAGT GCAAATTGAT AGGGTTTTAC TATTGTTTTT GGATTGAATT
-4860 ATTTATTTAA GTTCAAAATG CAATGGTTAA CATAACCACC CCACTCTGTT ACTTGATACA
-4800 ACTGCTGATA TACATATGTA TGTAAGAAGA TTTATGATTC GATTCCTCTA GTTTCTCCAA
-4740 GTGCATTGCT GCTTCTTAAT GATCGGTGGG CAGTATGCGC ATCAGTGCTT TCCTATTAGA
-4680 TCGCGGTATC TATCATTAGG TTCGGTGTGG TGTGCTTCGG TTCGGTTCGG TTCCGTTCGG
-4620 GCCGACTTTC GACCAGGCCA AAAGCAATTA CACCGAAAGG GGGAATTCTT TTGCCATCGA
-4560 ATCGGATCGC ATCTACCGTA CGATCGCTGA CCATGCAGCC GGCTGGAATG GGAATGGGT
-4500 ATGCGAATGG GAAGGAAAAA GGTAATGCCA GTGCCAGTAC CAGTGCTCTT GCCAGTCCCT
-4440 CCACGTCATA GGTGTGCTCC TCAAGTGGTG GTATATCGCG GCCCTGCTGA TAAGTTGTAT
-4380 TAATTATTTT TATGTCTCTG ACGTTGCTCC GTTGGTGTGG TAAATAGTAC AAACAGTCGG
-4320 TCGAAAGTCC AAGAAGCTTT CGATTGGGAA ATCTTGCTTG GTTTCCCTT TGTTTTTTTT
-4260 TTTTTTTCAA TTTTCTTTCA GCGGATAGAA GAGGAACAGA ACTCAATTTT CGCCTGAGGC
-4200 CTAATCTTTT CCACCCGCTA AGTGCCAGTG CCATGTGATT CAAACTTGAG TATTTTCGTA
-4140 CCCTTGCGCT ATGTTTGTGG CTACAGGGCT ATGGCATCAC ATGTCATTTA TAGTTGGGCC
-4080 TACCGTCTGT GGCCTGTGTA TAAGCCGTAG ATTGAGCGCG TGCTTTGTGA CTGGGCTGCT
-4020 TGGGTCTGGT TGCTCCGGGC CTTATTCGCG GTCTACCGAG GGGTCCACAC AGGTGTGTGT
-3960 ACACCTTCGA AATTCAGAA ATTCTTGCGT CAAGTAGCCG CCCCAGAAAC CTTATCACTC
-3900 AGACGATCGT CCATCCACTG ATTCCTGAGT TGCTCCACTG GAGGGCCGCG AAAGCGACGA
-3840 AAGCTTGTC AATGGATGGCA TTGATACGGG GACAGTTGGC TGGAATTGATT GGTTTGATTG
-3780 TGGGCCATCG TAAATACACC TGGCGCTCGG TGTATTTTCA GGAAATTGCT AATCAGAAAG
-3720 ATGCACAGGC TTAACCGAAT AGAATTTTAT ATTATTAGAT TAAATCAAGT AAATTTAAAG
-3660 ATCTCTTCAA GAAGAAAATC CATTCGAGTT CCATTCCCAT AAAGATCTAT ATCTAGATTT
-3600 AGTTCTAAAC AGAAATTACT TCTAGCTACT GAAAACCACG ATCAATCGGG CCTAATTTAT
-3540 TTCCGTTTTT GTGATATTTT CGAGCCAGTT GGGGATTGTC CCATTGGGCA TTTGATATGC
-3480 ATGCAGCCGA CCGATACAAC ACTCCTCCGC TTTTGGATCC AGTAGATCCC CCCAGCGATC
-3420 TGCGGCCATA AATAACCACT AAAGCCTATG GAATTTCTTA TAAATAAGTT CATGACGAAT
-3360 GTAACAAAAA TTCCCGGAGC AACCTTAGCC CCGCGCCCTT CTTTACAAAT GTGTGTGTGT
-3300 GTTGTAATAT ACCTCGTTCA CATAAAGTTC AGAAATTTCA TTTACAAACT TGTAATTGAA
-3240 AAAATCCACA CACACACGAG CGAGATTGTC TAGAGACAAA GTCAAACACG TTGGAATTTT
-3180 TGTTTTTTAC CGTTCAATGA CGAATTTTAC AGAGTGTGTG TGTGTGTGTG TGTGTGCGTT
-3120 GTTTACGAAA AACAAAAAAC AGAACGCCAC CAGCTACAAA CACACAAAGA AAAACAAAAT
-3060 AAAAAATAAA AAAAAACGAA AATTCCAAAA AGACACTTAC GAAAGCCCCG CAACATTTTT
-3000 TATTGTTCCG TAGATTACAA CACATAGGAA AACGCGAGAA GAGCTGAAAA ATTTTCGTTG
-2940 TCGAGGAGGA GAGTGCGCTT CACACCGATA TATCAGTATA CTGATGTGAC AAAATGCAAA
-2880 AGTAGCACAG ATACAAATGC AGATAGGGAT ACTCTTCTCG CAGTCTTCGA AAAAGAAAGG

```

```

-2820 GTCTGGAAGG GGATCGACTG GAAGGGGCAG TGTCGGTTTG TTGTGGAAT GCCGTTTGTG
-2760 AAGTTTCTTA TGCATGCGAC TTCAAACATA GTTCGGCATC GAAACTTTCT AGCACACCGA
-2700 CACACATACG AACGCGATCC AGCCGACACA CACACACACA CGCACGCAGC CACACACTTA
-2640 AGCGACTTTC GAAAGGTACA ACTTTTACG AAGTCGCTGC CTCGGCCGCT GTGCAGCCGA
-2580 CGCCACTGCC GCTGCCGCTG TCGCTGCCTC TGTCGACTTC GAATTCCAAC GCCAAGATGA
-2520 AAGATCGGCG CAAAAGAAAA GAAATATTCA TTCAGTAAAA TTTCATAGCT GCAGCCGCAT
-2460 GGTGTGTCCG CTCTCGCCTG CTCTTGCTTT TCGCGCAACA AACCGAAACG AGAAACACAT
-2400 AAATATAAAA GTGTGAACAT TGGCGTACAT ATAAAACTT AAAACTTAAC TTAACCTGAG
-2340 CAACATGAAA CAAATAAACA CGGGAAGCG GTTCCAGCGA AGAGGTTCCA AGGAGAGCAG
-2280 ACACAACCGC ATTCCAGAAA GTTTAAATAA CGCTGGAAGG AGGGGGAAG TGGAAAACTA
-2220 AACTCGAACT CGAACTCAGT GTGCCAGTGT ATGTGTGTGG AATGCAGAAG AGGAAGAAGC
-2160 AGCAGCAGCA GAATAAGCAG CGAATAGAAA ATATGTCTTC AAAGTGGTTT TTCGGTTTTC
-2100 AGACTGTCGT CGTCGGCCAA TCGGGTTCCA TTGACATCCG AACGAAAAAA ATAATGCCTA
-2040 ACCTTCGGG GGAACACTCG TAAGTCGGA TCCACACACA GCATGCACAC ACAACCCGT
-1980 TTATTGGCTG AAATTGGATG CTGTGTGTAT GTGCGGTTAT TTAGAAATTC AAATTGAAAT
-1920 TTTTCAAGCG TGAGTCATGC GACTGAGCGT GGGTTTTTGA GACCCGTTTC ATCTTCCCG
-1860 ACTCGACGAT CCTAACCTTC ACTGAGAACA GGAGTTAGCC GCCAGAACGT GAATGGGAAC
-1800 AGAATCGGGA ACGGGAACAG TCATAAAAGT TGCATCACTC AGCACAAAAA GACGAAGAGG
-1740 CGGGCAGACG GAGACACAAA CAAGTCAACC ACCAGCATAG AATGCGGCTG CCAGACAGGC
-1680 GAGACGCAAA TAGTAGTGGC GGCAGAGAAA GGCGCGACAA GCAGAAGAAC CGTTTTACTG
-1620 AGAAAAGAAG ACCGGGCACG CCGCGTCA GGTCGAGCGG GATGGCAGAA CAGGCAAAGG
-1560 GAAAAGGGAG CGAAAAACAC TGAGAGAAAT AAGAGTAAGG TGAACATGAA AATTAAAAATC
-1500 TTAAGTAACT CGTATATTCT TTGCAGCAAT ACTGTGGTTA AACGACAGTC AATTAAAAAT
-1440 TTGTTTTGTC ATCGTAAGAA AATGTACCAC ATTGAATATC TAAGTTTAGA ATGTTGAGAG
-1380 TCGTTTTTCC TTAGCCTCAA AACTTCGTAA TTCAAGCGAT ATTAAACGTA ATATTTTTTC
-1320 ACAGTGCAT CGGTCTGTCT TTCGCTCAG ACTTATCCCG TTGTTTTGTC AGTTCTCGT
-1260 CTGCATTCCG TTGTTTCGTC CGAAAAACAA ATTCAGCAGA AAAAAGGCC TTCAACGGGA
-1200 ATATCGATAT GATATCGATG GGAGAACCGA TTTTTCGGGA CCATTAATTT GCATATGCGA
-1140 AAATCGAAGG AGTTACAGAA AAGGGCAGCA AGCGGTGCGT TTAATATCCA CAACATAAAT
-1080 GTCAATTAAG AACGATATTT GTATTGTCAA GTGCGCCCG TCGCATCGCC ATAAATGTGT
-1020 TATAAAAAAG CTAACGGTTA ATGCTACGGT CTGCTGAAGT TCATGTGTGG AAGAGTGAAA
-960 AAAATGAGAA AAGAGGGAAG GAAACAAAAA CTATTCGCCG CTCAATAGAA AGTTTGTGTT
-900 AATAAAAAAT ACCTAAAAAC TTAACACAC AAAATATGTG TGTCGAAATA TGTATGCGAG
-840 CAACAAAAAA GAGTGAATGA AAAAAATGTT ACCTAATTTT CGGGGCCAG TTGGGGTTGT
-780 TGTTTTTGGT CTGTTTTATT TCAGCAACGT CGACGGTGGC AGAGGCGCG CATACTTTCC
-720 CACACAGCTT CCAGCTCATT CCCATTCCAG ATTCCAGGCC ATTCCCAGCA GCGTGCATC
-660 ATCGCGGGAG CAGCGCCACC GTTCCCTTCG CACGCTTTCC TCTCCGTCCC GCTGGAACGA
-600 CGTCTAAATT AATGATTGTT AAATGGAGAT TGTGTATTTT ATGTTAGTGT GTATGTGCTA
-540 GGCATCCAC ATACCAATGC AATTGGAGAA ATACGGGCGC GCCTGCGCAG AAACATTTTA
-480 TAAAGGTATG TAATCCCCAA TTTGATAACT CACAGGCATT TTACAGTTCA TGTCCCCCAC
-420 CAAAAAAGAA AAAAGCAAAA ACTCAGCGCC ACTAATTGTG TGCTATTTTT ATGAAACAAA
-360 AAAAAAAGAA AACGAAAGAA AAAGAAGGAA AGAATGAAAG ACTAAAACCT TAAGATCATT
-300 TTTTTTTTCT CGCGGCGCGT GTGAAAATAT TTAGGCTAGC CAAGGTATTT TTATTCTCGC
-240 CTCTTGTGGA TCTTTTGAAT CTCTCGTTCT TCGCTTCTCT GTGCTCTTTC TTGCTTTTTTA
-180 AAGTGTTAAC TGGCAGCATA TAATTTTCGGT CGACTTGACA TACATTATAA TTATAGTTAT
-120 TAAATGTGAG CCAGGCACGT GCGTGAAAAA CGCTCAGATG CAGATGTTGT TGATGTTATA
-60 AAGACCACGA TCGAAAGAGG AAAAAACGAA AACGAACGAA AAGCGTTTGT AACTCCAATG
1 ATTTGACTAC GAAACCGGTT TTCGATTGTT TTTGACTGTT TTTCATACAA GTGAGATCAT
61 TTTGAAAGCT GATTTTGTCA A

```




	Mad binding site (GRCGNC)	(36)
	Brk binding site (GGCGYY)	(16)
	Canonical Smad binding site (GTCT)	(39)

Figure 8. Sequence analysis of DNA 15kb upstream of *Drosophila bantam*.

Consensus binding sites for Mad (yellow), Brk (light red), and the canonical Smad binding site (green) are indicated. Note that some consensus sequences (orange) are identical for Mad and Brk due to variations in the consensus sequences.

Figure 2

Sequences in yellow box	Canonical Smad binding sites
Sequences in red	miRNA genes
Homo_sapiens >	chromosome:GRCh37.X:133674215:133677367:1
Gorilla_gorilla >	chromosome:gorGor3.X:132475478:132475656:1
	chromosome:gorGor3.X:132475657:132476819:1
Pongo_pygmaeus >	chromosome:PPYG2.X:133999430:133999604:1
	chromosome:PPYG2.X:133999605:134002584:1
Macaca_mulatta >	chromosome:MMUL_1.X:132765568:132765746:1
	chromosome:MMUL_1.X:132765747:132768705:1
Mus_musculus >	chromosome:NCBIM37.X:50401175:50401353:1
Rattus_norvegicus >	chromosome:RGSC3.4.X:139994793:139994969:1
Bos_taurus >	chromosome:Btau_4.0.Un.004.53:440327:440512:1
	chromosome:Btau_4.0.Un.004.53:440513:443497:1
Canis_familiaris >	chromosome:BROAD2.X:108239025:108239209:1
	chromosome:BROAD2.X:108239210:108241955:1
Equus_caballus >	chromosome:EquCab2.X:106948655:106948840:1
	chromosome:EquCab2.X:106948841:106951656:1
Homo_sapiens	ATACAAAACCTATGGATGCAAAATGATCCCAATACACTTATATTACATATTTCAGGAACATATTGC AAAAATAATTCTGCATCTTTACATTTATCACAGA-----AGTAAACCACAGATAG
Gorilla_gorilla	ATACAAAACCTATGGATGCAAAATGATCCCAATACACTTATATTACATATTTCAGGAACATATTGC AAAAATAATTCTGCATCTTTACATTTATCACAGA-----AGTAAACCACAGATAG
Pongo_pygmaeus	ATACAAAACCTATGGATGCAAAATGATCCCAATACACTTATATTACATATTTCAGGAACATATTGC AAAAATAATTCTGCATCTTTACATTTATCACAGA-----AGTAAACCACAGATAG
Macaca_mulatta	ATACAAAACCTATGGATGCAAAATGATCCCAATACGCTTATATCTACATATTTCAGGAACATATTGC AAAAATAATTCTGCATCTTTACATTTATCACAGA-----AGTAAACCACAGATAG
Mus_musculus	ATACAAAATTATGCATGCAAAATGTTCCCAATACGCTTATGTTATTCAGGAACATACTGC AAAAATAATTCTGTATCTGATTCCCTATTATAA-----AACAAACCATAAACAA
Rattus_norvegicus	ATACAAAATTATGTATGCCAAATGTTCCCAATACGCTTATGTTCTTATACAGGAACATACTGC AAAAAGAATTCCGTATCTGATTCCCTATTACAAA-----AACAACTCTCAAGTAA
Bos_taurus	ATACAAAACCTATGGATGCAAAATGTTCCCAATATACTTATATTAATATTTCAGGAACATATTGC AAAAATAATTTCGCATCTTACTTTTATCAGCTTTATGATATCATAAATCCACAGATAA
Canis_familiaris	ATACAAAACCTATGGATGCAAAATGTTCCCAATACACTTATATTACATATTTCAGGAACATATTGC AAAAATAATTTCGACCTTACCTTTATCTACTTTATCATATTGCAACCCACAGATAA
Equus_caballus	ATACAAAACCTATGGATGCAAAATGTTCCCAATACACTTATATTACATATTTCAGGAACATATTGC AAAAATAATTTCGACCTTCCCTTTATCTACTTTATCATATTGCAACCCACAGATAA
Homo_sapiens	CCGCTGTTAGATTTTTTGGCTTATTCCTCCCATCTTTTCATCTGTATATTGATACAAAACCTATACATGCAAAATGTTCCCAATATATTTATAGTGCATATTAGGAACACATCGCAAAAACA
Gorilla_gorilla	CCGCTGTTAGATTTTTTACTTATTCCTCCCATCTTTTCATCTGTATATTGATACAAAACCTATACATGCAAAATGTTCCCAATATATTTATAGTGCATATTAGGAACACATCGCAAAAACA
Pongo_pygmaeus	CCGCTGTTAGATTTTTT---TATTCCTCCCATCTTTTCATCTGTATATTGATACAAAACCTATACATGCAAAATGTTCCCAATATATTTATTTAGTGCATATTAGGAACACATCGCAAAAACA
Macaca_mulatta	CCAGCTGTTAGATTTTTTGGTTTATTCCTCCCATCGTTTTCATCTGTATATTGATACAAAACCTATACATGCAAAATGTTCCCAATATATTTATAGTGCATATTAGGAACACATCGCAAAAACA
Mus_musculus	CTATGGTTAGACTTTCAGCTTCTTCTTCCCAACCTTTTGCTCTGTATTGACACAAAGCTATTAT
Rattus_norvegicus	CTAGGCTTAGATTGTCAGCTTCTTCTTCCCAACCTT-TGCCTGTGTGCGATGTAACACTATTAT
Bos_taurus	CCATGATATAATTTTGGTTCTCTCGCAGCTCTTTATCTGTATATTGATACAAAACCTATACATGCAAAATGCTCCCAATATATTTATAGTGCATATTAGGAACACATCGCAAAAACA
Canis_familiaris	CCGTTACAAGATTTTTTGGTGATTCCTCCAGCCTTTTCATCTGTATATTGATACAAAACCTATGATGCAAAATGCTCCCAATATGTTCTACTCTGCATATTAGGAACACATCGCAAAAACA
Equus_caballus	CCATTATAAGATTTTTTGGTTTATTCCTTCCCTCAGCCTTTTGTCTGTATATTGATACAAAACCTATGATGCAAAATGCTCCCAATATATTTATAGTGCATATTAGGAACACATCGCAAAAACA
Homo_sapiens	GTTTAGTATCGTTT-TTGATTGCCTATAGTGACACAAGTCAGCGATAACCACTCTAGACTTTTGGTATACTTCCTGATAGCCTCTTTTCCCATAT-----TATTGATACAAA
Gorilla_gorilla	GTTTGGTATCATTT-TTGATTGCCTATAGTGACACAAGTCAGCGATAACCACTCTAGACTTTTGGTATACTTCCTGATAGCCTCTTTTCCCATAT-----TATTGATACAAA
Pongo_pygmaeus	GTTTAGTATCGTTT-TTGATTGCCTATAGTGACACAAGTCAGCAATACCACTCTAGACTTTTGGTATACTTCCTGATAGCCTCTTTTCCCATAT-----CATTGATACAAA
Macaca_mulatta	GTTTAGTATCATTTT-TTGATTGCCTATAGTGACACAAGTCAGCGATAACCACTCTAGACTTTTGGTATACTTCCTGATAGCCTCTTTTCCCATAT-----TATTGATACAAA
Mus_musculus
Rattus_norvegicus
Bos_taurus	GTTTAGCATCTTTCTTTGAT-----GGACTTTTGGTATCCGTCCTCTAGCCTTCTTTC-CATATAATAATATGAAGATTGATACAAA
Canis_familiaris	GTTTAGCATCTTTCTTTGCA-----GGGCTTTTGGCATGCTTCTCTCCAGCCTCTTCTTC-CATAT-----GATTGATACAAA
Equus_caballus	GTTTAGCATCTTTCTTTGAT-----AGACT-TTGGTATACTTCCTCTAGCCTCTTCTTC-CATAT-----TATTGATACAAA
Homo_sapiens	ACTATGAATGCAAAATGTCGCCAATACATTTATATTACATATTAGGAACACATCGCAAAATAGTTTAGCATCTTTCTTTGGTGCACTT-TTATACCACAACTCAGAGATA-ATCACAAT-
Gorilla_gorilla	ACTATGAATGCAAAATGTCGCCAATACATTTATATTACATATTAGGAACACATCGCAAAATAGTTTAGCATCTTTCTTTGGTGCACTT-TTATACCACAACTCAGAGATA-ATCACAAT-
Pongo_pygmaeus	ACTATGAATGCAAAATGTCGCCAATACATTTATATTACGATATTAGGAACACATCGCAAAATAGTTTAGCATCTTTCTTTGGTGCACTT-TTATACCACAACTCAGAGATA-ATCACAAT-
Macaca_mulatta	ACTATGAATGCAAAATGTCGCCAATACATTTATATTACATATTAGGAACACATCGCAAAATAGTTTAGCATCTTTCTTTGGTGCACTT-TTATACCACAACTCAGAGATA-ATCACAAT-
Mus_musculus
Rattus_norvegicus
Bos_taurus	ACTATGAATGCAAAATGTTCCCAATACATTTAGATTACATATTAGGAACACATCGCAAAATAGTTTAGCATCTTTCTTTGAACTCTTTTATACACAATTCATAGATA-ACCACITTTA
Canis_familiaris	ACTATGAATGCAAAATGTTCCCAATACACTTATAGTACATATTAGGAACACATCGCAAAATAGTTTAGCATCTTTCTTTGGTGCACTT---CCACAGCAACTCCAGACA-ACCACATTTA
Equus_caballus	ACTATGAATGCAAAATGTTCCCAATACATTTATATTACGATATTAGGAACACATCGCAAAATAGTTGAGCATCTTTCTTTGATCACTTATTATGCGCACAACTCAGAGATAAACACATTT
Homo_sapiens	AAAGTTTTTATATGTTTCCCTCCTAGCCTTTTATCTGTATGTTGATACAAAACCTATTATACAGAAATGCTCCCTATATACCTATATTGCAGAGATGGGAA-----AATATTTTGCACCT
Gorilla_gorilla	AAAGTTTTTATATGTTTCCCTCCTAGCCTTTTATCTGTATGTTGATACAAAACCTATTATACAGAAATGCTCCCTATATACCTATATTGCAGAGATGGGAA-----AATATTTTGCACCT
Pongo_pygmaeus	AAAGTTTTTATATGTTTCCCTCCTAGCCTTTTATCTGTATGTTGATACAAAACCTATTATACAGAAATGCTCCCTATATACCTATATTGCAGAGATGGGAA-----AATATTTTGCACCT
Macaca_mulatta	AAAGTTTTTATATGTTTCCCTCCTAGCCTTTTATCTGTATGTTGATACAAAACCTATTATACAGAAATGCTCCCTATATACCTATATTGCAGAGATGGGAA-----AATATTTTGCACCT
Mus_musculus
Rattus_norvegicus
Bos_taurus	AAAGTTTTGATACATTTCCCTCCAGCCTTTTATCTGTATATTGAAACAAAACCTA-CATACAGAATGCCCCCTGTACGCTCAGATTGCATAGATGGGAGAGTGCAAA-AATTGTGCTCAT
Canis_familiaris	AAAGCATTTGATATGTTTCTCACAGCCTTTTGTCTCCATATTGAAACAAAACCTG-CACACAGAAGCCTCCCTATATTGCTAGACTGGGCAGTTGGAAACT--GCAACCATTTGGCATGT
Equus_caballus	AAAGTTTTGATATATTTCCTCCAGCCTTTTATCTGTATGTTGAAACAAAACCTG-CACACAGAATGCGCCCTATATACTTAGATCATATAGATGGGAACAGACAAAAAATTGCACTT
Homo_sapiens	TTTTTCAATCGCTAAATGTTTTATCAGGAGCACATTCTCATGACATGAAATTACTTTCAGAAACATATTTTACATGAAAGCATCCTATTCTATTGTACTAGCTAGCTACGCTGTATTT
Gorilla_gorilla	TTTTTCAATCGCTAAATGTTTTATCAGGAGCACATTCTCATGACATGAAATTACTTTCAGAAACAT---TTTACATGAAAGCATCCTATTCTATTGTACTAGCTAGCTACGCTGTATTT
Pongo_pygmaeus	TTTTTCAATTGCTAAATGTTTTATCAGGAGCACATTCTCATGACATGAAATTACTTTCAGAAACATTATTTACATGAAAGCATCCTATTCTATTGTACTAGCTAGCCAGCGCTGATTT
Macaca_mulatta	TTTCTCAATCGCTAAATATTTTATCAGGAGCACATTCTCATGACATGAAATTAAGTTTCAGAAACATTACTTTACATGAAAGCATCCTATTCTATTGTACTA---GCTACACTGTATTT
Mus_musculus
Rattus_norvegicus
Bos_taurus	TTGTTTTATTGCTAAATACTTCAGCAGGAGCATATTCTCTTGCCA-----CATATTAGAGGACCATCTTT
Canis_familiaris	TTCTTTTTCACCAATATTATTCAACAGGAGCACATTCTCATGTCA-----CTTATTAGTAGCACCCTATTT
Equus_caballus	TTCTTTTATCACGAAATATTTCATCAGGAGCACATTGTCTATGTCA-----CTTATTAGTAGCACCATATTT
Homo_sapiens	TATTTGCTAATCCTTTTGTGTGGTCAT-TCAGGATGTTCCCTAACTTCCATCCTTA-AAATATTGAAATGAGCA-----
Gorilla_gorilla	TATTTGCTAATCCTTTTGTGTGGTCAT-TCAGGATGTTCCCTAACTTCCATCCTTA-AAATATTGAAATGAGCA-----
Pongo_pygmaeus	TATTTGCTAATCCTTTTGTGTGGTCAC-TCAGGATGTTCCCTAACTTCCATCCTTA-AAATATTGAAATGAGCA-----
Macaca_mulatta	TATTTGCCAATCCTTTTGTGTGGTCAT-TCAGGATGTTCCCTAACTTCCATCCTTA-AAATATTGAAATGAGCA-----
Mus_musculus
Rattus_norvegicus
Bos_taurus	TATTTACCCAATCCTTTTCTAGTGGTCAT--CAAGATTTTCTTAATTCTTATCTTTAAAAATACTGAAATGAGGACTTCCCTGGCAGTCGAGTGGTTAGACTCCATGCTTCCAAATGCA
Canis_familiaris	TATTTACCCAATCCTGCTGCTTGGCTGT--CAGACATTCCTTAATTTCCGCCCTTAAAAATACCGGAATCACTG
Equus_caballus	TATTTACCCGATCCTTTTGTGTGGTCATC-CCGATGTTCCCTAAATTTCCATCCTTCAAAATACTGAAATGAGTG


```

Homo_sapiens      TAAAC--TCATTGATCTTCCCCAA--ACATATTTTTTGAACCTAGTTTATTTTCATCTTACACAGC--CTCAGGAAAGCTGCCTAT-----AACTCCCATCTC-ATAGGCTCAGGTTT
Gorilla_gorilla   TAAAC--TCATTGATCTTCCCCAA--ACATATTTTTTGAACCTAGTTTATTTTCATCTTACACAGC--CTCAGGAAAGCTGCCTAT-----AACTCCCATCTC-ACAGGCTCAGGTTT
Pongo_pygmaeus     TAAAC--TCATTGATCTTCCCCAA--ACATATTTTTTGAACCTAGTTTATTTTCATCTTACACAGC--CTCAGGAAAGCTGCCTATAAGTTAACTCCCATCTC-ATAGGCTCAGGTTT
Macaca_mulatta     TAAAC--TCATTGATCTTCCCCAA--ACATATGTTTTGAACCTAGTTTATTTTCATCTTGCACAGT--CTCAGGAAAGCTGCCTGTAAGTTAACTCCCATCTC-ATAGGCTCAGGTTT
Mus_musculus       .....
Rattus_norvegicus  .....
Bos_taurus         TAAACCTTCATTGATTTTCAAAA---AATGCTTTTTTGAACCTATTTTATTTTCGTCTTGTCAGTTTCTCAGGAAAGCTGCCTAGAAGTTAGCTCACACCTGTGTAGGATGACTTTT
Canis_familiaris   TAAAC--TCCTTGATCTTCCAAAAGA-AATGCTTCTGAACCTATTTTACTTTTCATCTTGACCGTCTCTCAGCAAAGCTGCCTAGCAGTGAACCTCCACCTGTGTGGGAGCACTTCT
Equus_caballus     AAAAC--TCATTGGTCTCCCCAA---AATGCTTCTTGAACCTATTTTATTTTCATCTTGACCGTCTCTCAGGAAACCTGCCTAGAAGTGAACCTCCACCTGTGTAGGATCACTTTT

Homo_sapiens      TCTGCAAAATGTTGCCCTGAGCTCTA--TAGCAGTCCAGGATT-CAGGGAACGAACCCAGTCCCCCGCTGCCCATTTGCCTTGATGAGTTGATAGGTATGTTGTT--TTAAACAATCAG
Gorilla_gorilla   TCTGCAAAATGTTGCCCTGAGCTCTA--TAGCAGTCCAGGATT-CAGGGAACGAACCCAGTCCCCCGCTGCCCATTTGCCTTGATGAGTTGATAGGTATGTTGTT--TTAAACAATCAG
Pongo_pygmaeus     TCTGCAAAATGTTGCCCTGAGCTCTA--TAGTAGTCCAAGATGACAGGGAACGAACCCAGTCCCCCGCTGCCCATTTGCCTTGATGAGTTGATAGGTATGTTGTT--TTAAACAATCAG
Macaca_mulatta     TCTGCAAAATGTTGCCCTGAACCTCTA--TAGCAGTCCAGGATT-CAGGGAACGAACCCAGTCCCCGTGCCCATCTGCCTTGATGAGTTGATAGGTATGTTGTT--TTAAACAATCCG
Mus_musculus       .....
Rattus_norvegicus  .....
Bos_taurus         TCTCCAAGTGTGCCCTGAGCTCTA--G-----TTCCAGGATT-GGGTGAACAAACCCAGTCCCTGCTGCCCATCTGCCTTGATGATTGATGTTGTTGTTGTTGTTGTTTAAACAATCAG
Canis_familiaris   GCTCTAAGT-----GCCCCATCTGCCTTGAGGACTTGATGGGTCTGTTGTT--TGAAAC---AG
Equus_caballus     TCTCCAGTGTGCCCTGAGCTCTA--G-----GTGCTGGAT--GGGGGAACAAACCCAGTCCCTGCTGCCCATCTGCCTCGATGCTTTGATAGGTATGTTGTT--TTAAACAATCAG

Homo_sapiens      CAAAACAATTTGCACTGCAGAGT
Gorilla_gorilla   CAAAACAATTTGCACTGCAGAGT
Pongo_pygmaeus     CAAATCAATTTGCACTGCAGAGT
Macaca_mulatta     CAAAACAATTTGCACTGCAGAGT
Mus_musculus       .....
Rattus_norvegicus  .....
Bos_taurus         CAAAATAATTTGCACTGCAGAGT
Canis_familiaris   CAAAATAATTTGCACTGCAGGTT
Equus_caballus     CAAAATAATTTGCACTGCAGAGT

```

Figure 9. Conserved Smad binding sites in the regulatory sequences of *miR-450/542* cluster.

Alignments of the *miR-450/542* cluster among nine eutherian mammals. miRNA gene sequences are labeled in red. Smad binding sites are indicated by yellow boxes.

Tables

Table 1. Survival rates of haploinsufficient *dpp* alleles by two *ubi-Mad* transgenes.

	Straight wing	Total	Survival rate of <i>dpp</i> ^{H61} /+	Straight wing	Total	Survival rate of <i>dpp</i> ^{H46} /+
<i>yw</i>	21	2583	0.81%	1	2277	0.04%
<i>ubi-mad-m3'UTR #1</i>				287	1111	25.83%
<i>ubi-mad-m3'UTR #2</i>	676	1639	41.24%	458	1288	35.56%
<i>ubi-mad-m3'UTR #3</i>	572	1521	37.61%	218	583	37.39%
<i>ubi-mad-m3'UTR #5</i>				335	1194	28.06%
<i>ubi-mad-m3'UTR #6</i>	256	623	41.09%	589	1436	41.02%
<i>ubi-mad-m3'UTR #7</i>	517	1343	38.05%			
<i>ubi-mad-w3'UTR #1</i>	247	1116	22.13%	331	1394	23.74%
<i>ubi-mad-w3'UTR #2</i>	105	1195	8.79%	118	1139	10.36%
<i>ubi-mad-w3'UTR #4</i>	445	1066	41.74%			
<i>ubi-mad-w3'UTR #5</i>	336	1289	26.07%	288	1173	24.55%
<i>ubi-mad-w3'UTR #6</i>	278	1027	27.07%			

	Average survival rate of <i>dpp</i> ^{H61} /+	Average survival rate of <i>dpp</i> ^{H46} /+	S.D. of <i>dpp</i> ^{H61} /+	S.D. of <i>dpp</i> ^{H46} /+
<i>ubi-Mad-m3'UTR</i>	39.50%	33.57%	1.93%	6.41%
<i>ubi-Mad-w3'UTR</i>	25.16%	19.55%	11.80%	7.97%
<i>yw</i>	0.81%	0.04%		

Summary of the data of each individual transgenic *ubi-Mad* line used in viability experiments. S.D., standard deviation.

Table 2

Predicted target sites of miRNAs from *hsa-miR-450/542* cluster on Smad5 3'UTR.

miRNAs	Total miRNA sites	Position on Smad5	miRNA alignment	
hsa-miR-450b-3p	2	701	22 --AUACCUACG--U-UUUACUAGGGUU--- 1 701 AAAAUUUUUGCAAUAACUGAUCUCAAGUA 730	
		4744	22 -AUACCUACGUUUUACUAGGGUU- 1 4744 CAGUAAG-GCCAAAGAAUCCCAAG 4766	
hsa-miR-450b-5p	3	482	22 -AUAAGUCCUUGUAUAACGUUUU--- 1 482 CAAUUC---AUUGUUUUGCAAAAGUG 504	
		692	22 --AUAAGUCCUUGUAUAACGUUUU- 1 692 UUUUUUAAAAAAAAUUUUGCAAAUA 716	
		815	22 AUAAGUCCUUGUAUAACGUUUU- 1 815 GCUUUUGGACAAUGUUGCAAGAA 837	
hsa-miR-542-3p	2	731	22 --AAAGUCAAU-AG--UUAGACAGUGU--- 1 731 UAUGUCAUUUACUCAAAAUCUGUCAUAAGC 760	
		2476	22 AAAGUCAAUAGUUAGACAGUGU- 1 2476 UAUUUGGGGUCAUUAUGUCACAG 2498	

The table includes the target site positions in Smad5 for miRNAs in the *hsa-miR-450/542* cluster and shows the detailed alignments between miRNAs and their putative targets in the Smad5 3'UTR as predicted by miRanda and TargetScan.

CHAPTER IV

bantam microRNA functions in the optic lobe

My contribution to this chapter is involved in designing and performing all the experiments and the analysis of the data and writing the manuscript.

Summary

Drosophila has been a powerful model system for studying the underlying mechanisms controlling the precisely coordinated assembly of the visual system through the stepwise processes during development. *bantam*, a *Drosophila* microRNA, is involved in many functions, such as stimulating proliferation and inhibiting apoptosis. Here, we report the detailed expression pattern of *bantam* in the developing optic lobe for the first time, and demonstrate its essential role of promoting proliferation of mitotic cells in the optic lobe, including stem cells and differentiated glial cells. Changes in *bantam* levels autonomously affected glial cell number and distribution, and non-autonomously affected photoreceptor neuron axon projection patterns. Furthermore, we showed that *bantam* promotes the proliferation of mitotic active glial cells, and affects their distribution, largely through down regulation of T-box transcription factor, *omptomotor-blind* (*omb*). Co-expression of *omb* can rescue the *bantam* phenotype, and restore the normal glial cell number and proper glial cell positioning in 66% of brains. All these results suggest that *bantam* is critical for maintaining the stem cell pools in OPC and GPC regions of the optic lobe, and *bantam*'s expression in glial cells is crucial for their proliferation and distribution.

Introduction

The *Drosophila* visual system is composed of a pair of compound eyes and the optic ganglia. The compound eyes are composed of ~800 repeated units, called ommatidia. Each of these subunits contains eight photoreceptor neurons (R1-R8 neurons) and a complement of non-neural support cells arranged in an invariant pattern. The optic lobes are the visual processing centers of the brain and include three ganglia, the lamina, medulla, and lobula complex. During larval development, axons from photoreceptor neurons in the eye disc project through the optic stalk into different layers of the optic lobe. Axons from photoreceptor R1-R6 neurons end between two layers of lamina glial cells, the epithelial and marginal layers, and form the lamina plexus. R7 and R8 neurons connect to a deeper target site known as the medulla (reviewed in (Cutforth and Gaul, 1997; Ting and Lee, 2007)). During development, interactions between retinal innervations and optic lobe development are under stepwise control to ensure precisely coordinated assembly of the visual system. However, the molecular mechanisms underlying these processes remain unclear.

In addition to neurons, glial cells are another important component of the brain. In *Drosophila*, glial cells are normally classified by their relative position and morphology (Chotard and Salecker, 2007). In the third instar larval optic lobe, there are satellite glial cells, which are in close contact with lamina neurons, and epithelial, marginal and medulla glial cells, which are organized into three rows around the border of lamina and medulla. In medulla, there are medulla neuropil glial cells, which enwrap the axons, and separate medulla cortex from the central brain. Like their vertebrate counterparts,

Drosophila glial cells play important roles to support neuronal development as well, such as axon pathfinding, defining ganglion boundaries, neuronal proliferation and survival (Chotard and Salecker, 2007).

Glial cells and neurons are intimate partners. However, the origins of lamina glial cells are different from those of lamina neurons. Lamina neurons are differentiated from lamina precursor cells (LPCs). R-neuron axon afferents are known to be required for lamina neuron differentiation in the optic lobe. Two R-neuron derived anterograde extrinsic signals, Hedgehog (Hh) and an epidermal growth factor (EGF)-like ligand, Spitz, are needed to induce LPCs differentiation into lamina neurons (Huang and Kunes, 1996; Huang et al., 1998). Lamina epithelial and marginal glial cells are generated from glial precursor cell (GPC) areas located at the prospective dorsal and ventral margins of the optical lobe, and migrate to their final destination possibly by chain migration (Chotard and Salecker, 2007). GPC is characterized by the combination of the expressions of *Wingless* (*Wg*), the T-box transcription factor *optomotor blind* (*omb*), the Cadherin family member *Dachsous*, and the TGF β ligand *Decapentaplegic* (*Dpp*) (Dearborn and Kunes, 2004). However, the regulation of glial cell differentiation, proliferation, and migration by extrinsic and intrinsic factors is not well known. The transcription factors Glial cells missing (*Gcm*) and *Gcm2* were known to be required in the GPC precursor cells to promote glial cell differentiation (Chotard et al., 2005). *Dpp* signaling was reported to act upstream of *Gcm* in GPC areas to control lamina glial cell differentiation (Yoshida et al., 2005). So far, only one gene, *nonstop*, which encodes Ubiquitin-Specific Protease, has been reported to be required in glial cells and their precursor to mediate their migration (Poeck et al., 2001). Besides those, extrinsic signals

from R-cell axons are also important for lamina glial cell proliferation and migration, as in mutant animals lacking R-cell innervation, reduced lamina glial cells were seen and ectopic glial cells stuck at the GPC region (Perez and Steller, 1996). However, no such signals have been identified so far. Only *jab1* (*Jun-activation-domain binding protein1*) / *csn5* (*subunit 5 of the Arabidopsis COP9 signalosome*), a component of the COP9 signalosome, was genetically found to be required in the R cells for promoting lamina glial cell migration (Suh et al., 2002). R-cell axons also induce formation of the ‘scaffold axon’ of neurons within GPC regions, which act as a path for glial cell migration (Dearborn and Kunes, 2004).

microRNAs (miRNAs) are a newly identified, evolutionarily conserved, and abundant class of small, non-coding RNAs, which are about 22 nucleotides in length. To date, 940 miRNAs have been identified in the human and 171 miRNAs in *Drosophila melanogaster* (www.mirbase.org). Each miRNA is thought to target multiple genes in the genomes. In humans, over one-third of genes are predicted to be directly targeted by miRNAs (Lewis et al., 2005). Most miRNAs are transcribed by RNA polymerase II (Pol II) to generate a primary transcript (pri-miRNA). Pri-miRNA is processed in the nucleus into a stem-loop structure about 60–80 nt (pre-miRNA), which is then exported to the cytoplasm by Exportin-5 via a Ran-GTP-dependent mechanism. Next, another RNase III enzyme, Dicer, cleaves pre-miRNA, releasing the mature miRNA:miRNA* duplex. Finally, the 21–25 nt mature miRNA is assembled into the RNA-induced silencing complex (RISC), while the miRNA* strand is normally degraded (Bushati and Cohen, 2007; Yang et al., 2005). In metazoans, miRNAs typically down regulate gene expression by binding to complementary sequences in the three prime untranslated regions (3' UTR)

of their target mRNAs, usually resulting in inhibition of protein translation. miRNAs are known to play widespread and critical roles in a variety of cellular processes including proliferation, differentiation, apoptosis, development, and tumors (Bushati and Cohen, 2007). Numerous miRNAs were reported to be expressed in a spatially and temporally controlled manner in the nervous system, suggesting their important roles in brain function and development reviewed in (Liu and Zhao, 2009)).

Fly and vertebrate visual systems share similar features of organization, including the stereotyped retinotopic map and layer specific connectivity. With accessibility to the sophisticated genetic, molecular, and behavior analysis, *Drosophila* has been a powerful model system for studying the underlying mechanisms controlling axonal pathfinding and glial cell development. Studies from the fly will shed light on its more complicated vertebrate counterparts. In this chapter, we reported the detailed expression pattern of one *Drosophila* miRNA, *bantam*, in the optic lobe of the third instar larval brain, and showed that it is required in maintaining stem cell pools in the outer proliferation center (OPC), and GPC regions of the optic lobe, and *bantam*'s expression in glial cells are crucial for their proliferation and distribution. Our results showed that *bantam* autonomously affects glial cell number and distribution, and non-autonomously affects photoreceptor axon projection patterns. We also showed that *bantam*'s functions on glial cells are largely dependent on its down regulation of the T-box transcription factor, *omptomotor-blind* (*omb*).

Materials and Methods

Drosophila strains and genetics

Drosophila melanogaster were grown on standard media at 25 °C. For brain size comparisons, embryos were collected for 12–24 hrs, grown for 120–140 hrs, and wandering third instar larvae were selected for dissection.

Over expression of transgenes were done using the Gal4/UAS system (reviewed in (Elliott and Brand, 2008; Phelps and Brand, 1998)). The following drivers were used: Mz1369-Gal4 (Hiesinger et al., 1999); *ombC*-Gal4 (Hofmeyer et al., 2008); *omb*-Gal4, *repo*-Gal4, *elav*-Gal4, and *eyeless*-Gal4 (Bloomington Drosophila Stock Center, Bloomington, IN). The following reporters were used: *GS-bantam*, which contains an insertion of the Gene Search UAS element upstream near the *bantam* gene, allowing *bantam* to be over expressed by Gal4 (Cho et al., 2006); *UAS-ban* (obtained from I. Edery, RU), which contains around 300bp *bantam* gene (Robins et al., 2005) in pUAST vector. Since these two *bantam* lines yielded the same results, both were used in this work. *UAS-omb* (Hofmeyer et al., 2008); and *UAS-CD8-GFP* is the reporter used to express fused GFP only on the membrane (Lee and Luo, 1999). Other flies strains include: *bantam* sensor (a P element line which contains *tub-EGFP* and two copies of the *bantam* target sequence in the 3'UTR) (Brennecke et al., 2003), and *omb-lacZ* (Tsuneizumi et al., 1997).

Histology and Imaging

X-Gal staining the third instar larvae were rinsed and dissected in chilled 1x Ringers

solution by tearing them in half and inverting the heads (Van de Bor et al., 1999). Larval heads with discs attached were fixed in formalin (Sigma) for 10 min. and then rinsed 1x 10 min. in assay buffer (5 mM KH_2PO_4 , 5mM K_2HPO_4 , 2 mM MgCl_2 , 100 mM KCl , 4 mM $\text{K}_3[\text{Fe(III)(CN)}_6]$, 4 mM $\text{K}_4[\text{Fe(II)(CN)}_6]$). Next, they were incubated in pre-warmed reaction buffer (1.5mg/ml X-Gal in assay buffer) for four hours. Finally, the samples were rinsed in assay buffer to stop the reaction.

Antibody staining the third instar larvae were dissected in chilled 1x Ringers solution by tearing them in half and inverting the heads. Larval heads attached to the body wall were fixed in formalin (Sigma) for 18 min. at room temperature. PBST (0.3% Triton X-100 in 1x PBS) was used for the following washing and antibody incubation. Primary antibodies used for staining were from Developmental Studies Hybridoma Bank (DSHB), including: rat anti-DE-cadherin (DCAD2, diluted 1:20), mouse anti-Repo (8D12, diluted 1:20), mouse-anti-Chaopin (24B10, diluted 1:400), mouse anti-Dachshund (mAbdac2-3, diluted as 1:20), and rabbit anti- β -GAL (diluted 1:8000, Cappel). Secondary antibody was conjugated to Cy3 (diluted 1:200, Jackson ImmunoResearch Lab.), and Alexa fluor 633 (diluted 1:100, Invitrogen). All primary antibodies were diluted in PBST and incubated with tissue samples at 4°C overnight. Secondary antibodies were typically incubated with tissue samples for 2 hours at room temperature. Whole brains were dissected off from the larvae after secondary antibody incubation, washed, and mounted in Vectashield mounting medium (Vector Laboratories).

EdU staining (Salic and Mitchison, 2008) was performed using Click-iT EdU Alexa Fluor Imaging kits from Molecular probes (Invitrogen). Briefly, dissected larvae were incubated with EdU (20 μ M) at room temperature for 10 minutes, washed with PBS, and fixed in formalin (Sigma HT5011) for 18 min. After washing, these larvae were incubated with Alexa fluor azide conjugated to 594 for 30 min at room temperature. After washing, whole brains were dissected off the larvae and mounted in the Vectashield mounting medium.

All confocal images were taken on the Leica SP2 confocal microscope, viewed with LCS image browser, and processed with Adobe Photoshop and Illustrator.

Results

***bantam* is expressed differentially in the optic lobe.**

To study the function of *bantam* in the brain, we first checked *bantam* expression patterns in the optic lobe of third instar larval brain. The *bantam* sensor is the reporter expressing GFP under the control of *tubulin* promoter. At the 3'UTR of GFP, there are two copies of perfect *bantam* target sequence, which allow it to be targeted by *bantam* and strongly reduce GFP expression. *bantam* sensor is therefore used as the negative indicator of real *bantam* expression level (Brennecke et al., 2003). By examining *bantam* sensor expression in the third instar larval visual system, we found that *bantam* is expressed differentially in the third instar larval brain, with a high expression level in the optic lobe (Figure 1).

The *Drosophila* optic lobe is derived from an embryonic optic placode that is sitting at the posterior head region of ectoderm. The precursor cells in the optic lobe placode start to proliferate soon after larval hatching, and form two bracelet-like proliferation centers, the outer proliferation center (OPC) and inner proliferation center (IOC). In the OPC, a small group of mitotically active progenitor cells, which are located anterior to the lamina furrow on the surface of the optic lobe, give rise to the lamina precursor cells (LPCs). LPCs divide once posterior to the lamina furrow to produce lamina neurons. The OPC progenitor cells close to the central brain are responsible for producing outer medulla neurons. The IOC cells generate inner medulla and lobula neurons. At the tips of the OPC, superficially located at the dorsal ventral margin, are glial precursor cell (GPC) areas. GPC areas contain multipotent cells, which produce a subtype of neurons and lamina

glial cells (Egger et al., 2007; Green et al., 1993; Hofbauer and Campos-Ortega, 1990; Nassif et al., 2003) (Figure 1A and 1B).

To distinguish the detailed structure of the optic lobe, we used specific antibody staining to view different subtypes of cells in the optic lobe. DE-cadherin (DE-Cad) is the transmembrane protein located at the zonula adherens between epithelial cells. We used anti-DE-cadherin to view optic lobe neuroepithelia (Figure 1H and 1L), which have epithelial morphology, and act as progenitors of optic lobe neuroblasts (Egger et al., 2007). *decapentaplegic* (*dpp*) has been reported to be expressed in glial precursor cell (GPC) regions of optic lobe (Kaphingst and Kunes, 1994; Yoshida et al., 2005). We used Dpp expression, which is viewed by enhancer trap line Dpp-lacZ (Emerald and Roy, 1998) as the GPC region marker (Figure 1G and 1K). Reversed polarity (Repo) is a glial specific homeodomain protein expressed in all glial-cell subtypes in the visual system (Halter et al., 1995; Xiong et al., 1994). We used anti-Repo staining to view differentiated glial cells in the optic lobe (Figure 1D). By studying the expression level of *bantam* sensor, we found that *bantam* sensor displayed low expression levels in the neuroepithelial cells of OPC (white arrows in Figure 1C and 1F, 1I), cells at the GPC areas (yellow solid arrows in Figure 1F, 1I and 1J, 1M), and also in the mature glial cells (stars in Figure 1C, and 1E), which indicates high *bantam* expression in those cells (Figure 1). Whereas the *bantam* sensor showed high expression in differentiated neurons in the optic lobe and in the photoreceptor neuron cells (Figure 1C and 1J). This indicates that *bantam* expression level is low in those cells. Previous studies (Tompson et. al. 2006)

also found that low *bantam* level in the photoreceptor neurons (Thompson and Cohen, 2006).

***bantam* promotes proliferation in the optic lobe.**

bantam has been reported to promote growth in the wing and eye tissues (Brennecke et al., 2003). We found that *bantam* is highly expressed in the OPC, GPC areas and glial cells in the optic lobe, where cells are mitotically active. These observations made us reason that *bantam* might be critical for cell proliferation in those cells in the developing brain. To test this hypothesis, we first checked the brain size of wild type, *bantam* null mutant, and over expression of *bantam*. *ban^{Δ1}* is a null allele caused by *bantam* gene deletion (Hipfner et al., 2002). Homozygous *ban^{Δ1} / ban^{Δ1}* brain (Figure 2A) showed a smaller size compared to the wild-type one (Figure 2B). In wild type, we used an optic lobe driver, Mz1369-Gal4 (Hiesinger et al., 1999) to express *UAS-CD8-GFP*, the fusion GFP expressed on the cell membrane, to distinguish the optic lobe from central brain. When *bantam* was over expressed in the optic lobe by the Mz1369-Gal4 driver (Figure 2C), a bigger size of brain was seen compared to the wild type due to the expansion of the optic lobe, and expanded folded neuroepithelial cells were also been in *bantam* over-expressing brain (Figure 2C). To see further how cell proliferation is affected, EdU staining was performed, which is a superior alternative to traditional BrdU staining for detecting newly synthesized DNA, to view proliferation patterns in the optic lobe. EdU staining in the wild type showed active proliferation in OPC, LPCs, IPC and GPC regions (Figure 2E). Losing *bantam* in homozygous *ban^{Δ1} / ban^{Δ1}* animals (Figure 2D) led to decreased EdU staining in the OPC, LPCs and GPC regions, but showed almost normal

proliferation in IPC cells compared to the wild type. When *bantam* was over expressed in the optic lobe (Figure 2F), there was dramatically increased EdU staining in the OPC and GPC regions compared to the wild type. All these results indicate that *bantam* has critical roles in cell proliferation in OPC and GPC regions of the optic lobe.

***bantam* is acting in the brain for correct R axon projection patterns.**

OPC and GPC regions are sources of progenitor cells for neurons and glial cells for the optic lobe. Because *bantam* is highly expressed in these regions, and is also important for proliferation, we reasoned that expression level changes of the genes affecting proliferation in these regions might affect the pool of neural stem cells. It might eventually affect the final number of differentiated neurons and glia, causing abnormal structure of optic lobe, and therefore affecting the photoreceptor neuron (R neuron) axon projection pattern in the optic lobe. So we first checked R axon projection patterns in the optic lobe by modulating *bantam* expression. We used anti-Chaoptin to label R axons. In the horizontal view of the wild-type third instar larval brain (Figure 3C and Figure 3C'), R axon fibers are finely spaced by the lamina neurons, and R1-R6 are terminated at the bottom of lamina between two rows of glial cells, epithelial and marginal glial cells, and their growth cones form linear lamina plexus. R7 and R8 axons project deeper into medulla, forming a lattice-like network. In *ban^{Δ1} / ban^{Δ1}* larval brains (Figure 3E and Figure 3F), R projection patterns were disrupted from an intermediate to severe degree. In the severe case, R axons appeared in thick bundles, and stopped in the brain irregularly. In the intermediate case, there was visible lamina plexus, which did not appear evenly linear, and became shorter with some breaks. Projections in the medulla were also

disrupted. Surprisingly, when *bantam* was over expressed by Mz1369-Gal4 (Figure 3D and Figure 3D'), we found similar defects of R axon projection patterns like the ones observed in *ban^{Δ1}* / *ban^{Δ1}* larval brains, even though Mz1369-Gal4 > *ban* brains showed bigger size (compare Figure 3D and Figure 3E). These results indicate that *bantam* is required for maintaining the correct R axon projection patterns.

Altered R axon projection patterns might be the result of the change of genes affecting axon pathfinding, or the secondary effect of the disruption of the integrity of the brain structure. To find out where *bantam* acts to cause this phenotype, we compared the R axon projection patterns when different Gal4 drivers were used to over express *bantam*. Mz1369-Gal4 and *omb*-Gal4 are both expressed not only in the optic lobe, but also in the eye discs, while *eyeless*-Gal4 is only expressed in eye disc, and not in the optic lobe. In the lateral view of the wild-type larval brain (Figure 3H and Figure 3H'), R axon projection patterns in the brain appear in a crescent-like shape. When *bantam* was over expressed in the optic lobe by Mz1369-Gal4 driver, the crescent shape of R axon projection pattern was disrupted (Figure 3I and 3I'). The similar disrupted R axon projection patterns were also seen in *bantam* over expression with a different optic-lobe driver, *omb*-Gal4 (Figure 3J and 3J'). But when *bantam* was over expressed by *eyeless*-Gal4 (Figure 3G and 3G'), we discovered that although an overgrowth of eye discs was present, R axon projection patterns appeared the wild-type. This indicates that *bantam* is acting in the optic lobe but not in R neurons for the right R axon projection.

***bantam* is acting in glial cells, not in neurons.**

In the developing optic lobe, R axons and glial cells are two major partners, affecting each other to maintain the integrity of the visual system. Migration of lamina glial cells depends on the local signaling from R axons (Perez and Steller, 1996). Conversely, lamina glial cells function as intermediate targets of R1-R6 axons and are required for establishing the correct R axon projection pattern (Poeck et al., 2001; Ting and Lee, 2007). In *bantam* null mutants and when *bantam* is over expressed, we did not see much change in the number of R cells (Figure 3E and 3D). We reasoned that the altered R axon projection patterns in those cases might be the cause of the change in glial cells in the optic lobe. Thus, we examined cell number and distribution of glial cells in the optic lobe when *bantam* is eliminated or over expressed. Wild-type optic lobes have three distinct layers of glial cells in the lamina, called the epithelial, marginal and medulla glial cells (Figure 4D). In *bantam* null mutant larval brains, total glial cell number was less (Figure 4C) compared to the wild type (Figure 4A). When *bantam* was over expressed, total glial cell number increased (Figure 4B), and distribution of mature glial cells was disturbed, in that the three lamina glia layers were not clearly distinguishable, and less glial cells were present around the lamina plexus (Figure 4F). In the wild type, lamina epithelial and marginal glial cells were produced in GPC regions, and migrated under lamina furrow to their final destination (Perez and Steller, 1996). Therefore, only a few glial cells were present under lamina furrow at the single focal plane in wild type (Figure 4E). But when *bantam* was over expressed by Mz1369-Gal4, there were many glial cells present under the lamina furrow (Figure 4G). By using a different Gal4 line, *omb*-Gal4, we found the similar phenotype that *bantam* caused increased glial cells in the optic lobe with

disorganized distribution (Figure 7). All of these findings indicate that *bantam* is important for regulation of glial cell number and organization in the optic lobe.

Since Mz1369-Gal4 and *omb*-Gal4 are expressed both in neurons and glial cells, we cannot tell which type of cells *bantam* is acting in to cause the change of glial cells. To determine this, we used Gal4 lines, which are expressed only in glial cells or neurons, and then checked glial cell number and organization. *repo*-Gal4 was expressed in all differentiated glial cells, but not in neurons. When *bantam* was over expressed by *repo*-Gal4 (Figure 4H and Figure 4H'), brains were bigger because of the dramatic increase in the number of glial cells. At the brain surface, increased glial cells made multiple layers, forming a thicker glial sheath. On the border of the lamina and medulla, the three layers of glial cells were not able to be distinguished. Large ectopic glial cell clusters were seen in the lamina. *elav*-Gal4 driver strongly expresses in neurons, but not in glial cells. When *bantam* was over expressed by *elav*-Gal4 (Figure 4I and Figure 4I'), the brain was wild-type size, and there were a wild-type like glial cell distribution observed along with a wild-type R axon projection pattern. All together this indicates that *bantam* is acting in glial cells and autonomously affecting glial cell number and distribution.

***bantam* regulates glial cells through its regulation on *omb*.**

In our previous study, we learned *bantam* could down regulate the T-box gene, *optomotor-blind (omb)* (*Flybase, bifid*) in the wing disc. *omb* is known to be expressed in glial cells and is important for axonal projections (Hofmeyer et al., 2008). To determine how *bantam* regulates glial cell number and distribution, we checked whether *bantam*

could regulate *omb* in the optic lobe. We used the enhancer trap line, *omb-lacZ*, as a marker for *omb* expression in the optic lobe. *omb-lacZ* (Sun et al., 1995) is inserted 1.4 kb upstream of the 5' end of full length of *omb* cDNA (Pflugfelder et al., 1990). In wild type, *omb-lacZ* showed an expression pattern in the optic lobe consistent with RNA *in situ* (Poeck et al., 1993), with high expression in the GPC regions, in some differentiated glial cells in the lamina, and in the medulla (Figure 5A and Figure 5C). When *bantam* was over expressed by Mz1369-Gal4, *omb* expression is greatly decreased or even totally abolished in most lamina glial cells and medulla glial cells (Figure 5B and Figure 5D).

The next question we wanted to ask is whether the regulation of glial cells by *bantam* is dependant on its down regulation of *omb*. So, we tested whether expression of *omb* could rescue the glial cell phenotype caused by *bantam* over expression. We used Mz1369-Gal4 to express both *UAS-ban* and *UAS-omb*, and found that it was embryonic lethal. So, we thought it would be better to focus on a small group of glial cells by using a specific glial cell driver, *ombC*-Gal4 (Hofmeyer et al., 2008), which only expresses in medulla glial cells (meg) located at the base of the lamina plexus at the border of lamina and medulla, and in the medulla neuropil glial cells (mng) which enwrap the neuropil in the medulla (Figure 6A'). When *bantam* was over expressed by *ombC*-Gal4, the number of glial cells increased, and ectopic glial cells were found in the lamina (Figure 6B and Figure 6B'). Those ectopic glial cell clusters were in the position where DAC-positive neurons would normally be found (Figure 8). R axons were pushed to bypass the cluster, but the final destination of R1-R6 axon was not affected (Figure 9). These axons still stopped right at the lamina plexus. However, the line formed by their growth cone was

not linear. At the place where ectopic glial cells were present, the lamina plexus line was getting thinner than the rest of the lamina plexus (Figure 9). By observing the *omb-lacZ* levels in *ombC-Gal4 > UAS-ban*, we found very low levels of *omb* in those ectopic glial cells in the lamina (Figure 5F). To rescue, we used *ombC-Gal4* to over express both *UAS-ban* and *UAS-omb*, and found out about 66% brains (n=15) had almost wild-type like glial cell distribution (Figure 6C), and about 34% brains (n=15) had partially rescuing effect (Figure 6D), showing that less ectopic glial cells were present in the lamina compared to *bantam* alone (Figure 6B). All these results indicate that regulation *omb* by *bantam* is important in maintaining glial cell number and distribution in the optic lobe.

Discussion

***bantam* is important for maintaining the pool of stem cells in the larval optic lobe.**

During development, it is very important to maintain a constant stem/progenitor cell population while differentiated cells are produced. In *Drosophila*, the central nervous system is derived from neural stem cells called neuroblasts. The optic lobe neuroepithelium are important as they maintain the pool of optic lobe neuroblasts with symmetric division. The neuroblasts typically undergo asymmetric cell division to produce a large apical neuroblast for self-renewal and a smaller basal ganglion mother cell (GMC), which generally divides once more to produce two lineage-specific postmitotic ganglion cells (GCs) (Egger et al., 2007). Misregulation of the self-renewing capacity of the neuroblasts can lead to brain tumors. However, the mechanism underlying the precise regulation of proliferation and differentiation of the neuroepithelium and neuroblasts is not well known. miRNAs are crucial for stem cell maintenance. When the miRNA processing machinery is affected by loss of *Dicer-1* (*Dcr-1*), which is essential for generating mature miRNAs from their corresponding precursors (Lee et al., 2004), stem cells cannot be maintained and are lost rapidly in the *Drosophila* ovary. These *dcr-1* mutant stem cells are delayed in G1 to S transition (Hatfield et al., 2005; Jin and Xie, 2007). *bantam* is also known to be important for germline stem cell (GSC) maintenance in adult *Drosophila* (Shcherbata et al., 2007; Yang et al., 2009). However, the detailed underlying mechanism remains elusive. Our results provide evidence that *bantam* is important for stem cell maintenance in the optic lobe. First, *bantam* shows high expression in the OPC, GPC areas in the optic lobe, where stem cells are located. Second, *bantam* is critical for cell proliferation in OPC and GPC areas. *ban^{Δ1}/ban^{Δ1}* null mutants

have smaller brains with dramatic decrease of the proliferation in the OPC and GPC. On the other hand, *bantam* overexpression causes brain size to increase, along with increased proliferation in the OPC and GPC. *bantam* has been known to promote cell proliferation in the wing disc as well (Brennecke et al., 2003). The ability of *bantam* to promote cell proliferation in various tissues suggests that *bantam* might target molecules which directly but negatively affect cell-cycle machinery. Very recently, a report showed that *bantam* can target Mei-P26, which has ubiquitin ligase activity, causing oncogene c-Myc degradation in the wing imaginal disc (Herranz et al., 2010). c-Myc can respond to different growth factors to promote cell proliferation through positive regulation of the transcription factor E2F, which is a common G1-S master regulator and is involved in regulating the expression of a number of genes required for G1-S progress (Herranz et al., 2008). Future experiments studying whether *bantam* employs the same mechanism regulating cell-cycle in the stem cells of optic lobe will be informative.

***bantam* promotes glial cell proliferation but not differentiation**

During normal development, development of glial cells in the optic lobe is controlled by both extrinsic and intrinsic mechanisms (Chotard and Salecker, 2007). Glial cells rapidly increase during the third instar larval stage due to the mitosis of differentiated glia, and also more significantly from the proliferation of precursor cells (Pereanu et al., 2005; Read et al., 2009). In our work, we found that over expression of *bantam* caused a great increase of glial cell numbers in the optic lobe in a cell-autonomous manner. We believe that this is mainly because of *bantam*'s function in increasing proliferation of both glia precursor cells (Figure 2F) and differentiated glia (Figure 6B). On the other hand, we

think *bantam* does not affect glial cell differentiation most, if not at least. Because even with the loss of *bantam* in *ban^{Δ1}/ban^{Δ1}* null mutant, there were still Repo-positive differentiated glial cells, despite a decreased number. Transcriptional regulators, such as Glial cells missing (*Gcm*) and its closely related homolog *Gcm2*, have been well-studied for their roles of glial cell differentiation in embryonic and postembryonic nervous system of *Drosophila* (Alfonso and Jones, 2002; Chotard et al., 2005; Hosoya et al., 1995; Jones et al., 1995). *Gcm/Gcm2* are considered to be at the top of the hierarchy to initiate the differentiation of all glial cells at the transcriptional level. Their downstream targets are involved in maintaining terminal glial cell differentiation include *reverse polarity (repo)*, *pointed (pnt)* and *tramtrack (ttk)* (Jones, 2005; Soustelle and Giangrande, 2007). With antibody staining for Repo, we did not see any obvious change of Repo by *bantam*, further supporting the idea that *bantam* increases glial cell numbers independent of *Gcm*-Repo. In our work, we also provide evidence that *bantam*'s function on glial cell number is dependent from its negative regulation of *omb* in a small subgroup of differentiated glial cells, evidenced by the ability of *omb* to rescue *bantam*'s effect on glial cell numbers and distribution (Figure 6). *Omb* is a T-box transcription factor, highly conserved in all metazoans (Pflugfelder, 2009). The T-box family appears to play critical roles in development, including specification of the mesoderm and morphogenesis in the heart and limbs (Naiche et al., 2005; Wilson and Conlon, 2002). In the *Drosophila* optic lobe, *omb* is expressed in a subgroup of glial cells that are required for their proper glial cell positioning and morphology (Hofmeyer et al., 2008). However, the downstream targets of *omb* responsible for these functions are not clear. In wing discs, *bantam* can down regulate *omb* through its inhibitory effect on Dpp signaling (Chapter 3). Future

experiments to determine if the same mechanism is employed in the brain need to be performed.

Besides the effect on promoting glial cell numbers, *bantam* also affects the motility of glial cells, as we observed numerous glial cells stuck under the lamina furrow, which is the migrating path for glial cells. At their destination, the three-layer organization of glial cells was disturbed when *bantam* was over expressed. R-cell axon-derived signals were reported to be required for glial cell proliferation and migration in the lamina (Perez and Steller, 1996). However, our results demonstrated that glial cell defects by *bantam* are cell-autonomous, as neuronal over expression of *bantam* did not show any affect on glial cells. So far, *nonstop*, which encodes an ubiquitin-specific protease, was the only gene reported to be required in laminal glial cells for migration (Poeck et al., 2001). Future experiments to find out target genes of *bantam* responsible for glial cell migration will be of interest.

Acknowledgements

We would like to thank Drs. K. Irvine, I. Edery, K. Hofmeyer, S. Cohen and T. Tabata, the Bloomington Stock Center, and the Developmental Studies Hybridoma Bank at the University of Iowa for generously supplying the fly stocks and reagents.

Figure 1. *bantam* is differentially expressed within the optic lobe.

(A, B) Schematic diagram illustrates the third instar larval visual system. (A) Lateral view with anterior left, posterior right, dorsal up, and ventral down. All brains with the lateral view in this paper are oriented in the same way. Photoreceptor neuron axons from eye disc (ed) project through optic stalk (os) into optic lobe (crescent shape in gray). Glial precursor cell (GPC) regions are labeled in purple. Yellow arrows indicate the migrating paths of lamina glial cells from GPC to the lamina target region. OPC, outer proliferation center; LPC, lamina precursor cell; IPC, inner proliferation center; lb, lobula. (B) Horizontal view with anterior left, posterior right, lateral up, and middle down. All brains with the horizontal view in this paper are oriented in the same way. Neuroblasts in OPC closest to the lamina furrow (LF) give rise to LPC, which in turn divide to produce lamina neurons (ln). Neuroblasts in OPC close to medulla generate medulla neurons (mn). Three layers of lamina glial cells set the boundary of lamina and medulla. Subtypes of glia are labeled including satellite glia (sg), epithelial glia (epi glia), marginal glia (ma glia), medulla glia (me glia), and medulla neuropil glia (mng).

(C-E) One focal plane of horizontal view. The brain is outlined by the dashed line. (C) *bantam* sensor (green) is showing high expression in photoreceptor axons and neurons in the medulla, but very low expression in OPC cells (white arrows) and lamina glial cells (stars). (D) glial cells are labeled by anti-Repo staining (red). Three rows of lamina glial cells, epithelial, marginal and medulla glial cells are visible (stars). (E) merged.

(F-D) One focal plane of superficial horizontal view. (F) *bantam* sensor (green) is

showing low expression in OPC (white arrows) and GPC regions (solid yellow arrow heads). (G) GPC regions are labeled by *dpp-lacZ*, stained for β -galactosidase (megenta). (pointed by solid yellow arrow heads). (H) Anti-DE-cadherin staining (red) to view the neuroepithelial cells in OPC (pointed by white arrows). (I) merged.

(J-M) one focus plane of lateral view. (J) *bantam* sensor (green) shows high expression in the photoreceptor neurons in the eye discs, and low expression in OPC, IPC and GPC regions. (K) GPC regions (solid yellow arrow heads) are located at the dorsal and ventral margin at the posterior optic lobe, labeled by *dpp-lacZ*, stained for β galactosidase (megenta). (L) Anti-DE-cadherin staining (red) to view the neuroepithelial cells in the optic lobe. (M) merged.

Figure 2

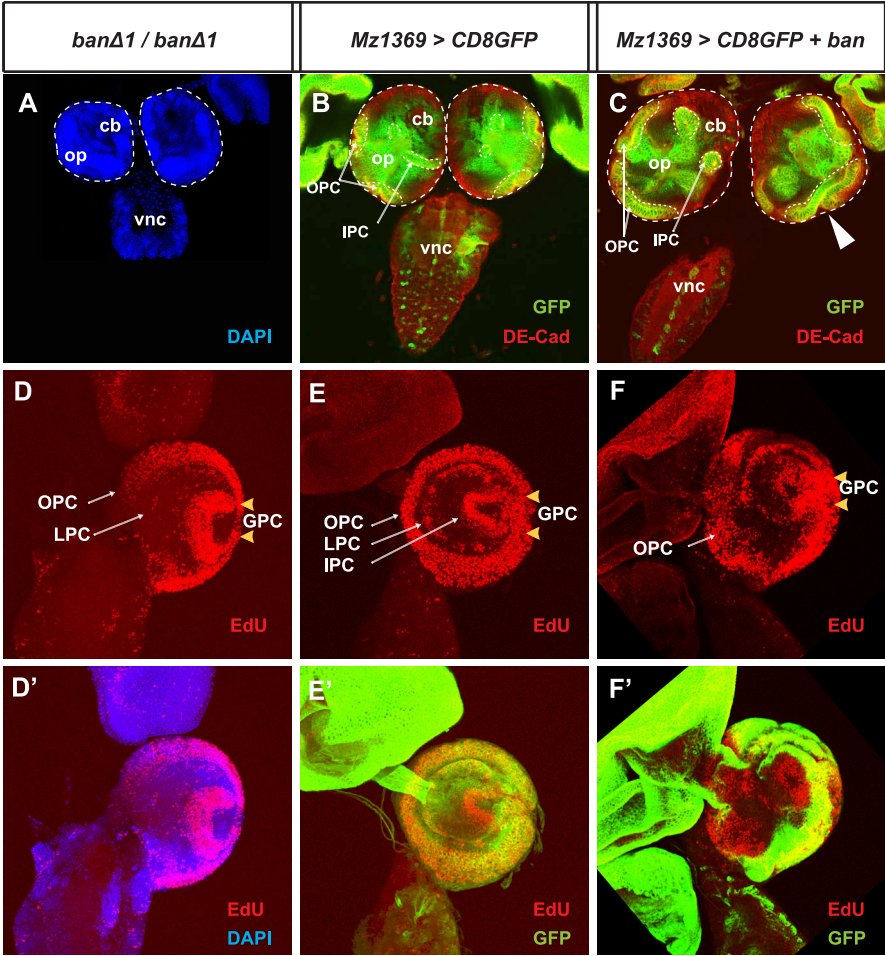


Figure 2. *bantam* is required for proliferation in the optic lobe.

(A, B, C) Brains are positioned in a horizontal view on a similar focal plane, and taken at the same magnification setting. Brain surface is outlined by dashed line for brain size comparison. (A) *bantam* null mutant. The brain is stained with DAPI (blue) to view all the cells. (B, C) *UAS-CD8-GFP* (green) is used to view the expression of *Mz1369-Gal4* in the optic lobe. DE-cadherin staining (red) is used to view neuroepithelial cells in the outer proliferation center (OPC) and inner proliferation center (IPC). Part of IPC and OPC can be seen at this focus plane, and outlined by the dashed line. op, optic lobe; cb, central brain; vnc, ventral nerve cord. (B) wild type; (C) over expression of *bantam* causes a broader size of the optic lobe, and folded neuroepithelia (white arrow head).

(D-F') Brains are positioned for lateral view. Projection images are from multiple section planes covering all proliferation centers in the optic lobe. EdU staining (red) shows cell proliferation in the brain. DAPI (blue) is used to view outline of the brain. *UAS-CD8-GFP* is used to view expression of *Mz1369-Gal4*. OPC, LPC, IPC, are labeled (white arrows), GPC are labeled (yellow arrow heads).

Genotypes: (D, D') *ban^{Δ1}/ban^{Δ1}*; (E, E') *UAS-CD8-GFP/+; Mz1369-Gal4/+;* (F, F') *UAS-CD8-GFP/+; Mz1369-Gal4/UAS-ban*

Figure 3

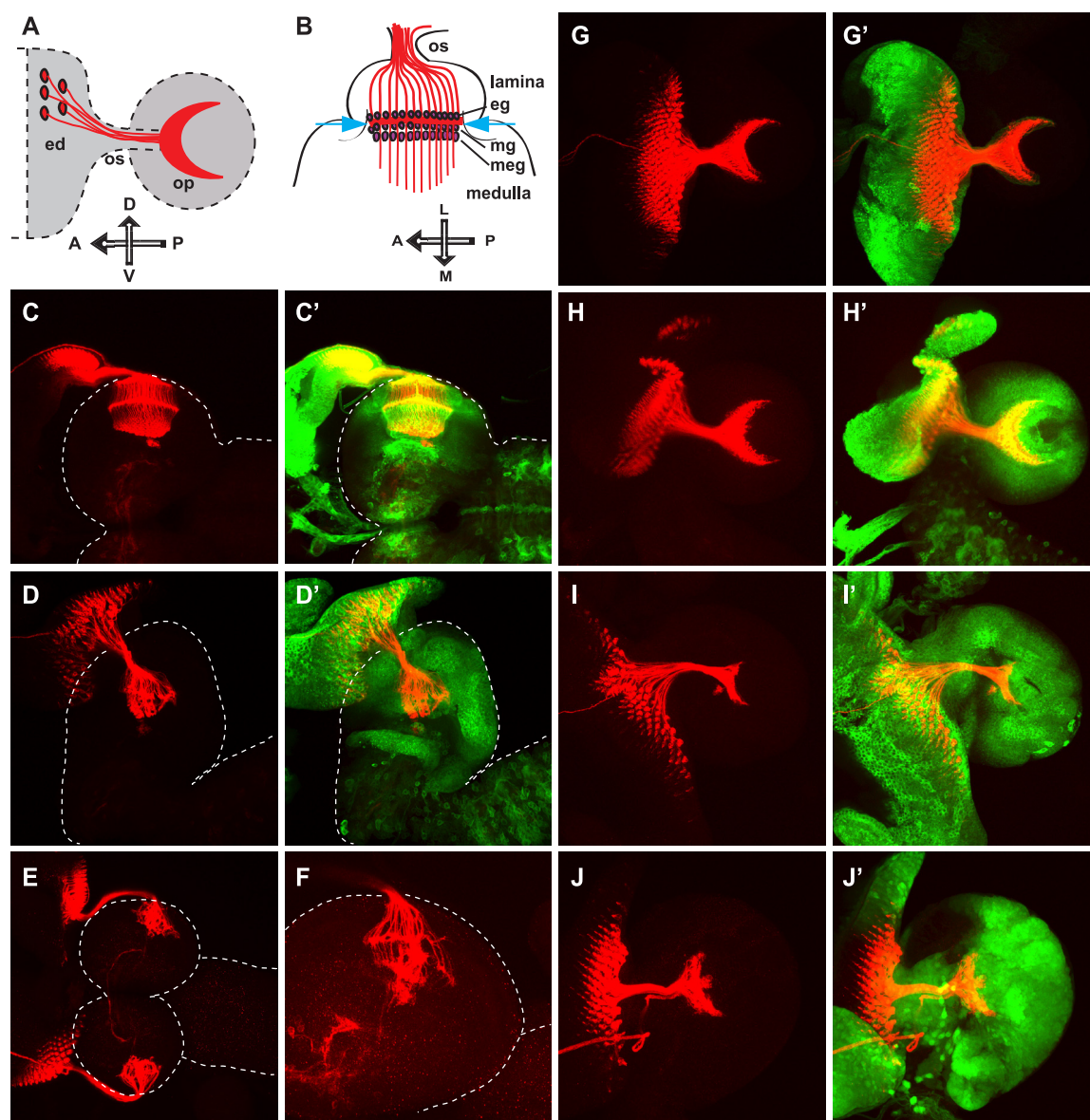


Figure 3. *bantam* affects photoreceptor-neuron axon projection in the optic lobe.

(A, B) Schematic illustration of the photoreceptor (R1-R8) axon projection patterns in the late third instar larval brain of *Drosophila*. (A) Lateral view. Axons from photoreceptor neurons (R1-R8) (red) in the eye disc (ed) project through the optic stalk (os) into the optic lobe (op). Projection pattern of R axons in the optic lobe is in crescent shape (red). (B) Horizontal view. Axons (red) of R cells project into different layers of the optic lobe. Axons from R1-R6 (red) stop between two layers of glial cells, the epithelial (eg) and marginal glial cells (mg) (magenta), in the lamina, and form the lamina plexus (red line between two blue arrows). R7 and R8 project deeper into the medulla. (A: anterior; P: posterior; D: dorsal; V: ventral; L: lateral; M: middle)

Anti-Chaopin staining (red) is used to view R-cell projection patterns. *UAS-CD8-GFP* (green) is used to visualize expression patterns of Gal4 drivers. Brain surface is outlined by dashed line based on the auto fluorescence exposure. (C-F) Brains are positioned for horizontal view. (C, C') wild type. (D, D') *bantam* is over expressed by Mz1369-Gal4. (E, F) *bantam* null mutant. (E) Lower magnification including two hemispheres. (F) Higher magnification only showing half hemisphere.

(G-J') Brains are positioned for lateral view. (G, G') *bantam* is over expressed by *eyeless*-Gal4 in the eye disc. (H, H') wild type. (I, I') *bantam* is over expressed by Mz1369-Gal4. (J, J') *bantam* is over expressed by *omb*-Gal4. Genotypes: (C, C', H, H') *UAS-CD8-GFP/+; Mz1369-Gal4/+; (D, D', I, I') UAS-CD8-GFP/+; Mz1369-Gal4/UAS-ban; (E, F) ban^{Δ1}/ban^{Δ1}; (G, G') UAS-CD8-GFP/+; eyeless-Gal4/UAS-ban; (J, J') omb-Gal4/+; UAS-CD8-GFP/+; UAS-ban/+.*

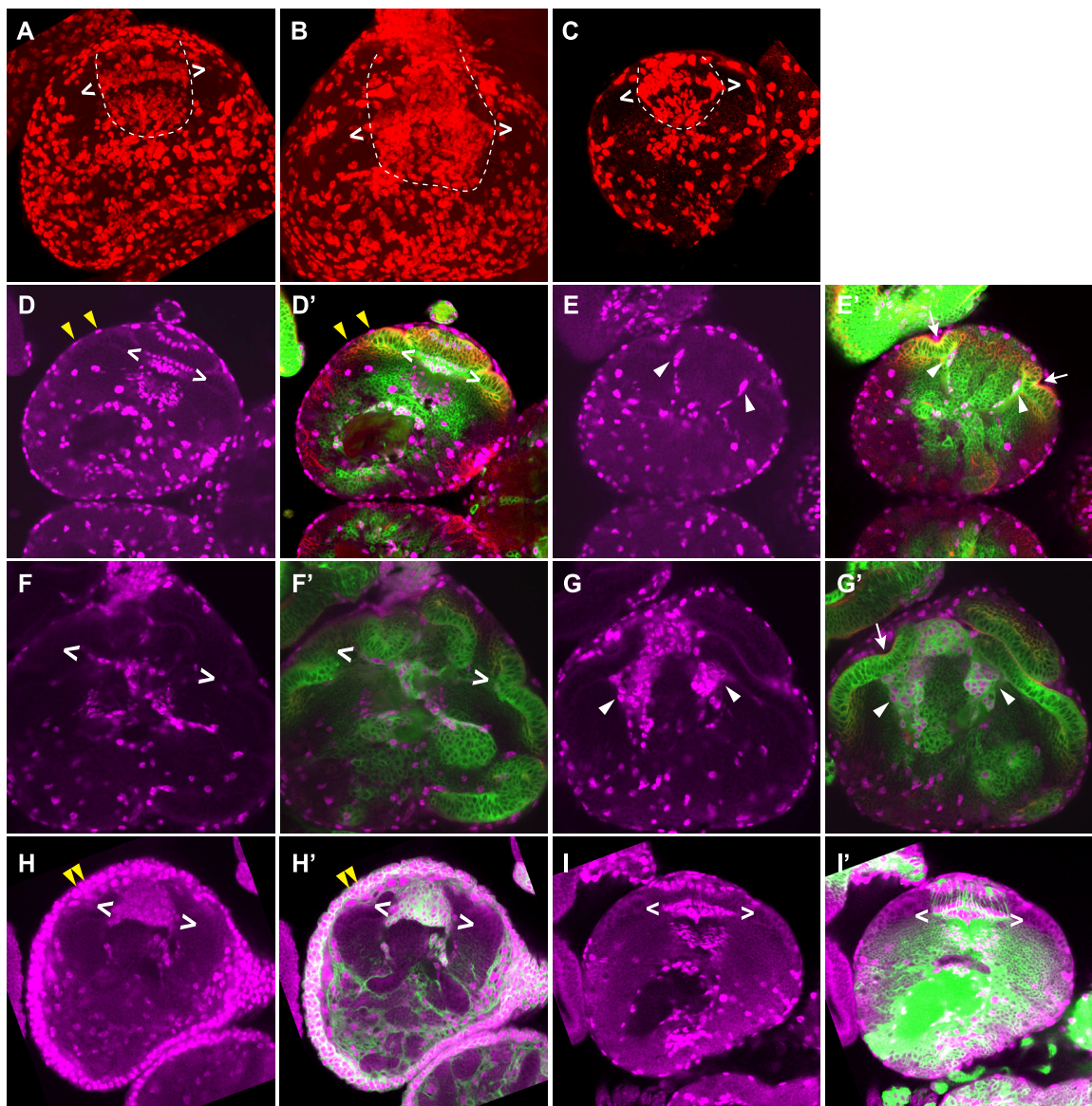
Figure 4

Figure 4. *bantam* promotes glial cell proliferation in the optic lobe.

All brains are positioned for horizontal view. (A-C) Maximum projection to view total number of glial cells, stained for anti-Repo (red). Glial cells in the lamina and medulla are circled inside the dashed line. Glial cells between brackets (two white $< >$) correspond to the three layers of laminar glial cells: epithelial, marginal and medulla glia. (A) wild type. (B) Mz1369-Gal4 $>$ *UAS-ban*. (C) *bantam* null mutant.

(D-I') Individual focus plane. Glial cells are stained by anti-Repo (magenta), *UAS-CD8-GFP* (green) is used to view the expression of Gal4. Neuroepithelial cells are viewed by anti-DE-cadherin (red). (D-E') wild type. (F-G') Mz1369-Gal4 $>$ *UAS-ban*. (D,D') and (F, F') are at the similar focus plane. (E, E') and (G, G') are at the similar focus plane. Glial cells between white brackets ($< >$) correspond to the three layers of laminar glial cells: epithelial, marginal, and medulla glia. Lamina furrows indicated by white arrows. Cell surface glia cells are indicated by yellow arrows.

Figure 5

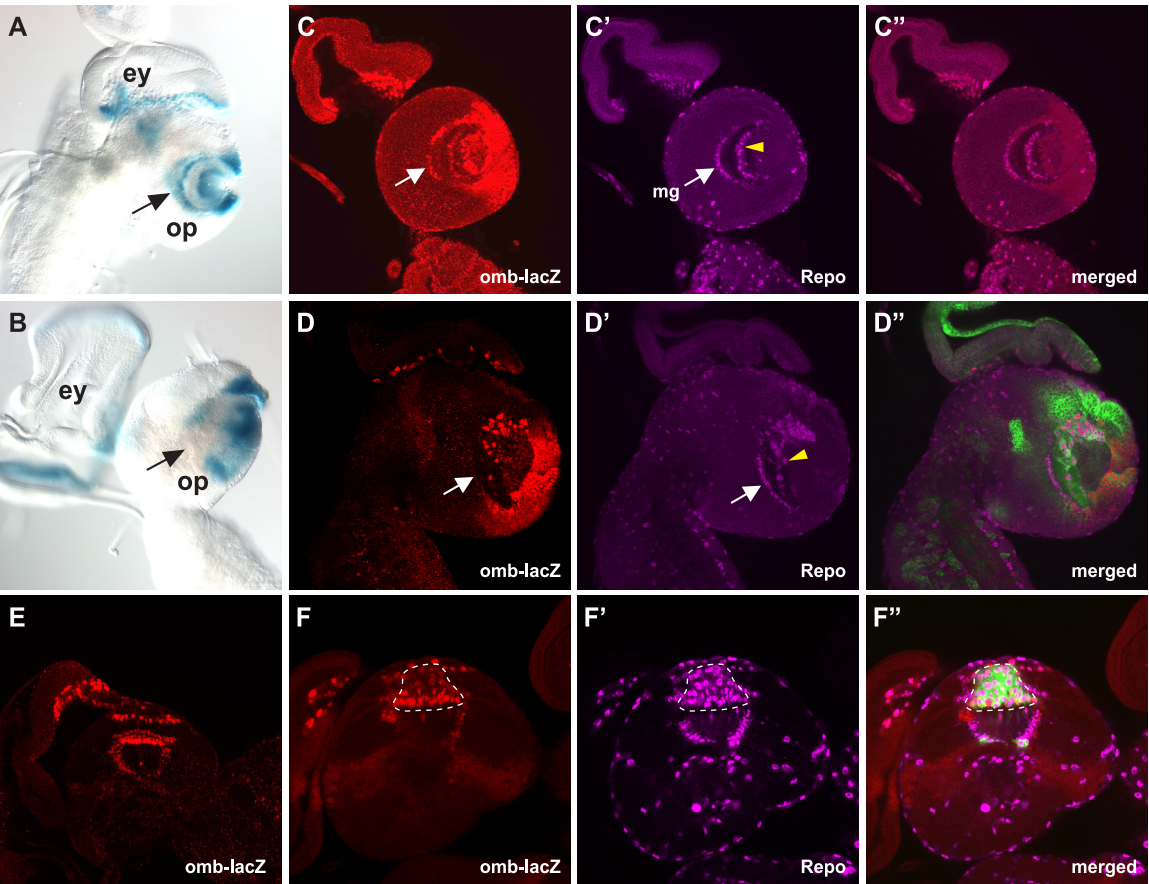


Figure 5. *bantam* down regulates *omb* in the optic lobe.

(A, B) brains are positions for lateral view. X-gal staining is to view *omb-lacZ* expression patterns in the optic lobe. (A) wild type; (B) Mz1369-Gal4 > *UAS-ban*.

(C-D'') single focal plane of lateral view. *UAS-CD8-GFP* (green) is used to view expression of Gal4. Anti- β galactosidase (red) is to view expression of *omb-lacZ*. Glia cells are viewed by anti-Repo (magenta). (C-C'') wild type; (D-D'') Mz1369-Gal4 > *UAS-CD8-GFP* + *UAS-ban*. (C-C'') and (D-D'') are at the similar focus plane. Medulla glia cells are indicated by white arrow and medulla neuropile glial cells are indicated by yellow arrow head.

(E-F'') single focal plane for horizontal view. *UAS-CD8-GFP* (green) is used to view expression of Gal4. Anti- β galactosidase (red) is to view expression of *omb-lacZ*. Glia cells are viewed by anti-Repo (magenta). (E) wild type; (F-F'') *ombC*-Gal4 > *UAS-CD8-GFP* + *UAS-ban*. Increased glial cells are circled by a dashed line.

Figure 6

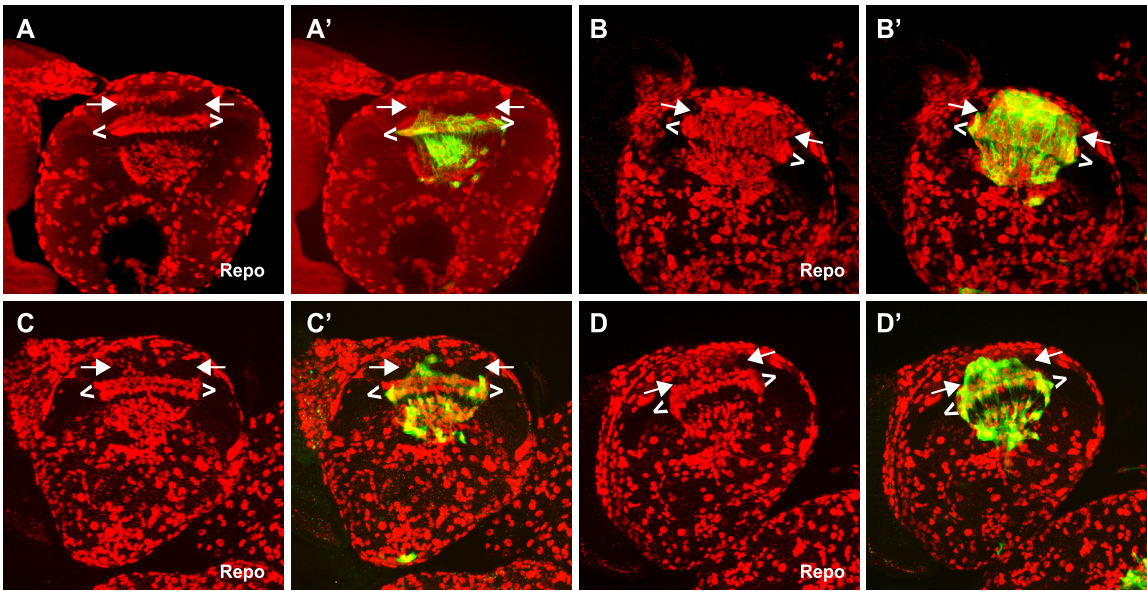


Figure 6. *omb* rescues *bantam*.

All brains are positioned for horizontal view. All pictures are maximum projection from multiple sections. anit-Repo staining (red) is used to label glial cells. *ombC*-Gal4 expression is visualized by *UAS*-CD8-GFP (green). Glial cells between white brackets (< >) correspond to the three layers of laminar glial cells: epithelial, marginal and medulla glia. Glial cells in the lamina are indicated between two arrows.

Genotypes: (A, A') *ombC*-Gal4 > *UAS*-CD8-GFP; (B, B') *ombC*-Gal4 > *UAS*-CD8-GFP + *UAS-ban*; (C-D') *ombC*-Gal4 > *UAS*-CD8-GFP + *UAS-ban* + *UAS-omb*

Figure 7

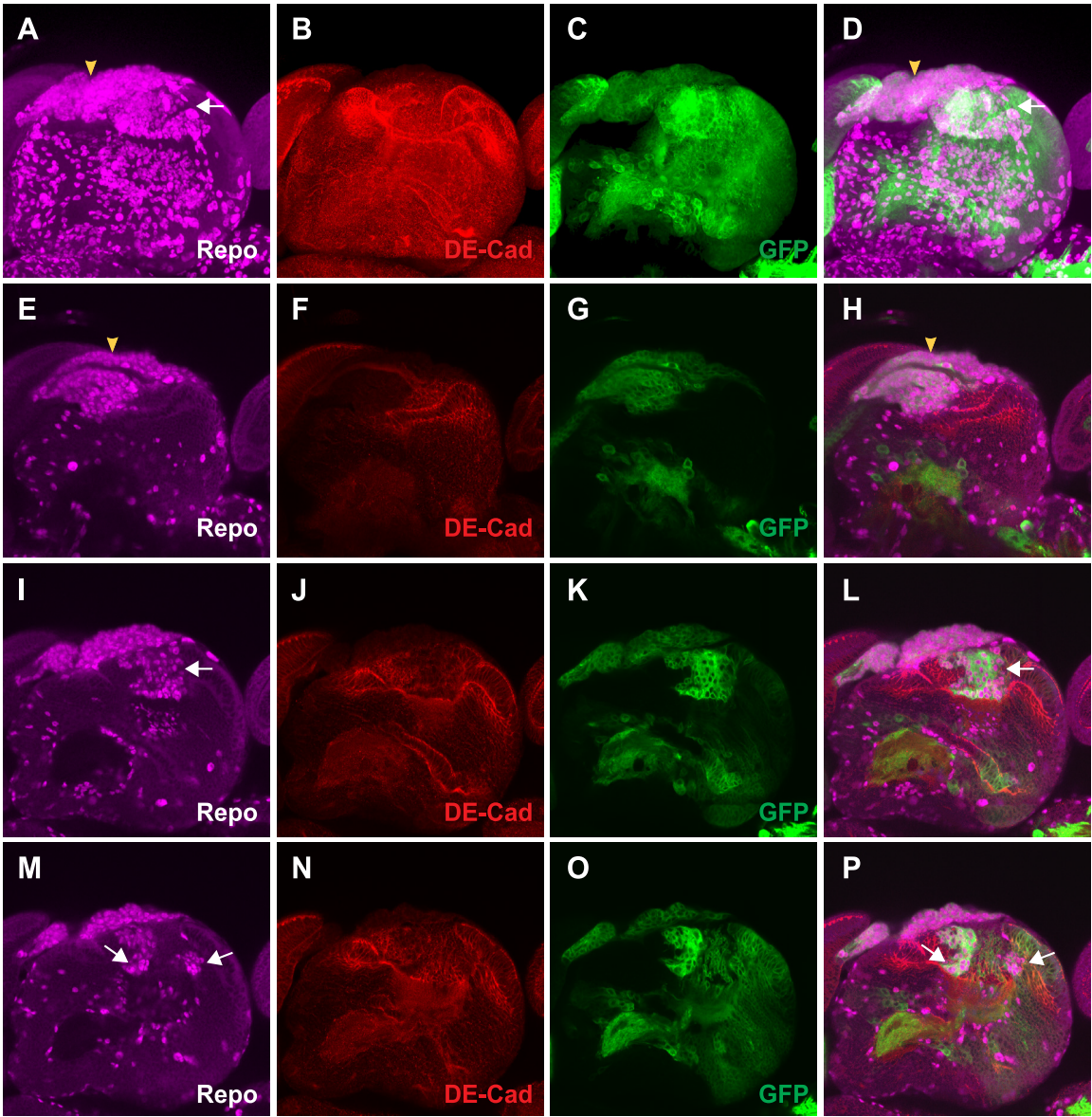


Figure 7. *bantam* causes abnormal distribution of glia cells with increased number in the optic lobe.

All brains are positioned for horizontal view. *bantam* is over expressed in the optic lobe by omb-GAL4. Glial cell are stained by the anti-Repo (magenta). Neuroepithelia are labeled by anti-DE-Cadherin (red). Expression of omb-GAL4 is visualized by GFP (green). (A, B, C, D) are maximum projection from multiple sections. (E, F, G, H) are single focal planes showing a greater number of glial cells in the optic stalk (yellow arrow head). (I, J, K, L) are single focal planes showing the disorganized glial cells at the base of lamina, and ectopic glial cells in the lamina (white arrow). (M, N, O, P) are single focal planes showing increased glial cells under the lamina furrow (white arrows).

Figure 8

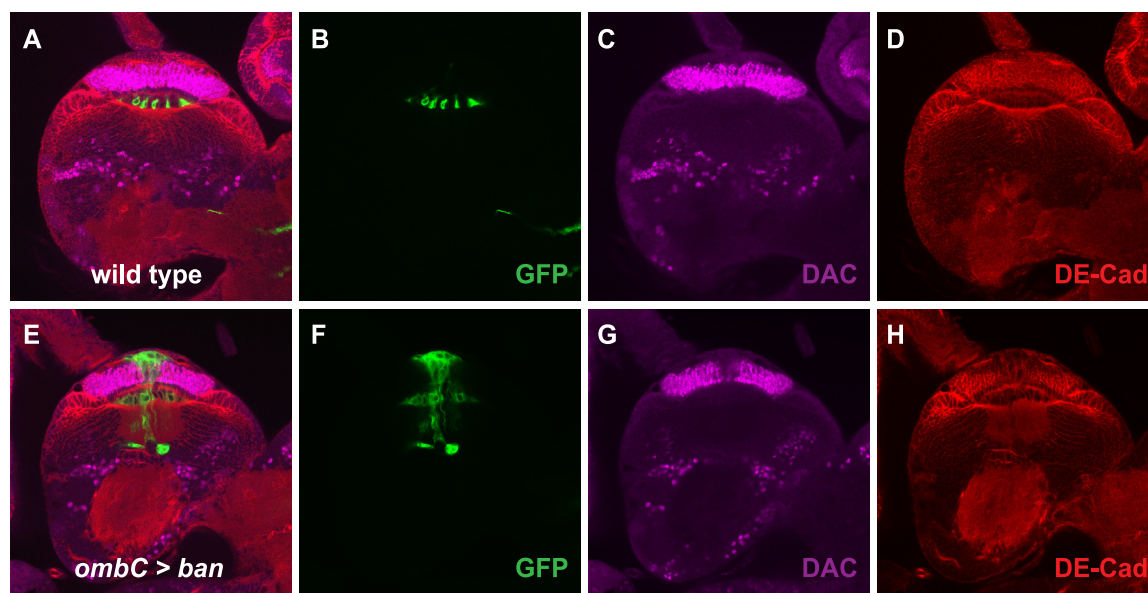


Figure 8. Over expression of *bantam* causes ectopic glial cells in the lamina.

A single focal plane for horizontal view is shown. *UAS-CD8-GFP* (green) is used to view expression of *ombC-Gal4*. anti-DAC (magenta) is used to label lamina neurons. DE-cadherin staining (red) is used to view neuroepithelial cells. (A, B, C, D) wild type; (E, F, G, H) *bantam* is over expressed by *ombC-Gal4*. Ectopic glial cells are present in the lamina (arrows).

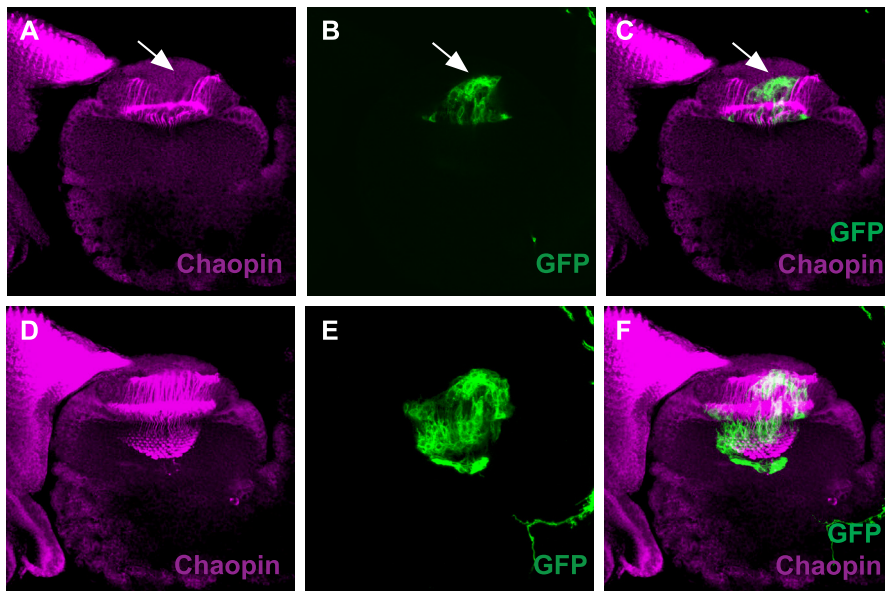
Figure 9

Figure 9. *bantam* causes ectopic glial cell cluster in the lamina.

Brains are positioned in a horizontal view. Anti-Chaopin staining (magenta) is used to view R-cell projection patterns. *UAS*-CD8-GFP (green) is used to visualize expression pattern of *ombC*-Gal4 driver. (A, B, C) is the single focal plane. R1-R6 terminate at the right position at the base of lamina even though they are taking detour to bypass the glial cell cluster (arrows) in the lamina. (D, E, F) is the maximum projection from multiple sections. The ectopic glial cell cluster is present in the lamina. The entire R axon projection pattern is like wild-type.

Appendix

Conserved microRNAs in brains

The work in this chapter is done as a collaboration with Maocheng Yang. My contribution to this chapter is involved in making small RNA samples from brain tissues, generating transgenic flies and analyzing the results.

Introduction

microRNAs (miRNAs) are a newly identified and abundant class of small non-coding RNAs found in a wide variety of organisms, from plants to insects to mammals. miRNAs are single stranded RNA of about 22nt in length that are generated from endogenous hair-pin transcripts encoded from the miRNAs genes (Kim, 2005). miRNAs function through base-pairing with their target mRNAs, usually in the 3' untranslated region (UTR). Based on the degree of complementary between miRNAs and mRNAs, there are two main mechanisms for miRNA action, translational repression or mRNA cleavage (Bagga et al., 2005; Yang et al., 2005). In animals, most miRNAs function through translation repression and also result in mRNA cleavage or degradation. More and more evidence showed that miRNAs play important roles in regulating diverse aspects of cellular and developmental processes, such as developmental timing, early embryogenesis, cell proliferation, cell differentiation, cell death, and neurogenesis. Aberrant miRNA expression levels are associated with lots of developmental disorders and diseases (Williams, 2008).

There are increasing number of the miRNA genes reported. At present, 940 in human, 171 in *Drosophila melanogaster*, and 175 in *Caenorhabditis elegans* (www.mirbase.org) (Griffiths-Jones, 2004). Many miRNAs are found evolutionarily conserved in vertebrates (Lagos-Quintana et al., 2003; Lim et al., 2003a). Moreover, some of them are conserved among distant related species. For example, about a third of the *C. elegans* miRNAs have conserved homologs in humans (Lim et al., 2003b), which strongly suggesting that these highly conserved miRNAs might have conserved functions.

To study the functions of miRNAs, miRNA targets, and spatial and temporal expression profiles of miRNAs would provide the best clues. In our work, we utilized a high-throughput miRNA microarray, miRMAX™ microarray, which has high sensitivity, to study the brain enriched miRNAs in different organisms, including *Drosophila*, mouse, rat and humans. Our results showed that about half of the known miRNAs are significantly up-regulated in the *Drosophila* third instar larval brain relative to the whole body. About 27 conserved miRNAs in mouse, rat, and human are significantly up-regulated in brains. Among those, six miRNAs including *miR-7*, *miR-9*, *miR-100*, *miR-124*, *miR-125* and *miR-219* were found enriched in brain tissues of *Drosophila*, mouse, rat and humans, suggesting their possible important conserved roles in central nervous system. Several of these miRNAs have already been associated with central nervous system or brain functions, such as *miR-9* and *miR-124* (described in the Chapter I).

Materials and Methods

The miRMAX Microarrays

The current miRMAX array chip (<http://cord.rutgers.edu/mirmax/index.html>) consists of 854 probes for all the existing miRNAs of *Caenorhabditis elegans*, *Drosophila melanogaster*, *Homo sapiens*, *Rattus norvegicus* and *Mus musculus* (Griffiths-Jones, 2004). This array has dimer oligonucleotides complementary to the mature miRNA sequences (or truncated miRNA sequences to allow for closer T_m values across all known miRNA sequences).

Small RNA Preparation

Drosophila melanogaster were grown on standard media at 25 °C. The wandering third-instar larvae and adults were collected for miRNA extraction. Approximately 60 larval brains were dissected and collected in 1X Ringers solution. Low molecular RNAs (small RNAs) were extracted with *mirVana*[™] miRNA isolation kit (Ambion, Austin, TX, USA) according to the manufacturer's protocol.

Fresh whole brains and livers of adult mice and rats were frozen and ground into a powder in liquid nitrogen for total RNAs extraction by using Trizol[™] (Invitrogen, Carlsbad, CA, USA). Small RNAs were extracted with *mirVana*[™] miRNA isolation kit (Ambion, Austin, TX, USA). Total RNAs of human brains and human livers were purchased from Ambion (Austin, TX, USA). Small RNAs were extracted from the total RNAs by passing through Microcon[®] YM-100 columns (Millipore, Bedford, MA, USA).

Two hundred nanograms of small RNAs from each tissue sample were directly labeled with 3DNA Array900 miRNA Direct labeling kit (Genisphere, Hatfield, PA, USA) for miRMAX™ miRNA microarray analysis.

Microarray data processing and normalization

Microarray chips were scanned using a GenePix 4000B scanner (Axon Instruments, Union City, CA, USA) and median spot intensities were generated using GenePix 4.0 (Axon Instruments, Union City, CA, USA). Microarray data were processed and normalized using GeneTraffic Duo (Stratagene, La Jolla, CA, USA). Three independent replicates for each sample were performed. Three identical replicates for human brain and liver RNAs were used for hybridization. Statistic and clustering analysis were done by using the JMP software (SAS Institute, Cary, NC, USA). Expression levels of miRNAs were subjected to a 1-way analysis of variance (Anova) for brain tissues vs. liver tissues in human, mouse and rat or larvae brains, whole larvae, adult heads and whole adults of flies. miRNAs were considered to be enriched in a tissue when either its average signal intensity is six fold higher than the other tissues or the fold change difference is over two (brain average/liver average or liver average/brain average) and statistically significant ($P < 0.05$, ANOVA, Tukey HSD).

Generation of miRNA sensor transgenes

***dme-miR-7* sensor**

To generate a *miR-7* sensor, a pair of oligos contain two copies of *miR-7* complementary sequences were used: 5'-

**GGCCGCACAACAAAATCACTAGTCTTCCAGTGCACAACAAAATCACTAGT
CTTCCAT -3' and 5'-**

**CTAGATGGAAGACTAGTGATTTTGTGTGCACTGGAAGACTAGTGATTTT
GTTGT GC -3'.** Oligos were annealed together, and inserted downstream of tub-EGFP into the 3'UTR between Not I and Xba I sites in CaSpeR4 for generating transgenic animals.

***dme-miR-125* sensor**

To generate a *miR-125* sensor, a pair of oligos contain two copies of *miR-125* complementary sequences were used: 5'-

**GGCCGCTCACAAGTTAGGGTCTCAGGGAGTGCTCACAAGTTAGGGTCTCA
GGGAT -3'**

and 5'-

**CTAGATCCCTGAGACCCTAACTTGTGAGCACTCCCTGAGACCCTAACTTG
TGAGC -3'.** Oligos were annealed together, and inserted downstream of tub-EGFP into the 3'UTR between Not I and Xba I sites in CaSpeR4 for generating transgenic animals.

Results and Discussion

miRNAs enriched in brains of *Drosophila*

Many miRNAs have been found temporally expressed in the developing mouse brain (Miska et al., 2004). Many are also regulated during neuronal differentiation (Sempere et al., 2004), suggesting important roles of miRNAs in brain development. Detailed miRNA expression profiles in the brains will provide useful first clue of functions they perform in the brain. We used the miMAX array technology to profile the expression of all known 78 *Drosophila* miRNAs in brain tissues of the third instar larvae, adult fly head, whole third instar larvae, and whole adult flies. In our results, there were 34 out of 78 miRNAs in *Drosophila* that are specifically enriched in brains of the 3rd instar larvae (Table 1). Eleven of them have more than 20 fold higher expression in larval brains compared to the levels in the whole larvae, including *miR-124*, *miR-125*, *miR-13a*, *miR-2c*, *miR-306*, *miR-307*, *miR-315*, *miR-7*, *miR-79*, *miR-92a*, and *miR-92b*. Eleven miRNAs, *miR-11*, *miR-124*, *miR-125*, *miR-133*, *miR-184*, *miR-210*, *miR-315*, *miR-317*, *miR-5*, *miR-7*, and *miR-87*, are enriched both in larval brains and in adult heads (Table 1). This large pool of miRNAs enriched in larval brains and fly heads suggests important role of miRNAs in *Drosophila* brain and neuronal development.

Brain miRNAs conserved across the species

Using the miMAX array technology, we also checked the brain miRNA expression profiles in human, mice and rats. miRNAs are considered to be enriched when either the array signal is six fold higher in the brain or the fold change is over two (brain /liver) and $P < 0.05$ (ANOVA). Compared to their own liver tissue samples, in human, there are 42

miRNAs are enriched in the brain, in rat, there are 61 miRNAs are enriched in the brain, in mice, there are 43 miRNAs are enriched in the brain. We compared brain enriched miRNA expression profiles in humans, mice, rats and *Drosophila*, and found that there are 27 miRNAs conserved expression among brain samples in humans, mice and rats, and six miRNAs, *miR-7*, *miR-9*, *miR-100*, *miR-124*, *miR-125* and *miR-219* were found enriched in the brain tissues of *Drosophila*, humans, mice and rats. (Table 2).

Many brain enriched miRNAs identified in our microarray were confirmed by the previous studies on the *in situ* expression patterns of miRNAs during brain development of zebrafish, mouse, and humans (Kloosterman et al., 2006; Nelson et al., 2006; Wienholds et al., 2005). *miR-124a* is specifically expressed in the CNS of zebrafish (Kloosterman et al., 2006; Wienholds et al., 2005) and mouse embryos (Kloosterman et al., 2006). In humans, *miR-124a* is expressed in the cerebral cortex in the fetal brain and exclusively in neurons of adult brain (Nelson et al., 2006). *miR-9* is expressed in the forebrain and the spinal cord of the mouse embryo (Kloosterman et al., 2006). In humans, *miR-9* is intensely expressed in the cells of the germinal matrix in fetal brain, and prominent in the dentate granule cells of the hippocampus but very low in the neurons of the cortex in adult brain (Nelson et al., 2006). *mir-125b* is strongly expressed at the midbrain-hindbrain boundary in mouse embryos (Kloosterman et al., 2006). In humans, *mir-125b* is strongly expressed in both the germinal matrix and cerebral cortex of the fetal brain, and in both neurons and glial cells of the adult brain (Nelson et al., 2006).

Among these six highly conserved brain enrich miRNAs, *miR-9* and *miR-124* have been most studied for their functions, playing important roles in the early neural patterning, and the proliferation and differentiation of neural stem cells (described in the Chapter I). Recently *miR-7* also was found to be down regulated at the early stage of the neuronal differentiation (Chen et al.). *miR-125* and *miR-219* are more associated with glial cells. *miR-125b* is strongly associated with glial cell proliferation and also found increased in astrogliosis associated neurological disorders, such as Alzheimer's disease and in Down's syndrome (Pogue et al., 2010). *miR-219* plays important roles in promoting oligodendrocyte differentiation (Nave, 2010).

miRNAs expression patterns in *Drosophila* developing brain

To further confirm our microarray data, we made transgenic flies containing miRNAs sensors for *Drosophila miR-7* and *miR-125*, which express GFP under the control of a ubiquitously active tubulin promoter. The sensors have two perfect miRNA binding sites in their 3'UTR. When miRNAs are present, miRNAs reduces GFP expression by RNAi effect, through reducing the mRNA levels of the reporter. Thus, sensors can be a negative indicators of miRNA expression levels.

We examined the sensor expression patterns in the third instar larval brain, and found low expression levels of *miR-125* and *miR-7* in the larval brain compared to the high expression level of the control sensor (Figure 1). This suggests that both miRNAs are abundantly expressed in the fly brain. Future studies of the expression of these miRNAs

in specific cell types in the developing brain will help elucidate their functions in brain development.

Identification of miRNA targets also will help in the function study of miRNAs. In our previous work, we identified two validated targets of *miR-7*, *fringe* and *HLHm5* (Robins et al., 2005). *fringe* is a negative regulator of Notch signaling, which has a role in nervous system development (Portin, 2002). *HLHm5* is required during early neurogenesis to give neuroectodermal cells access to the epidermal pathway of development (Schrons et al., 1992). Future experiments to test what effect *miR-7* has on *fringe* and *HLHm5* in the brain will be of interest.

Summary

In this work, we utilized a high-throughput miRNA microarray, miRMAX™ microarray, and identified the brain enriched miRNAs in different organisms, including *Drosophila*, mouse, rat and humans. Our results showed that about half of the known miRNAs are significantly up-regulated in the *Drosophila* third instar larval brain relative to the whole body. About 27 brain enriched miRNAs are significantly up-regulated in brains of mammals. But this number might be a low estimate, since some miRNAs are related but are not obvious homologs. Further our array did not have any of the newly identified miRNAs on it, so there may be more common miRNAs in the new group. Six miRNAs, including *miR-7*, *miR-9*, *miR-100*, *miR-124*, *miR-125* and *miR-219*, were found enriched in brain tissues of *Drosophila*, mouse, rat and humans, even after 500 million years of evolution. This suggests that these miRNAs likely participate in some basic neuronal functions rather than being involved in species-specific functions. These six miRNAs have already been confirmed to be enriched in the CNS of zebrafish, mouse or both.

Some of these miRNAs have also been associated with brain functions. *miR-9* and *miR-124* play important roles in proliferation and differentiation of neural stem cells. *miR-125* and *miR-219* have functions in glial cell proliferation and differentiation. Even though the architecture of fly and mammalian brains are quite different, they share similar mechanisms for basic neuronal functions, such as the proliferation and differentiation of neuronal stem cells, axon pathfinding of neurons, proliferation, differentiation, and migration of glial cells. The simple anatomy of the *Drosophila* brain and availability of sophisticated genetic tools make flies a great model for studying the role of these

conserved brain enriched miRNAs in brain development. Future experiments to validate predicted targets of these brain-enriched miRNAs examine their roles in the developing brain is of considerable interest.

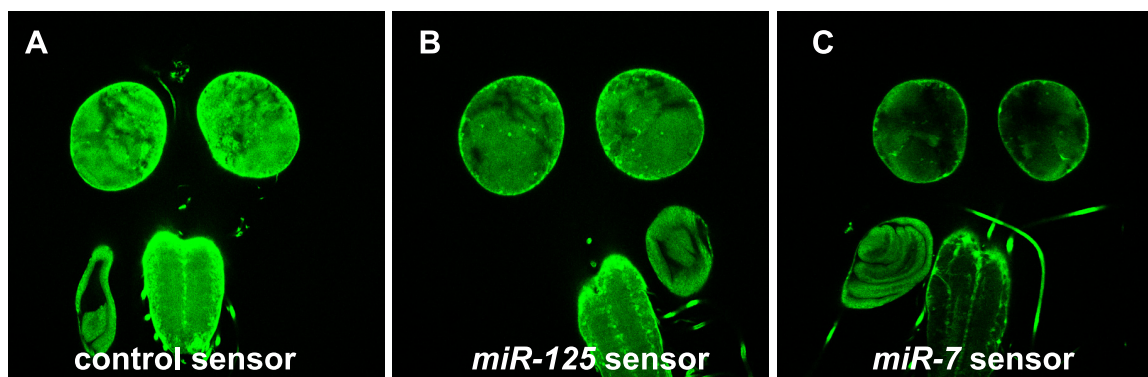
Figure 1

Figure 1. *miR-7* and *miR-125* are highly expressed in the *Drosophila* developing brain.

Single focal plane image of the third instar larval brains. All sensor constructs are expressed with a *tubulin* promoter driving EGFP. (A) Control sensor without miRNA binding sites shows high expression almost ubiquitously in both brain hemispheres and the ventral cord. (B) *miR-125* sensor containing two perfectly complementary copies of the *miR-125* binding sequence in the 3' UTR shows low expression level in the larval brain. (C) *miR-7* sensor containing two perfectly complementary copies of the *miR-7* binding sequence in the 3' UTR shows low expression level in the larval brain.

Table 1. miRNAs in *Drosophila* larval brains and adult heads.

miRNA	Larval Brain Average	Adult Head Average	Ratio (larval Brain/whole body)	Ratio (adult Head /whole body)
Larval brain enriched				
<i>dme-miR-92b</i>	20922	114	105.33	0.85
<i>dme-miR-13a</i>	22158	136	75.43	0.76
<i>dme-miR-307</i>	14917	376	44.09	1.66
<i>dme-miR-92a</i>	41341	393	43.61	0.60
<i>dme-miR-79</i>	25630	169	30.92	0.36
<i>dme-miR-306</i>	35393	200	26.33	0.43
<i>dme-miR-2c</i>	12060	387	24.60	0.80
<i>dme-miR-276b</i>	43518	1428	17.67	0.74
<i>dme-miR-276a*</i>	7138	394	16.69	0.87
<i>dme-miR-9b</i>	2978	118	15.58	0.71
<i>dme-miR-2b</i>	37906	1666	14.13	0.99
<i>dme-miR-100</i>	2493	299	12.85	0.95
<i>dme-miR-2a</i>	41985	1355	12.45	0.93
<i>dme-miR-9c</i>	7104	101	12.26	0.42
<i>dme-miR-275</i>	34770	958	12.13	1.52
<i>dme-miR-13b</i>	45202	702	9.24	0.31
<i>dme-miR-305</i>	42238	1832	8.87	1.37
<i>dme-miR-219</i>	383	65	8.54	1.11
<i>dme-miR-276a</i>	32728	3161	8.01	1.22
<i>dme-miR-279</i>	16463	641	5.72	0.42
<i>dme-bantam</i>	14716	973	4.96	0.35
<i>dme-miR-31a</i>	3219	496	4.77	1.01
<i>dme-miR-iab-4-5p</i>	320	36	4.14	1.31
<i>dme-miR-284</i>	3257	557	3.85	1.27
<i>dme-miR-10</i>	5726	123	3.68	0.19
<i>dme-miR-31b</i>	3145	479	3.42	1.04
<i>dme-miR-278</i>	1957	252	3.15	0.75
<i>dme-miR-6</i>	224	46	2.13	0.97
Brain and head enriched				
<i>dme-miR-125</i>	10200	13285	22.26	10.71
<i>dme-miR-184</i>	41857	26669	13.06	14.67
<i>dme-miR-133</i>	1769	7676	21.34	29.56
<i>dme-miR-210</i>	2695	14936	15.97	18.58
<i>dme-miR-315</i>	15270	241	99.97	8.42
<i>dme-miR-124</i>	16290	362	89.83	2.77
<i>dme-miR-7</i>	32589	2304	41.92	3.07
<i>dme-miR-317</i>	11541	2014	16.43	2.23
<i>dme-miR-11</i>	38688	6156	12.92	3.11
<i>dme-miR-87</i>	434	1054	2.58	2.51
<i>dme-miR-5</i>	83	276	2.22	6.94

Table 1

Each miRNA signal intensity of *Drosophila* third instar larval brains or adult heads is obtained from the average of three independent repeats. The ratio of signal intensities for each miRNA was analyzed by the ANOVA pair-wise method. Only miRNAs with more than two fold changes and statistically significant ($P < 0.05$ compared to all other samples) are considered brain enriched.

Table 2. Conserved expression of miRNAs in brain tissues across species.

miRNAs	Humans	Mouse	Rat	Fly
Brain enriched				
<i>miR-7</i>	2.3	2.8	2.4	41.9
<i>miR-100</i>	4.1	3.5	4	12.9
<i>miR-9</i>	201.1	26.8	24.5	b (15.6) c (12.3)
<i>miR-124</i>	a(23.5)	a (4.4)	a (9.8)	89.8
<i>miR-125</i>	a (8.0)	a (6.0)	a (6.9)	22.3
	b (6.7)	b (6.1)	b (6.1)	
<i>miR-219</i>	4.3	10.2	8.1	8.5
<i>miR-128a</i>	36.8	144.6	114.2	
<i>miR-128b</i>	42.7	49.5	100.1	
<i>miR-127</i>	4	30.6	31.5	
<i>miR-132</i>	21.3	23.2	22.8	
<i>miR-323</i>	10.8	25.3	98.2	
<i>miR-204</i>	19.6	63.7	21	
<i>miR-153</i>	69.5	34.1	14.8	
<i>miR-218</i>	6.6	37.9	19.7	
<i>miR-137</i>	26	29	19	
<i>miR-186</i>	15.4	8	12.3	
<i>miR-331</i>	6	10.5	10.5	
<i>miR-99a</i>	2.1	4.2	11.5	
<i>miR-181a</i>	17.2	10	6	
<i>miR-181b</i>	11.4	5.7	3.1	
<i>miR-181c</i>	6.6	8.9	3.8	
<i>miR-338</i>	17	6.3	4.6	
<i>miR-29b</i>	4.7	2.9	b (7.1) c (6.3) a(6.0)	
<i>miR-138</i>	3.8	4	2.7	
<i>miR-98</i>	5.3	2.2	2.6	
<i>miR-142-5p</i>	3.2	4.2	4.2	
<i>miR-222</i>	7.0	4.2	2.5	

Table 2 Conserved expression of miRNAs in brain tissues across species.

Brain enriched miRNAs are listed in the table. The ratio of signal intensities for each miRNA of the brain compared to the liver in mouse, rat or humans, or the third instar larval brains is shown. (a, b, c) in the table represents specific member in a miRNA family.

SUMMARY OF THESIS WORK

The TGF β superfamily plays important roles in controls a broad array of cellular functions, such as cell proliferation, differentiation, migration and apoptosis, in a variety of multicellular organisms ranging from worms and flies to humans. Fine tuned TGF β signaling is very important for its functions. Strength and duration of TGF β signaling are regulated at various steps and by multiple mechanisms. Aberrant TGF β signaling has been implicated in various developmental disorders and human diseases. The key components in the TGF β signal transduction are evolutionary conserved. With limited number of key molecules in the TGF β signaling pathways and availability of the sophisticated genetic tools, *Drosophila* has been considered a ideal model organism to study the regulators of the TGF β pathways, which will help to lead to potential treatments for various developmental disorders and diseases caused by aberrant TGF β signaling.

microRNAs (miRNAs) are an abundant class of small non-coding RNAs that play important roles in posttranscriptional gene regulation. In animals, miRNAs function through translational repression or mRNA cleavage to regulate gene expression. Many genetic and functional studies have indicated that miRNAs are involved in regulating diverse aspects of cellular and developmental processes.

My thesis work examines the regulation of TGF β -like pathways by miRNAs. Specifically, I did my early work in collaboration with H. Robins, where we successfully identified and validated putative targets of *Drosophila* miRNAs with the combination of the computational algorithm and tissue culture methods. We have developed an algorithm for predicting targets that does not rely on evolutionary conservation, but incorporates the

secondary structure of the mRNAs. In *Drosophila* S2 cells, we have validated our predictions in 10 of 15 genes tested. From that we found that *bantam*, a miRNA, can down regulate *Mad* (*Mothers against dpp*), the key component of Dpp signaling pathway.

Based on those results, I extended my work by using *Drosophila* as a model to study the role of *bantam* on regulation of Dpp *in vivo*. Our results showed that *bantam* down regulates *Mad* (*Mothers against dpp*) expression *in vivo* by targeting the *Mad* 3'UTR, resulting in changes in Dpp signaling. Over expression of *bantam* decreases P-MAD levels and negatively affects Dpp pathway transcriptional target genes. The removal of *bantam* binding sites in the 3'UTR of a *Mad* transgene results in a significant increase in the viability of haploinsufficient *dpp* animals compared to a *Mad* transgene carrying intact *bantam* binding sites in the 3'UTR. And I also found that *bantam* is up-regulated by Dpp in the wing imaginal disc, and thereby functions in a Dpp feedback loop. Furthermore, our results showed that this feedback loop between *bantam* and Dpp signaling is important for maintaining anterior-posterior (A/P) compartment boundary stability in the wing disc through regulation of *optomotor-blind* (*omb*). In terms of growth, our results showed that *bantam* only partially works in parallel to promote cell proliferation with Dpp signaling. Interestingly, by using comparative genomics, we found that *bantam* is evolutionarily conserved, and miRNA target predictions suggest that human *bantam* homologs selectively target Smad5, the homolog of *Mad* in BMP signaling, but do not target Smad2 in the activin/TGF β pathway. All together, our results support the hypothesis that *bantam* miRNA is a conserved negative regulator of BMP/Dpp signaling.

Besides the studies of the role of *bantam* in regulating Dpp, I expanded my work and examined the roles of *bantam* in fly brain development. My work revealed that the detailed expression pattern of *bantam* in the developing optic lobe for the first time, and demonstrated *bantam*'s essential role of promoting proliferation of mitotic cells in the optic lobe, including stem cells and differentiated glial cells. My results showed that change in *bantam* level autonomously affects glial cell number and distribution, and non-autonomously affects photoreceptor neuron axon projection patterns. Furthermore, I found that *bantam* promotes the proliferation of mitotic active glial cells, and affects their distribution, largely through down regulation of T-box transcription factor, *omptomotor-blind* (*omb*). Co-expression of *omb* can rescue *bantam* phenotype, and restore the normal glial cell number and proper glial cell positioning in 66% of brains. In summary, my results suggest that *bantam* is critical for maintaining the stem cell pools in OPC and GPC regions of the optic lobe, and *bantam*'s expression in glial cells is crucial for their proliferation and distribution.

In a side project with Maocheng (Tony) Yang, I did work studying the conservation miRNA expression in the brains. We collected small RNAs from brain tissues from *Drosophila*, rat, mouse, and human, and used miRNA microarray technology to study the miRNA expression profiles in the brains. Our results showed that about half of the miRNAs are significantly up-regulated in the *Drosophila* third instar larval brain relative to the body. About 27 miRNAs conserved in mouse, rat, and human are significantly up-regulated in brains. Among those, six miRNAs including *miR-7*, *miR-9*, *miR-100*, *miR-*

124, *miR-125* and *miR-219*, were found enriched in brain tissues of *Drosophila*, human, mouse and rat, suggesting that they might have important conserved roles in central nervous system.

During the development, organisms encounter many stimuli and need a way to tune molecular processes so that correct cellular responses occur. The use of positive and negative feedback regulation is an obvious way, and is found in many cases. My Ph.D. work identified that *bantam*, a microRNA, is important for fine-tuning of Dpp signaling in *Drosophila* through a negative feedback loop. Bioinformatics suggest that *bantam*/BMP interaction a conserved mechanism used in higher organisms as well. Studies in model organisms have revealed the conserved function of TGF β signaling and shed light on understanding normal development. These studies also provide possible new therapies on diagnoses and treatment of diseases. The future study on the human *bantam* homologs will be of interest.

REFERENCES

- Abrahante, J. E., Daul, A. L., Li, M., Volk, M. L., Tennessen, J. M., Miller, E. A. and Rougvie, A. E.** (2003). The *Caenorhabditis elegans* hunchback-like gene *lin-57/hbl-1* controls developmental time and is regulated by microRNAs. *Dev Cell* **4**, 625-637.
- Adachi-Yamada, T., Fujimura-Kamada, K., Nishida, Y. and Matsumoto, K.** (1999). Distortion of proximodistal information causes JNK-dependent apoptosis in *Drosophila* wing. *Nature* **400**, 166-169.
- Aegerter-Wilmsen, T., Aegerter, C. M., Hafen, E. and Basler, K.** (2007). Model for the regulation of size in the wing imaginal disc of *Drosophila*. *Mech Dev* **124**, 318-326.
- Affolter, M. and Basler, K.** (2007). The Decapentaplegic morphogen gradient: from pattern formation to growth regulation. *Nat Rev Genet* **8**, 663-674.
- Akiyama, T., Kamimura, K., Firkus, C., Takeo, S., Shimmi, O. and Nakato, H.** (2008). Dally regulates Dpp morphogen gradient formation by stabilizing Dpp on the cell surface. *Dev Biol* **313**, 408-419.
- Alfonso, T. B. and Jones, B. W.** (2002). *gcm2* promotes glial cell differentiation and is required with *glial cells missing* for macrophage development in *Drosophila*. *Dev Biol* **248**, 369-383.
- Ambros, V.** (2001). microRNAs: tiny regulators with great potential. *Cell* **107**, 823-826.
- Ambros, V.** (2003). MicroRNA pathways in flies and worms: growth, death, fat, stress, and timing. *Cell* **113**, 673-676.
- Arora, K., Levine, M. S. and O'Connor, M. B.** (1994). The *screw* gene encodes a ubiquitously expressed member of the TGF- β family required for specification of dorsal cell fates in the *Drosophila* embryo. *Genes Dev* **8**, 2588-2601.
- Arora, K. and Nusslein-Volhard, C.** (1992). Altered mitotic domains reveal fate map changes in *Drosophila* embryos mutant for zygotic dorsoventral patterning genes. *Development* **114**, 1003-1024.
- Bagga, S., Bracht, J., Hunter, S., Massirer, K., Holtz, J., Eachus, R. and Pasquinelli, A. E.** (2005). Regulation by *let-7* and *lin-4* miRNAs results in target mRNA degradation. *Cell* **122**, 553-563.
- Banerjee, D. and Slack, F.** (2002). Control of developmental timing by small temporal RNAs: a paradigm for RNA-mediated regulation of gene expression. *Bioessays* **24**, 119-129.

Bartel, D. P. (2004). MicroRNAs: genomics, biogenesis, mechanism, and function. *Cell* **116**, 281-297.

Belenkaya, T. Y., Han, C., Yan, D., Opoka, R. J., Khodoun, M., Liu, H. and Lin, X. (2004). Drosophila Dpp morphogen movement is independent of dynamin-mediated endocytosis but regulated by the glypican members of heparan sulfate proteoglycans. *Cell* **119**, 231-244.

Bernabeu, C., Lopez-Novoa, J. M. and Quintanilla, M. (2009). The emerging role of TGF- β superfamily coreceptors in cancer. *Biochim Biophys Acta* **1792**, 954-973.

Bierie, B. and Moses, H. L. (2006). TGF- β and cancer. *Cytokine Growth Factor Rev* **17**, 29-40.

Bilen, J., Liu, N. and Bonini, N. M. (2006). A new role for microRNA pathways: modulation of degeneration induced by pathogenic human disease proteins. *Cell Cycle* **5**, 2835-2838.

Bottinger, E. P., Factor, V. M., Tsang, M. L., Weatherbee, J. A., Kopp, J. B., Qian, S. W., Wakefield, L. M., Roberts, A. B., Thorgeirsson, S. S. and Sporn, M. B. (1996). The recombinant proregion of transforming growth factor β 1 (latency-associated peptide) inhibits active transforming growth factor β 1 in transgenic mice. *Proc Natl Acad Sci U S A* **93**, 5877-5882.

Brennecke, J., Hipfner, D. R., Stark, A., Russell, R. B. and Cohen, S. M. (2003). *bantam* encodes a developmentally regulated microRNA that controls cell proliferation and regulates the proapoptotic gene *hid* in Drosophila. *Cell* **113**, 25-36.

Brennecke, J., Stark, A., Russell, R. B. and Cohen, S. M. (2005). Principles of microRNA-target recognition. *PLoS Biol* **3**, e85.

Brummel, T., Abdollah, S., Haerry, T. E., Shimell, M. J., Merriam, J., Raftery, L., Wrana, J. L. and O'Connor, M. B. (1999). The Drosophila activin receptor *baboon* signals through *dSmad2* and controls cell proliferation but not patterning during larval development. *Genes Dev* **13**, 98-111.

Brummel, T. J., Twombly, V., Marques, G., Wrana, J. L., Newfeld, S. J., Attisano, L., Massague, J., O'Connor, M. B. and Gelbart, W. M. (1994). Characterization and relationship of Dpp receptors encoded by the *saxophone* and *thick veins* genes in Drosophila. *Cell* **78**, 251-261.

Bryant, P. J. (1988). Localized cell death caused by mutations in a Drosophila gene coding for a transforming growth factor- β homolog. *Dev Biol* **128**, 386-395.

Burke, R. and Basler, K. (1996). Dpp receptors are autonomously required for cell proliferation in the entire developing Drosophila wing. *Development* **122**, 2261-2269.

- Bushati, N. and Cohen, S. M.** (2007). microRNA functions. *Annu Rev Cell Dev Biol* **23**, 175-205.
- Calabrese, J. M., Seila, A. C., Yeo, G. W. and Sharp, P. A.** (2007). RNA sequence analysis defines Dicer's role in mouse embryonic stem cells. *Proc Natl Acad Sci U S A* **104**, 18097-18102.
- Campbell, G. and Tomlinson, A.** (1999). Transducing the Dpp morphogen gradient in the wing of *Drosophila*: regulation of Dpp targets by *brinker*. *Cell* **96**, 553-562.
- Carthew, R. W.** (2006). Gene regulation by microRNAs. *Curr Opin Genet Dev* **16**, 203-208.
- Chang, S., Johnston, R. J., Jr., Frokjaer-Jensen, C., Lockery, S. and Hobert, O.** (2004). MicroRNAs act sequentially and asymmetrically to control chemosensory laterality in the nematode. *Nature* **430**, 785-789.
- Chen, H., Shalom-Feuerstein, R., Riley, J., Zhang, S. D., Tucci, P., Agostini, M., Aberdam, D., Knight, R. A., Genchi, G., Nicotera, P. et al.** (2010). *miR-7* and *miR-214* are specifically expressed during neuroblastoma differentiation, cortical development and embryonic stem cells differentiation, and control neurite outgrowth in vitro. *Biochem Biophys Res Commun* **394**, 921-927.
- Chen, P., Nordstrom, W., Gish, B. and Abrams, J. M.** (1996). *grim*, a novel cell death gene in *Drosophila*. *Genes Dev* **10**, 1773-1782.
- Chen, X.** (2004). A microRNA as a translational repressor of APETALA2 in Arabidopsis flower development. *Science* **303**, 2022-2025.
- Chen, Y. G., Liu, F. and Massague, J.** (1997). Mechanism of TGF β receptor inhibition by FKBP12. *EMBO J* **16**, 3866-3876.
- Cheng, L. C., Pastrana, E., Tavazoie, M. and Doetsch, F.** (2009). *miR-124* regulates adult neurogenesis in the subventricular zone stem cell niche. *Nat Neurosci* **12**, 399-408.
- Cho, E., Feng, Y., Rauskolb, C., Maitra, S., Fehon, R. and Irvine, K. D.** (2006). Delineation of a Fat tumor suppressor pathway. *Nat Genet* **38**, 1142-1150.
- Chotard, C., Leung, W. and Salecker, I.** (2005). *glial cells missing* and *gcm2* cell autonomously regulate both glial and neuronal development in the visual system of *Drosophila*. *Neuron* **48**, 237-251.
- Chotard, C. and Salecker, I.** (2007). Glial cell development and function in the *Drosophila* visual system. *Neuron Glia Biol* **3**, 17-25.

- Conaco, C., Otto, S., Han, J. J. and Mandel, G.** (2006). Reciprocal actions of REST and a microRNA promote neuronal identity. *Proc Natl Acad Sci U S A* **103**, 2422-2427.
- Constam, D. B.** (2009). Riding shotgun: a dual role for the epidermal growth factor-Cripto/FRL-1/Cryptic protein Cripto in Nodal trafficking. *Traffic* **10**, 783-791.
- Cook, O., Biehs, B. and Bier, E.** (2004). *brinker* and *optomotor-blind* act coordinately to initiate development of the L5 wing vein primordium in *Drosophila*. *Development* **131**, 2113-2124.
- Crittenden, J. R., Skoulakis, E. M., Han, K. A., Kalderon, D. and Davis, R. L.** (1998). Tripartite mushroom body architecture revealed by antigenic markers. *Learn Mem* **5**, 38-51.
- Cutforth, T. and Gaul, U.** (1997). The genetics of visual system development in *Drosophila*: specification, connectivity and asymmetry. *Curr Opin Neurobiol* **7**, 48-54.
- Das, P., Inoue, H., Baker, J. C., Beppu, H., Kawabata, M., Harland, R. M., Miyazono, K. and Padgett, R. W.** (1999). *Drosophila dSmad2* and *Atr-I* transmit activin/TGF β signals. *Genes Cells* **4**, 123-134.
- Das, P., Maduzia, L. L., Wang, H., Finelli, A. L., Cho, S. H., Smith, M. M. and Padgett, R. W.** (1998). The *Drosophila* gene *Medea* demonstrates the requirement for different classes of Smads in *dpp* signaling. *Development* **125**, 1519-1528.
- Datar, S. A., Jacobs, H. W., de la Cruz, A. F., Lehner, C. F. and Edgar, B. A.** (2000). The *Drosophila cyclin D-Cdk4* complex promotes cellular growth. *EMBO J* **19**, 4543-4554.
- Datta, P. K. and Moses, H. L.** (2000). STRAP and Smad7 synergize in the inhibition of transforming growth factor β signaling. *Mol Cell Biol* **20**, 3157-3167.
- Davis, B. N., Hilyard, A. C., Lagna, G. and Hata, A.** (2008). SMAD proteins control DROSHA-mediated microRNA maturation. *Nature* **454**, 56-61.
- Day, S. J. and Lawrence, P. A.** (2000). Measuring dimensions: the regulation of size and shape. *Development* **127**, 2977-2987.
- de Celis, J. F. and Barrio, R.** (2000). Function of the *spalt/spalt-related* gene complex in positioning the veins in the *Drosophila* wing. *Mech Dev* **91**, 31-41.
- Dearborn, R., Jr. and Kunes, S.** (2004). An axon scaffold induced by retinal axons directs glia to destinations in the *Drosophila* optic lobe. *Development* **131**, 2291-2303.

- Decotto, E. and Ferguson, E. L.** (2001). A positive role for *Short gastrulation* in modulating BMP signaling during dorsoventral patterning in the *Drosophila* embryo. *Development* **128**, 3831-3841.
- del Alamo Rodriguez, D., Terriente Felix, J. and Diaz-Benjumea, F. J.** (2004). The role of the T-box gene *optomotor-blind* in patterning the *Drosophila* wing. *Dev Biol* **268**, 481-492.
- Didiano, D. and Hobert, O.** (2006). Perfect seed pairing is not a generally reliable predictor for miRNA-target interactions. *Nat Struct Mol Biol* **13**, 849-51.
- Doench, J. G., Petersen, C. P. and Sharp, P. A.** (2003). siRNAs can function as miRNAs. *Genes Dev* **17**, 438-442.
- Doench, J. G. and Sharp, P. A.** (2004). Specificity of microRNA target selection in translational repression. *Genes Dev* **18**, 504-511.
- Driever, W. and Nusslein-Volhard, C.** (1988). The *bicoid* protein determines position in the *Drosophila* embryo in a concentration-dependent manner. *Cell* **54**, 95-104.
- Egger, B., Boone, J. Q., Stevens, N. R., Brand, A. H. and Doe, C. Q.** (2007). Regulation of spindle orientation and neural stem cell fate in the *Drosophila* optic lobe. *Neural Dev* **2**, 1.
- Eivers, E., Demagny, H. and De Robertis, E. M.** (2009a). Integration of BMP and Wnt signaling via vertebrate Smad1/5/8 and *Drosophila* *Mad*. *Cytokine Growth Factor Rev* **20**, 357-365.
- Eivers, E., Fuentealba, L. C., Sander, V., Clemens, J. C., Hartnett, L. and De Robertis, E. M.** (2009b). *Mad* is required for *wingless* signaling in wing development and segment patterning in *Drosophila*. *PLoS One* **4**, e6543.
- Eldar, A., Dorfman, R., Weiss, D., Ashe, H., Shilo, B. Z. and Barkai, N.** (2002). Robustness of the BMP morphogen gradient in *Drosophila* embryonic patterning. *Nature* **419**, 304-308.
- Elliott, D. A. and Brand, A. H.** (2008). The GAL4 system : a versatile system for the expression of genes. *Methods Mol Biol* **420**, 79-95.
- Emerald, B. S. and Roy, J. K.** (1998). Organising activities of *engrailed*, *hedgehog*, *wingless* and *decapentaplegic* in the genital discs of *Drosophila melanogaster*. *Dev Genes Evol* **208**, 504-516.
- Enright, A. J., John, B., Gaul, U., Tuschl, T., Sander, C. and Marks, D. S.** (2003). MicroRNA targets in *Drosophila*. *Genome Biol* **5**, R1.

- Entchev, E. V., Schwabedissen, A. and Gonzalez-Gaitan, M.** (2000). Gradient formation of the TGF- β homolog Dpp. *Cell* **103**, 981-991.
- Farnworth, P. G., Stanton, P. G., Wang, Y., Escalona, R., Findlay, J. K. and Ooi, G. T.** (2006). Inhibins differentially antagonize activin and bone morphogenetic protein action in a mouse adrenocortical cell line. *Endocrinology* **147**, 3462-3471.
- Fazi, F., Rosa, A., Fatica, A., Gelmetti, V., De Marchis, M. L., Nervi, C. and Bozzoni, I.** (2005). A minicircuitry comprised of *microRNA-223* and transcription factors NFI-A and C/EBP α regulates human granulopoiesis. *Cell* **123**, 819-831.
- Feinbaum, R. and Ambros, V.** (1999). The timing of *lin-4* RNA accumulation controls the timing of postembryonic developmental events in *Caenorhabditis elegans*. *Dev Biol* **210**, 87-95.
- Feng, X. H. and Derynck, R.** (2005). Specificity and versatility in tgf- β signaling through Smads. *Annu Rev Cell Dev Biol* **21**, 659-693.
- Ferguson, E. L. and Anderson, K. V.** (1992). Decapentaplegic acts as a morphogen to organize dorsal-ventral pattern in the *Drosophila* embryo. *Cell* **71**, 451-461.
- Francois, V., Solloway, M., O'Neill, J. W., Emery, J. and Bier, E.** (1994). Dorsal-ventral patterning of the *Drosophila* embryo depends on a putative negative growth factor encoded by the *short gastrulation* gene. *Genes Dev* **8**, 2602-2616.
- Frankel, L. B., Christoffersen, N. R., Jacobsen, A., Lindow, M., Krogh, A. and Lund, A. H.** (2008). Programmed cell death 4 (PDCD4) is an important functional target of the *microRNA miR-21* in breast cancer cells. *J Biol Chem* **283**, 1026-1033.
- Fujise, M., Takeo, S., Kamimura, K., Matsuo, T., Aigaki, T., Izumi, S. and Nakato, H.** (2003). Dally regulates Dpp morphogen gradient formation in the *Drosophila* wing. *Development* **130**, 1515-1522.
- Furuhashi, M., Yagi, K., Yamamoto, H., Furukawa, Y., Shimada, S., Nakamura, Y., Kikuchi, A., Miyazono, K. and Kato, M.** (2001). Axin facilitates Smad3 activation in the transforming growth factor β signaling pathway. *Mol Cell Biol* **21**, 5132-5141.
- Gao, S., Steffen, J. and Laughon, A.** (2005). Dpp-responsive silencers are bound by a trimeric Mad-Medea complex. *J Biol Chem* **280**, 36158-36164.
- Gazzerro, E. and Canalis, E.** (2006). Bone morphogenetic proteins and their antagonists. *Rev Endocr Metab Disord* **7**, 51-65.
- Giraldez, A. J., Cinalli, R. M., Glasner, M. E., Enright, A. J., Thomson, J. M., Baskerville, S., Hammond, S. M., Bartel, D. P. and Schier, A. F.** (2005). MicroRNAs regulate brain morphogenesis in zebrafish. *Science* **308**, 833-838.

- Gonzalez-Gaitan, M., Capdevila, M. P. and Garcia-Bellido, A.** (1994). Cell proliferation patterns in the wing imaginal disc of *Drosophila*. *Mech Dev* **46**, 183-200.
- Goto, K., Kamiya, Y., Imamura, T., Miyazono, K. and Miyazawa, K.** (2007). Selective inhibitory effects of Smad6 on bone morphogenetic protein type I receptors. *J Biol Chem* **282**, 20603-20611.
- Green, P., Hartenstein, A. Y. and Hartenstein, V.** (1993). The embryonic development of the *Drosophila* visual system. *Cell Tissue Res* **273**, 583-598.
- Grether, M. E., Abrams, J. M., Agapite, J., White, K. and Steller, H.** (1995). The *head involution defective* gene of *Drosophila melanogaster* functions in programmed cell death. *Genes Dev* **9**, 1694-1708.
- Griffiths-Jones, S.** (2004). The microRNA Registry. *Nucleic Acids Res* **32**, D109-111.
- Grimm, S. and Pflugfelder, G. O.** (1996). Control of the gene *optomotor-blind* in *Drosophila* wing development by *decapentaplegic* and *wingless*. *Science* **271**, 1601-1604.
- Griswold-Prenner, I., Kamibayashi, C., Maruoka, E. M., Mumby, M. C. and Derynck, R.** (1998). Physical and functional interactions between type I transforming growth factor β receptors and α , a WD-40 repeat subunit of phosphatase 2A. *Mol Cell Biol* **18**, 6595-6604.
- Haerry, T. E. and O'Connor, M. B.** (2002). Isolation of *Drosophila* activin and follistatin cDNAs using novel MACH amplification protocols. *Gene* **291**, 85-93.
- Halter, D. A., Urban, J., Rickert, C., Ner, S. S., Ito, K., Travers, A. A. and Technau, G. M.** (1995). The homeobox gene *repo* is required for the differentiation and maintenance of glia function in the embryonic nervous system of *Drosophila melanogaster*. *Development* **121**, 317-332.
- Hassan, B. A., Bermingham, N. A., He, Y., Sun, Y., Jan, Y. N., Zoghbi, H. Y. and Bellen, H. J.** (2000). *atonal* regulates neurite arborization but does not act as a proneural gene in the *Drosophila* brain. *Neuron* **25**, 549-561.
- Hatfield, S. D., Shcherbata, H. R., Fischer, K. A., Nakahara, K., Carthew, R. W. and Ruohola-Baker, H.** (2005). Stem cell division is regulated by the microRNA pathway. *Nature* **435**, 974-978.
- Hayashi, H., Abdollah, S., Qiu, Y., Cai, J., Xu, Y. Y., Grinnell, B. W., Richardson, M. A., Topper, J. N., Gimbrone, M. A., Jr., Wrana, J. L. et al.** (1997). The MAD-related protein Smad7 associates with the TGF β receptor and functions as an antagonist of TGF β signaling. *Cell* **89**, 1165-1173.

Herranz, H., Hong, X., Perez, L., Ferreira, A., Olivieri, D., Cohen, S. M. and Milan, M. (2010). The miRNA machinery targets Mei-P26 and regulates Myc protein levels in the *Drosophila* wing. *EMBO J* **29**, 1688-1698.

Herranz, H., Perez, L., Martin, F. A. and Milan, M. (2008). A Wingless and Notch double-repression mechanism regulates G1-S transition in the *Drosophila* wing. *EMBO J* **27**, 1633-1645.

Hiesinger, P. R., Reiter, C., Schau, H. and Fischbach, K. F. (1999). Neuropil pattern formation and regulation of cell adhesion molecules in *Drosophila* optic lobe development depend on *synaptobrevin*. *J Neurosci* **19**, 7548-7556.

Hipfner, D. R., Weigmann, K. and Cohen, S. M. (2002). The *bantam* gene regulates *Drosophila* growth. *Genetics* **161**, 1527-1537.

Hocevar, B. A., Smine, A., Xu, X. X. and Howe, P. H. (2001). The adaptor molecule *Disabled-2* links the transforming growth factor β receptors to the Smad pathway. *EMBO J* **20**, 2789-2801.

Hofacker, I. L., Fontana, W., Stadler, P. F., Bonhoeffer, L. S., Tacker, M. and Schuster, P. (1994). Fast folding and comparison of RNA secondary structures. *Monatshefte für Chemie / Chemical Monthly* **125**, 167-188.

Hofbauer, A. and Campos-Ortega, J. A. (1990). Proliferation pattern and early differentiation of the optic lobes in *Drosophila melanogaster*. *Roux's Arch. Dev. Biol.* **198**, 264-274.

Hofmeyer, K., Kretzschmar, D. and Pflugfelder, G. O. (2008). *Optomotor-blind* expression in glial cells is required for correct axonal projection across the *Drosophila* inner optic chiasm. *Dev Biol* **315**, 28-41.

Hosoya, T., Takizawa, K., Nitta, K. and Hotta, Y. (1995). *glial cells missing*: a binary switch between neuronal and glial determination in *Drosophila*. *Cell* **82**, 1025-1036.

Houbaviy, H. B., Murray, M. F. and Sharp, P. A. (2003). Embryonic stem cell-specific MicroRNAs. *Dev Cell* **5**, 351-358.

Huang, Z. and Kunes, S. (1996). Hedgehog, transmitted along retinal axons, triggers neurogenesis in the developing visual centers of the *Drosophila* brain. *Cell* **86**, 411-422.

Huang, Z., Shilo, B. Z. and Kunes, S. (1998). A retinal axon fascicle uses *spitz*, an EGF receptor ligand, to construct a synaptic cartridge in the brain of *Drosophila*. *Cell* **95**, 693-703.

- Hufnagel, L., Teleman, A. A., Rouault, H., Cohen, S. M. and Shraiman, B. I.** (2007). On the mechanism of wing size determination in fly development. *Proc Natl Acad Sci U S A* **104**, 3835-3840.
- Ibáñez-Ventoso, C., Vora, M. and Driscoll, M.** (2008). Sequence relationships among *C. elegans*, *D. melanogaster* and human microRNAs highlight the extensive conservation of microRNAs in biology. *PLoS One* **3**, e2818.
- Imoto, S., Ohbayashi, N., Ikeda, O., Kamitani, S., Muromoto, R., Sekine, Y. and Matsuda, T.** (2008). Sumoylation of Smad3 stimulates its nuclear export during PIASy-mediated suppression of TGF- β signaling. *Biochem Biophys Res Commun* **370**, 359-365.
- Irish, V. F. and Gelbart, W. M.** (1987). The *decapentaplegic* gene is required for dorsal-ventral patterning of the *Drosophila* embryo. *Genes Dev* **1**, 868-879.
- Izzi, L. and Attisano, L.** (2006). Ubiquitin-dependent regulation of TGF β signaling in cancer. *Neoplasia* **8**, 677-688.
- Jackson, A. L., Burchard, J., Schelter, J., Chau, B. N., Cleary, M., Lim, L. and Linsley, P. S.** (2006). Widespread siRNA "off-target" transcript silencing mediated by seed region sequence complementarity. *RNA* **12**, 1179-1187.
- Jackson, S. M., Nakato, H., Sugiura, M., Jannuzi, A., Oakes, R., Kaluza, V., Golden, C. and Selleck, S. B.** (1997). *dally*, a *Drosophila* glypican, controls cellular responses to the TGF- β -related morphogen, Dpp. *Development* **124**, 4113-4120.
- Jazwinska, A., Rushlow, C. and Roth, S.** (1999). The role of *brinker* in mediating the graded response to Dpp in early *Drosophila* embryos. *Development* **126**, 3323-3334.
- Jiang, X., Xia, L., Chen, D., Yang, Y., Huang, H., Yang, L., Zhao, Q., Shen, L. and Wang, J.** (2008). Otefin, a nuclear membrane protein, determines the fate of germline stem cells in *Drosophila* via interaction with Smad complexes. *Dev Cell* **14**, 494-506.
- Jin, Z. and Xie, T.** (2007). Dcr-1 maintains *Drosophila* ovarian stem cells. *Curr Biol* **17**, 539-544.
- John, B., Enright, A. J., Aravin, A., Tuschl, T., Sander, C. and Marks, D. S.** (2004). Human MicroRNA targets. *PLoS Biol* **2**, e363.
- Johnston, R. J. and Hobert, O.** (2003). A microRNA controlling left/right neuronal asymmetry in *Caenorhabditis elegans*. *Nature* **426**, 845-849.
- Jones, B. W.** (2005). Transcriptional control of glial cell development in *Drosophila*. *Dev Biol* **278**, 265-273.

Jones, B. W., Fetter, R. D., Tear, G. and Goodman, C. S. (1995). *glial cells missing*: a genetic switch that controls glial versus neuronal fate. *Cell* **82**, 1013-1023.

Kadener, S., Menet, J. S., Sugino, K., Horwich, M. D., Weissbein, U., Nawathean, P., Vagin, V. V., Zamore, P. D., Nelson, S. B. and Rosbash, M. (2009). A role for microRNAs in the *Drosophila* circadian clock. *Genes Dev* **23**, 2179-2191.

Kamiya, Y., Miyazono, K. and Miyazawa, K. (2008). Specificity of the inhibitory effects of *Dad* on TGF- β family type I receptors, *Thickveins*, *Saxophone*, and *Baboon* in *Drosophila*. *FEBS Lett* **582**, 2496-2500.

Kanellopoulou, C., Muljo, S. A., Kung, A. L., Ganesan, S., Drapkin, R., Jenuwein, T., Livingston, D. M. and Rajewsky, K. (2005). Dicer-deficient mouse embryonic stem cells are defective in differentiation and centromeric silencing. *Genes Dev* **19**, 489-501.

Kang, J. S., Saunier, E. F., Akhurst, R. J. and Derynck, R. (2008). The type I TGF- β receptor is covalently modified and regulated by sumoylation. *Nat Cell Biol* **10**, 654-664.

Kaphingst, K. and Kunes, S. (1994). Pattern formation in the visual centers of the *Drosophila* brain: wingless acts via decapentaplegic to specify the dorsoventral axis. *Cell* **78**, 437-448.

Kapsimali, M., Kloosterman, W. P., de Bruijn, E., Rosa, F., Plasterk, R. H. and Wilson, S. W. (2007). MicroRNAs show a wide diversity of expression profiles in the developing and mature central nervous system. *Genome Biol* **8**, R173.

Kicheva, A., Pantazis, P., Bollenbach, T., Kalaidzidis, Y., Bittig, T., Julicher, F. and Gonzalez-Gaitan, M. (2007). Kinetics of morphogen gradient formation. *Science* **315**, 521-525.

Kim, J., Johnson, K., Chen, H. J., Carroll, S. and Laughon, A. (1997). *Drosophila* Mad binds to DNA and directly mediates activation of *vestigial* by Decapentaplegic. *Nature* **388**, 304-308.

Kim, V. N. (2005). MicroRNA biogenesis: coordinated cropping and dicing. *Nat Rev Mol Cell Biol* **6**, 376-385.

Kiriakidou, M., Nelson, P. T., Kouranov, A., Fitziev, P., Bouyioukos, C., Mourelatos, Z. and Hatzigeorgiou, A. (2004). A combined computational-experimental approach predicts human microRNA targets. *Genes Dev* **18**, 1165-1178.

Kirkbride, K. C., Townsend, T. A., Bruinsma, M. W., Barnett, J. V. and Blobe, G. C. (2008). Bone morphogenetic proteins signal through the transforming growth factor- β type III receptor. *J Biol Chem* **283**, 7628-7637.

Kloosterman, W. P., Wienholds, E., de Bruijn, E., Kauppinen, S. and Plasterk, R. H. (2006). In situ detection of miRNAs in animal embryos using LNA-modified oligonucleotide probes. *Nat Methods* **3**, 27-29.

Koli, K., Saharinen, J., Hyytiainen, M., Penttinen, C. and Keski-Oja, J. (2001). Latency, activation, and binding proteins of TGF- β . *Microsc Res Tech* **52**, 354-362.

Kowanetz, M., Lonn, P., Vanlandewijck, M., Kowanetz, K., Heldin, C. H. and Moustakas, A. (2008). TGF β induces SIK to negatively regulate type I receptor kinase signaling. *J Cell Biol* **182**, 655-662.

Krek, A., Grun, D., Poy, M. N., Wolf, R., Rosenberg, L., Epstein, E. J., MacMenamin, P., da Piedade, I., Gunsalus, K. C., Stoffel, M. et al. (2005). Combinatorial microRNA target predictions. *Nat Genet* **37**, 495-500.

Kretzschmar, M., Doody, J. and Massague, J. (1997). Opposing BMP and EGF signalling pathways converge on the TGF- β family mediator Smad1. *Nature* **389**, 618-622.

Krichevsky, A. M., Sonntag, K. C., Isacson, O. and Kosik, K. S. (2006). Specific microRNAs modulate embryonic stem cell-derived neurogenesis. *Stem Cells* **24**, 857-864.

Kutty, G., Kutty, R. K., Samuel, W., Duncan, T., Jaworski, C. and Wiggert, B. (1998). Identification of a new member of transforming growth factor- β superfamily in *Drosophila*: the first invertebrate *activin* gene. *Biochem Biophys Res Commun* **246**, 644-649.

Lagos-Quintana, M., Rauhut, R., Meyer, J., Borkhardt, A. and Tuschl, T. (2003). New microRNAs from mouse and human. *RNA* **9**, 175-179.

Landgraf, P., Rusu, M., Sheridan, R., Sewer, A., Iovino, N., Aravin, A., Pfeffer, S., Rice, A., Kamphorst, A. O., Landthaler, M. et al. (2007). A mammalian microRNA expression atlas based on small RNA library sequencing. *Cell* **129**, 1401-1414.

Lau, P., Verrier, J. D., Nielsen, J. A., Johnson, K. R., Notterpek, L. and Hudson, L. D. (2008). Identification of dynamically regulated microRNA and mRNA networks in developing oligodendrocytes. *J Neurosci* **28**, 11720-11730.

Lecuit, T. and Cohen, S. M. (1998). Dpp receptor levels contribute to shaping the Dpp morphogen gradient in the *Drosophila* wing imaginal disc. *Development* **125**, 4901-4907.

Lee, R. C. and Ambros, V. (2001). An extensive class of small RNAs in *Caenorhabditis elegans*. *Science* **294**, 862-864.

- Lee, R. C., Feinbaum, R. L. and Ambros, V.** (1993). The *C. elegans* heterochronic gene *lin-4* encodes small RNAs with antisense complementarity to *lin-14*. *Cell* **75**, 843-854.
- Lee, T., Lee, A. and Luo, L.** (1999). Development of the *Drosophila* mushroom bodies: sequential generation of three distinct types of neurons from a neuroblast. *Development* **126**, 4065-4076.
- Lee, T. and Luo, L.** (1999). Mosaic analysis with a repressible cell marker for studies of gene function in neuronal morphogenesis. *Neuron* **22**, 451-461.
- Lee, Y. S., Nakahara, K., Pham, J. W., Kim, K., He, Z., Sontheimer, E. J. and Carthew, R. W.** (2004). Distinct roles for *Drosophila* Dicer-1 and Dicer-2 in the siRNA/miRNA silencing pathways. *Cell* **117**, 69-81.
- Leucht, C., Stigloher, C., Wizenmann, A., Klafke, R., Folchert, A. and Bally-Cuif, L.** (2008). *MicroRNA-9* directs late organizer activity of the midbrain-hindbrain boundary. *Nat Neurosci* **11**, 641-648.
- Lewis, B. P., Burge, C. B. and Bartel, D. P.** (2005). Conserved seed pairing, often flanked by adenosines, indicates that thousands of human genes are microRNA targets. *Cell* **120**, 15-20.
- Lewis, B. P., Shih, I. H., Jones-Rhoades, M. W., Bartel, D. P. and Burge, C. B.** (2003). Prediction of mammalian microRNA targets. *Cell* **115**, 787-798.
- Lewis, K. A., Gray, P. C., Blount, A. L., MacConell, L. A., Wiater, E., Bilezikjian, L. M. and Vale, W.** (2000). Betaglycan binds inhibin and can mediate functional antagonism of activin signalling. *Nature* **404**, 411-414.
- Li, X. and Carthew, R. W.** (2005). A microRNA mediates EGF receptor signaling and promotes photoreceptor differentiation in the *Drosophila* eye. *Cell* **123**, 1267-1277.
- Li, Y., Wang, F., Lee, J. A. and Gao, F. B.** (2006). *MicroRNA-9a* ensures the precise specification of sensory organ precursors in *Drosophila*. *Genes Dev* **20**, 2793-2805.
- Lim, L. P., Glasner, M. E., Yekta, S., Burge, C. B. and Bartel, D. P.** (2003a). Vertebrate microRNA genes. *Science* **299**, 1540.
- Lim, L. P., Lau, N. C., Garrett-Engle, P., Grimson, A., Schelter, J. M., Castle, J., Bartel, D. P., Linsley, P. S. and Johnson, J. M.** (2005). Microarray analysis shows that some microRNAs downregulate large numbers of target mRNAs. *Nature* **433**, 769-773.
- Lim, L. P., Lau, N. C., Weinstein, E. G., Abdelhakim, A., Yekta, S., Rhoades, M. W., Burge, C. B. and Bartel, D. P.** (2003b). The microRNAs of *Caenorhabditis elegans*. *Genes Dev* **17**, 991-1008.

- Lin, S. Y., Johnson, S. M., Abraham, M., Vella, M. C., Pasquinelli, A., Gamberi, C., Gottlieb, E. and Slack, F. J.** (2003). The *C elegans hunchback* homolog, *hbl-1*, controls temporal patterning and is a probable microRNA target. *Dev Cell* **4**, 639-650.
- Liu, C. and Zhao, X.** (2009). MicroRNAs in adult and embryonic neurogenesis. *Neuromolecular Med* **11**, 141-152.
- Lonn, P., Moren, A., Raja, E., Dahl, M. and Moustakas, A.** (2009). Regulating the stability of TGF β receptors and Smads. *Cell Res* **19**, 21-35.
- Lopez-Casillas, F., Wrana, J. L. and Massague, J.** (1993). Betaglycan presents ligand to the TGF β signaling receptor. *Cell* **73**, 1435-1444.
- Makeyev, E. V., Zhang, J., Carrasco, M. A. and Maniatis, T.** (2007). The MicroRNA *miR-124* promotes neuronal differentiation by triggering brain-specific alternative pre-mRNA splicing. *Mol Cell* **27**, 435-448.
- Malzkorn, B., Wolter, M., Liesenberg, F., Grzendowski, M., Stuhler, K., Meyer, H. E. and Reifemberger, G.** (2010). Identification and functional characterization of microRNAs involved in the malignant progression of gliomas. *Brain Pathol* **20**, 539-550.
- Marques, G., Musacchio, M., Shimell, M. J., Wunnenberg-Stapleton, K., Cho, K. W. and O'Connor, M. B.** (1997). Production of a DPP activity gradient in the early *Drosophila* embryo through the opposing actions of the SOG and TLD proteins. *Cell* **91**, 417-426.
- Martin-Castellanos, C. and Edgar, B. A.** (2002). A characterization of the effects of Dpp signaling on cell growth and proliferation in the *Drosophila* wing. *Development* **129**, 1003-1013.
- Marty, T., Muller, B., Basler, K. and Affolter, M.** (2000). Schnurri mediates Dpp-dependent repression of *brinker* transcription. *Nat Cell Biol* **2**, 745-749.
- Mason, E. D., Konrad, K. D., Webb, C. D. and Marsh, J. L.** (1994). Dorsal midline fate in *Drosophila* embryos requires *twisted gastrulation*, a gene encoding a secreted protein related to human connective tissue growth factor. *Genes Dev* **8**, 1489-1501.
- Massague, J., Blain, S. W. and Lo, R. S.** (2000). TGF β signaling in growth control, cancer, and heritable disorders. *Cell* **103**, 295-309.
- Massague, J. and Gomis, R. R.** (2006). The logic of TGF β signaling. *FEBS Lett* **580**, 2811-2820.
- McEwen, D. G. and Peifer, M.** (2005). Puckered, a *Drosophila* MAPK phosphatase, ensures cell viability by antagonizing JNK-induced apoptosis. *Development* **132**, 3935-3946.

- Mendes, N. D., Freitas, A. T. and Sagot, M. F.** (2009). Current tools for the identification of miRNA genes and their targets. *Nucleic Acids Res* **37**, 2419-2433.
- Milan, M., Campuzano, S. and Garcia-Bellido, A.** (1996). Cell cycling and patterned cell proliferation in the *Drosophila* wing during metamorphosis. *Proc Natl Acad Sci U S A* **93**, 11687-11692.
- Miles, W. O., Jaffray, E., Campbell, S. G., Takeda, S., Bayston, L. J., Basu, S. P., Li, M., Raftery, L. A., Ashe, M. P., Hay, R. T. et al.** (2008). Medea SUMOylation restricts the signaling range of the Dpp morphogen in the *Drosophila* embryo. *Genes Dev* **22**, 2578-2590.
- Minami, M., Kinoshita, N., Kamoshida, Y., Tanimoto, H. and Tabata, T.** (1999). *brinker* is a target of Dpp in *Drosophila* that negatively regulates Dpp-dependent genes. *Nature* **398**, 242-246.
- Miska, E. A., Alvarez-Saavedra, E., Townsend, M., Yoshii, A., Sestan, N., Rakic, P., Constantine-Paton, M. and Horvitz, H. R.** (2004). Microarray analysis of microRNA expression in the developing mammalian brain. *Genome Biol* **5**, R68.
- Miyazono, K., Ichijo, H. and Heldin, C. H.** (1993). Transforming growth factor- β : latent forms, binding proteins and receptors. *Growth Factors* **8**, 11-22.
- Monteiro, R. M., de Sousa Lopes, S. M., Korchynskyi, O., ten Dijke, P. and Mummery, C. L.** (2004). Spatio-temporal activation of Smad1 and Smad5 in vivo: monitoring transcriptional activity of Smad proteins. *J Cell Sci* **117**, 4653-4663.
- Moss, E. G., Lee, R. C. and Ambros, V.** (1997). The cold shock domain protein LIN-28 controls developmental timing in *C. elegans* and is regulated by the *lin-4* RNA. *Cell* **88**, 637-646.
- Moustakas, A. and Heldin, C. H.** (2009). The regulation of TGF β signal transduction. *Development* **136**, 3699-3714.
- Muller, B., Hartmann, B., Pyrowolakis, G., Affolter, M. and Basler, K.** (2003). Conversion of an extracellular Dpp/BMP morphogen gradient into an inverse transcriptional gradient. *Cell* **113**, 221-233.
- Nahvi, A., Shoemaker, C. J. and Green, R.** (2009). An expanded seed sequence definition accounts for full regulation of the *hid* 3' UTR by *bantam* miRNA. *RNA* **15**, 814-822.
- Naiche, L. A., Harrelson, Z., Kelly, R. G. and Papaioannou, V. E.** (2005). T-box genes in vertebrate development. *Annu Rev Genet* **39**, 219-239.

Nakao, A., Afrakhte, M., Moren, A., Nakayama, T., Christian, J. L., Heuchel, R., Itoh, S., Kawabata, M., Heldin, N. E., Heldin, C. H. et al. (1997). Identification of Smad7, a TGF β -inducible antagonist of TGF- β signalling. *Nature* **389**, 631-635.

Nassif, C., Noveen, A. and Hartenstein, V. (2003). Early development of the *Drosophila* brain: III. The pattern of neuropile founder tracts during the larval period. *J Comp Neurol* **455**, 417-434.

Nave, K. A. (2010). Oligodendrocytes and the "micro brake" of progenitor cell proliferation. *Neuron* **65**, 577-579.

Nellen, D., Affolter, M. and Basler, K. (1994). Receptor serine/threonine kinases implicated in the control of *Drosophila* body pattern by *decapentaplegic*. *Cell* **78**, 225-237.

Nellen, D., Burke, R., Struhl, G. and Basler, K. (1996). Direct and long-range action of a DPP morphogen gradient. *Cell* **85**, 357-368.

Nelson, P. T., Baldwin, D. A., Kloosterman, W. P., Kauppinen, S., Plasterk, R. H. and Mourelatos, Z. (2006). RAKE and LNA-ISH reveal microRNA expression and localization in archival human brain. *RNA* **12**, 187-191.

Neul, J. L. and Ferguson, E. L. (1998). Spatially restricted activation of the SAX receptor by SCW modulates DPP/TKV signaling in *Drosophila* dorsal-ventral patterning. *Cell* **95**, 483-494.

Newfeld, S. J., Wisotzkey, R. G. and Kumar, S. (1999). Molecular evolution of a developmental pathway: phylogenetic analyses of transforming growth factor- β family ligands, receptors and Smad signal transducers. *Genetics* **152**, 783-795.

Nguyen, M., Park, S., Marques, G. and Arora, K. (1998). Interpretation of a BMP activity gradient in *Drosophila* embryos depends on synergistic signaling by two type I receptors, SAX and TKV. *Cell* **95**, 495-506.

Nolo, R., Morrison, C. M., Tao, C., Zhang, X. and Halder, G. (2006). The *bantam* microRNA is a target of the *hippo* tumor-suppressor pathway. *Curr Biol* **16**, 1895-1904.

Padgett, R. W. (1999). TGF β signaling pathways and human diseases. *Cancer Metastasis Rev* **18**, 247-259.

Padgett, R. W., Das, P. and Krishna, S. (1998). TGF- β signaling, Smads, and tumor suppressors. *Bioessays* **20**, 382-390.

Padgett, R. W., Wozney, J. M. and Gelbart, W. M. (1993). Human BMP sequences can confer normal dorsal-ventral patterning in the *Drosophila* embryo. *Proc Natl Acad Sci U S A* **90**, 2905-2909.

- Parker, L., Ellis, J. E., Nguyen, M. Q. and Arora, K.** (2006). The divergent TGF- β ligand Dawdle utilizes an activin pathway to influence axon guidance in *Drosophila*. *Development* **133**, 4981-4991.
- Parker, L., Stathakis, D. G. and Arora, K.** (2004). Regulation of BMP and activin signaling in *Drosophila*. *Prog Mol Subcell Biol* **34**, 73-101.
- Parrish, J. Z., Xu, P., Kim, C. C., Jan, L. Y. and Jan, Y. N.** (2009). The microRNA *bantam* functions in epithelial cells to regulate scaling growth of dendrite arbors in *Drosophila* sensory neurons. *Neuron* **63**, 788-802.
- Pascual, A. and Preat, T.** (2001). Localization of long-term memory within the *Drosophila* mushroom body. *Science* **294**, 1115-1117.
- Peng, H. W., Slattery, M. and Mann, R. S.** (2009). Transcription factor choice in the Hippo signaling pathway: *homothorax* and *yorkie* regulation of the microRNA *bantam* in the progenitor domain of the *Drosophila* eye imaginal disc. *Genes Dev* **23**, 2307-2319.
- Pentek, J., Parker, L., Wu, A. and Arora, K.** (2009). Follistatin preferentially antagonizes activin rather than BMP signaling in *Drosophila*. *Genesis* **47**, 261-273.
- Pereanu, W., Shy, D. and Hartenstein, V.** (2005). Morphogenesis and proliferation of the larval brain glia in *Drosophila*. *Dev Biol* **283**, 191-203.
- Perez, S. E. and Steller, H.** (1996). Migration of glial cells into retinal axon target field in *Drosophila melanogaster*. *J Neurobiol* **30**, 359-373.
- Pflugfelder, G. O.** (2009). *omb* and circumstance. *J Neurogenet* **23**, 15-33.
- Pflugfelder, G. O., Schwarz, H., Roth, H., Poeck, B., Sigl, A., Kerscher, S., Jonschker, B., Pak, W. L. and Heisenberg, M.** (1990). Genetic and molecular characterization of the *optomotor-blind* gene locus in *Drosophila melanogaster*. *Genetics* **126**, 91-104.
- Phelps, C. B. and Brand, A. H.** (1998). Ectopic gene expression in *Drosophila* using GAL4 system. *Methods* **14**, 367-379.
- Piccolo, S., Agius, E., Lu, B., Goodman, S., Dale, L. and De Robertis, E. M.** (1997). Cleavage of Chordin by Xolloid metalloprotease suggests a role for proteolytic processing in the regulation of Spemann organizer activity. *Cell* **91**, 407-416.
- Podos, S. D. and Ferguson, E. L.** (1999). Morphogen gradients: new insights from DPP. *Trends Genet* **15**, 396-402.

Poeck, B., Fischer, S., Gunning, D., Zipursky, S. L. and Salecker, I. (2001). Glial cells mediate target layer selection of retinal axons in the developing visual system of *Drosophila*. *Neuron* **29**, 99-113.

Poeck, B., Hofbauer, A. and Pflugfelder, G. O. (1993). Expression of the *Drosophila optomotor-blind* gene transcript in neuronal and glial cells of the developing nervous system. *Development* **117**, 1017-1029.

Pogue, A. I., Cui, J. G., Li, Y. Y., Zhao, Y., Culicchia, F. and Lukiw, W. J. (2010). Micro RNA-125b (*miRNA-125b*) function in astrogliosis and glial cell proliferation. *Neurosci Lett* **476**, 18-22.

Portin, P. (2002). General outlines of the molecular genetics of the Notch signalling pathway in *Drosophila melanogaster*: a review. *Hereditas* **136**, 89-96.

Poy, M. N., Eliasson, L., Krutzfeldt, J., Kuwajima, S., Ma, X., Macdonald, P. E., Pfeffer, S., Tuschl, T., Rajewsky, N., Rorsman, P. et al. (2004). A pancreatic islet-specific microRNA regulates insulin secretion. *Nature* **432**, 226-230.

Rafferty, L. A. and Sutherland, D. J. (1999). TGF- β family signal transduction in *Drosophila* development: from Mad to Smads. *Dev Biol* **210**, 251-268.

Rajewsky, N. and Socci, N. D. (2004). Computational identification of microRNA targets. *Dev Biol* **267**, 529-535.

Read, R. D., Cavenee, W. K., Furnari, F. B. and Thomas, J. B. (2009). A drosophila model for EGFR-Ras and PI3K-dependent human glioma. *PLoS Genet* **5**, e1000374.

Reguly, T. and Wrana, J. L. (2003). In or out? The dynamics of Smad nucleocytoplasmic shuttling. *Trends Cell Biol* **13**, 216-220.

Rehmsmeier, M., Steffen, P., Hochsmann, M. and Giegerich, R. (2004). Fast and effective prediction of microRNA/target duplexes. *RNA* **10**, 1507-1517.

Reinhart, B. J., Slack, F. J., Basson, M., Pasquinelli, A. E., Bettinger, J. C., Rougvie, A. E., Horvitz, H. R. and Ruvkun, G. (2000). The 21-nucleotide *let-7* RNA regulates developmental timing in *Caenorhabditis elegans*. *Nature* **403**, 901-906.

Rhoades, M. W., Reinhart, B. J., Lim, L. P., Burge, C. B., Bartel, B. and Bartel, D. P. (2002). Prediction of plant microRNA targets. *Cell* **110**, 513-520.

Robins, H., Li, Y. and Padgett, R. W. (2005). Incorporating structure to predict microRNA targets. *Proc Natl Acad Sci U S A* **102**, 4006-4009.

Rogulja, D. and Irvine, K. D. (2005). Regulation of cell proliferation by a morphogen gradient. *Cell* **123**, 449-461.

Ross, J. J., Shimmi, O., Vilmos, P., Petryk, A., Kim, H., Gaudenz, K., Hermanson, S., Ekker, S. C., O'Connor, M. B. and Marsh, J. L. (2001). *Twisted gastrulation* is a conserved extracellular BMP antagonist. *Nature* **410**, 479-483.

Salic, A. and Mitchison, T. J. (2008). A chemical method for fast and sensitive detection of DNA synthesis in vivo. *Proc Natl Acad Sci U S A* **105**, 2415-2420.

Sampath, T. K., Rashka, K. E., Doctor, J. S., Tucker, R. F. and Hoffmann, F. M. (1993). Drosophila transforming growth factor β superfamily proteins induce endochondral bone formation in mammals. *Proc Natl Acad Sci U S A* **90**, 6004-6008.

Schmierer, B. and Hill, C. S. (2007). TGF β -SMAD signal transduction: molecular specificity and functional flexibility. *Nat Rev Mol Cell Biol* **8**, 970-982.

Schmittgen, T. D. (2008). Regulation of microRNA processing in development, differentiation and cancer. *J Cell Mol Med* **12**, 1811-1819.

Schrons, H., Knust, E. and Campos-Ortega, J. A. (1992). The Enhancer of *split* complex and adjacent genes in the 96F region of *Drosophila melanogaster* are required for segregation of neural and epidermal progenitor cells. *Genetics* **132**, 481-503.

Schwank, G. and Basler, K. (2010). Regulation of organ growth by morphogen gradients. *Cold Spring Harb Perspect Biol* **2**, a001669.

Schwank, G., Restrepo, S. and Basler, K. (2008). Growth regulation by Dpp: an essential role for Brinker and a non-essential role for graded signaling levels. *Development* **135**, 4003-4013.

Sekelsky, J. J., Newfeld, S. J., Raftery, L. A., Chartoff, E. H. and Gelbart, W. M. (1995). Genetic characterization and cloning of *mothers against dpp*, a gene required for *decapentaplegic* function in *Drosophila melanogaster*. *Genetics* **139**, 1347-1358.

Sempere, L. F., Freemantle, S., Pitha-Rowe, I., Moss, E., Dmitrovsky, E. and Ambros, V. (2004). Expression profiling of mammalian microRNAs uncovers a subset of brain-expressed microRNAs with possible roles in murine and human neuronal differentiation. *Genome Biol* **5**, R13.

Serpe, M. and O'Connor, M. B. (2006). The metalloprotease tolloid-related and its TGF- β -like substrate Dawdle regulate *Drosophila* motoneuron axon guidance. *Development* **133**, 4969-4979.

Shcherbata, H. R., Ward, E. J., Fischer, K. A., Yu, J. Y., Reynolds, S. H., Chen, C. H., Xu, P., Hay, B. A. and Ruohola-Baker, H. (2007). Stage-specific differences in the requirements for germline stem cell maintenance in the *Drosophila* ovary. *Cell Stem Cell* **1**, 698-709.

- Shen, J., Dorner, C., Bahlo, A. and Pflugfelder, G. O.** (2008). *optomotor-blind* suppresses instability at the A/P compartment boundary of the *Drosophila* wing. *Mech Dev* **125**, 233-246.
- Sherr, C. J.** (1996). Cancer cell cycles. *Science* **274**, 1672-1677.
- Shi, W., Sun, C., He, B., Xiong, W., Shi, X., Yao, D. and Cao, X.** (2004). GADD34-PP1c recruited by Smad7 dephosphorylates TGF β type I receptor. *J Cell Biol* **164**, 291-300.
- Shi, Y., Wang, Y. F., Jayaraman, L., Yang, H., Massague, J. and Pavletich, N. P.** (1998). Crystal structure of a Smad MH1 domain bound to DNA: insights on DNA binding in TGF- β signaling. *Cell* **94**, 585-594.
- Shimell, M. J., Ferguson, E. L., Childs, S. R. and O'Connor, M. B.** (1991). The *Drosophila* dorsal-ventral patterning gene *tolloid* is related to human bone morphogenetic protein 1. *Cell* **67**, 469-481.
- Shimmi, O. and O'Connor, M. B.** (2003). Physical properties of Tld, Sog, Tsg and Dpp protein interactions are predicted to help create a sharp boundary in Bmp signals during dorsoventral patterning of the *Drosophila* embryo. *Development* **130**, 4673-4682.
- Shimmi, O., Umulis, D., Othmer, H. and O'Connor, M. B.** (2005). Facilitated transport of a Dpp/Scw heterodimer by Sog/Tsg leads to robust patterning of the *Drosophila* blastoderm embryo. *Cell* **120**, 873-886.
- Shraiman, B. I.** (2005). Mechanical feedback as a possible regulator of tissue growth. *Proc Natl Acad Sci U S A* **102**, 3318-3323.
- Silber, J., James, C. D. and Hodgson, J. G.** (2009). microRNAs in gliomas: small regulators of a big problem. *Neuromolecular Med* **11**, 208-222.
- Siomi, H. and Siomi, M. C.** (2010). Posttranscriptional regulation of microRNA biogenesis in animals. *Mol Cell* **38**, 323-332.
- Sivasankaran, R., Vigano, M. A., Muller, B., Affolter, M. and Basler, K.** (2000). Direct transcriptional control of the Dpp target *omb* by the DNA binding protein Brinker. *EMBO J* **19**, 6162-6172.
- Soustelle, L. and Giangrande, A.** (2007). Glial differentiation and the Gcm pathway. *Neuron Glia Biol* **3**, 5-16.
- Spencer, F. A., Hoffmann, F. M. and Gelbart, W. M.** (1982). *Decapentaplegic*: a gene complex affecting morphogenesis in *Drosophila melanogaster*. *Cell* **28**, 451-461.

- St Johnston, R. D. and Gelbart, W. M.** (1987). Decapentaplegic transcripts are localized along the dorsal-ventral axis of the *Drosophila* embryo. *EMBO J* **6**, 2785-2791.
- St Johnston, R. D., Hoffmann, F. M., Blackman, R. K., Segal, D., Grimaldi, R., Padgett, R. W., Irick, H. A. and Gelbart, W. M.** (1990). Molecular organization of the *decapentaplegic* gene in *Drosophila melanogaster*. *Genes Dev* **4**, 1114-1127.
- Stark, A., Brennecke, J., Russell, R. B. and Cohen, S. M.** (2003). Identification of *Drosophila* MicroRNA targets. *PLoS Biol* **1**, E60.
- Suh, G. S., Poeck, B., Chouard, T., Oron, E., Segal, D., Chamovitz, D. A. and Zipursky, S. L.** (2002). *Drosophila* JAB1/CSN5 acts in photoreceptor cells to induce glial cells. *Neuron* **33**, 35-46.
- Sun, Y. H., Tsai, C. J., Green, M. M., Chao, J. L., Yu, C. T., Jaw, T. J., Yeh, J. Y. and Bolshakov, V. N.** (1995). *White* as a reporter gene to detect transcriptional silencers specifying position-specific gene expression during *Drosophila melanogaster* eye development. *Genetics* **141**, 1075-1086.
- Tanaka-Matakatsu, M., Xu, J., Cheng, L. and Du, W.** (2009). Regulation of apoptosis of *rbf* mutant cells during *Drosophila* development. *Dev Biol* **326**, 347-356.
- Tanimoto, H., Itoh, S., ten Dijke, P. and Tabata, T.** (2000). Hedgehog creates a gradient of DPP activity in *Drosophila* wing imaginal discs. *Mol Cell* **5**, 59-71.
- Teleman, A. A. and Cohen, S. M.** (2000). Dpp gradient formation in the *Drosophila* wing imaginal disc. *Cell* **103**, 971-980.
- Thompson, B. J. and Cohen, S. M.** (2006). The Hippo pathway regulates the *bantam* microRNA to control cell proliferation and apoptosis in *Drosophila*. *Cell* **126**, 767-774.
- Ting, C. Y. and Lee, C. H.** (2007). Visual circuit development in *Drosophila*. *Curr Opin Neurobiol* **17**, 65-72.
- Tsumaki, N. and Yoshikawa, H.** (2005). The role of bone morphogenetic proteins in endochondral bone formation. *Cytokine Growth Factor Rev* **16**, 279-285.
- Tsuneizumi, K., Nakayama, T., Kamoshida, Y., Kornberg, T. B., Christian, J. L. and Tabata, T.** (1997). *Daughters against dpp* modulates *dpp* organizing activity in *Drosophila* wing development. *Nature* **389**, 627-631.
- Umemori, M., Takemura, M., Maeda, K., Ohba, K. and Adachi-Yamada, T.** (2007). *Drosophila* T-box transcription factor *Optomotor-blind* prevents pathological folding and local overgrowth in wing epithelium through confining Hh signal. *Dev Biol* **308**, 68-81.

Umulis, D., O'Connor, M. B. and Blair, S. S. (2009). The extracellular regulation of bone morphogenetic protein signaling. *Development* **136**, 3715-3728.

Van de Bor, V., Delanoue, R., Cossard, R. and Silber, J. (1999). Truncated products of the *vestigial* proliferation gene induce apoptosis. *Cell Death Differ* **6**, 557-564.

Varelas, X., Sakuma, R., Samavarchi-Tehrani, P., Peerani, R., Rao, B. M., Dembowy, J., Yaffe, M. B., Zandstra, P. W. and Wrana, J. L. (2008). TAZ controls Smad nucleocytoplasmic shuttling and regulates human embryonic stem-cell self-renewal. *Nat Cell Biol* **10**, 837-848.

Visvanathan, J., Lee, S., Lee, B., Lee, J. W. and Lee, S. K. (2007). The microRNA *miR-124* antagonizes the anti-neural REST/SCP1 pathway during embryonic CNS development. *Genes Dev* **21**, 744-749.

Wang, B., Suzuki, H. and Kato, M. (2008a). Roles of mono-ubiquitinated Smad4 in the formation of Smad transcriptional complexes. *Biochem Biophys Res Commun* **376**, 288-292.

Wang, X., Harris, R. E., Bayston, L. J. and Ashe, H. L. (2008b). Type IV collagens regulate BMP signalling in *Drosophila*. *Nature* **455**, 72-77.

Wang, Y., Baskerville, S., Shenoy, A., Babiarz, J. E., Baehner, L. and Blelloch, R. (2008c). Embryonic stem cell-specific microRNAs regulate the G1-S transition and promote rapid proliferation. *Nat Genet* **40**, 1478-1483.

Wang, Y. C. and Ferguson, E. L. (2005). Spatial bistability of Dpp-receptor interactions during *Drosophila* dorsal-ventral patterning. *Nature* **434**, 229-234.

Wharton, K. A., Ray, R. P. and Gelbart, W. M. (1993). An activity gradient of *decapentaplegic* is necessary for the specification of dorsal pattern elements in the *Drosophila* embryo. *Development* **117**, 807-822.

White, K., Grether, M. E., Abrams, J. M., Young, L., Farrell, K. and Steller, H. (1994). Genetic control of programmed cell death in *Drosophila*. *Science* **264**, 677-683.

Wicks, S. J., Haros, K., Maillard, M., Song, L., Cohen, R. E., Dijke, P. T. and Chantry, A. (2005). The deubiquitinating enzyme UCH37 interacts with Smads and regulates TGF- β signalling. *Oncogene* **24**, 8080-8084.

Wienholds, E., Kloosterman, W. P., Miska, E., Alvarez-Saavedra, E., Berezikov, E., de Bruijn, E., Horvitz, H. R., Kauppinen, S. and Plasterk, R. H. (2005). MicroRNA expression in zebrafish embryonic development. *Science* **309**, 310-311.

Wightman, B., Ha, I. and Ruvkun, G. (1993). Posttranscriptional regulation of the heterochronic gene *lin-14* by *lin-4* mediates temporal pattern formation in *C. elegans*. *Cell* **75**, 855-862.

Williams, A. E. (2008). Functional aspects of animal microRNAs. *Cell Mol Life Sci* **65**, 545-562.

Wilson, V. and Conlon, F. L. (2002). The T-box family. *Genome Biol* **3**, REVIEWS3008.

Winnier, G., Blessing, M., Labosky, P. A. and Hogan, B. L. (1995). Bone morphogenetic protein-4 is required for mesoderm formation and patterning in the mouse. *Genes Dev* **9**, 2105-2116.

Wong, P., Iwasaki, M., Somervaille, T. C., Ficara, F., Carico, C., Arnold, C., Chen, C. Z. and Cleary, M. L. (2010). The *miR-17-92* microRNA polycistron regulates MLL leukemia stem cell potential by modulating p21 expression. *Cancer Res* **70**, 3833-3842.

Wrana, J. L. (2000). Regulation of Smad activity. *Cell* **100**, 189-192.

Wrighton, K. H., Lin, X. and Feng, X. H. (2008). Critical regulation of TGF β signaling by Hsp90. *Proc Natl Acad Sci U S A* **105**, 9244-9249.

Xia, Y. and Schneyer, A. L. (2009). The biology of activin: recent advances in structure, regulation and function. *J Endocrinol* **202**, 1-12.

Xiong, W. C., Okano, H., Patel, N. H., Blendy, J. A. and Montell, C. (1994). *repo* encodes a glial-specific homeo domain protein required in the Drosophila nervous system. *Genes Dev* **8**, 981-994.

Xu, L., Yao, X., Chen, X., Lu, P., Zhang, B. and Ip, Y. T. (2007). Msk is required for nuclear import of TGF- β /BMP-activated Smads. *J Cell Biol* **178**, 981-994.

Xu, P., Vernoooy, S. Y., Guo, M. and Hay, B. A. (2003). The Drosophila microRNA *miR-14* suppresses cell death and is required for normal fat metabolism. *Curr Biol* **13**, 790-795.

Yakoby, N., Lembong, J., Schupbach, T. and Shvartsman, S. Y. (2008). Drosophila eggshell is patterned by sequential action of feedforward and feedback loops. *Development* **135**, 343-351.

Yamaguchi, T., Kurisaki, A., Yamakawa, N., Minakuchi, K. and Sugino, H. (2006). FKBP12 functions as an adaptor of the Smad7-Smurf1 complex on activin type I receptor. *J Mol Endocrinol* **36**, 569-579.

- Yang, M., Li, Y. and Padgett, R. W.** (2005). MicroRNAs: Small regulators with a big impact. *Cytokine Growth Factor Rev* **16**, 387-393.
- Yang, Y., Xu, S., Xia, L., Wang, J., Wen, S., Jin, P. and Chen, D.** (2009). The *bantam* microRNA is associated with drosophila fragile X mental retardation protein and regulates the fate of germline stem cells. *PLoS Genet* **5**, e1000444.
- Yao, X., Chen, X., Cottonham, C. and Xu, L.** (2008). Preferential utilization of Imp7/8 in nuclear import of Smads. *J Biol Chem* **283**, 22867-22874.
- Yekta, S., Shih, I. H. and Bartel, D. P.** (2004). MicroRNA-directed cleavage of HOXB8 mRNA. *Science* **304**, 594-596.
- Yoo, A. S. and Greenwald, I.** (2005). LIN-12/Notch activation leads to microRNA-mediated down-regulation of Vav in *C. elegans*. *Science* **310**, 1330-1333.
- Yoshida, S., Soustelle, L., Giangrande, A., Umetsu, D., Murakami, S., Yasugi, T., Awasaki, T., Ito, K., Sato, M. and Tabata, T.** (2005). DPP signaling controls development of the lamina glia required for retinal axon targeting in the visual system of Drosophila. *Development* **132**, 4587-4598.
- Zars, T.** (2000). Behavioral functions of the insect mushroom bodies. *Curr Opin Neurobiol* **10**, 790-795.
- Zawel, L., Dai, J. L., Buckhaults, P., Zhou, S., Kinzler, K. W., Vogelstein, B. and Kern, S. E.** (1998). Human Smad3 and Smad4 are sequence-specific transcription activators. *Mol Cell* **1**, 611-617.
- Zecca, M., Basler, K. and Struhl, G.** (1995). Sequential organizing activities of *engrailed*, *hedgehog* and *decapentaplegic* in the Drosophila wing. *Development* **121**, 2265-2278.
- Zhang, H., Levine, M. and Ashe, H. L.** (2001). Brinker is a sequence-specific transcriptional repressor in the Drosophila embryo. *Genes Dev* **15**, 261-266.
- Zhang, Y.** (2005). miRU: an automated plant miRNA target prediction server. *Nucleic Acids Res* **33**, W701-W704.
- Zhao, C., Sun, G., Li, S. and Shi, Y.** (2009). A feedback regulatory loop involving *microRNA-9* and nuclear receptor TLX in neural stem cell fate determination. *Nat Struct Mol Biol* **16**, 365-371.
- Zheng, X., Wang, J., Haerry, T. E., Wu, A. Y., Martin, J., O'Connor, M. B., Lee, C. H. and Lee, T.** (2003). TGF- β signaling activates steroid hormone receptor expression during neuronal remodeling in the Drosophila brain. *Cell* **112**, 303-315.

Zheng, X., Zugates, C. T., Lu, Z., Shi, L., Bai, J. M. and Lee, T. (2006). Baboon/dSmad2 TGF- β signaling is required during late larval stage for development of adult-specific neurons. *EMBO J* **25**, 615-627.

Zhu, C. C., Boone, J. Q., Jensen, P. A., Hanna, S., Podemski, L., Locke, J., Doe, C. Q. and O'Connor, M. B. (2008). Drosophila Activin- and the Activin-like product Dawdle function redundantly to regulate proliferation in the larval brain. *Development* **135**, 513-521.

Zwijssen, A., Verschueren, K. and Huylebroeck, D. (2003). New intracellular components of bone morphogenetic protein/Smad signaling cascades. *FEBS Lett* **546**, 133-139.

Curriculum Vitae

Ying Li

EDUCATION:

- 2004-2010 Ph.D., Cell and Developmental Biology, Rutgers University, New Jersey, U.S.A.
- 1998-2001 M.S., Biochemistry and Molecular Biology, Peking University Health Science Center, Beijing, P.R.China
- 1993-1998 M.B., Clinic Medicine, Peking University Health Science Center, Beijing, P.R.China

AWARDS AND HONORS:

- 2004-2008 Predoctoral Fellowship, Rutgers University, Waksman Institute and the Department of Molecular Biology and Biochemistry.
- 2002-2003 Predoctoral Fellowship, University of Illinois at Urbana - Champaign, Cell and Structural Biology
- 1996-1997 Peking University Outstanding Medical Student Award
- 1993-1994 Peking University Outstanding Medical Student Award

PUBLICATIONS:

Li Y, Robins H, Kane NS, Padgett RW. *bantam microRNA is a Negative Regulator of the decapentaplegic Pathway*. Plos Genetics (submitted)

Li Y, Padgett RW. *bantam microRNA functions in the optic lobe*. (to be submitted in Nov. 2010)

Robins H, Li Y, Padgett RW. (2005) *Incorporating structure to predict microRNA targets*. Proc Natl Acad Sci U S A. 102(11):4006-4009.

Yang M, Li Y, Padgett RW. (2005) *MicroRNAs: Small regulators with a big impact*. Cytokine Growth Factor Rev. 16(4-5)

Minin AA, Kulik AV, Gyoeva FK, Li Y, Goshima G, Gelfand VI. (2006) *Regulation of mitochondria distribution by RhoA and formins*. Journal of Cell Science. 119(Pt 4):659-670